

**Over-expression and Biophysical Characterisation of Membrane  
Proteins Solubilised in a Styrene Maleic Acid Polymer**

**Yu-pin Lin**

A thesis submitted to the University of Birmingham

For the degree of Doctor of Philosophy

School of Biosciences  
University of Birmingham  
Birmingham  
B15 2TT

February 2011

UNIVERSITY OF  
BIRMINGHAM

**University of Birmingham Research Archive**

**e-theses repository**

This unpublished thesis/dissertation is copyright of the author and/or third parties. The intellectual property rights of the author or third parties in respect of this work are as defined by The Copyright Designs and Patents Act 1988 or as modified by any successor legislation.

Any use made of information contained in this thesis/dissertation must be in accordance with that legislation and must be properly acknowledged. Further distribution or reproduction in any format is prohibited without the permission of the copyright holder.

## **Acknowledgements**

Firstly, I very much appreciate to my supervisor, Dr. Tim Dafforn for his supervision. I have studied under his supervision over 4 years (MRes+PhD). He always gives me a lot of support and encouragement throughout my years of study, especially when I stuck in A<sub>2a</sub>R purification, he continuously encouraged me and provided many useful solutions which have aided my research. It has been a real pleasure to work with him. I will never forget all his help !!!

Huge thanks to Prof. Mark Wheatley, Dr. David Poyner, Miss Zharain Bawa for their help on GPCRs and radioligand binding assay. Many thanks to Prof. Michael Overduin and Dr. Tim Knowles to provide and teach me the most important technique of my PhD project, SMALP. I would like to thank Dr. Corinne Smith for electron microscopy and Mrs. Rosemary Parslow for her very kind help on everything in the lab. I would also like to thank Dr. Roslyn Bill, Dr. Richard Darby and Dr. Mohammed Jamshad for their help on A<sub>2a</sub>R expression and yeast membrane preparation.

Especially thank Dr. Raul Pacheco-Gomez for his huge help on my PhD project, his friendship, encouragement and keep me to stay in positive attitude. My thanks also go to the members of 7<sup>th</sup> floor, Prof. Chris Wharton, Dr. Eva Hyde, Rich, Rachel, Hsing, Martin,

Umbreen, Yukie, Michelle, Matt, Craig, Sandy for making a very friendly working environment. I would also like to thank all my friends, Da-Chung, Colin, Kai, Leo, Libby, Nat.....in UK and Taiwan for keeping me away from the science sometimes throughout my PhD. I am forever appreciated to my parents, my wife, Hsuan-Chi and my sisters for their enthusiasm, support and unlimited love.

## **Abstract**

Membrane proteins are the gateways into cells and therefore a critical part of pharmaceutical research. Membrane proteins, in fact, have been shown to be the target of over 50% of all medicinal drugs. The development of drugs that acts on membrane proteins, however, has been limited by the lack of high resolution structural data. This lack of information results from a lack of a generic method to extract active membrane proteins from the cell membrane.

We have developed a novel styrene maleic acid (SMA) / lipid particle system termed SMALP that preserves the structural and functional integrity of membrane proteins. We have optimised this system and used it to solubilise two membrane proteins with different architectures and functions. The first, human adenosine 2a receptor ( $A_{2a}R$ ), is a G-protein coupled receptor, a 7 transmembrane helix protein that is involved in cell signalling, whereas the second, FtsZ-interacting protein A (ZipA), is a protein involved in bacterial cell division that contains a single transmembrane domain.

In this project, standardised purification protocols were developed that produced pure proteins without the need to add any detergents. The subsequent biophysical characterisation that included circular dichroism, mass spectrometry and sedimentation velocity analytical ultracentrifugation indicated that these purified SMALP solubilised proteins were natively

folded once encapsulated. The activities of both proteins were then tested and shown to be close to that expected for the intact proteins in the cell membrane. Taken together these data suggest that the SMALP system offers the solution to membrane protein purification into the future.

**Keywords:** Membrane proteins; SMALP; Human adenosine 2a receptor; FtsZ-interacting protein A; Detergent; Biophysical characterisation

## Abbreviations

A<sub>2a</sub>R: Human adenosine 2a receptor

Abs<sub>280</sub>: Absorbance at wavelength 280 nm

BCA: Bicinchoninic acid

B<sub>max</sub> : Maximum binding capability

bR: Bacteriorhodopsin

BSA: Bovine serum albumin

CD: Circular dichroism

CHS: Cholesteryl hemisuccinate

CMC: Critical micelle concentration

CTAB: Cyltrimethylammonium bromide

DDM solubilised A<sub>2a</sub>R: A<sub>2a</sub>R extracted from cell membrane by DDM method (not purified yet, only the solubilised material)

DDM: n-dodecyl-β-D-maltoside

DLS : Dynamic light scattering

DMPC: 1,2-Dimyristoyl-sn-Glycero-3-Phosphocholine

DNA: Deoxyribonucleic acid

DPHC: 1,2-Dihexanoyl-sn-Glycero-3-Phosphocholine

DTT: Dithiothreitol

*E. coli* : *Escherichia coli*

EDTA: Ethylenediaminetetraacetic acid

EM: Electron microscopy

FPLC: Fast protein liquid chromatography

FT-ICR: Fourier transform ion cyclotron resonance

FtsZ: Filamentous temperature sensitive protein Z

GDP: Guanosine diphosphate

GPCRs: G-protein coupled receptors

GTP: Guanosine triphosphate

GUVs: Giant unilamellar vesicles

×g :Centrifugal force

HPLC: High performance liquid chromatography

IDA: Iminodiacetic acid

IMAC: Immobilized-metal affinity chromatography

IPTG: Isopropyl-β-D-thiogalactopyranoside

$K_d$  : Dissociation constant

kDa: Kilodalton

LB: Luria-Bertani

LD: Linear dichroism



LUVs: Large unilamellar vesicles

M: Molar

MESG: 2-amino-6-mercapto-7-methylpurine/methylthioguanosine

mg: Milligram

ml: Millilitre

MLVs: Multilamellar vesicles

mM: Millimolar

MSPs: Membrane scaffold proteins

MW: Molecular weight

MWCO: Molecular weight cut-off

NECA: *N*-ethylcarboxamidoadenosine

ng: Nanogram

NMR: Nuclear magnetic resonance

OG: Octyl  $\beta$ -D-glucoside

PCR: Polymerase chain reaction

PDB: Protein Data Bank

pH:  $-\log_{10} [H^+]$

Pi: Inorganic phosphate

PNP: Purine nucleoside phosphorylase

Purified DDM-A<sub>2a</sub>R: pure A<sub>2a</sub>R solubilised by DDM method and then purified by standardised purification protocols

Purified SMALP-A<sub>2a</sub>R (or ZipA): pure A<sub>2a</sub>R (or ZipA) solubilised by SMALP method and then purified by standardised purification protocols

RALS: Right angle light scattering

rpm: Revolutions per minute

SDS-PAGE: Sodium dodecyl sulphate polyacrylamide gel electrophoresis

SMA: Styrene maleic acid

SMALP solubilised A<sub>2a</sub>R: A<sub>2a</sub>R extracted from cell membrane by SMALP method (not purified yet, only the solubilised material)

SMALP: Styrene maleic acid lipid particle

SUVs: Small unilamellar vesicles

svAUC: Sedimentation velocity analytical ultracentrifugation

Tris: Tris (hydroxymethyl) aminomethane

UV: Ultraviolet

v/v: Volume to volume ratio

V: Volts

w/v: Weight to volume ratio

XAC : Xanthine amine congener

ZipA: FtsZ-interacting protein A

# Table of Contents

<b>CHAPTER 1: INTRODUCTION .....</b>	<b>1</b>
<b>1.1 WHY STUDY MEMBRANE PROTEINS .....</b>	<b>1</b>
<b>1.2 MEMBRANE PROTEINS AND LIPIDS.....</b>	<b>3</b>
<b>1.3 THE CURRENT CHALLENGES AND APPROACHES FOR MEMBRANE PROTEIN STUDY .....</b>	<b>6</b>
1.3.1 MEMBRANE PROTEINS EXPRESSION .....	9
1.3.2 MEMBRANE PROTEIN PURIFICATION .....	10
1.3.3 ANALYTICAL STUDIES .....	22
<b>1.4 A NOVEL MEMBRANE PROTEIN STUDY METHOD: STYRENE MALEIC ACID LIPID PARTICLES .....</b>	<b>23</b>
<b>1.5 TARGET PROTEIN SELECTION: HUMAN ADENOSINE 2A RECEPTOR, A GPCR.....</b>	<b>29</b>
1.5.1 G-PROTEIN COUPLED RECEPTORS .....	29
1.5.2 HUMAN ADENOSINE 2A RECEPTOR.....	33
<b>1.6 TARGET PROTEIN SELECTION: FTSZ-INTERACTING PROTEIN A, A BACTERIAL CELL DIVISION PROTEIN .....</b>	<b>36</b>
1.6.1 BACTERIAL CELL DIVISION PROTEINS .....	36
1.6.2 FILAMENTOUS TEMPERATURE SENSITIVE PROTEIN Z .....	41
1.6.3 FtsZ-INTERACTING PROTEIN A .....	43
1.6.4 THE FtsZ-ZipA INTERACTION.....	45
<b>1.7 OBJECTIVES.....</b>	<b>46</b>
<b>1.8 AIMS.....</b>	<b>47</b>
<b>CHAPTER 2: MATERIALS AND METHODS .....</b>	<b>49</b>
<b>2.1 MATERIALS.....</b>	<b>49</b>
2.1.1 Reagents for Protein Expression .....	49
2.1.2 Reagents for Protein Purification .....	50
2.1.3 Reagents for Protein Characterisation.....	51
<b>2.2 METHODS: EXPRESSION AND PURIFICATION OF A2AR.....</b>	<b>51</b>
2.2.1 YEAST STRAINS, TRANSFORMATION AND EXPRESSION SCREENING .....	51
2.2.2 LARGE-SCALE FLASK CULTURE.....	54
2.2.3 BIOREACTOR CULTURE.....	54
2.2.4 YEAST MEMBRANE PREPARATION.....	56

2.2.5 YEAST MEMBRANE SOLUBILISATION WITH SMA POLYMER.....	57
2.2.5.1 Preparation of SMA polymer .....	57
2.2.5.2 Solubilisation with SMA polymer.....	58
2.2.6 YEAST MEMBRANE SOLUBILISATION WITH DETERGENT .....	58
2.2.7 PURIFICATION OF A2AR.....	59
2.2.7.1 SMALP Solubilised A2aR Purification Trails .....	63
2.2.7.2 Final SMALP Solubilised A2aR Purification Procedure .....	64
2.2.7.3 Purification of Detergent Solubilised A2aR.....	65
2.2.8 SDS-PAGE AND WESTERN BLOTTING .....	66
2.2.9 IDENTIFICATION OF A2AR .....	68
2.2.10 PROTEIN QUANTITATION .....	69
<b>2.3 METHODS: CHARACTERISATION OF A2AR.....</b>	<b>70</b>
2.3.1 RADIOLIGAND BINDING ASSAYS .....	70
2.3.2 CIRCULAR DICHROISM.....	73
2.3.3 SEDIMENTATION VELOCITY ANALYTICAL ULTRACENTRIFUGATION .....	76
2.3.4 ELECTRON MICROSCOPY .....	77
<b>2.4 METHODS: EXPRESSION AND PURIFICATION OF ZipA .....</b>	<b>78</b>
2.4.1 PLASMID CONSTRUCTION, ESCHERICHIA COLI STRAINS AND TRANSFORMATION .....	78
2.4.1.1 Extraction of Escherichia coli Genomic DNA.....	78
2.4.1.2 Polymerase Chain Reaction .....	79
2.4.1.3 Agarose Gel Electrophoresis .....	80
2.4.1.4 Purification of PCR Product from Agarose Gel.....	81
2.4.1.5 Ligation Reaction.....	81
2.4.1.6 Transformation of TOP10 Chemical Competent Cells.....	85
2.4.1.7 Isolation of Recombinant Plasmid DNA .....	86
2.4.1.8 DNA Sequencing .....	87
2.4.1.9 Transformation of BL21 Star (DE3) One Shot E.coli Cells .....	87
2.4.2 SMALL-SCALE FLASK CULTURE.....	88
2.4.3 LARGE-SCALE FLASK CULTURE.....	89
2.4.4 E.COLI MEMBRANE PREPARATION.....	89
2.4.5 SOLUBILISATION WITH SMA AND PURIFICATION OF SMALP SOLUBILISED ZipA.....	90
2.4.6 SDS-PAGE AND WESTERN BLOTTING OF ZipA .....	90
2.4.7 IDENTIFICATION OF ZipA.....	90
2.4.8 THE N-TERMINAL SEQUENCING OF ZipA.....	90
2.4.9 FtsZ PROTEIN PREPARATION .....	91
2.4.9.1 FtsZ Protein Expression.....	91
2.4.9.2 FtsZ Protein Purification .....	92

2.4.10 PROTEIN QUANTITATION .....	93
<b>2.5 METHODS: CHARACTERISATION OF ZipA.....</b>	<b>94</b>
2.5.1 CIRCULAR DICHROISM AND SEDIMENTATION VELOCITY ANALYTICAL ULTRACENTRIFUGATION .....	94
2.5.2 RIGHT ANGLE LIGHT SCATTERING .....	94
2.5.3 LINEAR DICHROISM .....	95
2.5.4 GTPASE ASSAY .....	96
2.5.5 SEDIMENTATION ASSAY .....	99
2.5.6 ELECTRON MICROSCOPY .....	100
2.5.7 RECONSTITUTION OF FtsZ-RING INSIDE A GUV .....	101
<b>CHAPTER 3: EXPRESSION AND PURIFICATION OF A2AR.....</b>	<b>103</b>
<b>3.1 INTRODUCTION .....</b>	<b>103</b>
<b>3.2 RESULTS.....</b>	<b>104</b>
3.2.1 EXPRESSION SCREENING OF A2AR .....	104
3.2.2 LARGE-SCALE PROTEIN EXPRESSION .....	105
3.2.3 A COMPARISON OF SMA SOLUBILISATION WITH DETERGENT SOLUBILISATION .....	107
3.2.4 PURIFICATION OF A2AR.....	110
3.2.4.1 SMALP Solubilised A2aR Purification Trails .....	110
3.2.4.2 Final SMALP Solubilised A2aR Purification Procedure .....	113
3.2.4.3 Purification of Detergent Solubilised A2aR.....	118
3.2.5 RECEPTOR IDENTIFICATION AND WESTERN BLOTTING ANALYSIS .....	122
<b>3.3 DISCUSSION.....</b>	<b>125</b>
<b>CHAPTER 4: CHARACTERISATION OF A2AR.....</b>	<b>128</b>
<b>4.1 INTRODUCTION .....</b>	<b>128</b>
<b>4.2 RESULTS.....</b>	<b>129</b>
4.2.1 RADIOLIGAND BINDING ASSAYS .....	129
4.2.2 CIRCULAR DICHROISM STUDIES .....	133
4.2.3 SEDIMENTATION VELOCITY ANALYTICAL ULTRACENTRIFUGATION .....	138
4.2.4 ELECTRON MICROSCOPY .....	140
<b>4.3 DISCUSSION.....</b>	<b>142</b>
<b>CHAPTER 5: EXPRESSION AND PURIFICATION OF ZipA .....</b>	<b>145</b>
<b>5.1 INTRODUCTION .....</b>	<b>145</b>
<b>5.2 RESULTS.....</b>	<b>146</b>
5.2.1 PLASMID CONSTRUCTION, ESCHERICHIA COLI STRAINS AND TRANSFORMATION .....	146

5.2.1.1	<i>Extraction of Escherichia coli Genomic DNA</i> .....	146
5.2.1.2	<i>Polymerase Chain Reaction</i> .....	147
5.2.1.3	<i>Ligation, Transformation and Extraction of Plasmid DNA</i> .....	150
5.2.2	EXPRESSION SCREENING AND SMALL-SCALE OF PROTEIN PURIFICATION .....	151
5.2.3	LARGE-SCALE OF PROTEIN EXPRESSION AND PURIFICATION .....	154
5.2.4	PROTEIN IDENTIFICATION AND WESTERN BLOTTING ANALYSIS.....	157
5.2.5	FtsZ PROTEIN EXPRESSION AND PURIFICATION .....	160
5.2.5.1	<i>Expression Screening of FtsZ</i> .....	160
5.2.5.2	<i>Large-scale FtsZ Expression and Purification</i> .....	161
5.2.5.3	<i>Activity Test for FtsZ</i> .....	162
<b>5.3</b>	<b>DISCUSSION</b> .....	<b>164</b>
<b>CHAPTER 6:</b>	<b>CHARACTERISATION OF ZipA</b> .....	<b>166</b>
<b>6.1</b>	<b>INTRODUCTION</b> .....	<b>166</b>
<b>6.2</b>	<b>RESULTS</b> .....	<b>167</b>
6.2.1	CIRCULAR DICHROISM.....	167
6.2.2	SEDIMENTATION VELOCITY ANALYTICAL ULTRACENTRIFUGATION .....	168
6.2.3	ELECTRON MICROSCOPY .....	170
6.2.4	RIGHT ANGLE LIGHT SCATTERING .....	172
6.2.5	SEDIMENTATION ASSAY .....	179
6.2.6	GTPASE ASSAY .....	183
6.2.7	LINEAR DICHROISM .....	185
6.2.8	ELECTRON MICROSCOPY .....	188
6.2.9	RECONSTITUTION OF FtsZ-RING INSIDE A GIANT UNILAMELLAR VESICLE.....	189
<b>6.3</b>	<b>DISCUSSION</b> .....	<b>193</b>
<b>CHAPTER 7:</b>	<b>GENERAL DISCUSSION, CONCLUSIONS AND FUTURE WORK</b> .....	<b>195</b>
<b>7.1</b>	<b>GENERAL DISCUSSION</b> .....	<b>195</b>
<b>7.2</b>	<b>CONCLUSIONS</b> .....	<b>204</b>
<b>7.3</b>	<b>FUTURE WORK</b> .....	<b>205</b>
<b>CHAPTER 8:</b>	<b>REFERENCES</b> .....	<b>207</b>
<b>CHAPTER 9:</b>	<b>APPENDICES</b> .....	<b>222</b>

# **CHAPTER 1: Introduction**

## **1.1 Why Study Membrane Proteins**

At the present time, the biggest challenge to our understanding of the structure and functionality of membrane proteins is the lack of a simple and universal protocol for extracting membrane proteins from the native membrane environment while at the same time maintaining their native structures and functions. Membrane proteins are extremely important for human biology research as they are central to a wide range of biological processes including signal transduction, molecular transport, cell division and respiration [1]. The human genome project has shown that over 30% of genes encode for membrane proteins, and these membrane proteins are the targets for over 50% of the marketed pharmaceuticals [2, 3]. The development of drugs, however, has been limited by the lack of atomic level structural information.

The first high resolution protein structure, myoglobin, was reported in 1960 [4]. However, the first membrane protein structure was solved after a further 26 years [5], and since then a relatively small number of membrane protein structures have been solved (compared to total protein structures, Figure 1-1) [6, 7]. To date, there are nearly 65,000 protein structures solved by X-ray crystallography, nuclear magnetic resonance (NMR) or electron microscopy

(EM), but only approximately 1% these structures are membrane proteins. (All known protein structures: 64,353; membrane proteins: 717) [6, 7].

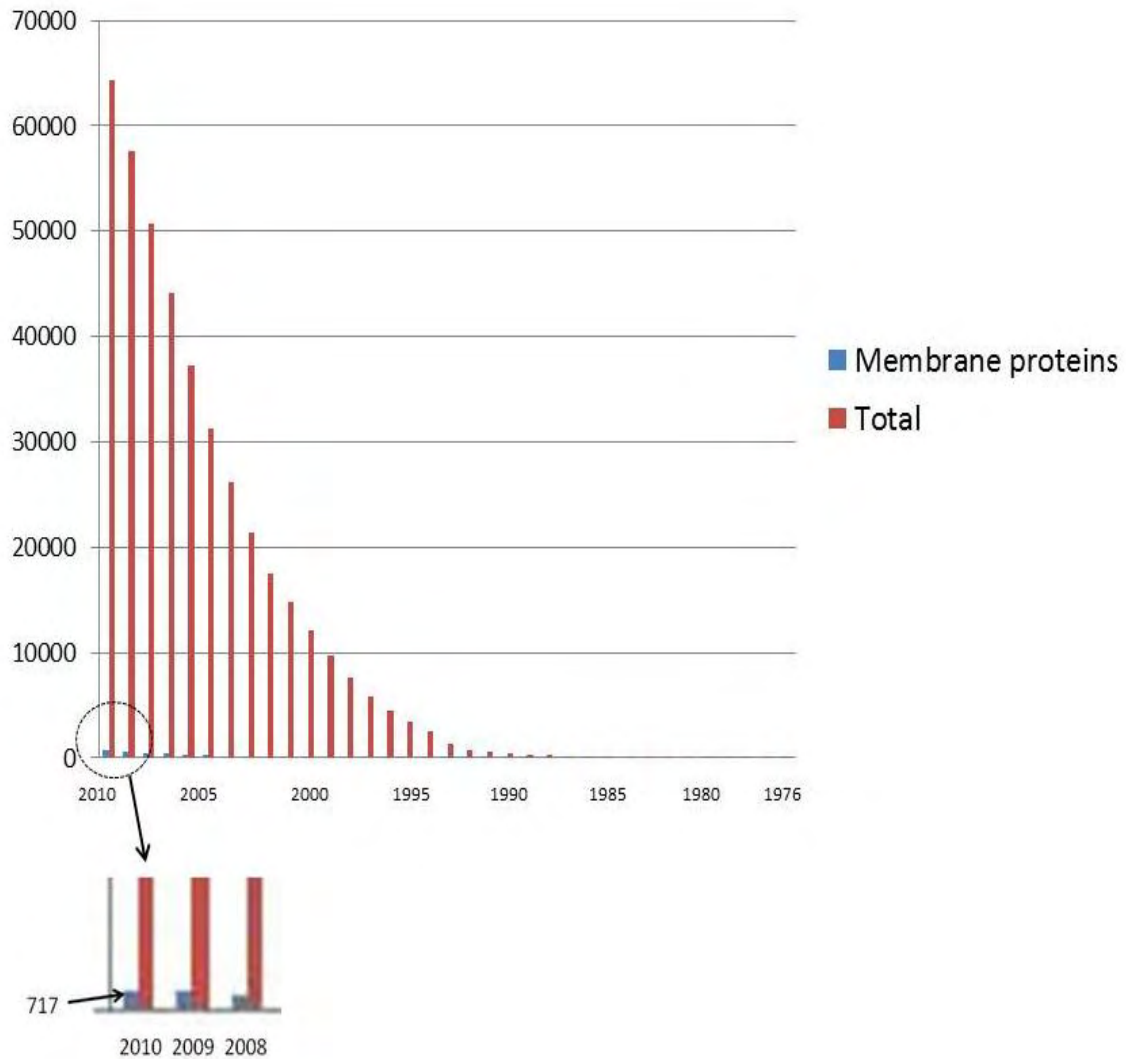


Figure 1-1. The chart shows the number of total protein structures (red) and membrane protein structures (blue) resolved from 1976 to 2010. The number of total protein structures is accumulated to ~ 65,000 in 2010, but the number of membrane protein structures is only 717. Within the figure of 717, it is noteworthy that only 261 represent truly unique membrane protein structures.



The main reason which makes membrane proteins extremely difficult to study is their low solubility in water, which leads to instability when extracted from the cell membrane. Moreover, only few membrane proteins are naturally abundant [8, 20]. This results in challenges at all levels including protein expression, purification and analytical study for membrane proteins.

In this chapter, we will describe the current challenges and review the current approaches for membrane protein study. We have also illustrated a novel system, styrene maleic acid lipid particle (SMALP), which offers a new route for membrane protein study. Furthermore, we describe two membrane proteins with different architectures and functions which we have successfully applied to this novel system, SMALP. The first, human adenosine 2a receptor ( $A_{2a}R$ ) contains 7 transmembrane helices and belongs to G-protein coupled receptors (GPCRs) family. The second, FtsZ-interacting protein A (ZipA) is a bacterial cell division protein that contains a single transmembrane domain.

## **1.2 Membrane Proteins and Lipids**

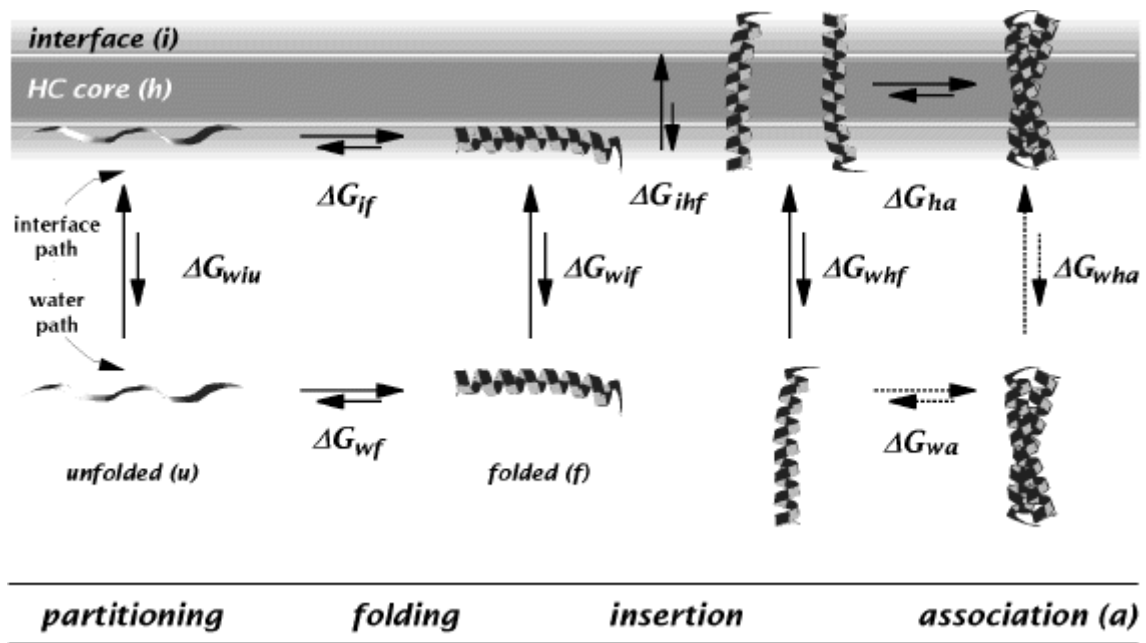
Membrane proteins can be classified to two main categories according to how easily they are removed from the membrane. The first, peripheral membrane proteins: as they can be isolated by changing the ionic strength or the pH. The second, integral membrane proteins: require

disruption of the membrane using chemical agents such as detergents [8]. Whichever extraction technique is used, it is clear that the removal from biological membrane has a significant influence on structure and function of membrane proteins. Phospholipids, sphingolipids and sterol are the main components found in the biological membrane [8]. Numerous reports have shown these lipids protect the hydrophobic regions of the membrane proteins, increase protein structural stability, control insertion and directly influence the function of membrane proteins [8, 12-17].

The lipids in a membrane can be classified into three types according to their positions and functions with respect to membrane proteins. The first, the bulk, forms the major part of the lipid bilayer which provides a special milieu for membrane proteins. The lipid bilayer is thought to provide a specific lateral pressure for membrane proteins [13, 14]. Moreover, the lipid makeup of a membrane also effects the folding of a membrane protein. Work by Booth *et al.* has shown that the lateral pressure of lipid bilayer influences the folding of a membrane protein [15, 16]. The second type of lipids is called the annular lipids; these lipids encircle and directly contact the proteins and have been thought to affect the function of membrane proteins [8]. In addition to the bulk and annular lipids, there is a third type of lipids called lipid cofactors. Lipid cofactors are often found bound tightly to a cleft or in between the subunits of the membrane proteins. These lipids are directly involved in the function of the

membrane proteins. For example,  $\text{Ca}^{2+}$ -ATPase requires phosphatidylinositol-4-phosphate and cholesterol for acetylcholine receptor [17, 18]. It is therefore clear that an ideal solution to the problem of membrane protein extraction would maintain these lipids around the chosen membrane protein.

Furthermore, White and Wimley proposed a four-step thermodynamic model to describe membrane protein folding (for  $\alpha$ -helix membrane proteins) including partitioning, folding, insertion and association (Figure 1-2) [19]. The hydrophobic side chain can provide enough free energy for partitioning. While the  $\Delta G$  (standard transfer free energy) of the partitioning of the folded peptide is smaller than (more negative) the partitioning of the unfolded peptide, the partitioning could induce the folding to  $\alpha$ -helix. The insertion of the  $\alpha$ -helix is affected by its rotational degrees of freedom and the space [8, 19]. Finally these helices assemble by packing together.



[19]

Figure 1-2. Four-step thermodynamic model for membrane protein folding.

The model describes the energetics of the partitioning, folding, insertion, and association of  $\alpha$ -helix. The process can go through an interface path, a water path, or a combination of both. The  $\Delta G$  symbol represents the standard transfer free energies. w= water, i = interface, h = hydrocarbon core, f = folded, u = unfolded, and a = association. For example, the standard free energy of transfer from water path to interface path of a folded peptide is represented as  $\Delta G_{wif}$  [19].

### **1.3 The Current Challenges and Approaches for Membrane Protein Study**

Membrane proteins have proved difficult to be investigated due to their natural low abundance and their amphipathic nature which tends to lead to aggregation in aqueous buffer [20]. In addition, the requirement to use detergent as an extraction agent from the cell membrane often leads to the stripping of lipids from the protein, can alter its activity. The imbedding of membrane proteins in lipids also limits the use of many techniques used for

further functional and structural studies [8, 20]. In this section, we describe current challenges in membrane protein study and recent approaches to membrane protein expression, purification and analytical studies. Figure 1-3 shows the standard flow chart of membrane proteins study from designing the primers to the characterisation of proteins.

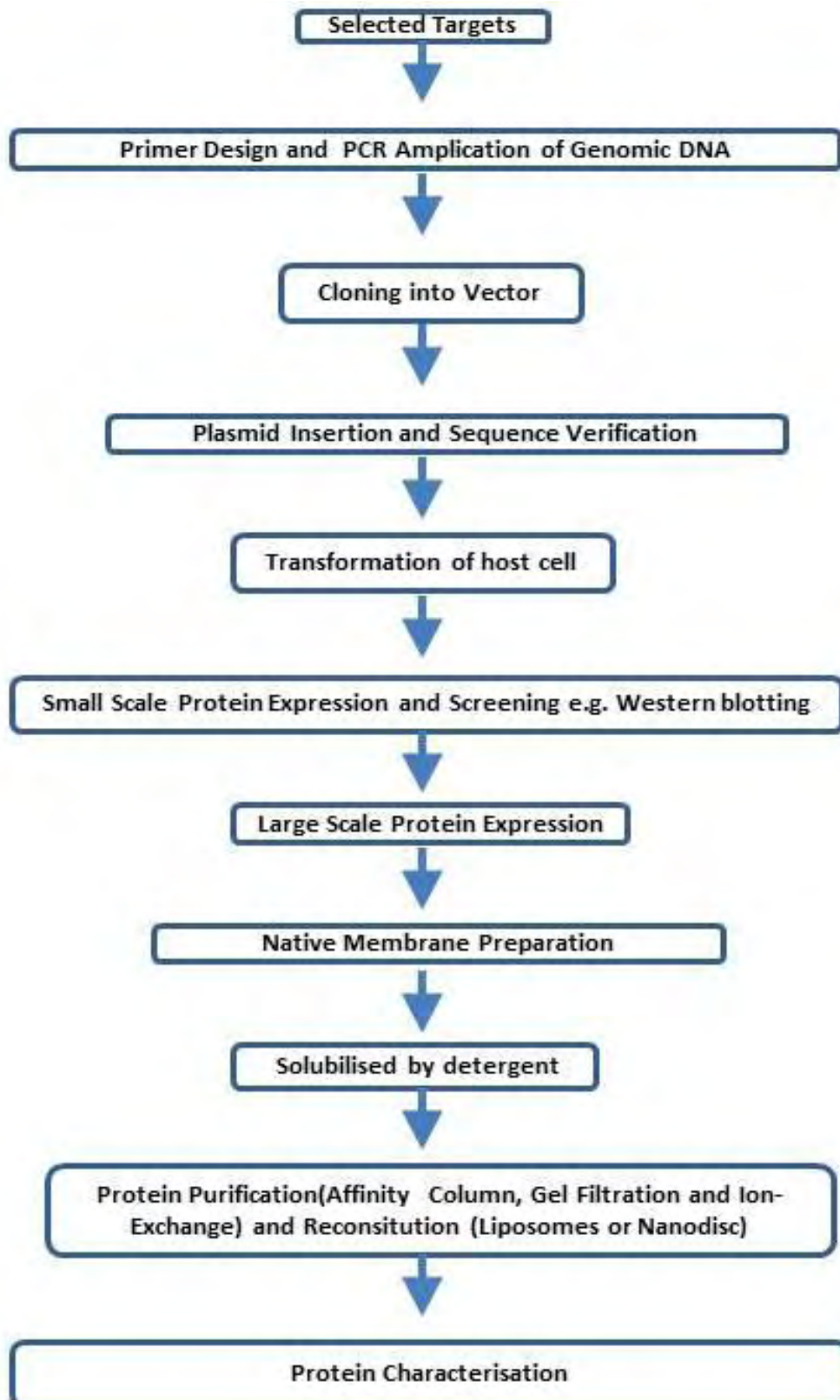


Figure 1-3. Flow chart showing the standard process of membrane proteins study from designing the primer to the characterisation of protein.

### **1.3.1 Membrane Proteins Expression**

The current challenges on expression of membrane proteins are mainly low protein expression yield, cellular toxicity, protein misfolding and aggregation. These result in a significant impact on the final purification yield and protein quality [11, 21]. To overcome these expression problems, it is important to choose the right expression system for each particular membrane protein [11]. Membrane proteins have been successfully expressed in several of expression systems, such as bacteria (e.g. *Escherichia coli* and *Lactococcus lactis*) [22-24], yeasts (e.g. *Pichia pastoris* and *Saccharomyces cerevisiae*) [25, 26], insect cells (e.g. *Baculovirus*) [27], mammalian cells [28], and cell free systems [29]. The proteins purified from these sources have been successfully used for functional and structural studies. Choosing a suitable expression system should consider several factors including the expression yield, post-translational modifications and the lipid composition of cellular membranes [21]. Furthermore, it should be understood that establishing an expression system to obtain the high quality and yield of membrane protein is usually difficult, therefore, it can take several months to a year to establish a satisfying expression system.

For example, expression of membrane proteins by bacterial cells such as *E. coli* is simple, quick, inexpensive, and a large number of constructs can be screened, however, most post-translational modifications of recombinant eukaryotic membrane proteins require eukaryotic

systems for protein expression [8, 12]. Moreover, membrane proteins are embedded in a complex and dynamic lipid bilayer, and the components of the lipids are different for bacterial and eukaryotic cells. Therefore, consideration should be given to the lipid composition when choosing an expression system for membrane proteins.

Additionally, in most of traditional eukaryotic culture systems, the protein yield is extremely low, e.g. the flask culture of yeast cells. This can be mitigated by using a bioreactor which maximises cell densities and hence increases the yield of the target protein. For example, the expression level of human adenosine 2a receptor ( $A_{2a}R$ ) is approximately 0.2 mg of protein per litre of flask culture. By growing  $A_{2a}R$  in a bioreactor results in up to 10 times biomass, therefore, the expression level per litre of bioreactor culture can be increased to 2 mg of protein. This level of protein is sufficient for many functional and structural studies [25, 30].

### **1.3.2 Membrane Protein Purification**

Membrane proteins can be purified by a range of chromatographic methods such as affinity column, ion-exchange and gel filtration. However, before application to a chromatography column, for membrane proteins, the first step is to remove proteins from their cell membrane using a chemical agent such as detergent. Unfortunately, this step often leads proteins to lose their native function. This issue can sometimes be mitigated by the addition of specific lipids



during the purification which stabilise membrane proteins and maintain their activity. For example, the presence of cholesterol can increase the activity of some mammalian membrane proteins [11, 21, 31-33]. In addition, temperature and pH are also important factors for the stability of purified membrane proteins, most of purified membrane proteins are stable at 4°C, pH 6 - 8. Additions of glycerol and protease inhibitors can also stabilise these purified membrane proteins [20]. Furthermore, once the complex process of purification has been completed, many functional and structural studies of membrane proteins require the reinsertion of the purified membrane protein into a mimic native membrane environment, termed model systems. Achieving this process in the presence of detergent presents a larger challenge than the purification itself. Here, we illustrate a number of current methods for producing of membrane proteins including using detergents and model systems.

#### *Current Methods for Studying Membrane Proteins: Detergents and Model Systems*

There are a wide range of methods in the literature that use detergents and several model systems, such as the use of liposomes, amphipols, nanodiscs, and bicelles which allow membrane protein study *in vitro* in a native-like membrane environment [8-10, 35-37].

Detergent is the most common tool to extract membrane proteins from their cell membranes and prevent protein aggregation [20]. However, detergents also remove lipids from membrane proteins resulting in loss of its biological activity. Inserting proteins into a model

system can provide proteins a native-like membrane environment for their structural and functional studies [8].

### Detergents

Detergents are amphiphilic molecules and water soluble surfactants, these have been widely used to solubilise membrane proteins in aqueous solutions [8]. A variety of detergents have been used to solubilise membrane proteins, including ionic detergents such as sodium dodecyl sulfate (SDS) and cetyltrimethylammonium bromide (CTAB) and non-ionic detergents: Triton X-100, octyl  $\beta$ -D-glucoside (OG) and n-dodecyl- $\beta$ -D-maltoside (DDM) [148, 149]. Ionic detergents bind to the hydrophobic parts of membrane proteins disrupting ionic and hydrogen bonds due to their charge. Some ionic detergents, such as SDS usually denature proteins by binding to each side chain. Non-ionic detergent, for example, Triton X-100 has aromatic ring that interferes with some biophysical studies such as circular dichroism (CD) [8]. So far, **no single** detergent has been shown to be satisfactory for all membrane proteins. It is therefore an essential and time-consuming part of the purification process to test several different detergents and select an effective solubilising, non-denaturing detergent prior to use [20].

The mechanism of most detergent to solubilise membrane protein involves micelle formation [20]. The solubilisation action of membrane proteins by detergents is strongly related to the critical micelle concentration (CMC). Below the CMC (low concentration), detergent penetrates the lipid bilayer but does not form micelles. As the concentration increases above the CMC (high concentration), the detergent disrupts the bilayer and results in mixed micelles (Figure 1-4) [8, 150]. Detergent micelles are commonly used for study membrane proteins, although they lack a lipid bilayer [47, 151]. Maintaining the micelles structure, however, requires careful control of the experimental conditions within narrow limits, and this is often not possible during the purification and further biophysical studies of membrane proteins.

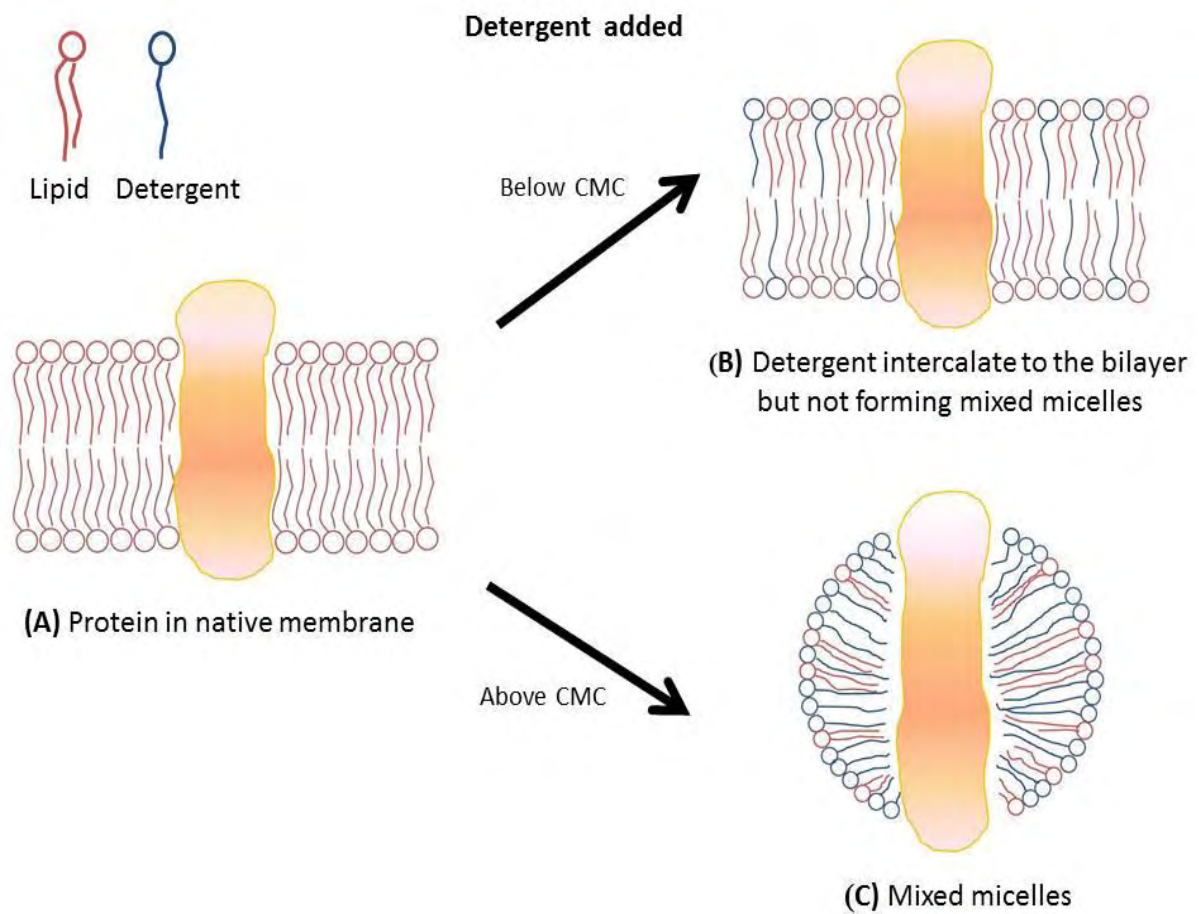


Figure 1-4. Solubilisation of membrane proteins by detergents. Detergents are used to solubilise membrane protein from their cell membrane. (A) Initially, the membrane protein is in the native membrane. (B) While low concentration of detergent is added (lower than CMC), some detergent molecules bind to the membrane without forming mixed micelles. (C) As more detergent is added (higher than CMC), it leads to the formation of mixed micelles containing the protein, lipids and detergent molecules.

Model systems: Liposomes, Amphipols, Nanodiscs and Bicelles

1. Liposomes

Liposomes are the most common model systems used in membrane proteins studies. A liposome is a closed spherical vesicle containing an aqueous core enclosed in lipid layer [37, 152]. Liposomes can be classified as multilamellar vesicles (MLVs) contain an “onion” like arrangement of membrane layers and unilamellar vesicles containing a single bilayer (Figure 1-5) [153]. Unilamellar vesicles are also classed by size including small unilamellar vesicles (SUVs), large unilamellar vesicles (LUVs) and giant unilamellar vesicles (GUVs) [154-157].

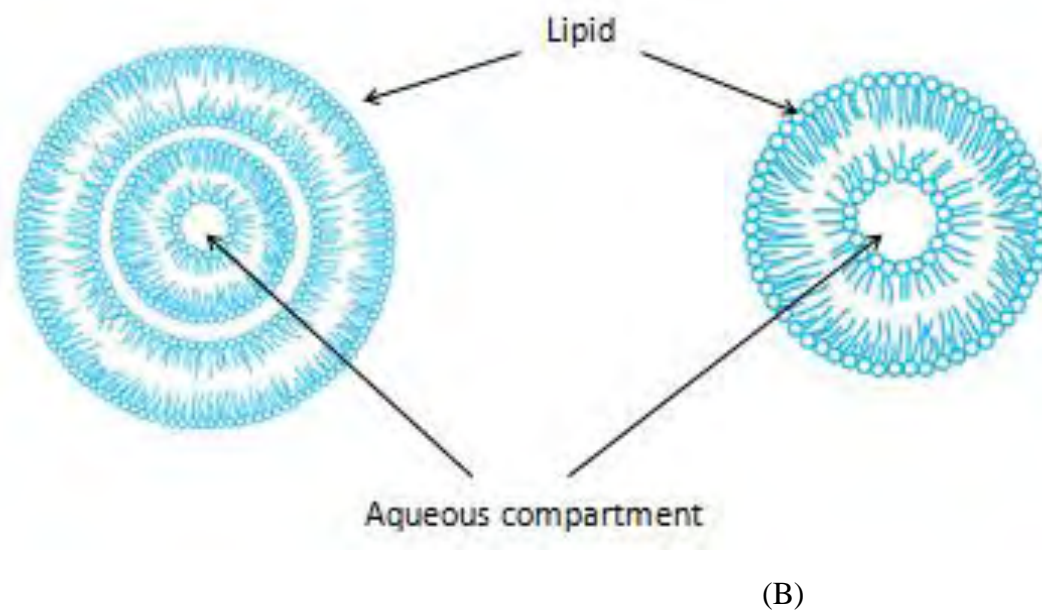


Figure 1-5. Different type of liposomes

Liposomes can be classified to two major types depending on whether they have single or multi bilayers.

(A) Multilamellar vesicles (MLVs): the size is up to 10  $\mu\text{m}$ . (B) Unilamellar vesicles include SUVs, LUVs, and GUVs and the size varies from 20 nm to 300  $\mu\text{m}$ .

MLVs can be prepared by simply shaking a dried lipid within an aqueous solution and have been previously used in many enzyme and peptide binding studies. SUVs are vesicles with a diameter of 20 ~50 nm and can be easily made by sonicating MLVs [8, 34]. Although SUVs are very simple to prepare, it is often difficult to incorporate proteins due to the excessive bilayer curvature. LUVs (diameters between 100 nm and 5  $\mu\text{m}$ ) can be prepared from induced fusion of SUVs by freeze-thaw cycles. LUVs have more encapsulated lipid and a lower curvature than SUVs, but also are fragile and often have a heterogeneous size distribution [8, 34]. GUVs can be prepared by different methods, including the use of Teflon disks (§ 2.5.7), LUVs fusion or Electroformation - Pt Wire [34]. In general, GUV preparation is more complicated than preparation of SUVs and LUVs. GUVs are very large vesicles with diameter between 5  $\mu\text{m}$  to ~300  $\mu\text{m}$  and hence have a very low surface curvature, they can also be visualised by optical microscopy, however, the large size also makes them very fragile [8]. Table 1-1 summarises the advantages and disadvantages of the methods for GUVs preparation.

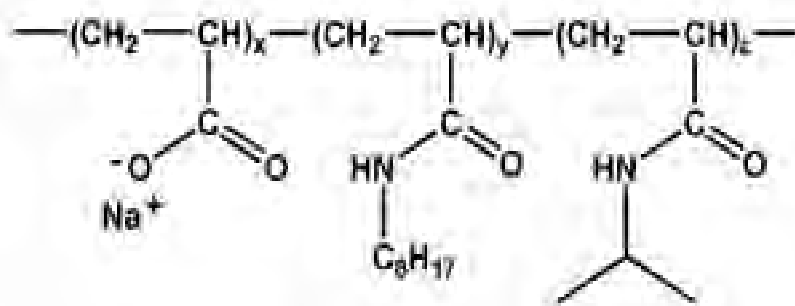
<b>Teflon disk</b>	
Advantages	Most of the GUVs are unilamellar
Disadvantages	It is hard to remove vesicles from the substrate surface
<b>LUVs fusion</b>	
Advantages	Very simple method
Disadvantages	The size of GUVs is relatively small, ~10 $\mu\text{m}$
<b>Electroformation - Pt Wire</b>	
Advantages	GUVs size is well controlled
	GUVs are unilamellar
Disadvantages	Only a few GUVs can be prepared per experiment since only small amounts of lipids can be used for each sample
	Requires many hours to clean the chamber

Table 1-1: Advantages and disadvantages of different methods for GUVs preparation

## 2. Amphipols

Amphipols are amphipathic polymers that allow membrane proteins to be solubilised in aqueous solutions (polymers with strongly hydrophilic backbone and grafted with hydrophobic chains) [35, 36]. These amphipathic polymers are short chain polymer, which must be flexible, highly soluble in water and also able to be adsorbed onto the hydrophobic transmembranes segments of membrane proteins. They can retain the lateral pressure of membrane proteins, increase protein stability and maintain their native state [37]. There are several amphipathic polymers that have been used for the study of membrane proteins so far,

these include A8-35 and PC-amphipol [36-39]. A8-35 is the most studied amphipol since it has been developed by Tribet *et al.* in 1996 (Figure 1-6). It has been applied to numerous membrane proteins including GPCRs [35, 36, 40, 41]. Although useful, the major drawback of these polymers is their requirement of detergent usage to solubilise the target proteins from their cell membrane before being added the polymer [37].



[35]

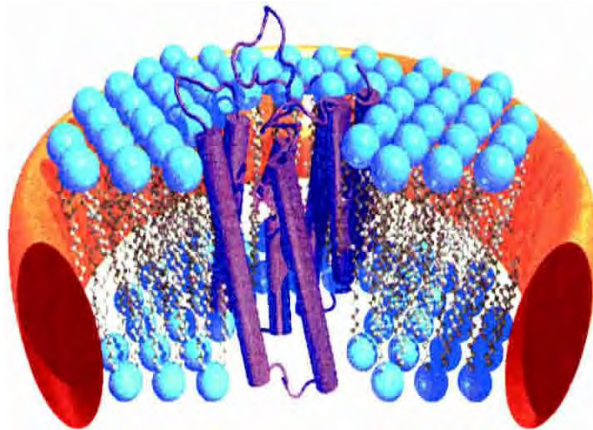
Figure 1-6. A8-35: the most studied amphipathic polymer used for membrane protein studies.

### 3. Nanodiscs

Nanodiscs are a novel model system for supporting membrane proteins during studies which has been developed in the last decade. It is proposed that membrane proteins incorporated into nanodiscs may avoid the aggregation and purification problems associated with other systems [9, 10]. The nanodisc is a 10 nm diameter disc structure composed of phospholipids and membrane scaffold proteins (MSPs) (Figure 1-7). In order to incorporate membrane proteins to nanodiscs, the membrane protein of interest is first solubilised in a detergent such



as Triton X-100. The mixture of MSPs stock solution and lipid are then added into the sample. The detergent is removed and the protein can be purified using a general purification procedure. The nanodisc contains the purified target protein which can then be used to further analytical studies. In practice, MSPs may interfere with some analytical investigations, for example their proteinaceous nature means that they have disruptive signals in techniques such as CD [9, 42].



[9]

Figure 1-7. Model of a nanodisc (cutaway view)

The nanodisc is a nanometer scale soluble bilayer structure which consists of phospholipids (blue) and encircled by a 200 amino acid scaffold protein (orange) containing the target protein (purple) [9].

#### 4. Bicelles

Bicelles are self-assembled disc-like structures which are usually made of two lipids. Bicelles can be formed from phospholipids which contain the combinations of head-group/acyl chain that favour the form of the curved bilayers, for example, the mixtures of 1,2-Dihexanoyl-sn-Glycero-3-Phosphocholine (DHPC) and 1,2-Dimyristoyl-sn-Glycero-3-Phosphocholine (DMPC). The diameter of the bicelle is usually between 5 - 40 nm depending on the DMPC:DHPC ratio (Figure 1-8) [43-46]. Previous study on bicelles has shown that biophysical studies of membrane proteins can be performed on this system [46]. This system, however, still requires using detergents to solubilise the membrane proteins from their biological membranes. Table 1-2 summarises the advantages and disadvantages of these current methods for membrane proteins study.

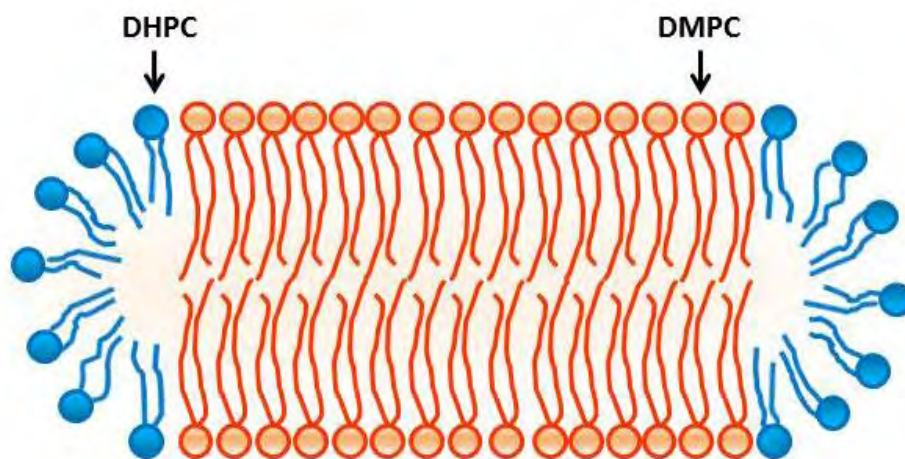


Figure 1-8. Cross section representation of the central planar bilayer of a bicelle.

The bicelle is formed by the long-chain phospholipid (DMPC) and it is surrounded by the of short-chain phospholipid (DHPC) that protects DMPC hydrophobic tails from water [46].

<b>Detergents</b>	
Advantages	Size homogeneity
Disadvantages	Lateral pressure is decreased
	Detergent sometimes leads to activation of unfolded protein
	Native lipid is disrupted
	Concentrations below CMC results in membrane protein aggregation
<b>Liposomes</b>	
Advantages	Provide native lipid environment
	Maintain lateral pressure
Disadvantages	Size heterogeneity
	One side of the membrane protein is inaccessible to the bulk solvent
	Requires detergent solubilisation of membrane protein prior to formation
<b>Amphipols</b>	
Advantages	Size homogeneity
	Maintain membrane lateral pressure
Disadvantages	Requires detergent solubilisation of membrane protein prior to formation
<b>Nanodiscs</b>	
Advantages	Size homogeneity
	Provide native lipid environment
	Maintain lateral pressure
Disadvantages	Membrane scaffold proteins (MSPs) may interfere with the functional and structural studies
	Require detergent solubilisation of membrane protein prior to formation
<b>Bicelles</b>	
Advantages	Suitable for many biophysical studies of membrane proteins
Disadvantages	Require detergent solubilisation of membrane protein prior to formation
	Limited choice of lipid combinations

Table 1-2: Advantages and disadvantages of detergents and model systems for membrane protein studies.

### 1.3.3 Analytical Studies

To study the native structure and function of membrane proteins *in vitro*, membrane proteins are generally prepared in the detergent micelles or in the model systems such as those discussed above. However, **no single** system has been universally satisfactory for all techniques used to characterise membrane proteins. This is mainly due to interference with the signals produced by the subsequent analytical studies. In addition, maintaining the protein in the micelles or a model system requires careful control of experimental conditions (e.g. pH and temperature) [8, 20], within narrow limits and it is often not possible to achieve this during the subsequent analytical studies. Therefore, different detergents or model systems are often required for different functional and structural studies of the same membrane protein. Table 1-3 summarises current hurdles for membrane protein studies.

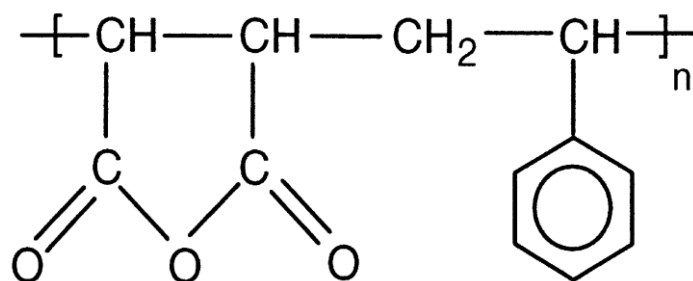
<b>Expression</b>	Most membrane proteins are naturally low in abundance
	Tend to aggregate
<b>Purification</b>	Need to solubilise using detergent
	Need insertion to a model system to maintain their native structure and function for further study
	Low yields
<b>Analytical Study</b>	Detergents and model systems may interfere with the signals of analytical studies
	Rapid degradation, and aggregation

Table 1-3. A summary of current hurdles for membrane protein studies.

#### **1.4 A Novel Membrane Protein Study Method: Styrene Maleic Acid Lipid Particles**

As described above, many methods have been used to produce monodispersed preparations of membrane proteins. These include the use of the detergent micelles and the model systems. However, all these methods require the use of detergents to solubilise proteins from the cell membrane, and hence the stripping away of their native lipids. Furthermore, no single method has been universally satisfactory to study and characterise these membrane proteins. It is therefore important to develop a novel system which can be used to produce membrane proteins, ideally keeping them in their native environment without adding any detergents as well as being suitable for most techniques used to characterise membrane proteins.

Styrene maleic anhydride polymer is an anionic hypercoiling polymer (Figure 1-9) [48]. The only anionic polymers that have been found to hypercoil are polyacids containing carboxylic acid pendant groups either in the form of acrylic acid or maleic anhydride (requires hydrolysing to maleic acid). Styrene pendant groups provide a hydrophobic moiety, which together with maleic acid form a hypercoiling polymer [48].



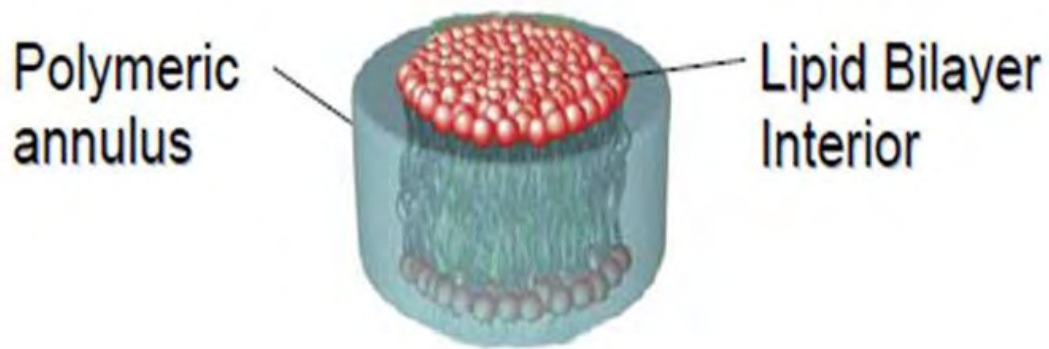
[48]

Figure 1-9. Styrene maleic anhydride

Prior to use, maleic anhydride requires hydrolysing to maleic acid. Styrene pendant groups provide a hydrophobic moiety and together with maleic acid they form a hypercoiling polymer [48].

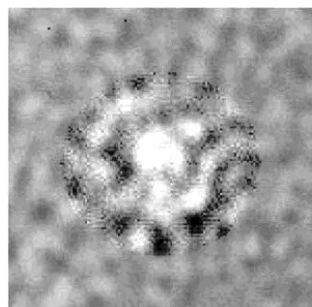
In the presence of lipids, styrene maleic acid (SMA) polymer self assembles to form a polymer-lipid nanostructure (Figure 1-10) [48,158]. This lipid-polymer nanostructure disassociates at pH 4 due to the pH-dependence of the ionization of the maleic groups within the polymer (Figure 1-11) [158]. The polymer-lipid particle is formed again when pH increases to 8. This polymer-lipid nanostructure was termed “Lipodisq” and it has been

developed by Malvern Cosmeceutics Ltd for use in hydrophobic pharmaceutical delivery systems [49].



[158]

(A)



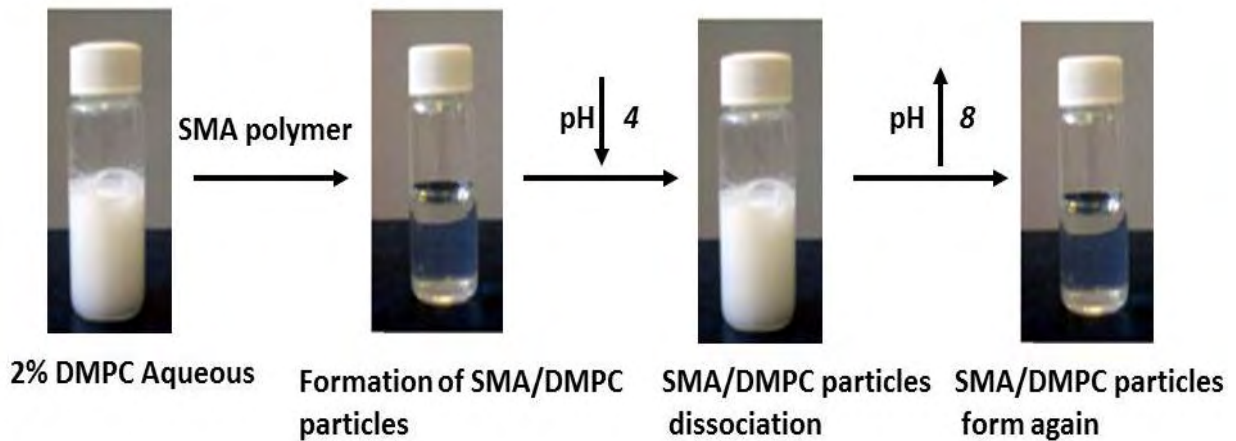
[48]

(B)

Figure 1-10.

(A) The cartoon of styrene maleic acid/DLPC (lipid)

(B) Cryo-TEM electron micrograph (x 120,000) of styrene maleic acid/DLPC particles. The diameter of this nano-disc structure is 10 nm [48].



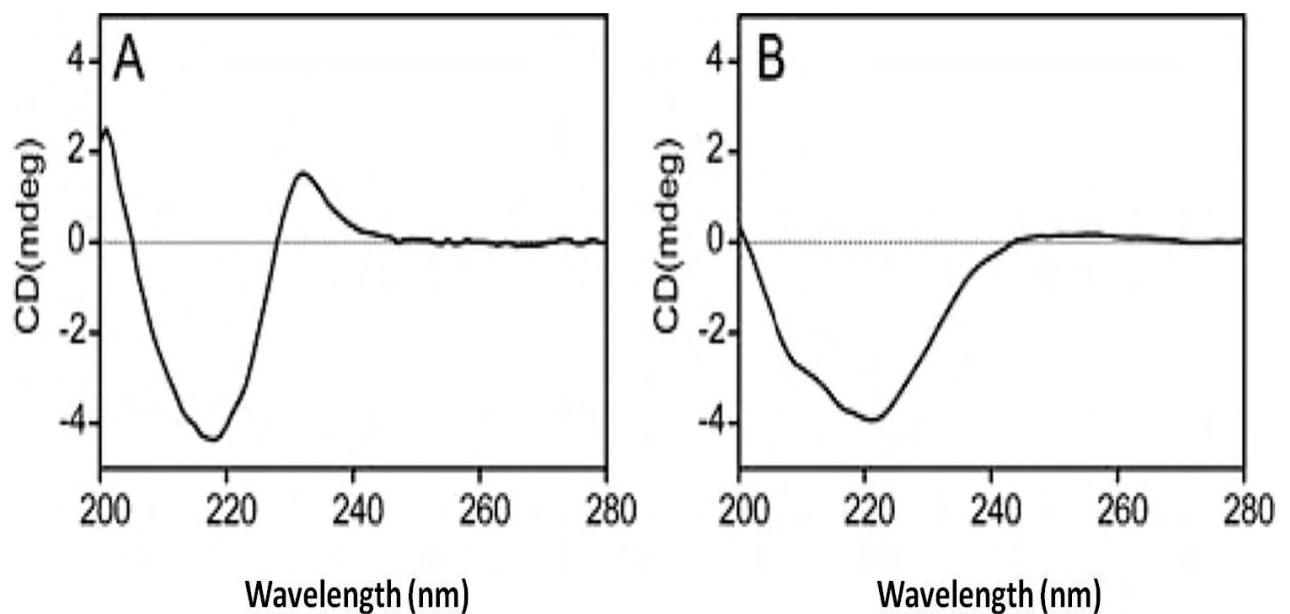
[158]

Figure 1-11. The addition of SMA polymer into a 2% lipid (1, 2-dimyristoyl-glycero-3-phosphocholine, DMPC) aqueous solution, makes it form SMA/DMPC nanostructure and hence becomes clear. This lipid-polymer nanostructure disassociates at pH 4. The SMA/DMPC nanostructure forms again when pH increases to 8.

Knowles *et al.* have recently applied this SMA/lipid nanoparticle system, termed SMALP, to bacterial membrane proteins, PagP and bacteriorhodopsin (bR) [49]. The empty SMALP has been shown with average  $9.0 \pm 1.1$  nm diameter estimated by dynamic light scattering (DLS). The size of SMALP was slightly larger when PagP was incorporated into SMALP, with an average diameter of  $11.2 \pm 1.4$  nm as estimated by DLS. It is clear that SMALP is flexible and may be able to incorporate with different architectures of proteins. Additionally, the subsequent biophysical experiments the proteins have shown proteins were folded, thermostable and active. For example, CD spectroscopy has shown that proteins were

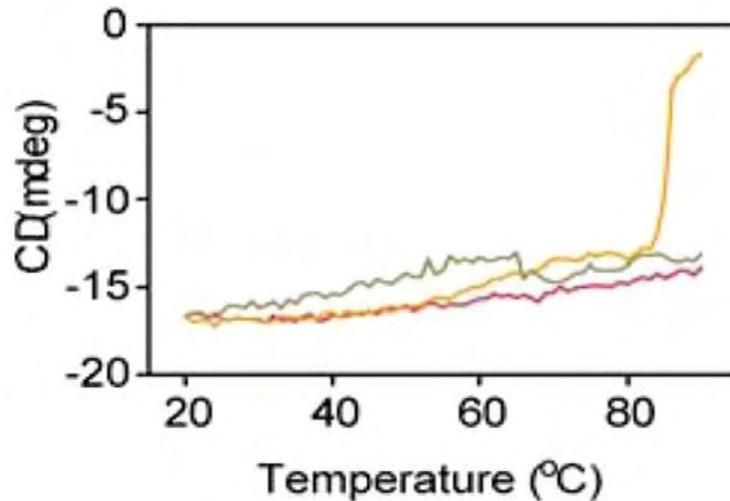


correctly folded within SMALP and more thermostable than protein within detergent (Figure 1-12) (Figure 1-13) [49].



[49]

Figure 1-12. Far UV CD of (A) purified SMALP-PagP and (B) purified SMALP-bR. Both of samples showed a folded structure. The CD spectrum of purified SMALP-PagP showed a minimum at 218 nm and shoulders at 222 and 208 nm, consistent with the expected  $\beta$ -barrel and  $\alpha$ -helical structures. The CD spectrum of purified SMALP-bR showed a minimum at 222 nm and shoulder at 208 nm, consistent with the expected high  $\alpha$ -helical components [49].



[49]

Figure 1-13. CD spectrum of the thermal stability experiment. 218 nm CD unfolding profiles for PagP in SMALP (grey line), liposomes (red line), and detergent ( $\beta$ -octylglucoside, ( $\beta$ -OG)) (orange line). The data showed  $\beta$ -OG-PagP denatured at 84°C, both purified SMALP-PagP and liposomes-PagP maintained fold state at 84°C. It showed that PagP in SMALP offers corresponding stability to liposomes-PagP and a better stability to detergent-PagP [49].

These preliminary studies showed that SMALP offers a solution to preserve the integrity of transmembrane proteins and form a thermostable and soluble nanoparticle which is suitable for their biophysical studies in the lipid environment. It is clear that SMALP may provide a solution to other more challenging membrane proteins, such as G-protein coupled receptors.

## **1.5 Target Protein Selection: Human Adenosine 2a Receptor, a GPCR**

### **1.5.1 G-Protein Coupled Receptors**

The G-protein coupled receptors (GPCRs) are the largest family of membrane proteins in the human genome with over 1000 unique members, and have been shown to have vital roles in maintaining normal function in humans [50, 51]. These proteins are implicated in diverse acute and chronic diseases ranging from HIV infection to Parkinson's disease. GPCRs are integral membrane proteins, embedded within the cellular plasma membrane with 7 transmembrane helices linked by extracellular and intracellular loops [52].

GPCRs bind to a wide variety of extracellular ligands including peptides and small molecules. The receptors are activated by agonists while neutral antagonists prevent activation by agonists. In addition to agonists and neutral antagonists, a third type of ligand, the inverse agonist, reduces the activity of GPCRs by inhibiting their constitutive activity [12, 52]. The neutral antagonist "blocks" the action of the agonist or inverse agonist without altering the existing conformation of the receptor. Agonist-activated receptors undergo a conformational change which results in their intracellular interaction with G-proteins which are involved in downstream cellular signalling [12, 52]. These G-proteins are trimers made of  $\alpha$ ,  $\beta$ , and  $\gamma$  subunits (known as  $G\alpha$ ,  $G\beta$ , and  $G\gamma$ ) (Figure 1-14). Moreover, GPCRs also interact with other proteins apart from G-proteins, in particular,  $\beta$ -arrestin, can bind to

phosphorylated GPCRs, and prevent further coupling of the receptor to G protein [53].  $\beta$ -arrestin is thought to play an important role in agonist-mediated desensitisation of GPCRs, and leads to the mitigation of cellular responses to stimuli such as hormones, neurotransmitters, etc. (Figure 1-15) [54-56,160].

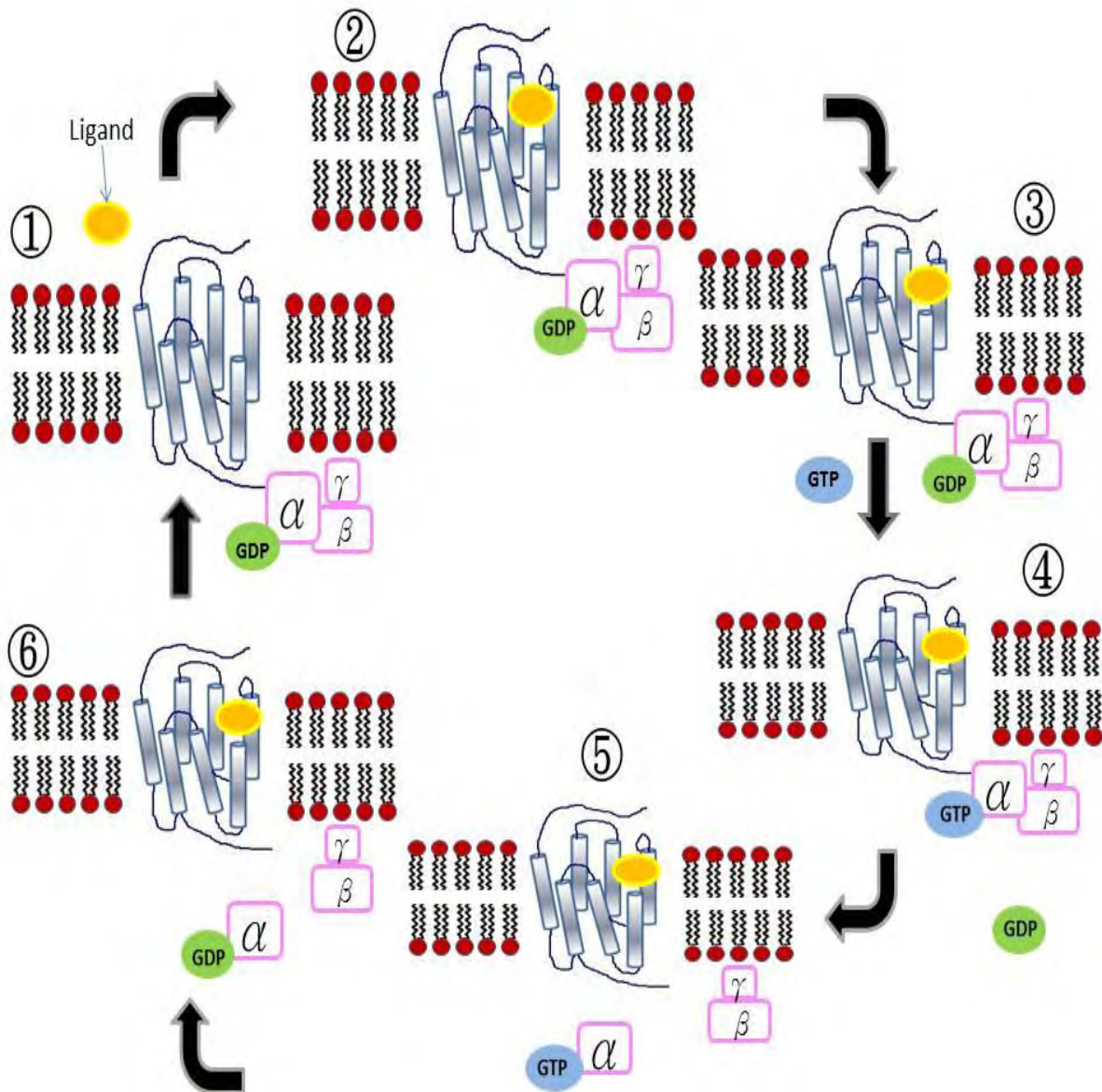


Figure 1-14. GPCRs signalling pathway.

(1) Ligand (agonist) does not bind to the receptor. (2) Ligand binds to the receptor which causes a conformational change of the receptor and results in activation of the trimeric G-protein. (3) and (4) GDP is released and GTP binds to the trimeric G-protein. (5) While GTP binds to the trimeric G-protein, the G-protein dissociates into two parts, G alpha and G betagamma. (6) The GTP has been hydrolysed to GDP and Pi by the GTPase activity of the alpha subunit, the separated two parts of the G-protein can recombine again and restart a new signalling cycle (back to(1)) [159].

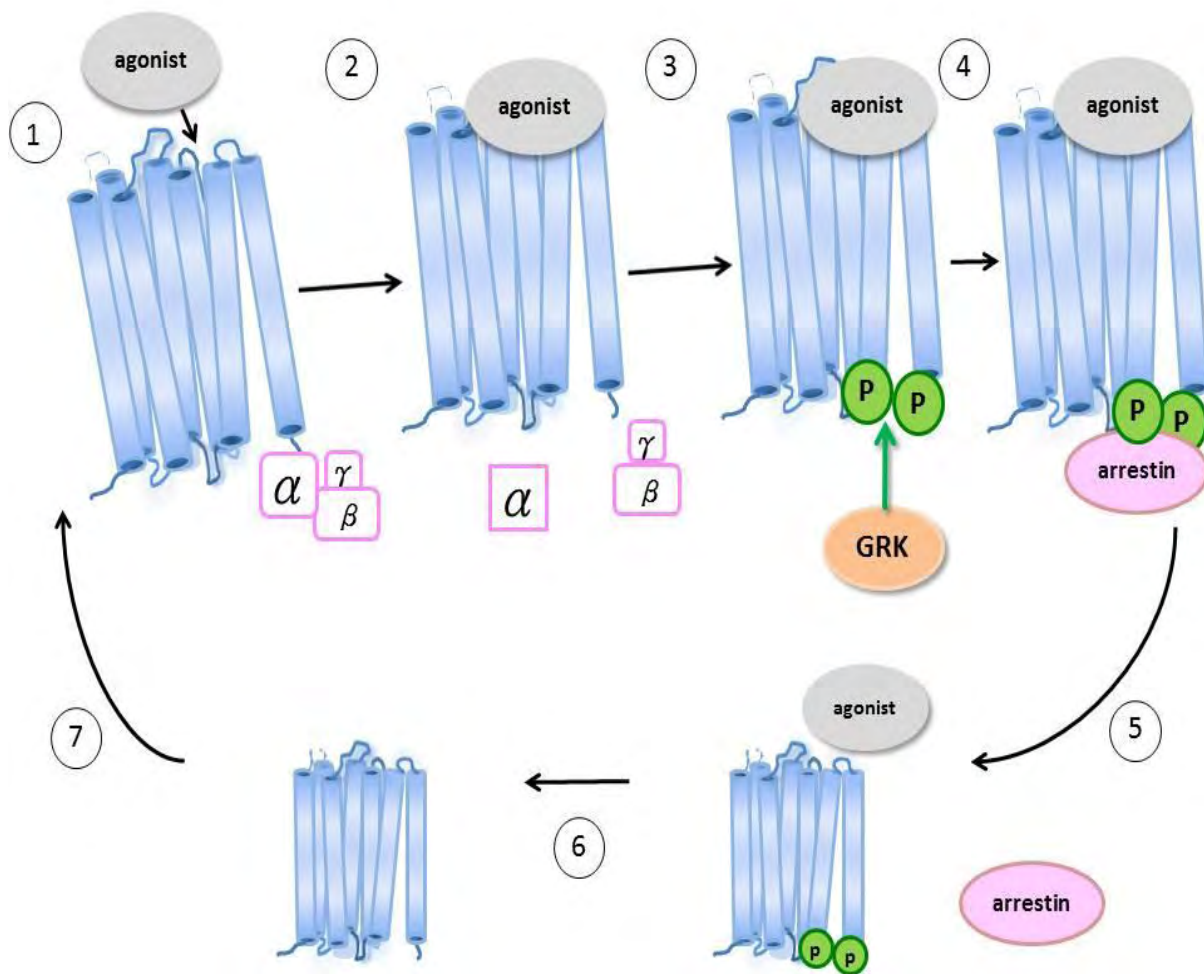


Figure 1-15. (1) The GPCR is activated by agonist. (2) The G-protein dissociates into two parts, G alpha and G betagamma (see above, Figure 1-14). (3) The receptor is phosphorylated by a G protein-coupled receptor kinase (GRK). (4)  $\beta$ -arrestin can bind to phosphorylated GPCR, which prevents further coupling of the receptor to G protein (desensitisation) (5) Internalisation and (6) dephosphorylation. (7) The receptor is ready for the new cycle (back to (1)) [160].

GPCRs are central to cellular signalling and thus these receptors have emerged as desirable targets for the pharmaceutical research. In fact, approximately 40% of pharmaceuticals on the market are targeted to GPCRs [2]. However, merely six crystal structures of GPCRs have been discovered in this largest class of membrane proteins: rhodopsin,  $\beta$ 2-adrenoceptor,  $\beta$ 1-

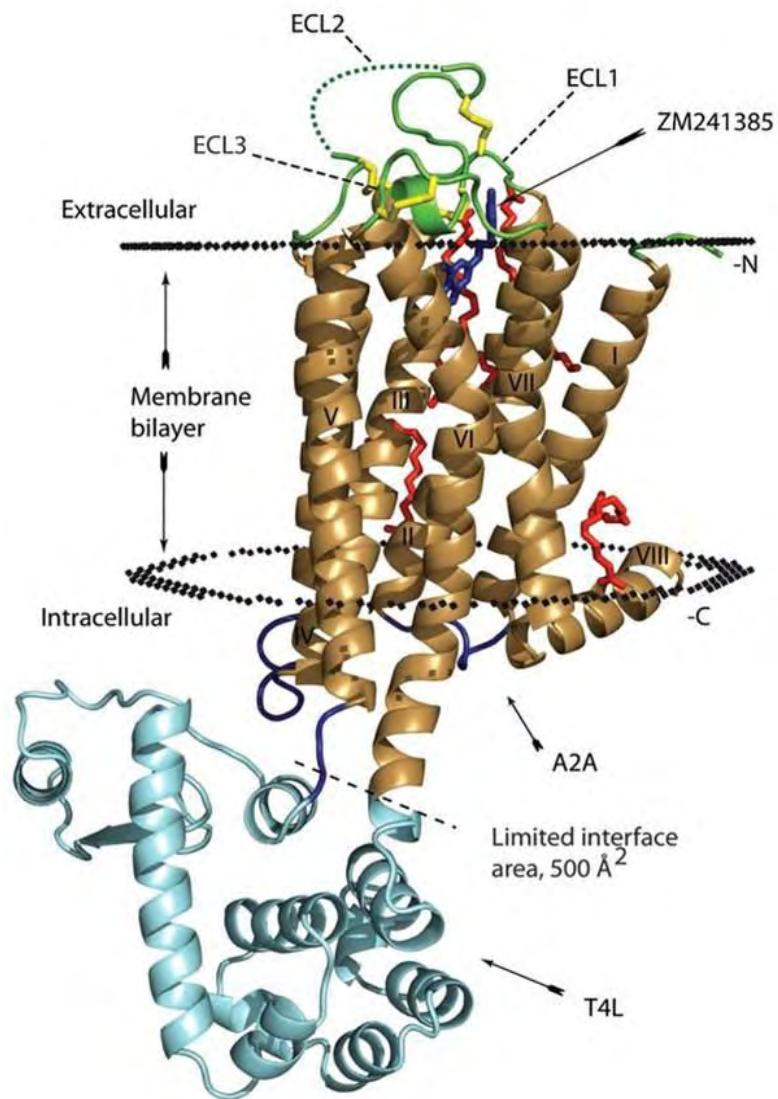
adrenoceptor, A<sub>2a</sub>R adenosine receptor, CXCR4 chemokine receptor and Dopamine D3 receptor [57-63]. The first crystal structure of GPCR was rhodopsin, it is a molecule of the retina which is responsible for light detection. Rhodopsin consists of the opsin apoprotein and the 11-*cis*-retinal. It is activated while light causes photoisomerisation of the 11-*cis*-retinal (the inverse agonist of the receptor) to all-*trans*-retinal (an agonist of rhodopsin). This makes the protein “inflexible” as it is held in an inactive state bound to 11-*cis* retinal [58]. In other cases, receptors had been “locked” by binding to an antagonist or plus other modifications. For example, the A<sub>2a</sub>R is bound to its antagonist ZM241385, and for the β<sub>2</sub>-adrenoceptor, intracellular loop 3 is replaced with T4 lysozyme [57, 60]. Although it became possible to obtain GPCRs crystal structure in the last decade, however, it is still a big challenge to obtain the crystal structure of GPCRs without any modifications.

### **1.5.2 Human Adenosine 2a Receptor**

Adenosine receptors play an essential role in local regulatory processes in humans such as control of cerebral blood flow and respiration. Four subtypes of human adenosine receptors have been identified (A<sub>1</sub>R, A<sub>2a</sub>R, A<sub>2b</sub>R, and A<sub>3</sub>R) [64-66]. The human adenosine 2a receptor (A<sub>2a</sub>R) is a GPCR and one of adenosine receptors found in humans. Until today, the first and the only crystal structure of human adenosine receptors is A<sub>2a</sub>R, which was solved by Jaakola *et al.* in 2008 (Figure 1-16) [57].

$A_{2a}R$  binds to ligands present in the extracellular domain and then changes shape leading to the activation of an intracellular G-protein. This activation has been summarised in a two-state model. State one represents the active state and state two represents the inactive.  $A_{2a}R$  is activated by agonists such as 2-chloroadenosine, and blocked by antagonists such as caffeine [161].  $A_{2a}R$  is abundant in polymorphonuclear leukocytes, blood vessels, and platelets.  $A_{2a}R$  is found in high concentrations in the central nervous system and is expected to have a therapeutic effect in central nervous system (CNS) disorders such as Parkinson's disease [67]. Clinical evidence suggests that coffee drinkers have a lower risk of Parkinson's disease [68]. Therefore, understanding the binding mechanism of  $A_{2a}R$  with its ligands and obtaining  $A_{2a}R$  crystal structure without any modifications should help drug discovery for these diseases.





[57]

Figure 1-16. Human adenosine 2a receptor bound to an antagonist (ZM-241385). The resolution of the structure is  $2.6\text{\AA}$ . The third cytoplasmic loop of the receptor was replaced with lysozyme from T4 bacteriophage. In addition, the C-terminal tail (Ala317–Ser412) was removed to improve the likelihood of crystallization. The transmembrane domain of  $A_{2a}R$  is colored brown (helices I to VIII), and the T4L is in cyan. ZM241385 is colored blue. Five lipid molecules bound to the receptor are in red, and four disulfide bonds are colored yellow. The intracellular loops are colored blue, and the extracellular loops are in green. PDB identifier: 3EML [57].

## **1.6 Target Protein Selection: FtsZ-Interacting Protein A, a Bacterial Cell Division Protein**

### **1.6.1 Bacterial Cell Division Proteins**

Cell division is the critical mechanism by which a cell divides into two or more daughter cells in all living organism. In prokaryote cells, cell division occurs by a process called binary fission which starts with DNA replication. The single, circular DNA replicates by semiconservative replication. The chromosome replicates resulting in two identical chromosomes. The actual physical division process then proceeds. The cell elongates, two identical chromosomes separate into daughter cell [12]. In the *E. coli* cells, several cell division genes have been identified in temperature-sensitive mutants these have been named Fts genes, filamentous temperature sensitive. Fts genes such as FtsA, FtsB, FtsL, FtsI, FtsQ, FtsN, FtsW, FtsK and FtsZ are believed to be involved in cell division [69-71].

Apart from the Fts proteins there are also more than 5 other proteins have been identified that play a role during cell division of *E. coli* cells [72-74]. The protein encoded by FtsZ gene is called FtsZ protein, the first protein appears at the division site (in the middle of the bacterial cell) where FtsZ protein assembles into FtsZ-ring (§ 1.6.2, symbol § represents “describe in”). In the last decade, numerous pieces of evidence have suggested FtsZ-ring drives cell division by which FtsZ-ring creates enough force in constricting the cytoplasmic membrane [72-75].

Two proteins, ZipA and FtsA, are important for formation of FtsZ-ring by directly interacting with FtsZ [75]. ZipA is an integral inner-membrane protein (§ 1.6.3). FtsA, although a cytoplasmic protein, has been found to contain an amphipathic helix that forms a labile anchor to the membrane [76]. It has been observed that the FtsZ-ring can form while either ZipA or FtsA protein is absent, however, FtsZ-ring can not form if both of proteins are absent [75]. Another protein, ZapA, has also been shown to be an FtsZ binding protein that can stabilise FtsZ-ring [77].

The localisation of FtsZ-ring is regulated by three proteins, MinC, MinD and MinE. These three proteins prevent the formation of FtsZ-ring away from the mid-cell (Figure 1-17) [78, 162]. MinC has been shown to inhibit the formation of FtsZ-ring and is found at its highest concentration at the poles and the lowest at mid-cell [79, 80]. MinC is active only while bound to MinD as free MinC remains in the cytoplasm and is unable to prevent FtsZ assembly. MinD belongs to a family of bacterial ATPase that binds to the membrane by its C-terminal amphipathic helix only while it is bound to ATP. The third Min protein, MinE has been shown to prevent the formation of MinC/D complexes at mid-cell. MinE can displace MinC from the MinC/D complex [81-83]. Consequently, MinC is unable to prevent FtsZ from forming the FtsZ-ring and then allows the cell to divide in the middle of the cell. MinE is able to stimulate the ATPase activity of MinD which results in MinD dissociating from the

membrane. MinD can then rebind to membrane at the opposite pole where MinE concentration is the lowest, MinC then bind to MinD to start of the new cycle.

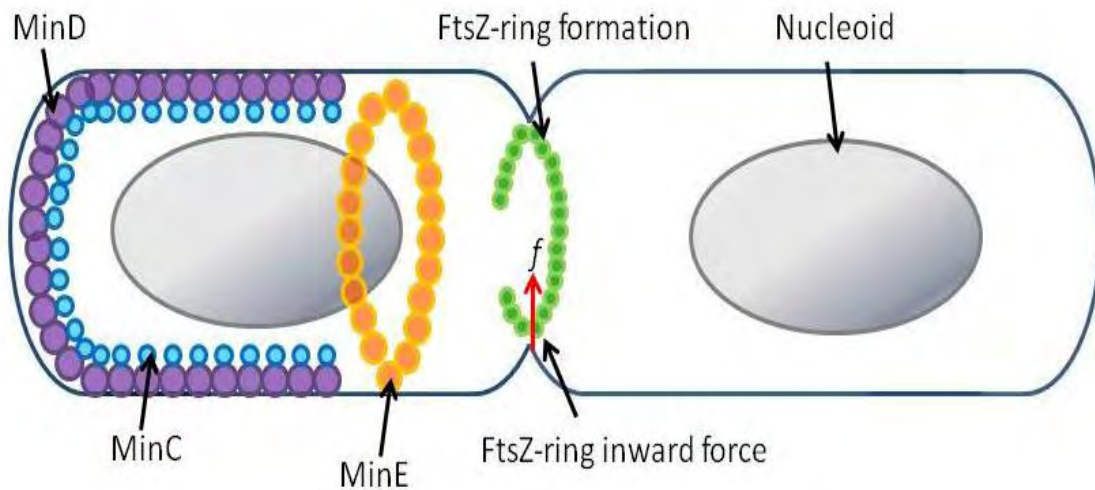


Figure 1-17. The localisation of FtsZ-ring regulated by MinCDE proteins.

In the *Escherichia coli* cell, positioning of the FtsZ-ring is regulated by three proteins, MinC, MinD and MinE. MinD-ATP binds to the cell membrane and it also binds MinC to form the MinC/D complex which prevents the formation of FtsZ-ring. MinE has been shown to prevent the formation of MinC/D complexes at mid-cell. Consequently, FtsZ-ring forms at mid-cell which then allows cell to divide in the middle of the cell [162].

After the FtsZ-ring has been formed, the remaining proteins involved in cell division are recruited; all these proteins are predicted to contain either single or multiple transmembrane spanning helices (apart from AmiC, amidase required for cell division). However, the

functions of some of these proteins are still not clear. Table 1-4 summarises 15 proteins are required for cell division of the *E. coli* cell.

Protein	Function
<b>FtsZ-ring associated</b>	
1. FtsZ	Tubulin homologue ; forms FtsZ-ring
2. ZipA	Stabilises FtsZ-ring; serves as a membrane anchor for FtsZ-ring
3. FtsA	It belongs to the actin superfamily; stabilises FtsZ-ring
4. ZapA	Stabilises FtsZ-ring
<b>Regulator of the location of FtsZ-ring</b>	
1. MinC	FtsZ inhibitor
2. MinD	Required to activate MinC; a family of bacterial ATPase
3. MinE	Min topological regulator ; prevents the formation of MinC/D complexes at mid-cell
<b>Proteins involve in “late” cell division</b>	
1. FtsK	Chromosome partitioning; acts as a DNA motor
2. FtsW	Division and Sporulation proteins
3. FtsI	Division specific transpeptidase
4. FtsN	It is only found among gamma-proteobacteria ; unknown function
5. FtsQ	Unknown function
6. FtsL	Unknown function
7. FtsB	Unknown function
8. AmiC	Amidase required for cell division

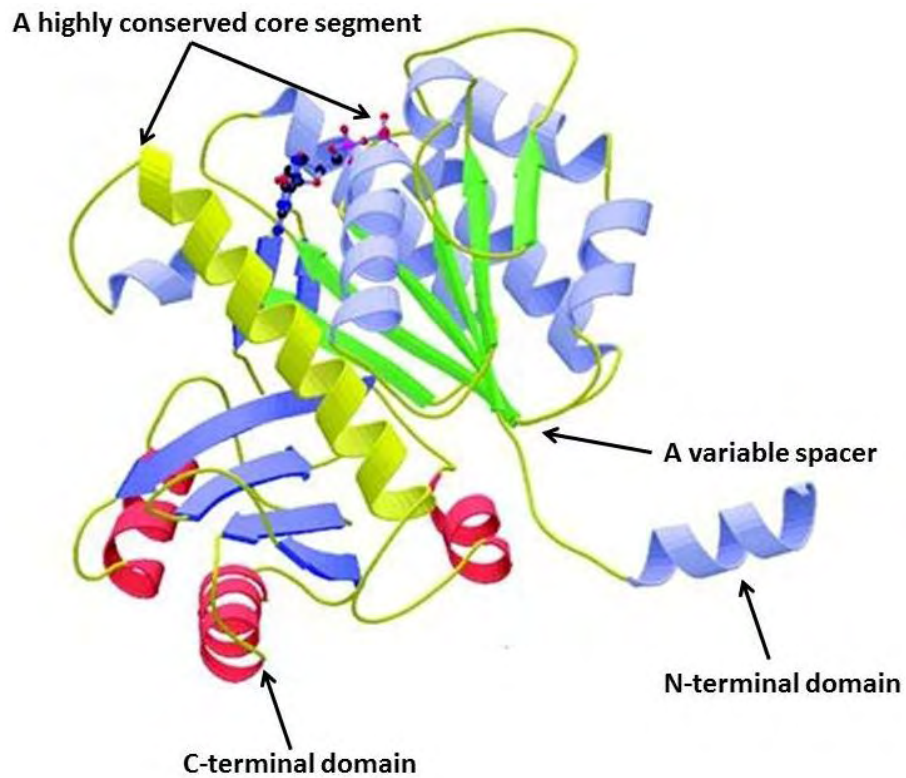
Table 1-4: At least 15 proteins are required for cell division of *E. coli* cell. These proteins include cytoplasmic, integral inner-membrane proteins and enzymes. These proteins can be classified into three groups according to their function, including FtsZ-ring associated, regulator of the location of FtsZ-ring and the proteins involved in “late” cell division [72-74].

### **1.6.2 Filamentous Temperature Sensitive Protein Z**

Filamentous temperature sensitive protein Z (FtsZ) is a GTPase protein, essential for cell division [84, 85]. It exists in most of the major groups of bacteria and *Euryarchaeal* branch of the *archaea* [86-88]. It is a highly conserved protein among the prokaryotes with only a few exceptions [89-91]. FtsZ has also been found in eukaryotic cells, for example, it is involved in the division of chloroplasts and mitochondria [92, 93].

The first crystal structure of FtsZ has been solved by Lowe and Amos in 1998 (Figure 1-18) [94]. FtsZ consists of four main protein domains, and these domains include the N-terminal region, a highly conserved core segment, a variable spacer and a C-terminal conserved domain. The N-terminal region is variable, and the function of this region is not clearly understood. Following the N-terminal region lies a conserved core segment which contains a tubulin-like motif of 7 amino acids responsible for GTP binding and hydrolysis. Flanking this are two independent N-terminal and C-terminal regions called Nt core and Ct core. The Nt core binds to the bottom portion of the adjoining monomer in an FtsZ protofilament, and the Ct core binds to the top portion of the adjoining monomer in the protofilament [94, 95]. Following the core segment is a variable spacer, but its function is still not clear. Finally, a C-terminal conserved domain, although this domain is not required for assembly, it is an

essential part for the interaction with other FtsZ-ring associated proteins such as ZipA, FtsA and ZapA which are important for stabilising FtsZ- ring [96, 97].



[164]

Figure 1-18. The structure of FtsZ. The protein consists of four main protein domains including the N-terminal region, a highly conserved core segment, a variable spacer and a C-terminal conserved domain.

PDB identifier: 1FSZ



### 1.6.3 FtsZ-Interacting Protein A

FtsZ-interacting protein A (ZipA) is an integral inner-membrane protein that contains an N-terminal membrane anchor which has been identified by Hale and de Boer in 1997 [100]. ZipA consists of 328 amino acids with a predicted molecular weight of 36.4 kDa. ZipA plays an essential role in the assembly of the FtsZ-ring by anchoring the FtsZ protein to the membrane during cell division (Figure 1-19). Its importance is reflected by the fact that cells depleted of ZipA can grow, but can not divide [100].

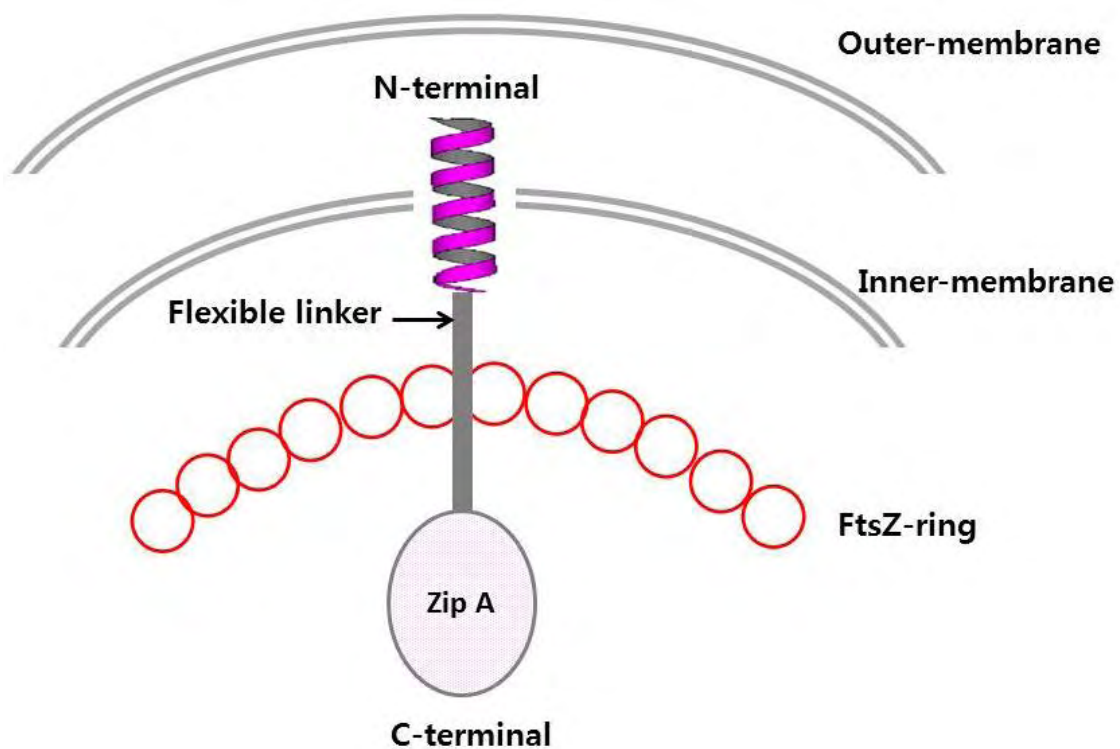
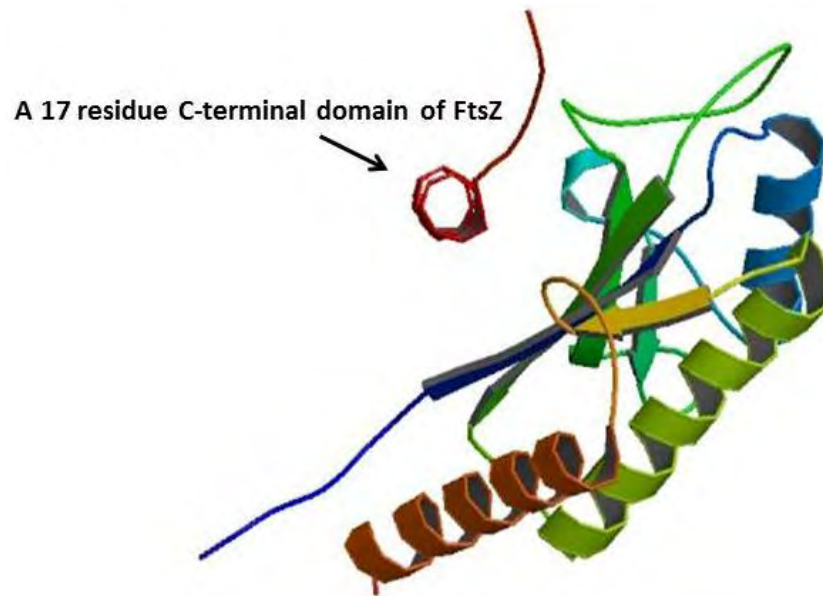


Figure 1-19. Representation of ZipA binds to the FtsZ-ring.

The periplasmic domain and transmembrane segment (N-terminal) acts as a membrane anchor for FtsZ-ring. The P/Q domain is unfolded and serves as flexible linker for FtsZ-ring to the membrane. The globular domain of ZipA (C-terminal) has been shown to bind to the C-terminus of FtsZ.

ZipA contains five regions [99]: a short periplasmic domain (amino acids 1 to 6) followed by a hydrophobic transmembrane segment (amino acids 7 to 28) which serves as a membrane anchor for FtsZ-ring. The removal of this N-terminal region of the protein results in a soluble ZipA [100]. The third region is a highly charged region (amino acids 29 to 85) which has been shown to block membrane transport and prevent further export of the protein [100,101]. The fourth region (amino acids 86 to 185) is a proline/glutamine rich domain named P/Q domain. The P/Q domain is the largely an unfolded polypeptide and plays a role as flexible linker that tethers FtsZ-ring to the membrane [100,102]. Immediately following P/Q domain lays a globular domain (amino acids 186 to 328). The globular domain of ZipA has been shown to bind to C-terminus of FtsZ [103-107]. The atomic structure of C-terminal has been solved and reveals this region to contain 3  $\alpha$ -helices motifs and 6  $\beta$ -sheets (Figure 1-20) [104,105].



<http://www.pdb.org/pdb/home/home.do>

Figure 1-20. Crystal structure for the C-terminal domain of ZipA

The complex with a 17 residue C-terminal domain of FtsZ [105]. The Resolution of the structure is 1.95 Å .

PDB identifier: 1F47

#### **1.6.4 The FtsZ-ZipA Interaction**

ZipA protein has been shown to stabilise FtsZ-ring at the membrane in the early stages of cell division. In the last decade, several reports have described the interaction between FtsZ and ZipA [107,108,110,111]. Ray and Chaudhuri and Hale *et al.* have shown that ZipA stabilises FtsZ polymers and that ZipA can induce bundling of FtsZ polymers [110,111]. Liu *et al.* found no evidence to suggest that ZipA affect FtsZ GTPase activity [107, 146].

Recent studies of the FtsZ-ZipA interaction have been carried out using methods that probe the GTPase activity of FtsZ as well as the structure of FtsZ by electron microscopy and sedimentation assays [107,110-112]. However, the information from these techniques does not fully address all aspects of the FtsZ-ZipA interaction.

Linear dichroism (LD) is a spectroscopic technique that can be used to characterise the interaction between FtsZ and ZipA. Previous studies have reported that LD can be used to measure the changes of rigidity or length of FtsZ polymers when FtsZ interacts with other proteins [113]. LD can be used in describing the orientations of biomolecules in ordered arrays [114]. LD is defined as the difference in absorbance between parallel and perpendicular linearly polarized light with respect to an orientation axis [115]. This can be used to determine the angle and the length of FtsZ polymers in the presence/absence of ZipA.

## **1.7 Objectives**

Membrane proteins present critical targets in biological research. However, the development of drugs that acts on membrane proteins has been limited by the lack of data on their structure and function. This is partly due to low expression level of most membrane proteins. Nevertheless, the major problem for membrane protein studies is the requirement of detergent

to extract from the native membrane, which often results in a loss of native structure and function. In this project we explore the use of a novel extraction reagent (SMA) for extraction of membrane proteins. This reagent negates the need of detergents and preserves the lipid annulus around the protein. In order to examine the applicability of the technique we use the reagent to purify two structurally and functionally diverse membrane proteins, A<sub>2a</sub>R and ZipA. Finally, we can use these purified SMALP membrane proteins for the subsequent characterisation studies.

## **1.8 Aims**

### *1. Expression and purification of SMALP and detergent solubilised A<sub>2a</sub>R*

An A<sub>2a</sub>R expression plasmid obtained from Dr. Niall Fraser (University of Glasgow). This is transferred to *Pichia pastoris* strain X-33 for protein expression. In order to obtain large quantities of protein, a bioreactor culture was used to grow A<sub>2a</sub>R. The SMALP system is then used to solubilise A<sub>2a</sub>R and compared to an established system using detergent.

### *2. Characterisation of A<sub>2a</sub>R*

Purified SMALP-A<sub>2a</sub>R and purified DDM-A<sub>2a</sub>R (pure A<sub>2a</sub>R solubilised by SMALP or DDM methods and then purified by standardised purification protocols) was studied using the

ligand-binding assay, circular dichroism (CD) and sedimentation velocity analytical ultracentrifugation (svAUC). These experiments can be used to characterise A<sub>2a</sub>R within SMALP, and also assess the advantages and disadvantages of the SMALP method compared with detergent solubilised sample.

### 3. Cloning, expression and purification of ZipA

A ZipA construct was made and the protein solubilised using the SMALP method as well as previous protocol used to purify A<sub>2a</sub>R.

### 4. Characterisation of ZipA, the interaction studies between FtsZ and ZipA

The structure of purified SMALP-ZipA (pure ZipA solubilised by SMALP method and then purified by standardised purification protocols) will be characterised using CD and svAUC.

This material will then be used for studying the FtsZ-ZipA interaction.

## **CHAPTER 2: Materials and Methods**

### **2.1 Materials**

Unless stated otherwise all chemicals used in this project were purchased from Sigma-Aldrich (Dorset, UK) and Fisher Scientific (Leicestershire, UK).

#### **2.1.1 Reagents for Protein Expression**

Synthetic oligonucleotides used for PCR reactions and primer DNA sequencing reactions were synthesized by Alta biosciences (University of Birmingham, UK). GoTaq Flexi DNA Polymerase was purchased from Promega (Southampton, UK). Restriction enzyme, *PmeI*, was purchased from NEB (Hitchin, UK). DNA loading buffer and Hyperladder I (ranging from 200 to 10,000 bp) were purchased from Bioline (London, UK). The pET 101/D-TOPO plasmid vector, One Shot<sup>®</sup> TOP10 Chemically Competent *E. coli* and One Shot<sup>®</sup> BL21 Star<sup>™</sup> (DE3) Chemically Competent *E. coli* were purchased from Invitrogen (Paisley, UK). FtsZ expression plasmid was kindly provided from Dr. Raul Pacheco-Gomez (University of Birmingham, UK). A<sub>2a</sub>R expression plasmid was obtained from Dr. Niall Fraser (University of Glasgow, UK). *Pichia pastoris* strains X-33 was kindly provided from Dr. Roslyn Bill (Aston University, UK). QIA quick gel extraction kit and QIAprep<sup>®</sup> Spin miniprep kit were purchased from Qiagen (Crawley, UK). LB medium and antibiotics, Ampicillin, used in *E.*

*coli* culture were purchase from Sigma-Aldrich (Dorset, UK). Isopropyl- $\beta$ -D-thiogalactopyranoside (IPTG) was purchase from Bioline (London, UK). BMMY/BMGY media used in yeast culture containing yeast extract and peptone were purchased from Merck (Feltham, UK), yeast nitrogen base without amino acids, biotin and antibiotics, Zeocin, were purchased from Invitrogen (Paisley, UK), glycerol and methanol were purchased from Fisher Scientific (Leicestershire, UK).

### **2.1.2 Reagents for Protein Purification**

Styrene maleic anhydride was supplied by Malvern Cosmeceutics Ltd. (Malvern, UK). DDM detergent was purchased from Sigma-Aldrich (Dorset, UK). All lipids were purchased from Avanti polar lipids (Alabaster, USA). Ni-NTA agarose was purchased from Qiagen (Crawley, UK). Colorplus prestained protein marker was purchased from NEB (Hitchin, UK). Instant blue was purchased from Expedeon (Harston, UK). Silver stain kit and BCA protein assay reagent were purchased from Thermo scientific (Northumberland, UK). CBQCA protein quantitation kit was purchased from Invitrogen (Paisley, UK). For western blotting: 6xHis Monoclonal antibody was purchased from Clontech (Saint-Germain-en-Laye, France), rabbit anti-A<sub>2a</sub>R receptor antibodies was purchased from Thermo scientific (Northumberland, UK), anti-mouse or rabbit IgG HRP-conjugated , ECL western blotting detection solution and autoradiography film were purchased from GE Healthcare (Buckinghamshire,UK).



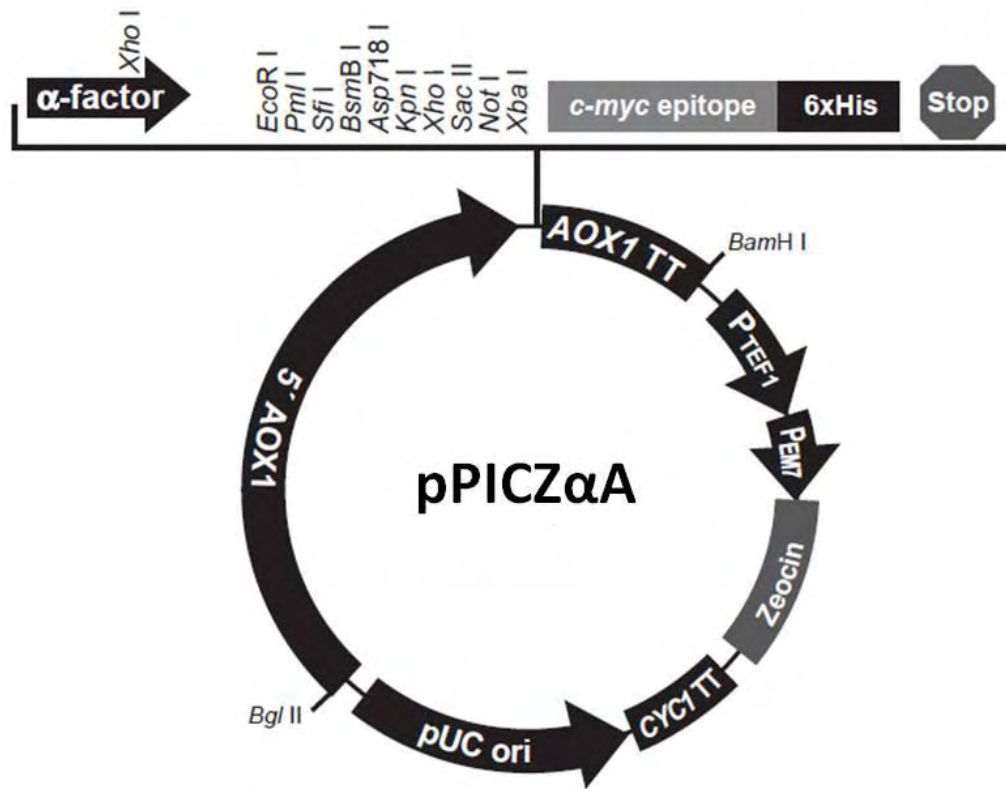
### **2.1.3 Reagents for Protein Characterisation**

GTP was purchased from Sigma-Aldrich (Dorset, UK). EnzChek® Phosphate Assay Kit was purchased from Invitrogen (Paisley, UK).

## **2.2 Methods: Expression and Purification of A<sub>2a</sub>R**

### **2.2.1 Yeast Strains, Transformation and Expression Screening**

A glycosylation deficient version of human adenosine 2a receptor (A<sub>2a</sub>R) expression plasmid was obtained from Dr. Niall Fraser (University of Glasgow). The N-linked glycosylation site at Asn154 in A<sub>2a</sub>R was changed to Gln in order to decrease overglycosylation due to yeast has a tendency to hyperglycosylate. The A<sub>2a</sub>R gene was excised by digestion with *Eco*RI and *Not*I before being cloned into the *Pichia pastoris* expression vector pPICZαA (Invitrogen) (Figure 2-1). The construct contained an N-terminal Flag-tag followed by a 10xHis-tag which can be used for the protein purification (Figure 2-2) as well as a Zeocin selection marker [25].



pPICZαA- 3593 nucleotides

5' *AOX1* promoter region: bases 1-941

5' *AOX1* priming site: bases 855-875

α-factor signal sequence: bases 941-1207

Multiple cloning site: bases 1208-1276

*c-myc* epitope: bases 1275-1304

Polyhistidine (6xHis) tag: bases 1320-1337

3' *AOX1* priming site: bases 1423-1443

*AOX1* transcription termination region: bases 1341-1682

*TEF1* promoter: bases 1683-2093

EM7 promoter: bases 2095-2162

*Sh ble* ORF: bases 2163-2537

*CYC1* transcription termination region: bases 2538-2855

pUC origin: bases 2866-3539 (complementary strand)

<http://www.invitrogen.com>

Figure 2-1. The *Pichia pastoris* expression vector pPICZαA

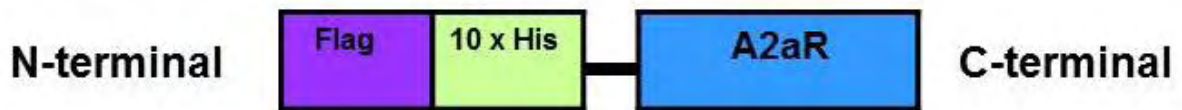


Figure 2-2 Diagram of the A<sub>2a</sub>R fusion protein, the protein contains a Flag-tag and a 10xHis-tag in the N-terminal.

The plasmid was linearized with the restriction endonuclease *PmeI*. It was then purified and concentrated to 0.5 - 1 µg DNA/µl using a centrifugal vacuum concentrators (Labconco), and used to transform into *Pichia pastoris* wild type strain X-33 by electroporation, as described by Cereghino *et al.* [116]. 20 transformants were cultured in BMGY medium (1% yeast extract, 2% peptone, 1.34% yeast nitrogen base without amino acids, 0.00004% biotin, 1% glycerol, 0.1 M phosphate buffer, pH 6) containing 100 µg/ml Zeocin. The cells were grown at 30°C and 220 rpm overnight to yield an optical density at 600 nm (OD<sub>600</sub>) of 2 - 10. 200 µl of 80% glycerol was added to 0.8 ml of the cell cultures and the mixture was stored at -80°C. Clones were then screened for production of A<sub>2a</sub>R by inducing production in 3 ml BMMY medium (BMGY containing 0.5% methanol instead of 1% glycerol) at 30°C and 220 rpm with an initial OD<sub>600</sub> of 1 in 24-well uniplates (Whatman). Protein production was maintained by addition of methanol (to a final concentration of 0.5% (v/v)) at 24 hours and 48 hours of post-induction. Samples were collected by centrifugation at 13,000 rpm for 3 minutes in a bench microcentrifuge (Labnet, Model 16M) at 6 hours, 24 hours and 54 hours of post-

induction to analyse production yields and determine the optimal harvest time by Western blotting.

### **2.2.2 Large-scale Flask Culture**

Five litres of A<sub>2a</sub>R expressing cells were routinely grown as 10 x 500 ml cultures. The frozen stock glycerol culture was used to inoculate to 50 ml of BMGY medium containing 100 µg/ml Zeocin at 30°C, 220 rpm until OD<sub>600</sub> between 2 and 6. A 500 ml conical flask containing BMGY was then inoculated with 25 ml of the initial culture and grown at 30°C and 220 rpm until OD<sub>600</sub> reached a value between 8 and 12. The cells were centrifuged at 6,000 x g in a Beckman JA-10 rotor for 20 minutes, and the pellet was then resuspended in 500 ml BMMY with 10 mM theophylline for induction. This was further incubated at 22°C and 220 rpm. At the 12 and 24 hours of post-induction, 0.5% methanol was added to the culture. The cells were harvested by centrifuging at 6,000 x g in a Beckman JA-10 rotor for 20 minutes at the 36 hours of post-induction. The pellet was then washed once with 10 mM Tris-HCl buffer, pH 8.

### **2.2.3 Bioreactor Culture**

A bioreactor, also known as a fermentor, allows precise regulation of pH, carbon source and the aeration that in return allows maximising cell densities and expression of the target

protein. Several factors should be considered carefully before optimizing the protocols such as pH, dissolved oxygen, the level of methanol for induction. For example, a large amount of methanol can induce cytotoxic effects and thus decrease the expression level [117]. The osmotic stress happens during high cell density which can adapt cell response mechanisms, e.g. change in the component of lipid [118]. Bioreactor cultures may yield up to 10 times more biomass compared to flask cultures and then increase the expression level of protein [25, 30].

## Methods

The frozen glycerol stock culture was used to inoculate to 50 ml of BMGY containing 100  $\mu\text{g/ml}$  Zeocin at 30°C, 220 rpm which was grown until an  $\text{OD}_{600}$  between 2 and 6 was reached. 50 ml of this culture was used to inoculate a 1 litre fermentor (Applikon) containing basal salts medium (BSM) 26.7 ml 85%  $\text{H}_3\text{PO}_4$ , 0.93 g  $\text{CaSO}_4$ , 18.2 g  $\text{K}_2\text{SO}_4$ , 14.9 g  $\text{MgSO}_4\cdot 7\text{H}_2\text{O}$ , 4.13 g KOH, and 40.0 g glycerol in 1 litre and 4.35 ml PTM1 trace salts (PTM1 (filter-sterilized) consists of 6.0 g  $\text{CuSO}_4\cdot 5\text{H}_2\text{O}$ , 0.08 g NaI, 3.0 g  $\text{MnSO}_4\cdot \text{H}_2\text{O}$ , 0.2 g  $\text{Na}_2\text{MoO}_4\cdot 2\text{H}_2\text{O}$ , 0.02 g  $\text{H}_3\text{BO}_3$ , 0.5 g  $\text{CoCl}_2$ , 20.0 g  $\text{ZnCl}_2$ , 65.0 g  $\text{FeSO}_4\cdot 7\text{H}_2\text{O}$ , 0.2 g biotin and 5.0 ml  $\text{H}_2\text{SO}_4$  in 1 litre) to a starting at  $\text{OD}_{600}$  of 0.3. The fermentation was run in fed-batch mode at 30°C, and pH was maintained at 5.0 using undiluted (28%) ammonium hydroxide. Dissolved oxygen (DO) was maintained above 20% saturation by adjusting

agitation rate and pure oxygen supply. When the initial glycerol (40 g/l) in batch phase was depleted, as indicated by an abrupt increase in DO reading, a 50% (w/v) glycerol solution containing 1.2% (v/v) PTM1 was fed at a feed rate of 30 ml/hr for 4 hours. Glycerol feed was terminated and a 3 hours starvation period was initiated in order to ensure complete glycerol consumption. During the final hour of starvation the temperature was at 30°C or reduced to 22°C and allowed to stabilise. Theophylline was added into the culture with a final concentration of 10 mM to increase A<sub>2a</sub>R expression. The induction phase is then started, in which 100% methanol or mixture of 60% sorbitol and 40% methanol containing 1.2% (v/v) PTM1 was fed at a programmed initial feed rate of 1.92 ml/hr for 17 hours to allow culture adaptation to methanol. When a steady DO rate and fast DO spike time was obtained, indicative of adaptation to methanol utilisation the feed rate was increased to 3.96 ml/hr for the remainder of the fermentation. The entire methanol fed-batch phase lasts approximately 40 hours with a total of approximately 125 ml methanol fed per litre of initial volume. The cells were then harvested by centrifuging at 6,000 x g in a Beckman JLA-8.1 rotor and washed once with 10 mM Tris-HCl buffer, pH 8.

#### **2.2.4 Yeast Membrane Preparation**

All work involving membrane preparation was carried out at 0 - 4°C to preserve protein integrity. Typically 10 g of cells were suspended in 50 ml ice-cold breaking buffer (5%

glycerol, 2 mM EDTA, 50 mM Tris-HCl, pH 7.4, 0.2% protease inhibitor cocktail set IV (Merck)) and poured into an Avestin-C3 cell disrupter (Avestin). The cells were broken by 3 passages through the chilled cell with homogenizing pressures ~30,000 psi. The breaking efficiency was > 90% when inspected with a light microscope. Unbroken cells and cell debris were removed from the membrane suspension by low-speed centrifugation (10,000 x g in a Beckman JA-25.5 rotor for 30 minutes). Membrane was collected using an ultracentrifuge (150,000 x g in a Beckman Type 70.1 Ti rotor for 45 minutes) and then resuspended in resuspension buffer (10% glycerol, 500 mM NaCl, 50 mM Tris-HCl, pH 8). Membrane was rapidly-frozen in liquid nitrogen and stored at -80°C.

### **2.2.5 Yeast Membrane Solubilisation with SMA Polymer**

#### **2.2.5.1 Preparation of SMA polymer**

Styrene maleic anhydride required hydrolysis to styrene maleic acid (SMA) before use. A 10% styrene maleic anhydride polymer was prepared by dissolving in 1 M NaOH and stirred at room temperature for overnight. The mixture was refluxed for two hours and then incubated at 4°C for 48 hours. The sample of stock of SMA polymer was stored at -80°C until it was required. When required, the stock SMA polymer was dialyzed overnight against 50 mM Tris-HCl, pH 8 using dialysis membranes (3,500 MWCO, Thermo Scientific) to remove NaOH before being applied to a solubilisation step.

#### 2.2.5.2 Solubilisation with SMA polymer

Solubilisation with SMA polymer was carried out in the solubilisation buffer I (10% glycerol, 500 mM NaCl, 2.5% (w/v) SMA, 1% (w/v) DMPC, 50 mM Tris-HCl, pH 8) with a protein concentration between 20 - 40 mg/ml. The slurry was stirred for one to two hours at room temperature and then centrifuged at 150,000 x g in a Beckman Type 70.1 Ti Rotor for 45 minutes to remove the unsolubilised materials. The supernatant containing SMALP solubilised A<sub>2a</sub>R (A<sub>2a</sub>R extracted from cell membranes by SMALP method, not purified yet, only the solubilised material) was reserved for further use.

#### 2.2.6 Yeast Membrane Solubilisation with Detergent

Solubilisation with n-dodecyl-β-D-maltoside (DDM) was performed in solubilisation buffer II (10% glycerol, 500 mM NaCl, 2.5% (w/v) DDM, 0.5% (w/v) Cholesteryl hemi-succinate (CHS), 50 mM Tris-HCl, pH 8) with a protein concentration of 20 mg/ml. After incubation with slow rotation at 4°C for 2 to 3 hours, the sample was centrifuged at 150,000 x g in a Beckman Type 70.1 Ti Rotor for 45 minutes to remove the unsolubilised materials. The supernatant containing DDM solubilised A<sub>2a</sub>R (A<sub>2a</sub>R extracted from cell membranes by DDM method, not purified yet, only the solubilised material) was saved for further use.



### **2.2.7 Purification of A<sub>2a</sub>R**

There are several purification methods that can be used for A<sub>2a</sub>R purification, these include Immobilized-metal affinity chromatography (IMAC), gel filtration, ion-exchange chromatography and affinity methods via an immobilized xanthine ligand.

The first, IMAC was first used for protein purification using the chelating ligand iminodiacetic acid (IDA) [119]. IDA was charged with metal ions used for protein purification [120]. However, IDA has only three metal-chelating sites results in metal ion leaching and leads to low purification yields or impure protein. Nitrilotriacetic acid (NTA) has a tetradentate chelating adsorbent site and can be charged with metal ions such as nickel ion. NTA binds to four of the six ligand binding sites in the coordination sphere of the nickel ion, leaving other two binding sites of nickel ion to bind to His-tagged of protein (Figure 2-3) [163]. This method overcomes low purification yields or impure protein. To date, Ni<sup>2+</sup>- NTA technology has become one of the most common method for protein purification.

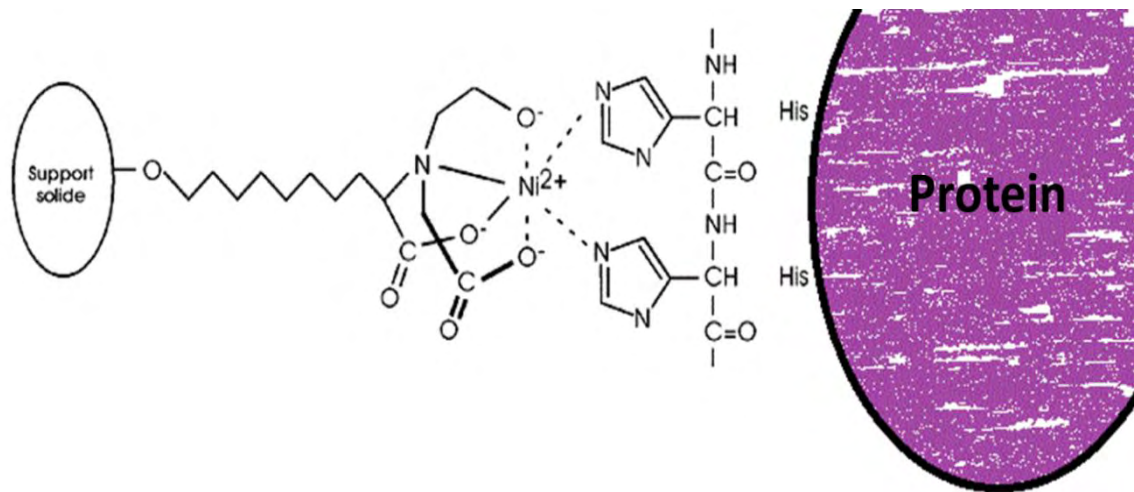


Figure 2-3. NTA occupies four of the six ligand binding sites of the nickel ion, leaving two sites free to interact with the His tag of protein.

The second, gel filtration, also called size exclusion, separates molecules and proteins according to the differences in size. It is a very useful method to separate monomers from aggregates for the protein purification. The gel filtration medium is a porous matrix that consists of a cross-linked polymer with pores of selected size and packed into the column to form a packed bed. Larger molecules migrate faster than smaller ones due to too large to enter the pores in the beads, therefore, larger molecules take more direct path through the column. The smaller proteins enter the pores in the beads hence take more labyrinthine route through the column (Figure 2-4) [12].

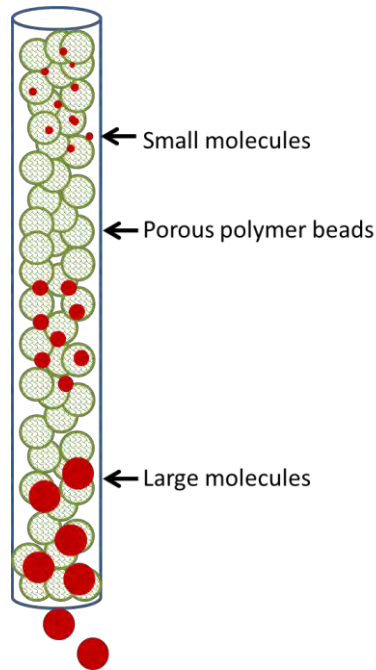


Figure 2-4. Gel filtration. Smaller molecules enter the pores in the beads, therefore, migrate slower than larger molecules.

The third, ion-exchange, ion-exchange chromatography separates compounds according to the net electric charges of protein. The column matrix is a synthetic polymer bound anionic or cationic groups. Cationic exchange resins, such as sulphopropyl (strong cationic exchangers) and carboxymethyl (weak cationic exchangers), bound anionic group (negative charge) and can be used to purify positively charged compounds. Anionic exchange resins, for example, quaternary amine (strong anionic exchangers) and diethylaminoethyl (weak anionic exchangers), bound cationic group (positive charge) can be used to separate negatively charged molecules (Figure 2-5) [12]. The affinity of protein binds to resin is affected by the pH (depend on isoelectric point of protein) and the concentration of salt in the buffer,

therefore, optimization of purification protocol can be approached by changing the pH or salt concentration [12].

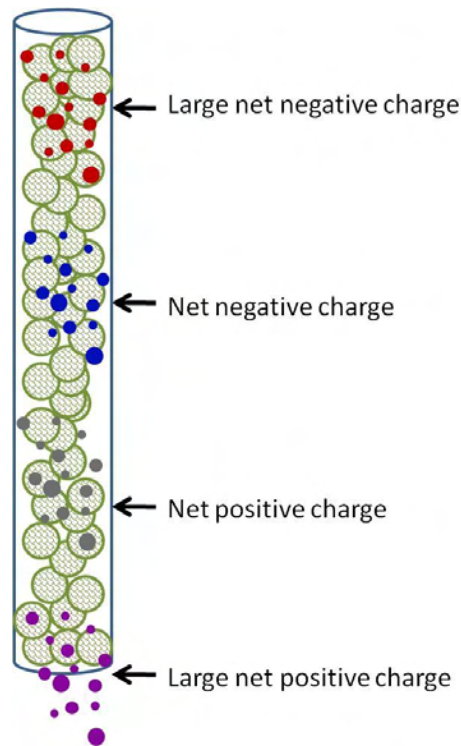


Figure 2-5. Ion-exchange. The column matrix contains anionic or cationic groups. In this example, bound cationic group (positive charge), the strongest positive charged compounds are eluted first, followed by those with positive charged molecules, negative charged compounds and strongest negative charged molecules are eluted last. pH, salt concentration and even temperature all act important roles in controlling the separation.

The fourth, affinity methods via an immobilized xanthine ligand, the principle of this method is similar to IMAC method: The ligand, in the case of  $A_{2a}R$ , Xanthine amine congener (XAC, an antagonist of  $A_{2a}R$ ) was used to bind to the receptor. The  $A_{2a}R$  can then be eluted by competition elution with other ligands, such as theophylline, an antagonist of  $A_{2a}R$  [121,122].

## Methods

### 2.2.7.1 SMALP Solubilised A<sub>2a</sub>R Purification Trails

Several methods were used to develop a protocol for purification of SMALP solubilised A<sub>2a</sub>R. In all cases experiments were carried out at 0 - 4°C to preserve protein integrity.

IMAC method: The supernatant containing the solubilised A<sub>2a</sub>R was diluted with 80 mM imidazole in the resuspended buffer (10% glycerol, 500 mM NaCl, 50 mM Tris-HCl, pH 8), so that the mixture had final concentration of 20 mM imidazole in the resuspended buffer. The solubilised sample (from 30 g of original culture) was then passed over the 1 ml, 5 ml or 15 ml of pre-packed His Trap column (GE healthcare) at 4°C overnight, with a flow rate of 1 ml/min. Alternately, the sample was incubated with 1.5 ml or 15 ml of Ni<sup>2+</sup>-NTA resin (Qiagen) with slow rotation at 4°C overnight. The sample was eluted with 20 times column volumes of elution buffer (10% glycerol, 500 mM NaCl, 50 mM Tris-HCl, pH 8, plus a linear gradient of imidazole up to 500 mM of imidazole). The sample was collected every 0.5 ml.

Gel filtration: The sample was injected into a Superdex 200 10/300 GL column attached to an ÄKTA™ purifier FPLC purification system (GE Healthcare) or BioCAD HPLC system. The fractions were eluted with gel filtration elution buffer and collected every 0.5 ml (10% glycerol, 150 mM NaCl, 50 mM Tris-HCl, pH 8).

Ion-exchange: The sample was washed extensively with ion-exchange buffer (10% glycerol, 100 mM NaCl, 50 mM Tris-HCl, pH 8) before loading onto 3 ml Q Sepharose resin (GE Healthcare). The resin was washed with 10 times resin volumes of ion-exchange buffer. The receptor was eluted with different concentration of NaCl (from 100 mM to 2 M) in ion-exchange buffer. The sample was collected every 0.5 ml.

Affinity methods via an immobilized xanthine ligand: The method has been developed and reported in the several publications [26, 121,122]. The experiment was approached according to previous publish protocol using synthesized Xanthine amine congener resin (XAC, an antagonist of A<sub>2a</sub>R) [26].

#### 2.2.7.2 Final SMALP Solubilised A<sub>2a</sub>R Purification Procedure

A two-step purification process for SMALP solubilised A<sub>2a</sub>R after numerous of trials (§ 3.2.4.2) was found to be sufficient. The purification process included IMAC and gel filtration step. The supernatant containing the solubilised A<sub>2a</sub>R was diluted with 80 mM imidazole in resuspension buffer (10% glycerol, 500 mM NaCl, 50 mM Tris-HCl, pH 8), so that the mixture had final concentration of 20 mM imidazole. The sample was incubated with 1.5 ml of Ni<sup>2+</sup>-NTA resin (Qiagen) with slow rotation at 4°C overnight. Typically, 1.5 ml of resin was used in 30 g cell pellet of original culture, the resin was washed with 5 times resin

volumes of wash buffer (resuspension buffer plus 60 mM imidazole, pH 8) before receptor was eluted using the elution buffer (resuspension buffer plus 250 mM imidazole, pH 8) within 20 times resin volumes.

The fractions containing A<sub>2a</sub>R were concentrated using a Vivaspin 20 concentrator (30 kDa cut-off, Sigma-Aldrich) and washed extensively with gel filtration elution buffer (10% glycerol, 150 mM NaCl, 50 mM Tris-HCl, pH 8) before being injected onto a Superdex 200 10/300 GL column attached to an ÄKTA™ purifier FPLC purification system (GE Healthcare) or BioCAD HPLC. The fractions were eluted with gel filtration elution buffer and collected every 0.5 ml (10% glycerol, 150 mM NaCl, 50 mM Tris-HCl, pH 8).

#### 2.2.7.3 Purification of Detergent Solubilised A<sub>2a</sub>R

Purification of detergent solubilised A<sub>2a</sub>R was approached using a three-step purification process which included IMAC, ion-exchange and gel filtration [25]. All buffers were contained 0.05% DDM and 0.01% CHS. Purification of detergent solubilised A<sub>2a</sub>R was performed as for the SMALP solubilised A<sub>2a</sub>R based protocol except the following steps which were altered: first, all buffers included 0.05% DDM and 0.01% CHS. Second, the samples eluted from the IMAC step required an ion-exchange step before being loaded onto Superdex 200 10/300 GL. The fractions from IMAC eluted containing A<sub>2a</sub>R were concentrated using Vivaspin 20 concentrator (30 kDa, cut-off) and washed extensively with

ion-exchange buffer (10% glycerol, 100 mM NaCl, 50 mM Tris-HCl, pH 8) before loading onto a 3 ml Q Sepharose resin (GE Healthcare). The resin was washed with 10 times resin volumes of ion-exchange buffer. The receptor was eluted with 250 mM NaCl in ion-exchange buffer. The fractions containing A<sub>2a</sub>R were then concentrated and washed extensively with gel filtration elution buffer before being loaded onto Superdex 200 10/300 GL.

### **2.2.8 SDS-PAGE and Western Blotting**

Unless noted otherwise all work in this section were performed at room temperature. Whole cell pellet samples for expression screening were heated at 95°C for 10 minutes in SDS-PAGE (Laemmli) sample buffer (Table 2-1), and pure receptor samples were incubated with sample buffer at 37°C for 15 minutes before being loaded onto the SDS-PAGE gel (Table 2-2) [123]. Prestained protein marker (range 7-175 kDa, NEB) was used as molecular weight marker. The PAGE was run for 50 minutes at 200 volts (V) in SDS-PAGE running buffer (25 mM Tris-HCl, 192 mM Glycine and 0.1% SDS). The protein was visualised by coomassie blue staining (dissolving 0.25 g of coomassie blue in 45 ml methanol, 45 ml water and 10 ml glacial acetic acid) for 15~30 minutes and destained in destaining buffer (5:4:1 ratio of methanol: water: acetic acid) for one hour to overnight, or used instant blue (Expedeon) and destained with water. Alternatively, gel can be visualised by silver staining (Thermo scientific) according to the manufacturer's instructions from Thermo scientific.



Components	Concentration
SDS	10% (w/v)
$\beta$ -mercapto-ethanol	10 mM
Glycerol	20 % (v/v)
Tris-HCl buffer, pH 6.8	0.2 M
Bromophenolblue	0.05% (w/v)

Table 2-1. Recipe of 5x SDS-PAGE sample buffer [123].

10% resolving gel (volumes)	Components	5% stacking gel (volumes)
5.9 ml	H <sub>2</sub> O	3.4 ml
5 ml	30% (w/v) Acrylamide	0.83 ml
3.8 ml	1.5M Tris-HCl buffer, pH 8.8 / 1M Tris-HCl buffer, pH 6.8	0.63 ml
0.15 ml	10% (w/v) SDS	0.05 ml
0.15 ml	10% (w/v) Ammonium persulfate	0.05 ml
0.006 ml	TEMED	0.005 ml

Table 2-2. Components of 10% resolving gel and 5% stacking gel [123].

For Western blotting, gel was transferred to a nitrocellulose membrane (Sigma-Aldrich) in transfer buffer (25 mM Tris-HCl, 192 mM Glycine and 20% methanol) for 60 minutes at 80 V. The membrane was transferred to blocking buffer (TBST buffer: 10 mM Tris-HCl, pH 7.3, 100 mM NaCl, 0.2% tween 20, plus 5% non-fat dried milk ) for 1 hour to reduce non-specific binding. The membrane was then placed in blocking buffer with 1 : 5,000 diluted 6xHis Monoclonal antibody (Clontech) for one hour or with 1 : 250 to 1 : 1,000 diluted rabbit anti-A<sub>2a</sub>R receptor antibody (Thermo scientific) for between 1 and 12 hours. The membrane was then washed with TBST buffer for 5 minutes and repeated 3 times to remove unbound antibody before being placed in blocking buffer with 1 : 10,000 diluted anti-mouse or anti-rabbit IgG HRP-conjugated (GE Healthcare) for 1 hour. The next step was carried out before the bands were visualised using ECL Western blotting detection solution (GE Healthcare) and autoradiography film (GE Healthcare) or Gel documentation System (UVItec).

### **2.2.9 Identification of A<sub>2a</sub>R**

The band corresponding to the expected mass of A<sub>2a</sub>R was excised from SDS-PAGE gel and then identified by Functional Genomics and Proteomics Laboratory within the School of Biosciences at University of Birmingham. The sample was digestion with trypsin before identification using Fourier Transform Ion Cyclotron Resonance (FT-ICR) mass

spectrometry. The data were then run a search on Mascot to identify the protein and then further analysed using MassLynx software.

### **2.2.10 Protein Quantitation**

Although there are several methods to quantitate proteins in solution, quantitation of a membrane protein is difficult since the lipid membrane and detergents may interfere with the assay. To address these three different methods were used to measure protein concentration.

(1) Ultraviolet (UV) spectrophotometry absorption at 280 nm: This method is a fast and easy, however, it is not ideal for membrane proteins. The absorbance maximum in the near UV (280 nm) was due to the amino acids with aromatic residues such as Tyrosine and Tryptophan [12, 20]. (2) Bicinchoninic acid (BCA) method: This method is a modification of the Lowry method improved by Smith et al in 1985 [124]. This method, however, can be influenced by the presence of lipid. (3) CBQCA protein quantitation kit: this is a commercially available kit which shows a good response in the presence of lipids and detergents. It is an ideal method to measure membrane protein concentration. In this project, we found CBQCA protein quantitation kit (Invitrogen) does not show interference with lipids, DDM and SMA. Therefore, this method is the best way to obtain accurate protein concentration in the presence of lipids, DDM and SMA.

## Methods

Determining the protein concentration using UV spectrophotometry at 280 nm was based on

following equation:

$$\text{Absorbance (280 nm)} = [\text{Protein}] (\text{M}) \times \text{Extinction coefficient (M}^{-1} \text{cm}^{-1}) \times \text{pathlength (cm)}$$

In the case of A<sub>2a</sub>R, extinction coefficient is 66,850 [125].

BCA assay (Thermo scientific) and CBQCA protein quantitation (Invitrogen) methods were performed as described by the manufacturer's instructions from Thermo scientific and Invitrogen. An aqueous solution of bovine serum albumin (BSA) was used as a standard.

## **2.3 Methods: Characterisation of A<sub>2a</sub>R**

### **2.3.1 Radioligand Binding Assays**

A radioligand binding assay is based on the use of a radioactively labelled compound which interacts with a receptor. Tritium [<sup>3</sup>H] is the most common isotopes used to label these compounds due to its long half-life (12.3 years) [52]. The radioligand binding assays are not only used for studying membrane-bound receptor, but also widely used to analyse purified receptors. This tool can also use to analyse the interactions of hormones, neurotransmitters, and drugs with the related receptors. There are three main types of information can be given

by radioligand binding assays: saturation binding, competitive binding, and kinetics assays [52, 126].

#### Saturation binding assay

This assay is used for measuring total binding and non-specific binding at various concentrations of the radioligand. The specific binding can be calculated by non-specific binding is subtracted from total binding. The maximum binding capability ( $B_{\max}$ ) and equilibrium dissociation constant ( $K_d$ ) are calculated from specific binding using Scatchard plots [127, 128].

#### Competitive binding assay

The experiment can determine equilibrium binding of a radioligand with a fixed concentration at various concentrations of displacing ligand. The data are used to analyse the affinity of the receptor for the competitor (displacing ligand) [127, 128].

#### Kinetics assay

The experiment can measure the binding at different times and then used to determine the association rate (ligand associating with the receptor) and dissociation rate (ligand dissociating from the receptor) constants of radioligand [127, 128].

## Method

All radioligand binding assays were performed using [<sup>3</sup>H]ZM241385, an A<sub>2a</sub>R antagonist, in binding assay buffer (0.5 mM EDTA, 50 mM sodium phosphate, pH 7.4). The assays were carried out by Dr. David Poyner (Aston University, UK). For membrane-bound A<sub>2a</sub>R, the assay was performed as described previously [25]. For SMALP/ detergent solubilised or purified A<sub>2a</sub>R (typically at 0.1 mg/ml), the assay was modified for saturation binding analysis by incubating the various concentrations of [<sup>3</sup>H] ZM241385 with diluted A<sub>2a</sub>R for 90 minutes at room temperature in the binding assay buffer. For displacement studies, the solubilised receptor was incubated with a fixed concentration of [<sup>3</sup>H]-ZM241385 (nominally 1 nM; the actual concentration was measured in each experiment) with varying concentrations of displacing ligand.

For thermal stability experiments the receptor was pre-incubated at the desired temperature for 30 minutes prior to incubation with 1nM [<sup>3</sup>H] ZM241385. Non-specific binding was determined in parallel incubations with 1 μM ZM241385. The samples were loaded onto P30 mini-spin gel filtration columns (Bio-Rad Laboratories Inc.) that had been pre-equilibrated in the binding assay buffer and the eluate was collected by centrifugation (3,000 rpm for 4 minutes). For the displacement and thermal stability experiments, crude SMALP solubilised samples were used, rather than purified receptor. Saturation and displacement binding curves

were analysed using PRISM Graphpad v4.0, fitting the data to sigmoidal curves with a Hill slope constrained to unity. In the displacement studies,  $K_i$  values were calculated from  $IC_{50}$ 's using the Cheung-Prussoff equation. Thermostability curves were fitted to a Boltzmann sigmoidal function to calculate the temperature at which binding was reduced by 50% ( $T_{1/2}$ ).

### **2.3.2 Circular Dichroism**

Circular dichroism (CD) spectroscopy has been widely used to determine the secondary structure of proteins, for example,  $\alpha$ -helix,  $\beta$ -sheet,  $\beta$ -turn and polyproline (describe below). The different secondary structures of proteins absorb different amounts of right and left circularly polarized light providing CD signals [129, 130]. The CD spectrum between the far-UV region (190 - 260 nm) is a specific region for the peptide backbone and allows the identification of secondary structure elements within a protein. By examining the shape CD spectra of proteins of known structure, it has been shown that certain features in the spectrum correlate with the presence of each secondary structure type (Figure 2-6) [131].

#### **$\alpha$ -helix**

The CD spectrum of  $\alpha$ -helix exhibits a double minimum at 208 nm and 222 nm. It also presents positive CD signals between 190 nm - 200 nm [130,131].

### *β-sheet*

Unlike  $\alpha$ -helix, the CD spectrum of  $\beta$ -sheet is not so well defined. However it is accepted that in general  $\beta$ -sheets display a minimum between 216 - 220 nm and a positive peak approximately at 195 nm [130,131].


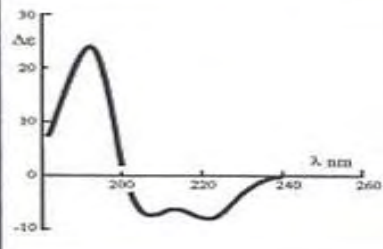
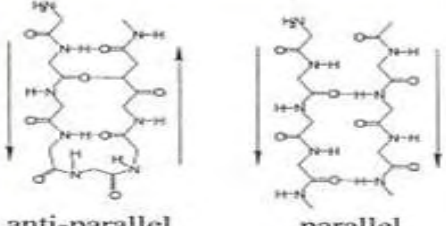
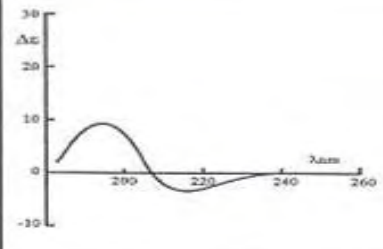
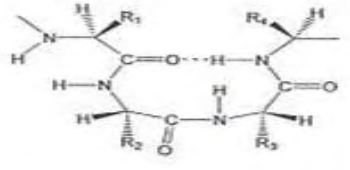
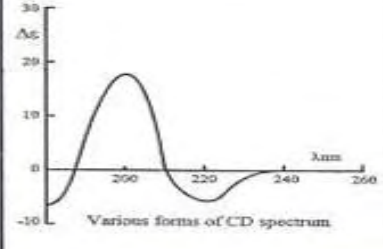
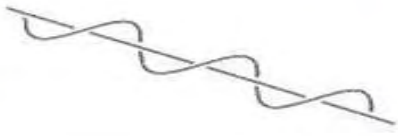
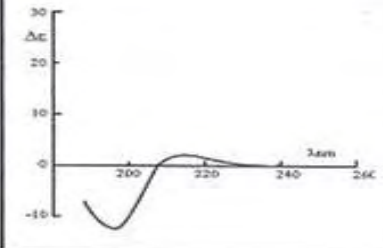

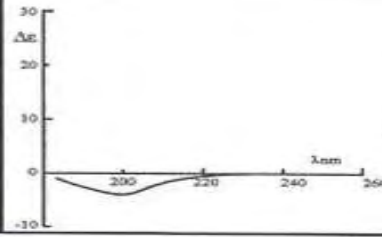
### *β-turn*

The CD spectra of  $\beta$ -turns are quite difficult to define because of it can include numerous kinds of turn in a protein. The common shape of  $\beta$ -turn is included a positive peak between 200 nm and 205 nm and a negative peak between 220 - 225 nm. In addition, it also presents a strong negative signal between 180 nm and 190 nm [130,131].

### *Polyproline*

The CD spectrum of polyproline is unusual in that it has a positive peak between 225 and 230 nm [130,131].



Protein conformation, shape and circular dichroism		
Conformation	Molecular Shape	CD Spectrum
$\alpha$ -helix (H-bonded)		
$\beta$ -sheet parallel and anti-parallel (H-bonded)		
$\beta$ -turn, (Type I, II, II', ...) $\gamma$ -turns Some turns not H- bonded in proteins		
Polyproline $P_{II}$ helix $3_1$ -helix (Left handed extended helix) (No intra-molecular H-bonds)		
<b>Irregular</b> (Disordered)		

[131]

Figure 2-6. CD spectra of various secondary structure motifs. Each type of secondary structure of protein presents different shape. For a protein containing a mix of structures the shape of spectrum is made up of the sum of signals from each element.

## Method

The protein sample was dialysed using dialysis membrane (14,000 MWCO) against 3 litres of 10 mM sodium phosphate, pH 8, prior to the CD spectrum was measured. The far-UV (190 - 260 nm) CD spectrum was recorded in a JASCO J-715 spectrophotometer using 1 mm pathlength quartz cuvette. The thermal stability experiments were performed using 1 mm pathlength on a JASCO J-810 spectrophotometer fitted with a Peltier heating block. The thermal stability experiments involved two methods: The first, monitoring the change in CD signals at 222 nm as a function of increasing temperature (0.5°C steps between 25°C and 95°C). The second, involved recording full wavelength scans between 190 nm and 260 nm every 10°C between 25°C and 95°C.

### **2.3.3 Sedimentation Velocity Analytical Ultracentrifugation**

Sedimentation velocity analytical ultracentrifugation (svAUC) allows the characterisation mass of sample in their native state in the solution. The sedimentation velocity experiments used in this study separates the molecules by the difference in mass and shape and provides information about the solution homogeneity, mass of the sample particle and identifies any aggregation [130].

## Methods

Receptor sample was equilibrated in 10 mM sodium phosphate, pH 8, prior to analytical ultracentrifugation. Velocity experiments were performed using a Beckman Coulter XL-I analytical ultracentrifuge and a Ti50 rotor at 40,000 rpm, 4°C. The protein concentration within the cell was monitored at 280 nm. These data were then analysed using the c(S) and c(M) routines implemented within SEDFIT [132]. Parameters for  $A_{2a}R$   $v_{bar}$  and solvent density and viscosity were calculated using SEDNTERP. The value for  $v_{bar}$  is only an estimate for the SMALP encapsulated particle as value SMA is not available.

### **2.3.4 Electron Microscopy**

Receptor sample was equilibrated in 10 mM sodium phosphate, pH 8, and then centrifuged at 10,000 rpm for 5 minutes to remove any aggregated protein or large particles. 5  $\mu$ l of the mixture was transferred to the carbon side of an electron microscopy grid for 1 minute. The sample was stained by incubating in 1% uranyl acetate solution for 45 seconds before the excess solution was removed. The electron microscopy (EM) experiment was carried out using a JEOL 2011 Transmission electron microscope (TEM). The samples were visualised at magnification of 10,000 and 40,000 times.

## **2.4 Methods: Expression and Purification of ZipA**

### **2.4.1 Plasmid Construction, *Escherichia coli* Strains and Transformation**

#### **2.4.1.1 Extraction of *Escherichia coli* Genomic DNA**

ZipA exists as a single copy in the genome of most gram-negative bacteria. In this study, we extracted genomic DNA from *E. coli* strain TOP10 and used it as the template for polymerase chain reaction (PCR) to amplify ZipA gene.

#### **Methods**

TOP10 *E. coli* cells were grown in 5 ml of LB medium at 37°C overnight and then centrifuged at 13,000 rpm for 2 minutes in a bench microcentrifuge (Labnet, Model 16M). The cell pellet was resuspended in NaCl/EDTA buffer (0.15 M NaCl, 0.1 M EDTA, pH 8.0). 0.5 mg lysozyme and 0.2 mg RNaseA were added into the sample, and then incubated at 37°C for 30 minutes. A 25% SDS (w/v) stock solution was added to the sample, so that the final mixture had a SDS concentration of 2% (w/v). The sample was incubated at 60°C for 10 minutes and cooled in a cold water bath to lyse the cells. A 5 M NaCl stock solution was added to raise the NaCl concentration to 2 M before adding a mixture of Phenol/CHCl<sub>3</sub>/IAA (Phenol: chloroform: isoamyl alcohol = 25:24:1). The sample was centrifuged at 10,000 rpm for 10 minutes using a bench microcentrifuge (Labnet, Model 16M) and added CHCl<sub>3</sub>/IAA (chloroform: isoamyl alcohol = 24:1) to the supernatant. The mixture was centrifuged again

at 10,000 rpm for 5 minutes in a bench microcentrifuge (Labnet, Model 16M) and the supernatant was kept. Finally, the DNA was precipitated by adding 100% ethanol, followed by washing the pellet with 70% ethanol and drying in the air. The dried DNA was then resuspended in deionised water for further use.

#### 2.4.1.2 Polymerase Chain Reaction

The primer sequences (synthesized by Alta biosciences) used to carry out a PCR to amplify ZipA gene is described in Table 2-3. 1.25 U Taq DNA polymerase, 0.2 mM dNTPs, 2 mM MgCl<sub>2</sub>, 0.5 mM primers and 1 µg genomic DNA which was extracted from previous experiment (§ 2.4.1.1) were used in a PCR reaction according to the procedures in the manual from Promega. The PCR reaction cycle parameters are shown in Table 2-4. The PCR products were examined by 1% agarose gel electrophoresis.

	Sequence	Tm(°C)	GC(%)
Forward Primer	5' <u>CACCATG</u> ATGCAGGATTTGCGTCT 3'	67.8	50
Reverse Primer	5' GCGTGTGCTTTGACTTCGCG 3'	67	57.1

Table 2-3: Synthetic oligonucleotides used to amplify ZipA gene. A CACC sequence (underlined) allows topoisomerase I to ligate the blunt end PCR product to the pET101/D- TOPO plasmid vector (See Figure 2-7 and 2-8).

Cycle	Step	Temperature (°C)	Time (minute)
x1	Initialization	95	2
x30	Denaturation	95	1
	Annealing	58	1
	elongation	72	1
x1	Final elongation	72	5

Table 2-4: The PCR reaction cycle

#### 2.4.1.3 Agarose Gel Electrophoresis

The 1% (w/v) of agarose solution was prepared by dissolving 0.5 g of agarose in 50 ml of 1×TAE buffer (40 mM Tris-HCl, 20 mM Acetate, 2 mM EDTA) followed by heating in microwave for 1 minute at full power. Ethidium bromide was added to a final concentration

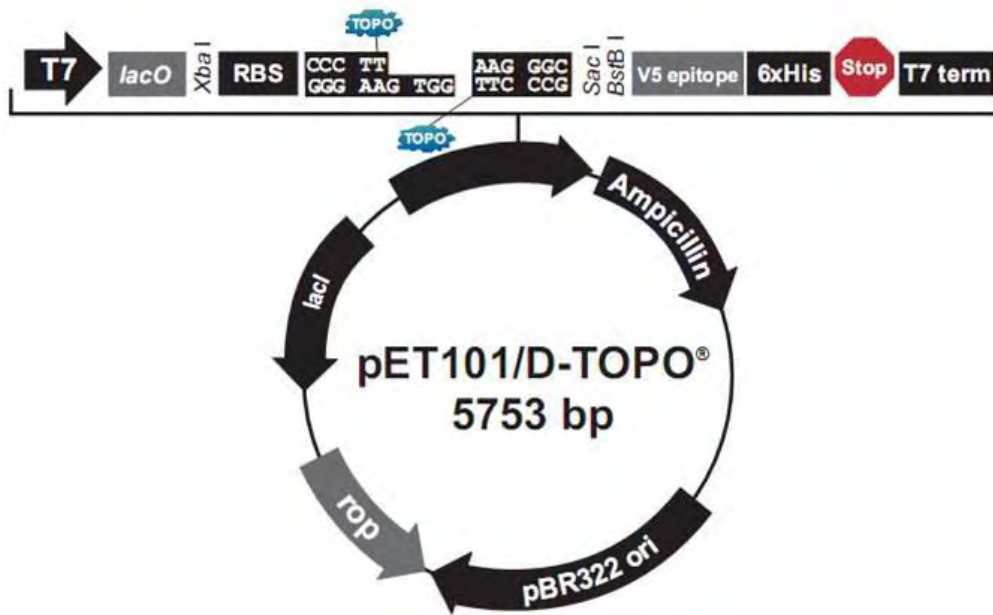
of 0.5 µg/ml after agarose solution was cooled down to 50°C in a cold water bath. The mixture was poured into a mould with a comb and allowed it to cool to room temperature. The gel was placed in an electrophoresis tank filled with 1×TAE buffer. The DNA sample was mixed with 5×DNA loading buffer (Bioline) before loading into the gel. A HyperLadder I (Bioline) was loaded to the gel as a molecular weight marker. The gel was run at 80 V for 50 minutes and then examined using UV light.

#### 2.4.1.4 Purification of PCR Product from Agarose Gel

PCR product was purified from agarose gel using a QIA quick gel extraction kit for ligation experiment. The kit was designed for DNA size from 70 bp to 10 kb and contains a silica membrane assembly for binding of DNA. The impurities such as enzymes, agarose and ethidium bromide, were removed during the purification procedure. A purification procedure using a QIA quick gel extraction kit was followed the manufacturer's instructions from Qiagen.

#### 2.4.1.5 Ligation Reaction

The ligation reaction was performed using Champion pET101 Directional TOPO plasmid vector which contains a T7 promoter, a 6×His tag at C-terminus and Ampicillin resistance gene (Figure 2-7).



T7 promoter: bases 209-225

T7 promoter priming site: bases 209-228

*lac* operator (*lacO*): bases 228-252

Ribosome binding site (RBS): bases 282-288, 292-296

TOPO® cloning site (directional): bases 297-310

V5 epitope: bases 333-374

Polyhistidine (6xHis) region: bases 384-401

T7 reverse priming site: bases 455-474

T7 transcription termination region: bases 416-544

*bla* promoter: bases 845-943

Ampicillin (*bla*) resistance gene (ORF): bases 944-1804

pBR322 origin: bases 1949-2622

*ROP* ORF: bases 2990-3181 (complementary strand)

*lacI* ORF: bases 4493-5584 (complementary strand)

<http://www.invitrogen.com>

Figure 2-7. Vector map of pET101/D- TOPO. In the pET TOPO vectors, expression of the gene of interest under control of T7 promoter. When T7 RNA polymerase is present, it binds to T7 promoter and transcribes the gene of interest. T7 RNA polymerase gene is controlled of the *lacUV5* promoter, when IPTG (inducer) is added that allows expression of T7 RNA polymerase from the *lacUV5* promoter. The vector contains a 6xHis tag for affinity purification of protein of interest and Ampicillin resistance gene as selection marker.



Topoisomerase I binds to DNA at specific sites (after 5'-CCCTT in one strand). Topoisomerase I cleaves the phosphodiester backbone and the energy from the broken phosphodiester backbone is used for the formation of a covalent bond between the 3' phosphate of the cleaved strand and tyrosyl residue of topoisomerase I. This phospho-tyrosyl bond can be attacked by the 5' hydroxyl of the original cleaved strand this results in reversing the reaction and releasing topoisomerase I. The vector contains a single-stranded GTGG overhang on the 5' end and a blunt end on the 3' end [98]. Therefore, PCR product contains CACC sequence at 5' end allows topoisomerase I to ligate PCR product to the pET101/D-TOPO plasmid vector (Figure 2-8). Figure 2-9 shows a diagram of the ZipA fusion protein containing a V5 epitope-tag and a 6 x His-tag in the C-terminal.

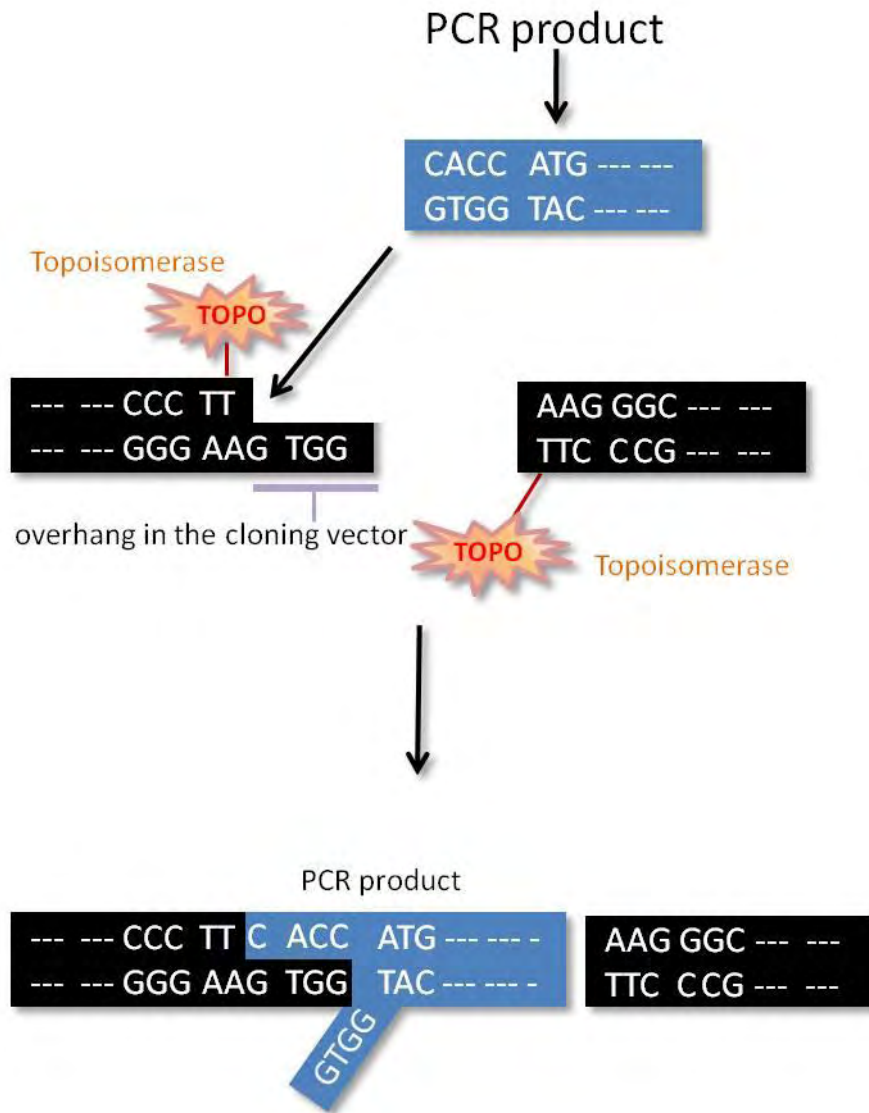


Figure 2-8. Directional TOPO cloning. The vector contains a single-stranded GTGG overhang on the 5' end and a blunt end on the 3' end. PCR product contains CACC sequence at 5' end allowing topoisomerase I to ligate PCR product to the vector.

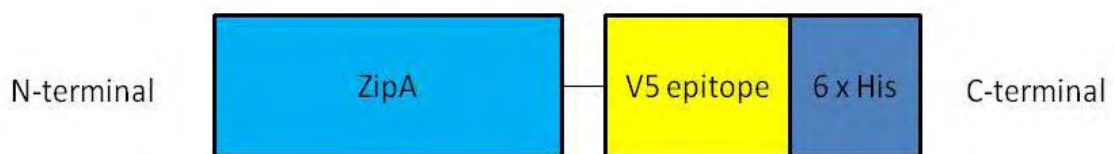


Figure 2-9 .Diagram of the ZipA fusion protein, the protein contains a V5 epitope-tag and a 6 x His-tag in the C-terminal.

## Methods

The 0.5:1 to 2:1 molar ratio of PCR product: vector was used in ligation reaction. The volume of vector was 1  $\mu$ l. The reaction composition was described at Table 2-5. The mixture was incubated at room temperature for 5 minutes and stored at 4°C for further use.

Component and final concentration	Quantity
PCR product	0.5 to 4 $\mu$ l
Salt solution (0.2M NaCl and 0.01M MgCl <sub>2</sub> )	1 $\mu$ l
Sterile water	Added to a final volume of 5 $\mu$ l
TOPO vector	1 $\mu$ l

Table 2-5. The composition of ligation reaction.

### 2.4.1.6 Transformation of TOP10 Chemical Competent Cells

TOP10 chemical competent cells (Invitrogen) were used as a host for plasmids DNA. T7 RNA polymerase is absent in TOP10 *E.coli* cell, therefore, the cell is ideal for maintenance reproduction and propagation of plasmid DNA.

## Methods

1 to 5  $\mu$ l of ligation products were added to one vial (50  $\mu$ l) of TOP10 chemical competent cells and then the mixture was incubated on ice for 30 minutes. The cells were heat-shocked

for 30 seconds at 42°C using water bath and then immediately placed on ice 2 minutes. 250 µl of S.O.C. medium (2% Tryptone, 0.5% Yeast extract, 10 mM MgSO<sub>4</sub> 10 mM NaCl, 2.5 mM KCl, 10 mM MgCl<sub>2</sub>, 20 mM glucose) was added to the sample and incubated at 37°C ,180 rpm for 1 hour. 20 µl to 100 µl of mixture was plated onto an LB agar plate containing the 100 µg/ml Ampicillin at 37°C overnight.

#### 2.4.1.7 Isolation of Recombinant Plasmid DNA

TOP10 *E.coli* cell is an excellent candidate for maintenance reproduction and propagation of plasmid DNA. Qiagen mini/midi prep extraction kit was used to isolation of plasmid DNA. The kit consists of a disposable chromatography column which is used for absorption and elution of plasmid DNA. The recombinant plasmid DNA is used for transform into BL21 star (DE3) One Shot *E.coli* cells for protein expression.

#### Methods

Selected fresh colonies from previously transformants (TOP10 *E.coli* cell) were inoculated into 5 ml of LB medium containing 100 µg/ml Ampicillin and incubated at 37°C, 180 rpm overnight. The cultures were used to extract plasmid DNA. The experiment was then carried out using a Qiagen mini/midiprep extraction kit according to the manufacturer's instructions.

#### 2.4.1.8 DNA Sequencing

200 - 500 ng of plasmid DNA isolated from TOP10 *E.coli* cells were sequenced by Functional Genomics and Proteomics Laboratory within the School of Biosciences at University of Birmingham. The sample prepared for sequencing was shown at Table 2-6. Experiment was carried out using an ABI 3730 Analyser and checked using programme BLAST sequence alignment programme [109].

Component	Quantity
Template (plasmid DNA)	200-500 ng
Primer (used PCR to amplify ZipA gene)	3.2 pmol
Deionised water	x $\mu$ l
Terminator Reaction Mix (from Genomics lab)	10 $\mu$ l
Total volume	20 $\mu$ l

Table 2-6. The sample prepared for DNA sequence.

#### 2.4.1.9 Transformation of BL21 Star (DE3) One Shot *E.coli* Cells

BL21 star (DE3) One Shot *E.coli* cells (Invitrogen) were used for high level expression of genes cloned to vector contains bacteriophage T7 promoter such as pET series. The cells contain lysogen of DE3 and carry a chromosomal copy for T7 RNA polymerase gene under the control of *lacUV5* promoter, therefore, allowing protein expression to be induced by

IPTG. OmpT, an outer membrane protease, and *lon* protease are absent in BL21 star (DE3) *E.coli* cells to reduce heterologous protein degradation.

## Methods

5 - 10 ng of recombinant plasmid DNA containing correct sequence (in 1 to 5  $\mu$ l volume) was added to one vial (50  $\mu$ l) of BL21 star (DE3) *E.coli* cells and incubated on ice for 30 minutes. The cells were heat-shocked for 30 seconds at 42°C using water bath and then immediately placed on ice. 250  $\mu$ l of S.O.C. medium was added to the cultures and incubated at 37°C, 180 rpm for 30 minutes. 20  $\mu$ l to 100  $\mu$ l of mixture were plated onto an LB agar plates containing 100  $\mu$ g/ml Ampicillin at 37°C overnight.

### 2.4.2 Small-scale Flask Culture

Selected colonies from successful transformants were inoculated into 5 ml of LB medium containing 100  $\mu$ g/ml Ampicillin. The cells were incubated at 37°C overnight with shaking at 180 rpm. 200  $\mu$ l of 80% glycerol was added to 0.8 ml of the initial culture, and the mixture as the glycerol stock can be stored at -80°C. 3 ml of the initial cultures were diluted into 50 ml of LB medium containing 100  $\mu$ g/ml Ampicillin. The cultures were grown at 37°C and 180 rpm until OD<sub>600</sub> of 1. A stock IPTG was added into culture to make a final IPTG concentration of 0.84 mM, and the cells were grown for another 3 hours. The cells were

harvested by centrifuging at 6,000 x g in a Beckman JA-25.5 rotor for 30 minutes, and the pellets were washed once with 10 mM Tris-HCl buffer, pH 8.

#### **2.4.3 Large-scale Flask Culture**

The *E.coli* colonies expressing ZipA protein were inoculated to 5 ml LB medium with 100 µg/ml Ampicillin. The cells were incubated at 37°C and 180 rpm overnight. A 500 ml of LB medium containing 0.04% sterile glucose and 100 µg/ml Ampicillin was then inoculated with 5 ml of the initial culture, grown at 37°C and 180 rpm until OD<sub>600</sub> of 1. A stock IPTG was then added into culture to make a final IPTG concentration of 0.84 mM and the cells were grown another 3 hours then harvested by centrifuging at 6,000 x g in a Beckman JA-10 rotor for 20 minutes, and the pellets were washed once with 10 mM Tris-HCl buffer, pH 8.

#### **2.4.4 E.coli Membrane Preparation**

*E.coli* membrane preparation was performed as yeast membrane preparation based protocol except the following step which was altered: the homogenizing pressure was 25,000 psi for *E.coli* cells.

#### **2.4.5 Solubilisation with SMA and Purification of SMALP Solubilised ZipA**

Solubilisation step was carried out as previously describe in 2.2.5. Purification of SMALP solubilised ZipA was performed as purification of SMALP solubilised A<sub>2a</sub>R based protocol (§ 2.2.7.2) with the exception of the following changes. The first, 1.5 ml of resin was used in 15 g cell pellet of original culture. The second, an additional wash step with 5 times resin volumes of wash buffer (resuspension buffer plus 80 mM imidazole, pH 8) was required.

#### **2.4.6 SDS-PAGE and Western Blotting of ZipA**

SDS-PAGE and western blotting was achieved according to previously protocol (§ 2.2.8) using 6xHis Monoclonal antibody (Clontech) as the primary antibody.

#### **2.4.7 Identification of ZipA**

The band representing ZipA was excised from SDS-PAGE gel and then submitted to the Functional Genomics and Proteomics Laboratory as previously described (§ 2.2.9).

#### **2.4.8 The N-terminal Sequencing of ZipA**

The purified SMALP-ZipA was loaded into SDS-PAGE gel. The Gel was run for 50 minutes at 200 volts (V) in SDS-PAGE running buffer and then transferred to Polyvinylidene fluoride



(PVDF) membrane. The PVDF membrane was stained with coomassie blue and a band at ~52 kDa was excised from PVDF membrane. The sample was identified by Alta Biosciences at University of Birmingham. The system used for the N-terminal protein sequencing chemistry first devised by Edman. The equipment used by the laboratory is an Applied Biosystems Procise 494HT machine.

#### **2.4.9 FtsZ Protein Preparation**

FtsZ protein used for the interaction experiments between FtsZ and ZipA was kindly provided by Dr. Raul Pacheco-Gomez (University of Birmingham, UK). FtsZ protein was also purified following the protocol described below [133]. Expression plasmid for FtsZ protein was kindly provided from Dr. Raul Pacheco-Gomez.

##### **2.4.9.1 FtsZ Protein Expression**

Plasmid DNA was transformed to BL21 star (DE3) *E.coli* cell was previously describe in 2.4.1.9. The cells were plated onto an LB agar plate containing the 100 µg/ml Ampicillin at 37°C overnight. Selected colonies from the successful transformation experiment were inoculated to 5 ml LB medium with 100 µg/ml Ampicillin. The cells were incubated at 37°C and 180 rpm overnight. A 500 ml of LB medium containing 100 µg/ml Ampicillin and 0.04% sterile glucose was inoculated with 5 ml of the initial culture, grown at 37°C and 180 rpm until OD<sub>600</sub> of 0.4. A stock IPTG was then added into culture to make a final IPTG

concentration of 0.84 mM and allowed cells to grow for another 3 hours. The cells were harvested by centrifuging at 6,000 x g in a Beckman JA-10 rotor for 20 minutes, and the pellets were washed once with 10 mM Tris-HCl buffer, pH 7.9.

#### 2.4.9.2 FtsZ Protein Purification

All work involving protein purification was carried out at 0 - 4°C. Typically 10 g of cells were suspended in 50 ml ice-cold lysing buffer (50 mM Tris-HCl, pH 7.4, 2 mM EDTA, 0.2% protease inhibitor cocktail set IV (Calbiochem)) and poured into an Avestin-C3 cell disrupter. *E.coli* cells were broken by 3 passages through the chilled cell. Unbroken cells and cell debris were removed from the membrane suspension by low-speed centrifugation (10,000 x g in a Beckman JA-25.5 rotor for 30 minutes). The membrane fraction was removed using an ultracentrifuge (150,000 x g in a Beckman Type 70.1 Ti Rotor for 45 minutes). A 30% ammonium sulfate (16.6 g/100 ml of extract) was then slowly added to the supernatant with stirring for 20 minutes. The ammonium sulphate precipitate was collected using a centrifugation (20,000 x g in a Beckman JA-25.5 Rotor for 15 minutes) and resuspended in buffer A (50 mM Tris-HCl, pH 7.9, 50 mM KCl, 1 mM EDTA, 10% glycerol). The sample was dialysed using dialysis membrane (3,500 MWCO, Thermo Scientific) overnight against 3 x 1 litre of buffer A.

The dialysed ammonium sulphate fraction was loaded to Q Sepharose resin (GE Healthcare) with slow rotation for 1 hour. Typically, 3 ml of resin was used in 1 litre of original culture. The resin was washed with 5 times resin volumes of buffer A before the protein was eluted with 250 mM KCl in buffer A. Fractions of 2 ml were collected and examined by SDS-PAGE. The eluted fractions containing pure FtsZ were mixed. Further purification steps were then used to remove contaminating acetate kinase activity [133, 134]. A 20% ammonium sulfate (11 g/100 ml of extract) was added to mixture containing FtsZ with stirring for 20 minutes. The ammonium sulphate precipitate was collected using centrifugation (20,000 x g in a Beckman JA-25.5 rotor for 15 minutes) and resuspended in buffer A. The sample dialyzed overnight against extensive buffer A. The further ion-exchange chromatography was then carried out following the same procedure previously described. The fractions containing pure FtsZ were concentrated using a Vivaspin 20 concentrator (30 kDa cut off, Sigma-Aldrich) and washed extensively with 50 ml of buffer A. The FtsZ protein can be stored at -80°C for more than 1 year.

#### **2.4.10 Protein Quantitation**

ZipA and FtsZ protein quantitation were carried out according to previously described (§ 2.2.10).

## **2.5 Methods: Characterisation of ZipA**

### **2.5.1 Circular Dichroism and Sedimentation Velocity Analytical Ultracentrifugation**

CD and svAUC of ZipA were carried out according to previously protocol (§ 2.3.2 and 2.3.3).

### **The Interaction Experiments Between FtsZ and ZipA**

The sections from 2.5.2 to 2.5.7 described the methods used to characterise the FtsZ-ZipA interaction.

### **2.5.2 Right Angle Light Scattering**

The dynamics of FtsZ polymerisation, steady state and depolymerisation could be measured by Right-Angle Light-Scattering assay (RALS). The experiment was performed according to the preliminary work developed by Mukherjee and Lutkenhaus [135]. This study showed that FtsZ polymerisation reached steady state within the first minute of the reaction, the length of steady state was proportional to the GTP concentration. FtsZ depolymerisation followed this steady state as a result of GTP hydrolysis by FtsZ [135]. In the presence of ZipA protein, the dynamics of FtsZ polymerisation, steady state and depolymerisation could be changed and it provides us the information about the size of FtsZ polymer affected by ZipA.

## Methods

11  $\mu\text{M}$  FtsZ and appropriate ZipA were incubated at 25°C for 10 minutes in polymerization buffer (50 mM MES, pH 6.5, 50 mM KCl, and 10 mM  $\text{MgCl}_2$ ) to give a final volume of 100  $\mu\text{l}$ . The sample was placed into a 0.3 cm path length fluorescence cuvette. The experiments were performed using a Perkin Elmer LS50B spectrofluorimeter. The excitation and emission wavelengths were set at 500 nm, and the excitation and emission slit widths were set at 2.5 nm. A baseline was collected for 2 minutes before 0.2 mM GTP was added to the sample.

### **2.5.3 Linear Dichroism**

Linear dichroism (LD) is a spectroscopic technique that can be used for studying on the orientations of biomolecules in ordered arrays [115]. For example, it has been used to study of oriented peptide in liposomal membrane [136]. Linear dichroism is defined as the difference in absorbance of light polarized parallel and perpendicular to an orientation axis [115]. LD spectrum can be obtained by modifying circularly polarised light of CD spectropolarimeter to linearly polarised light by the addition of a quarter wave plate or by modifying the phase of the lock-in amplifier [133].

## Methods

11  $\mu\text{M}$  FtsZ and appropriate ZipA were incubated at 25°C for 10 minutes in polymerisation buffer (50 mM MES, pH 6.5, 50 mM KCl, and 2.5 mM  $\text{MgCl}_2$ ) to give a final volume of 90  $\mu\text{l}$ . The experiments were performed at room temperature using a Jasco J-715 spectropolarimeter adapted for LD spectroscopy. The sample was then placed into a quartz capillary Couette cell which induces long assemblies to align by applying a shear flow (generated by spinning the capillary). The experiment was carried out with a rotation (7 V) and a blank (non-rotation) was subtracted from each sample measured. Data were recorded using an interval scan measurement programme. The wavelength range was set between 190 nm and 350 nm with a scanning speed of 200 nm/min and data pitch of 0.5 seconds.

### **2.5.4 GTPase Assay**

The inorganic phosphate ( $\text{P}_i$ ) released from enzymatic reactions can be determined by a spectrophotometric method. This method is based on the conversion of 2-amino-6-mercapto-7-methylpurine riboside (MESG) to ribose 1-phosphate and 2-amino-6-mercapto-7-methylpurine by an enzymatic reaction leading to a shift in the wavelength of maximum absorbance from 330 nm to 360 nm [138]. Purine nucleoside phosphorylase (PNP) uses  $\text{P}_i$  released from the action of FtsZ on GTP to convert MESG to ribose 1-phosphate and 2-amino-6-mercapto-7-methylpurine leading to an increase in the absorbance at 360 nm. The

increase in the absorbance at 360 nm can thus be used to quantitate  $P_i$ . The assay can therefore be used to determine the GTPase activity of FtsZ produced when the FtsZ monomer forms FtsZ polymers [133]. It also allows the measurement of the catalytic activity of FtsZ in the presence/or absence of ZipA (Figure 2-10).

In the presence/or absence of ZipA

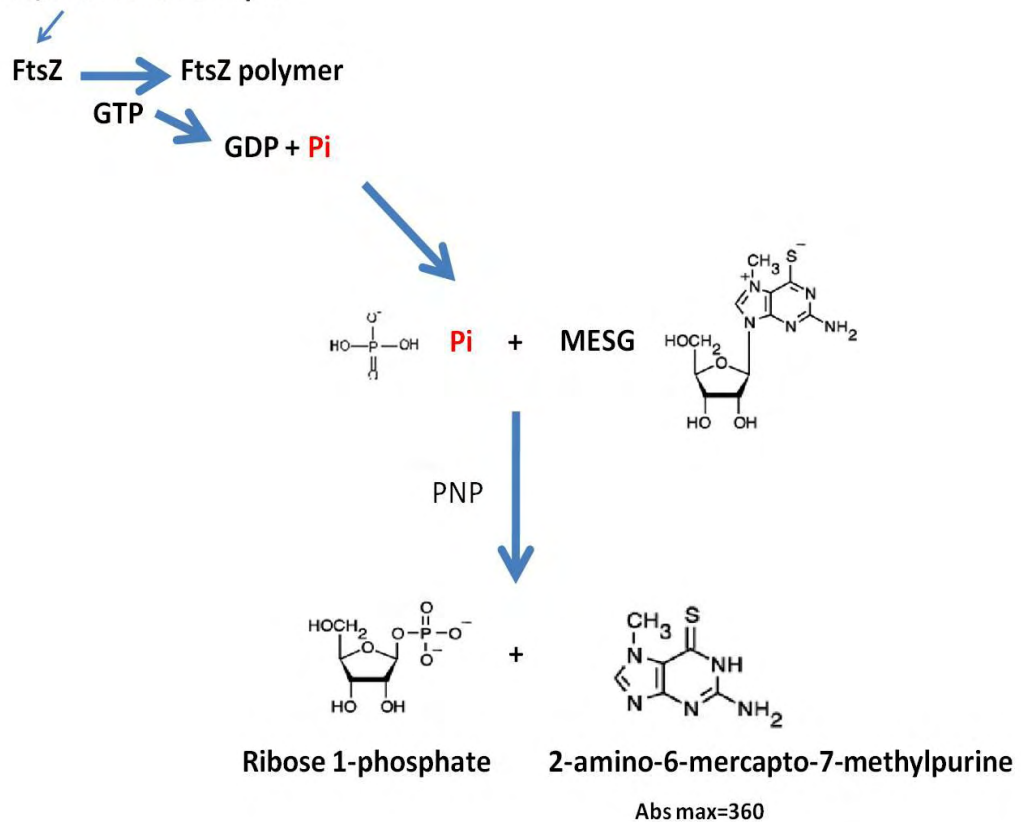


Figure 2-10. Schematic diagram for measuring the catalytic activity of FtsZ in the presence/or absence of ZipA.  $P_i$  is released from GTP hydrolysis catalysed by FtsZ. PNP uses  $P_i$  to convert MESG to ribose 1-phosphate and 2-amino-6-mercapto-7-methylpurine results in shift in the wavelength of maximum absorbance from 330 nm to 360 nm. The change in absorption at 360 nm allows quantification of  $P_i$  and thus determine the catalytic activity of FtsZ in the presence/or absence of ZipA.

## Methods

The experiment was performed using an EnzChek® Phosphate Assay Kit (Invitrogen) based on manufacturer's instructions from Invitrogen. The sample was prepared as described in Table 2-7. The mixture was incubated at 25°C for 10 minutes and placed into a 0.5 cm cuvette. The experiment was carried out using a Jasco V-550 spectrometer at room temperature, and the wavelength was set up at 360 nm. The Abs<sub>360</sub> was zeroed before adding 0.2 mM GTP into the sample.

Compound	Final concentration
dH <sub>2</sub> O	x
MES pH 6.5	50 mM
KCl	50 mM
MgCl <sub>2</sub>	2.5 mM
MESG	0.4 mM
PNP	1 U/ml
FtsZ	11 μM
ZipA	Appropriate

Table 2-7. The components for GTPase assay.



### 2.5.5 Sedimentation Assay

A previous study has described that a sedimentation assay can be used for determining the effect of the FtsZ co-protein YgfE on FtsZ polymerisation [113,137]. The FtsZ polymers can be selectively sedimented to form a pellet leaving unincorporated monomers in the solution.

#### Methods

A protocol for sedimentation assay was similar to published protocol [139]. The samples were prepared as described in Table 2-8. 250 µl mixture containing FtsZ and/or ZipA was made up in the polymerisation buffer and then incubated at 25°C for 10 minutes. 2 mM GTP was added to the sample immediately before centrifugation. Experiments were carried out at 20°C using a rotor TLA 100.2 in Beckman Coulter XL-I analytical ultracentrifuge at 80,000 rpm for 10 minutes. 125µl of supernatant was collected and the remainder was carefully removed. The pellet was resuspended in 250 µl of polymerisation buffer. 20 µl of samples were then taken for analysis by SDS-PAGE gel.

Compound	Sample 1	Sample 2	Sample 3	Final concentration
dH <sub>2</sub> O	+	+	+	x
MES pH 6.5	+	+	+	50 mM
KCl	+	+	+	50 mM
MgCl <sub>2</sub>	+	+	+	2.5 mM
FtsZ	Not added	+	+	11 μM
ZipA	+	Not added	+	Appropriate
GTP	+	+	+	2 mM

Table 2-8. Table 2-7. The components for sedimentation assay.

### **2.5.6 Electron Microscopy**

The proteins were centrifuged at 10,000 rpm for 5 minutes to remove any aggregation protein or large particles. 100 μl reactions containing 11 μM FtsZ with appropriate ZipA were made up in the polymerisation buffer and then incubated at 25°C for 10 minutes. 0.2 mM GTP was added to the mixture immediately before 5 μl of the mixture was transferred to the carbon side of carbon-coated copper grids for 1 minute. The sample was stained by incubating in 1% uranyl acetate solution for 45 seconds before the excess solution was removed. The experiment was carried out using a JEOL 2011 Transmission electron microscope (TEM). The samples were visualised at magnification of 10,000, 30,000 and 50,000.

### **2.5.7 Reconstitution of FtsZ-ring Inside A GUV**

SMA polymer can be removed from purified SMALP solubilised protein by decreasing pH or adding  $MgCl_2$ , the process we termed “de-SMALP”. However, reducing pH can destabilise encapsulated proteins. De-SMALP allows protein to be inserted to the different model system such as GUVs for further studies.

GUVs are large vesicles with diameters of 5  $\mu m$  ~300  $\mu m$  that can to be visualised using optical microscopy [8]. The bilayer can be labelled with rhodamine 6G were prepared by following published protocol allowing GUVs to be seen by confocal microscope [140,141].

#### **Methods**

A stock of  $MgCl_2$  was added to the purified SMALP solubilised ZipA to give a final  $MgCl_2$  concentration of 50 mM. The sample was then dialysed overnight against polymerisation buffer using dialysis membrane (14,000 Molecular weight cut-off, MWCO) that allowed the SMA to exit the sample. The protein can be stored at 4°C for further use.

A 10 mg/ml of lipid mixture contains 40% of DMPC and 60% of egg phosphocholine (PC), were dissolved in methanol. Methanol was evaporated in a fume cabinet under the air current then resuspended lipid with a final concentration of 10 mg/ml in 10  $\mu M$  rhodamine 6G by

vigorous vortexing. Small drops of the mixture was placed on a 4 cm diameter Teflon disc and allowed to dry. The films were then hydrated by covering them with 5 ml of the polymerisation buffer and incubated at 37°C for 3 hours. GUVs were suspended by gentle pipetting to form a turbid layer. 50 µl ~100 µl of GUVs were removed from this layer and used for further experiments.

The de-SMALP ZipA and FtsZ were prepared in the polymerisation buffer to give a final protein concentration of 3.3 µM (or in the absence of de-SMALP ZipA) and 11 µM, respectively. The 67.5 µl of protein sample in the polymerisation buffer were added into GUVs to make up a final volume of 135 µl, the sample was mixed by gentle pipetting and then incubated at 37°C for 15 minutes. GTP was added into the sample to give a final concentration of 2 mM, and then the reaction was observed immediately by Nikon AIR Inverted Confocal microscope at 60 times magnification, the samples were observed for up to 30 minutes.

## **CHAPTER 3: Expression and Purification of A<sub>2a</sub>R**

### **3.1 Introduction**

GPCRs are the largest family of membrane proteins, and these proteins represent, pharmaceutically, the most important receptors in human biology. Research on drugs that target GPCRs currently accounts ~40% of all spending drugs discovery [2]. However, structural characterisation of GPCRs has been limited by problems with protein expression, solubilisation, purification, and preservation of activity *in vitro*.

SMALP, SMA/lipid particle, is a novel nano-reagent that enables a quick and easy purification of membrane proteins without adding any detergent. The preliminary protocol for solubilising and purifying bacterial membrane proteins using this method was recently developed by Knowles *et al.* [49]. These data showed SMALP can stabilise the bacterial membrane protein forming thermostable and soluble nanoparticles suitable for biophysical studies [49]. In this study, the SMALP method was applied for the first time to the purification of a GPCR (human adenosine 2<sub>a</sub> receptor, A<sub>2a</sub>R) directly from the cell membranes.

Earlier studies have shown that A<sub>2a</sub>R has been successful expressed in *Pichia pastoris*, and it was solubilised and purified with detergent [25]. However, the yield of pure receptor was

low and detergents had been shown to hamper further structural characterisation as it disturbs the interplay between conformational states within the GPCR. In this project, we have used the same expression plasmid used in the previous studies in order to compare the SMALP with the detergent method [25].

## **3.2 Results**

### **3.2.1 Expression Screening of A<sub>2a</sub>R**

The A<sub>2a</sub>R expression plasmid consisted of a 10xHis-tag in the N-terminal that enabled detection of A<sub>2a</sub>R expression by Western blotting using anti-His-tagged Monoclonal antibody. A band at 83 kDa was observed from all transformants including the negative control (the sample only containing plasmid without the A<sub>2a</sub>R gene) (Figure 3-1, data not shown for negative control). Previous *Pichia pastoris* studies have shown that this represents non-specific binding to the AOX1 gene product (Dr. Mohammed Jamshad, personal communication). A second band at 58 kDa was observed in most of transformants. However, this was considerably heavier than the calculated value of A<sub>2a</sub>R (47 kDa). Anomalous migration of membrane proteins on SDS-PAGE is a well-known phenomenon [142, 143], so to ascertain whether this band represented A<sub>2a</sub>R, two samples, sample 7 and 8 were chosen for an A<sub>2a</sub>R specific radioligand binding assay. Both samples showed the specific binding to [<sup>3</sup>H]ZM241385, with sample 8 showing better binding capability ( $B_{\max}$  ~9.5 pmol/mg) than

sample 7 ( $B_{\max}$  at fmol/mg level). Therefore, sample 8 was chosen for the further experiments.

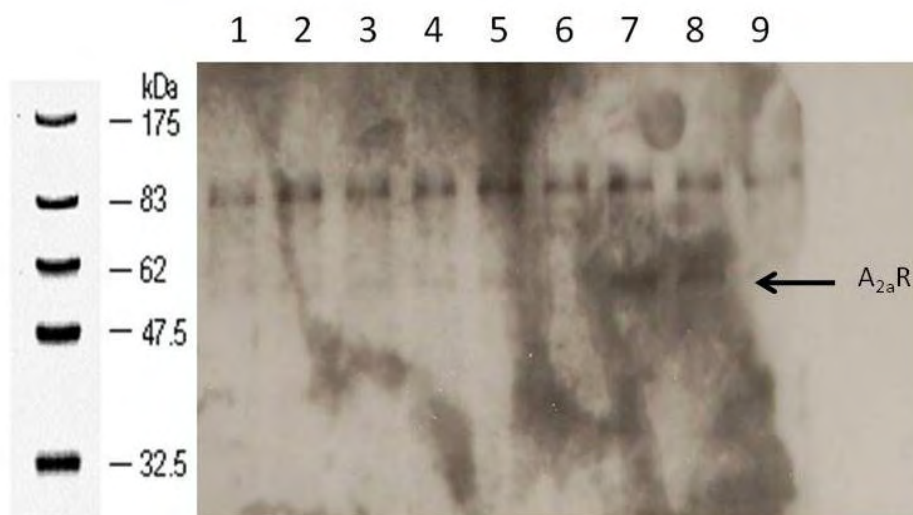


Figure 3-1. Western blotting of an SDS-PAGE using anti-His-tagged antibody for A<sub>2a</sub>R expression screening. Two bands were found on the blot. A band at 83 kDa was observed from all transformants including negative control. This could be non-specific binding with AOX1. The other band at 58 kDa was observed from most of transformants, this band could be A<sub>2a</sub>R. Sample 7 and 8 were chosen for specific radioligand binding assay (since they had the strongest signal on the band of 58 kDa). Sample 8 showed higher binding capability ( $B_{\max}$ ~9.5 pmol/mg).

### **3.2.2 Large-scale Protein Expression**

Obtaining a high protein yield is essential for biophysical and structural analysis of A<sub>2a</sub>R. Two cultures systems were investigated in this study, the flask culture and the bioreactor culture. However, it was found that the bioreactor produced higher biomass (typically 110 g of yeast cells per litre) and hence greater yields. To enhance this yield further a modified

bioreactor protocol was implemented using a mixture of 60% sorbitol and 40% methanol for induction leading to biomasses of up to 160 g wet weight per litre. This compared favourably with the bioreactor culture using solely methanol and at 30°C for induction which obtained an average of ~130 g wet weight per litre. Comparing to the flask culture (with average ~16 g of cell was obtain from one litre culture), the bioreactor culture produced up to 10 times more biomass. Unfortunately, the radioligand binding assays showed low  $B_{\max}$  value on the membrane preparation using a mixture of sorbitol and methanol for induction ( $B_{\max}$  at fmol/mg level). The bioreactor culture inducted using solely methanol at 30°C showed a  $B_{\max}$  value of 3.8 pmol/mg.

The bioreactor cultures (using methanol and at 22°C for induction) and flask cultures (using methanol and at 22°C for induction) had a similar  $B_{\max}$  value ~ 9.5 pmol/mg. Given the high production of sample from the bioreactor cultures it was decided that only bioreactor cultures provided sufficient samples for functional and structural analysis, therefore, the bioreactor cultures were used for large-scale protein expression with the induction conditions utilising methanol at 22°C. Table 3-1 shows A<sub>2a</sub>R expression results by different culture methods and conditions.



Culture methods	$B_{\max}$ (pmol/mg)	Yeast cells obtained (g/litre culture)
Bioreactor cultures (using methanol at 22°C for induction)	9.5	110
Bioreactor cultures (using a mixture of sorbitol and methanol at 22°C for induction)	Only at fmol/mg level	160
Bioreactor cultures (using methanol at 30°C for induction)	3.8	130
Flask cultures (using methanol at 22°C for induction)	9.5	16

Table 3-1. A<sub>2a</sub>R expression results using different culture methods and induction conditions. Bioreactor cultures gave much higher production than flask culture, and using methanol at 22°C for induction showed the highest  $B_{\max}$  (green colour).

### **3.2.3 A Comparison of SMA Solubilisation with Detergent Solubilisation**

So far, solubilisation membrane protein using SMA polymer has only been applied to the protein from bacterial cells by adding SMA and exogenous lipid into membrane sample [49].

SMA had until this point not been used to solubilise a protein from yeast. The first

observation during the experiment showed that SMA successfully solubilised the yeast membranes. The data showed yeast membrane sample became clearer after adding SMA. In addition, smaller pellet after centrifugation of the processed membrane when compared to the control without SMA added (Figure 3-2).

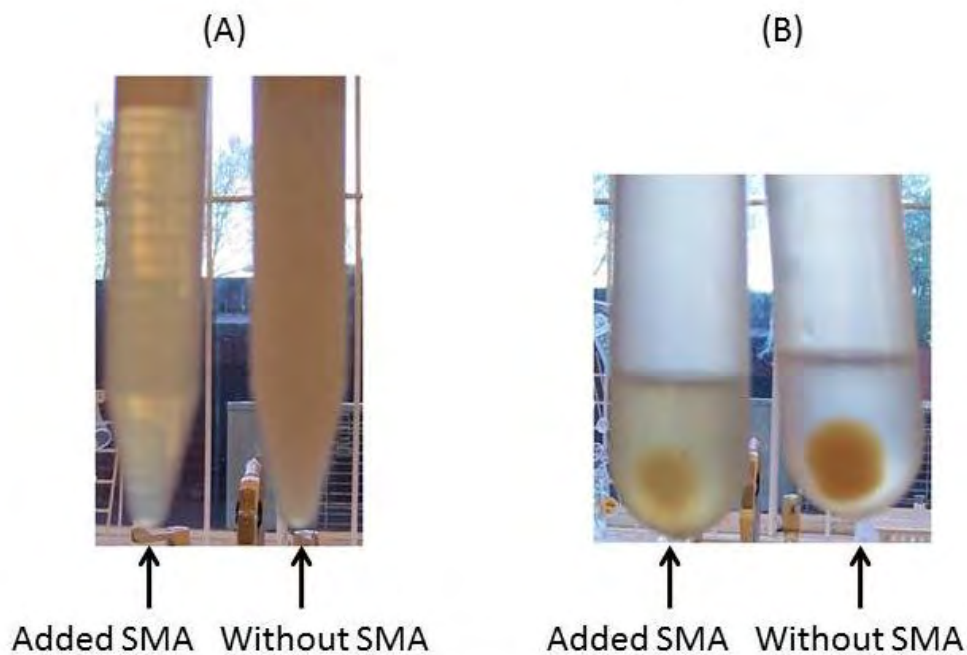


Figure 3-2. (A) The figure showed yeast membrane sample became clearer after adding SMA. (B) The figure showed a smaller pellet in the SMA solubilisation sample after being centrifuged at 150,000 x g.

Previously, n-dodecyl- $\beta$ -D-maltoside (DDM) has been shown to solubilise  $A_{2a}R$  from cell membrane preparations [25, 26, 122]. In order to compare the solubilisation efficiency between SMA and detergent, experiments were carried out using both SMA and DDM. In addition, two types of SMA experiments were carried out with and without exogenous lipid

(1,2-Dimyristoyl-sn-Glycero-3-Phosphocholine, DMPC) (Table 3-2). These experiments were devised to examine whether the SMA method could be used for membrane protein solubilisation in its native environment. In each case, the solubilisation was monitored using radioligand binding assay. These data showed that there was no decrease in the  $B_{\max}$  value upon SMA extraction from the yeast membranes, indicating that the SMA method preserves the function and hence structure of  $A_{2a}R$ . There was also a two fold increase in  $B_{\max}$  value achieved by the addition of DMPC during the course of solubilisation by SMA. The comparison between SMA and DDM solubilisation indicated DDM solubilisation sample had a slightly higher  $B_{\max}$  value (13.6 pmol/mg) than SMA solubilisation sample (9.6 pmol/mg), but  $K_d$  data showed SMA solubilisation had higher affinity (12 nM) than DDM solubilisation sample (43 nM).

Solubilisation condition	$B_{\max}$ (pmol/mg)	$K_d$ (nM)
2.5% SMA with 1% DMPC	9.6	12
2.5% SMA only	4.8	12
2.5% DDM with 0.5% CHS	13.6	43

Table 3-2.  $A_{2a}R$  solubilisation experiments performed using different conditions. These data showed that adding DMPC during solubilisation by SMA results in a two fold increase in  $B_{\max}$  value. DDM solubilisation showed a little higher value in  $B_{\max}$ , but it also showed larger  $k_d$  value (lower affinity).

### **3.2.4 Purification of A<sub>2a</sub>R**

#### **3.2.4.1 SMALP Solubilised A<sub>2a</sub>R Purification Trails**

The IMAC method was chosen to purify SMALP solubilised A<sub>2a</sub>R due to its simplicity and high specificity to the target protein. There were two different methods allowed protein to load onto IMAC resin. The first, involved applying the samples into a pre-packed column by passing the sample over the column with a flow rate of 1 ml/min (column loading). The second, involved loading samples by adding the sample directly onto the resin followed by mixing by slow rotation (batch loading). The data indicated a significant difference between column loading and batch loading method. Column loading (15 ml of resin) led to end yield of less than 0.2 mg of protein per litre bioreactor culture (Figure 3-3). In contrast batch loading of resin (15 ml of resin) produced an end yield of > 3.5 mg of protein per litre bioreactor culture (Figure 3-4). However, this method also yielded samples with significant contamination by other proteins. To resolve this, elutions were then applied onto ion-exchange resin or XAC affinity resin to attempt to increase purity.



Figure 3-3. Silver stained of SDS-PAGE gel showed the very low binding efficiency using column loading method for SMALP solubilised A<sub>2a</sub>R. Lane 1 to 5: elution with 250 mM imidazole. Lane 6: wash with 60 mM imidazole. Lane 7: Flow through: the materials did not bind to the resin.

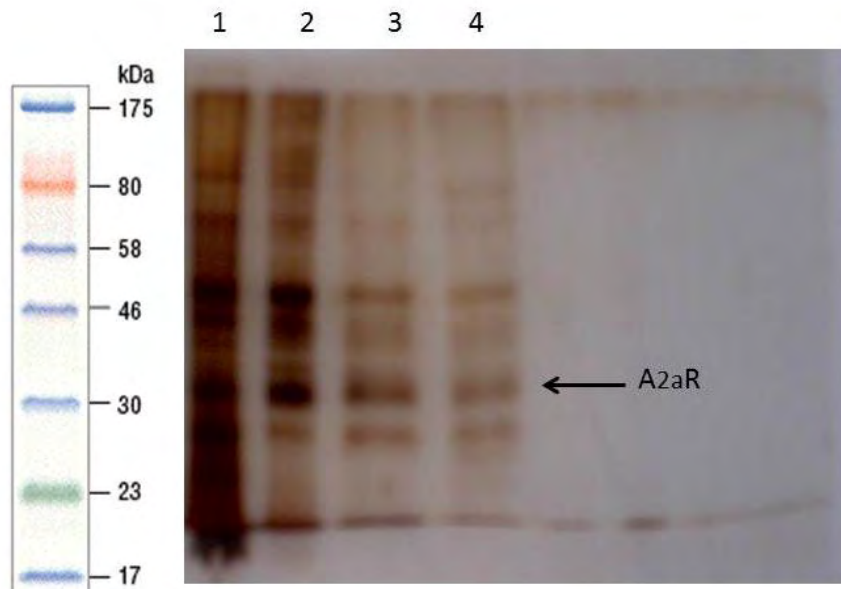


Figure 3-4. Silver stained of SDS-PAGE gel showed the improved binding efficiency using batch loading method for SMALP solubilised A<sub>2a</sub>R. Lane 1 to 4: elution with 250 mM imidazole.

The data from the ion-exchange chromatography experiment showed no improvement in the purity of A<sub>2a</sub>R (Figure 3-5, lane 2). Moreover, the receptor required higher concentration of NaCl (1M) for elution, indicated that the large negative charge of SMALP solubilised A<sub>2a</sub>R interacted strongly the positively charged resin.

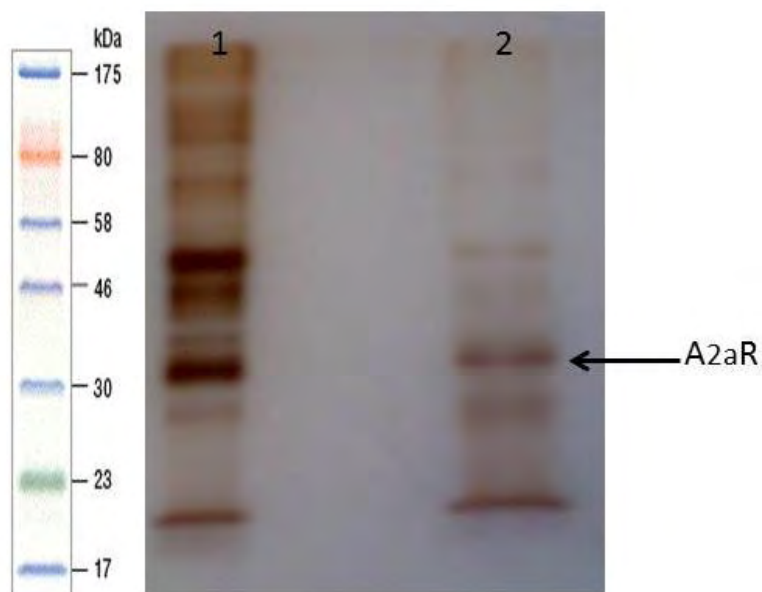


Figure 3-5. Purification of SMALP solubilised A<sub>2a</sub>R using ion-exchange method. Silver stained SDS-PAGE gel showed the purification using ion-exchange method did not improve the purity of protein. Lane 1: IMAC elution. Lane 2: Ion-exchange elution: the protein was eluted in a high concentration of NaCl (1M).

Synthesised XAC resin (XAC, an antagonist of A<sub>2a</sub>R) was also used as an affinity resin to improve the purity of A<sub>2a</sub>R. However, the data showed the purification using XAC resin caused a serious aggregation problem (Figure 3-6). Most of proteins were aggregated and the

radioligand binding assay also showed a low  $B_{\max}$  value (0.5 nmol/mg) for purified SMALP- $A_{2a}R$  purified via this method.

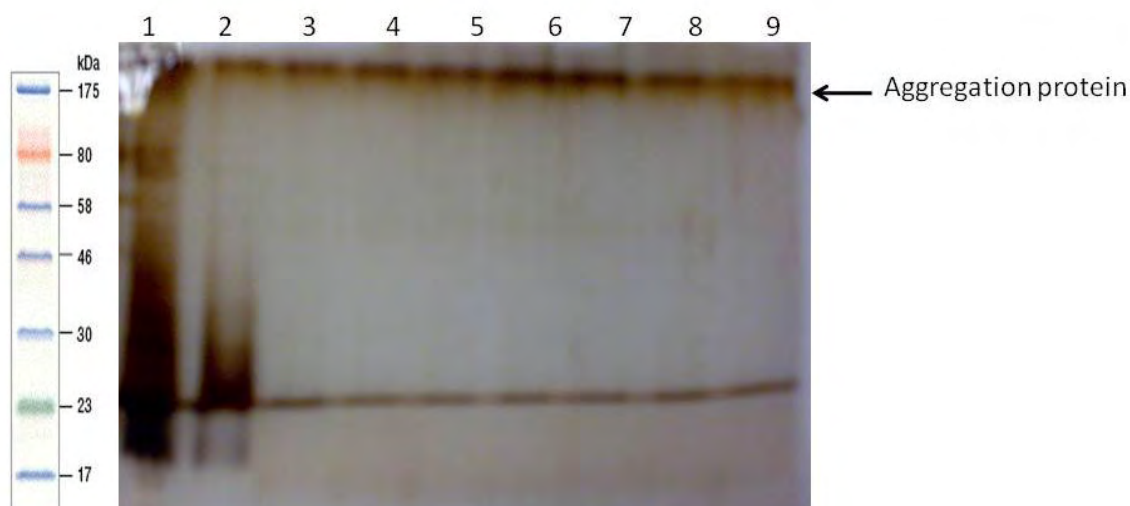


Figure 3-6. Purification of SMALP solubilised  $A_{2a}R$  using synthesized XAC resin. Silver stained SDS-PAGE gel showed the purification using XAC resin caused a serious aggregation problem. Most of proteins were aggregated. Lane 1: Flow through: the materials did not bind to the resin. Lane 2: wash with resuspended buffer (10% glycerol, 500 mM NaCl, 50 mM Tris-HCl, pH 8). Lane 3-9: elutions with resuspended buffer plus 20 mM theophylline.

#### 3.2.4.2 Final SMALP Solubilised $A_{2a}R$ Purification Procedure

Previous study has shown that reducing the volume of IMAC resin used in the purification can have an effect on the purity of the final product (Dr. Eva Hyde, personal communication).

To address the issues of purity in this project, a smaller volume (1.5 ml) of IMAC resin was used for the first stage of purification. Data from this purification showed a substantial increase in purity of the  $A_{2a}R$  with a resulting increase in  $B_{\max}$ . The protein yield was > 1.6

mg (calculated from all eluted fractions) per litre of bioreactor culture after the IMAC purification stage, with a high degree of purity (Figure 3-7).

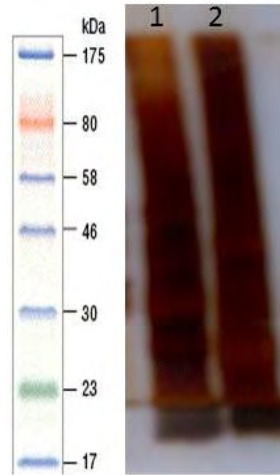


Figure 3-7 (A)

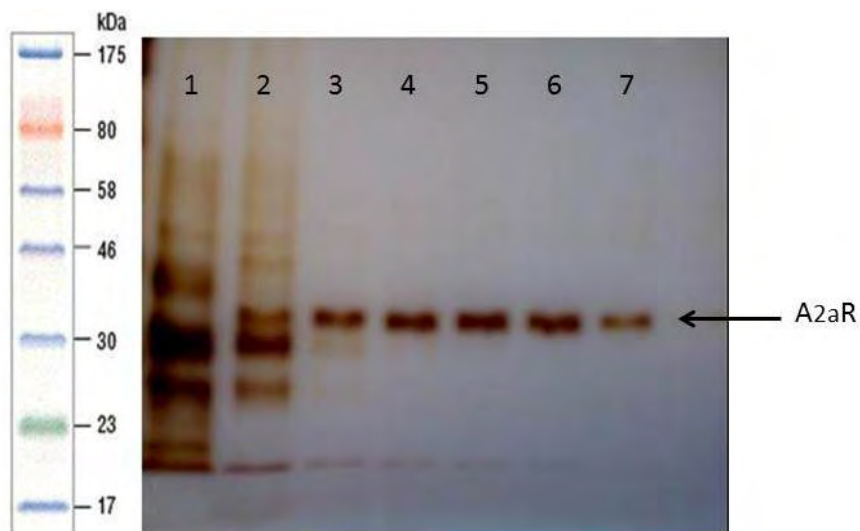


Figure 3-7 (B)

Figure 3-7. Silver stained SDS-PAGE gel showing the increased purification efficiency by IMAC method (small volume of resin and batch loading method). (A) Lane 1: yeast crude membrane .Lane 2:SMALP solubilised materials. (B) Lane 1: wash with 60 mM imidazole. Lane 2 to 7: elution with 250 mM imidazole. These two figures showed the good purification efficiency by this simple SMALP purification method.



Silver stained SDS-PAGE gel showed the receptor from IMAC elutions except eluted fraction 1 (Figure 3-7, lane 2) was already substantially pure, but radioligand binding assay only showed approximately half of theoretical  $B_{\max}$  (21.3 nmol/mg, § 4.2.1). To improve  $B_{\max}$ , the receptors from IMAC elutions (Figure 3-7, lane 3 to 7) were further purified by gel filtration Superdex 200 10/300 GL column to remove any aggregated protein or small peptides (Figure 3-8) (Figure 3-9). The radioligand binding assay for the gel filtered sample showed a  $B_{\max}$  of 20.1 nmol/mg, close to the theoretical  $B_{\max}$  value of 21.3 nmol/mg. These data suggest purified SMALP-A<sub>2a</sub>R from two-step purification process had reached homogeneity and retained its functionality. The final protein yield was ~0.55 mg from one litre bioreactor culture (~ 0.1 mg of A<sub>2a</sub>R can be obtained from one litre flask culture) after this two-step purification process. Table 3-3 shows a summary of purification results by different purification methods.

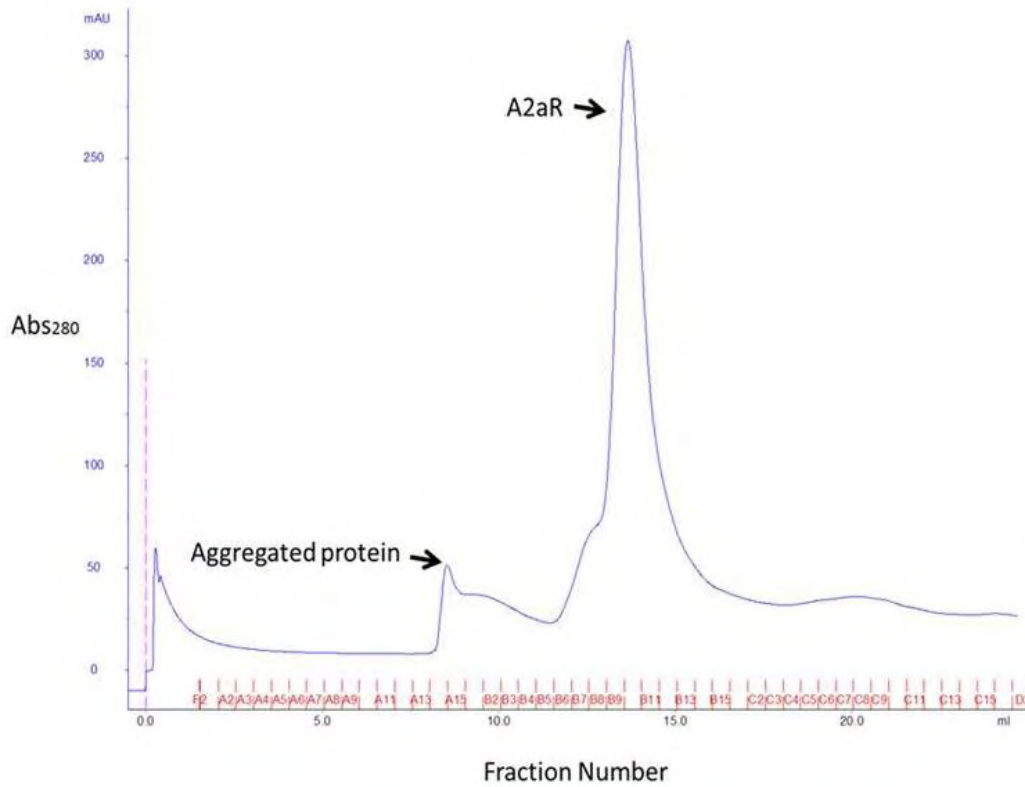


Figure 3-8. Gel filtration of A<sub>2a</sub>R. The data showed some aggregation protein was eluted before the major protein (A<sub>2a</sub>R) was eluted. The fractions of different peak were then examined by silver stained SDS-PAGE gel (Figure 3-9). The experiments were carried out using a Superdex 200 10/300 GL column attached to an ÄKTA™ FPLC purification system. A flow rate was set at 1 ml/min. Absorbance measurements were recorded at 280 nm.

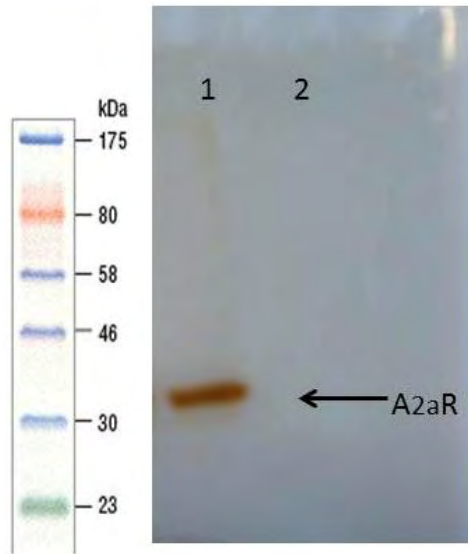


Figure 3-9. Silver stained SDS-PAGE gel for the purification of SMALP solubilised A<sub>2a</sub>R using gel filtration. The gel showed the major peak (Figure 3-8) was A<sub>2a</sub>R. Lane 1: the protein from major peak. Lane 2: the fraction from aggregated peak.

Purification methods	Results
IMAC method by column loading (1 ml of resin)	Very low yield, can not be detected by silver stained SDS-PAGE gel
IMAC method by column loading (5 ml of resin)	Very low yield, can not be detected by silver stained SDS-PAGE gel
IMAC method by column loading (15 ml of resin)	Very low yield, only showed very slight band on silver stained SDS-PAGE gel
IMAC method by batch loading (1.5 ml of resin)	Showing a good purification efficiency
IMAC method by batch loading (15 ml of resin)	Low purity
Ion-exchange method	Did not improve the purity. Requires a very high concentration of NaCl to elute
XAC resin	Serious aggregation problem
Gel filtration	Removes aggregation protein to improve the purity of protein

Table 3-3. A summary for the purification results of SMALP solubilised A<sub>2a</sub>R by different purification methods. The results showed that using two-step purification process including IMAC and gel filtration (green colour) can obtain the best purification result.

#### 3.2.4.3 Purification of Detergent Solubilised A<sub>2a</sub>R

DDM solubilised sample required the use of a three-step purification process to reach homogeneity [25]. We observed an increased level of impurities after the IMAC stage was

applied to the detergent sample compared to the SMALP solubilised sample (1.5 ml resin, batch loading, Figure 3-10).

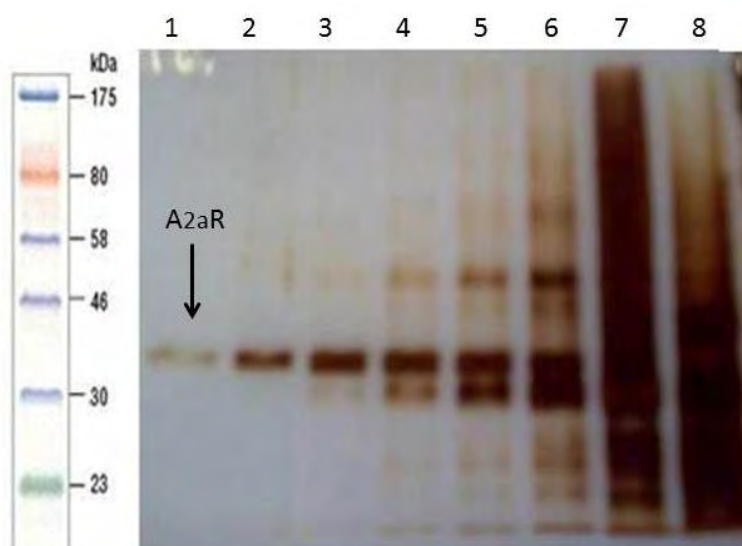


Figure 3-10. Silver stained 10% SDS-PAGE gel of DDM solubilised  $A_{2a}R$  by IMAC method. Lane 1 to 7: elution with 250 mM imidazole. Lane 8: wash with 60 mM imidazole. The elutions (lane 1 to 6) were mixed and further purified by ion-exchange column.

Hence, it was necessary to use ion-exchange column before loading to gel filtration Superdex 200 10/300 GL column. Figure 3-11 and Figure 3-12 showed DDM solubilised  $A_{2a}R$  after ion-exchange and gel filtration step. The protein reached homogeneity after three-step purification process and the final protein yield was ~ 0.5 mg per litre bioreactor culture ( ~ 0.1 mg of  $A_{2a}R$  can be obtained from one litre flask culture). Table 3-4 is the purification table for purified  $A_{2a}R$  by SMALP and detergent methods.

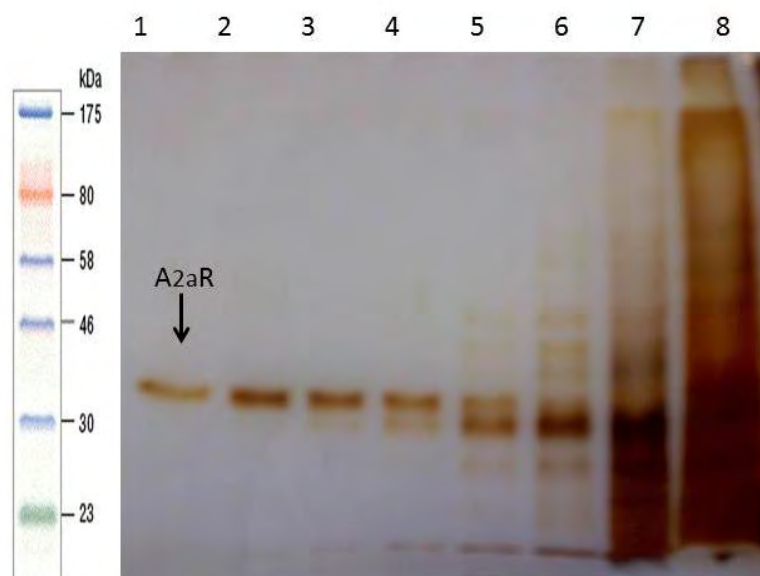


Figure 3-11. Silver stained SDS-PAGE for the purification of DDM solubilised A<sub>2a</sub>R using ion-exchange.

Lane 1 to 6: the protein was eluted with 250 mM NaCl. Lane 7: the protein was washed with 100 mM NaCl. Lane 8: Flow through: the materials did not bind to the resin. The elutions (lane 1 to 4) were mixed and further purified by gel filtration.

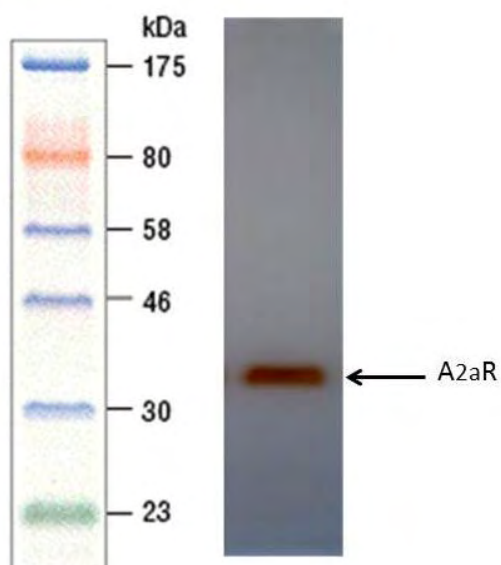


Figure 3-12. Silver stained SDS-PAGE gel for the purification of DDM solubilised A<sub>2a</sub>R using gel filtration. The purified A<sub>2a</sub>R was approached by a three purification step. Only single band was observed on the gel.

Purification step	Total protein (mg)	Specific binding ( $B_{max}$ , pmol/mg)	Total A <sub>2a</sub> R (pmol)	Relative yield (%)	Purification (fold)
Solubilised materials	2835	9.6	27216	100	1
IMAC eluate	1.61	9300	14973	55	968
Gel filtration eluate	0.55	20100	11055	40.6	2093

Table 3-4 (A)

Purification step	Total protein (mg)	Specific binding ( $B_{max}$ , pmol/mg)	Total A <sub>2a</sub> R (pmol)	Relative yield (%)	Purification (fold)
Solubilised materials	2420	13.6	32912	100	1
IMAC eluate	3.82	4500	17190	52.2	330
Q Sepharose eluate	1.51	10200	15402	46.7	750
Gel filtration eluate	0.50	18200	9100	27.6	1338

Table 3-4 (B)

Table 3-4. (A) Purified SMALP-A<sub>2a</sub>R (B) Purified DDM-A<sub>2a</sub>R. Assuming 1 litre yield of A<sub>2a</sub>R purification. Calculating from 0.5 litre bioreactor culture. The purification was carried out as described in the materials and methods section. Protein concentration was determined with CBQCA protein quantitation method. Specific binding was the  $B_{max}$  value of radio-ligand binding assay using [<sup>3</sup>H] ZM241385. Total A<sub>2a</sub>R was calculated by total protein × specific binding. Relative yield was calculated by total A<sub>2a</sub>R of each step ÷ total A<sub>2a</sub>R at solubilised materials. Purification (fold) was calculated by specific binding of each step ÷ specific binding at solubilised materials. The data showed on this table were representative data. Data varies for each preparation, but the final relative yields were always between 30~40.6% for SMALP sample and 25~35% for DDM sample.

### **3.2.5 Receptor Identification and Western Blotting Analysis**

*A band at 34 kDa is an intact A<sub>2a</sub>R*

The purified A<sub>2a</sub>R (for both of SMALP and DDM solubilised samples) ran in SDS-PAGE gels was incubated at 37°C before being loaded into SDS-PAGE gel due to membrane proteins can aggregate in SDS at temperatures over 50°C [147]. The gel showed a single band with an apparent molecular mass of 34 kDa. This is less than the predicted molecular weight of 47 kDa, and that observed in a previous paper [25]. This could be some membrane proteins bind to more SDS than water soluble protein [142, 143]. To demonstrate that the anomalous migration resulted from atypical running behaviour, rather than from proteolysis, we used FT-ICR mass spectrometry and Western blotting to identify and analyse the proteins. The band at 34 kDa was cut from SDS-PAGE gel stained by silver staining, and digested with trypsin before the fragments were identified by FT-ICR. Three peptides were found which were cross referenced with the human proteome. The protein was identified as human adenosine 2a receptor. (Table 3-5).



Peptide Fragments	Peptide Sequence	Peptide Location (amino acid)	Peptide Location
1	YNGLVTTGTR	112-120	Intracellular loop 2
2	QMESQPLPGER	210-220	Intracellular loop 3
3	SHVLRQQEPEFK	305-315	Cytoplasmic domain

Table 3-5. Three Peptide fragments identified by FT-ICR. Purified A<sub>2a</sub>R was determined by SDS-PAGE following stained with silver stain, a band was cut at *ca.* 34 kDa, for trypsin digestion before identified by FT-ICR. The data were then run a search on Mascot to identify the protein and carried out the further analysis using MassLynx software. Peptide location (amino acid) represents the location of this peptide, for example, 112-120 represents this peptide located from 112 to 120 amino acid residue of A<sub>2a</sub>R protein.

Furthermore, Western blotting analysis using both the anti-A<sub>2a</sub>R antibodies and the anti-His-tagged antibodies as a primary antibody, both showed a single band at 34 kDa. The positive result with the anti-A<sub>2a</sub>R antibodies indicated that the C-terminus of A<sub>2a</sub>R was also intact as this antibody bound at the C-terminus of A<sub>2a</sub>R (Figure 3-13, data only shown purified DDM-A<sub>2a</sub>R). The positive result with the anti-His-tagged antibodies indicated that the N-terminus of A<sub>2a</sub>R was also intact as this antibody bound at the N-terminus of A<sub>2a</sub>R (Figure 3-14). These data added to the results of the specific radioligand binding assay provide strong evidence that the purified A<sub>2a</sub>R had retained is an intact, functional A<sub>2a</sub>R.

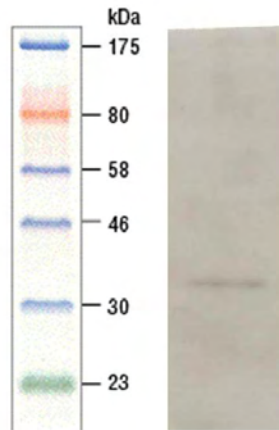


Figure 3-13. Western blotting of purified DDM-A<sub>2a</sub>R. The pure receptor was analysed by Western blotting. Only one band was observed on blot. The primary antibody was anti-A<sub>2a</sub>R antibody with 1: 500 dilutions and the secondary antibody used anti-rabbit IgG HRP-conjugated with 1: 10,000 dilutions. The anti-A<sub>2a</sub>R antibody bound close to the C-terminus of A<sub>2a</sub>R, therefore, indicating that the C-terminus of A<sub>2a</sub>R was intact.

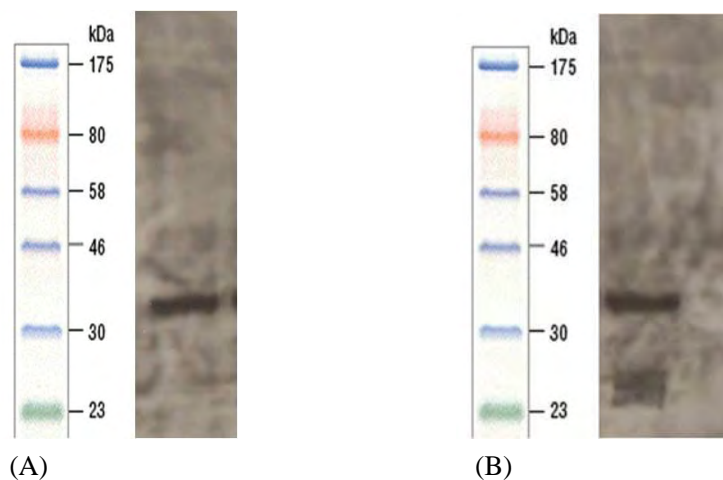


Figure 3-14. Western blotting of purified SMALP and DDM A<sub>2a</sub>R  
 (A) The purified SMALP-A<sub>2a</sub>R (B) The purified DDM-A<sub>2a</sub>R. The pure receptor was analysed by Western blotting using an anti-His-tagged antibodies as primary antibody. Only one band was observed on both blots. The anti-His-tagged of A<sub>2a</sub>R bound close to the N-terminus, therefore, the presence of a band indicates that the N-terminus of both purified SMALP and DDM A<sub>2a</sub>R were intact. The primary antibody was anti-His-tagged antibody with 1: 5,000 dilutions and the secondary antibody was anti-mouse IgG HRP-conjugated with 1: 10,000 dilutions.

### **3.3 Discussion**

Previous published data showed bacterial membrane proteins, PagP and bR can be incorporated into SMALP. These proteins preserve their folded state and activity in SMALP. Here, we have applied SMALP to more difficult protein, A<sub>2a</sub>R, a GPCR. To date, one of the major challenges in the study of GPCRs has been the problem of obtaining a large amount of soluble and functional of protein. This is, in general, due to difficulties in purification, low expression of receptor and difficulty in maintaining the native environment around the protein. We have shown A<sub>2a</sub>R can be expressed in *Pichia pastoris* in bioreactor culture system allowing the production of around 10 times higher cell density compared to flask cultures. Approximately 0.5 mg of purified A<sub>2a</sub>R was produced from a litre bioreactor culture, a sufficient quantity for initial functional and structural studies.

During purification of the receptor, it was found that the SMA solubilisation material produced a higher better  $B_{\max}$  when DMPC was added. It is possible that DMPC makes this disk structure larger, and hence more native lipids can surround the protein to stabilise A<sub>2a</sub>R, or DMPC directly stabilise A<sub>2a</sub>R. Whatever the mechanism, however, this investigation indicates that the lipid is vital importance for preserve receptor functionality. A similar result was also observed in DDM solubilisation A<sub>2a</sub>R indicating that the presence of CHS (an analogue of cholesterol), also results in higher  $B_{\max}$  values during the solubilisation and

purification process [122]. These observations are consistent with demonstrations that membrane protein activity is preserved to a higher degree in the correct lipid environment.

Experiments also showed that purification process of SMALP solubilised A<sub>2a</sub>R is improved by loading sample to a small amount of resin as a slurry rather than loading on resin *in situ* in a column. This may reflect a decreased on-rate for the interaction between the SMALP and the resin. Previous studies on the purification of membrane proteins with His-tagged have also shown that batch loading provides better yield than column loading [122]. Our experiments, remarkably also shown that even a single purification step (IMAC) provides SMALP-A<sub>2a</sub>R that is potentially pure enough for many further analytical studies. Conventionally, purifications of GPCRs and other membrane proteins take a much larger number of steps [25, 122]. For example, unlike purified SMALP-A<sub>2a</sub>R, purified DDM-A<sub>2a</sub>R needs three-step purification process to approach homogeneity [25]. An additional purification step (ion-exchange) was needed to remove the contamination by other proteins to produce a preparation with a  $B_{\max}$  value close to the theoretical  $B_{\max}$  value. The purification table (Table 3-4) shows the relative yield decreased by increase purification step. Therefore, it is important to reduce the number of purification steps to increase the final relative yield.

In addition to purify SMALP solubilised A<sub>2a</sub>R using IMAC and gel filtration methods, we also attempted to use synthesised XAC affinity resin. However, this resin caused a serious aggregation problem, but the reason is still not clear. Additionally, ion-exchange method seems not suitable for SMALP due to the negative charge of polymer.

FT-ICR mass spectrometry, Western blotting and radioligand binding assay showed the band at 34 kDa is an intact and functional A<sub>2a</sub>R. Overall, we have shown that SMALP provides us several advantages for A<sub>2a</sub>R purification. The first, the protein can be solubilised by SMA without any detergent added. The second, quicker method to obtain pure protein than detergent solubilised sample. The third, low cost, SMA polymer is much cheaper than DDM, and simple purification process also decrease the cost of research.

## **CHAPTER 4: Characterisation of A<sub>2a</sub>R**

### **4.1 Introduction**

In order to maintain GPCRs in a native-like membrane environment for their structural and functional studies, these proteins must be isolated in detergent micelles or inserted into a model system such as liposomes or bicelles. However, no single system has been universally satisfactory for use with all techniques used to characterise membrane proteins. In addition, sometimes, maintaining the protein in detergent micelles or a model system requires careful control of experimental conditions within narrow limits, for example, bicelles are very sensitive to solution conditions, and the temperature is defined by the lipid combinations [46,144]. It is therefore often a requirement to use the different systems for different functional and structural studies of a membrane protein. In the chapter 3, we have shown that we have successfully applied SMALP to purify A<sub>2a</sub>R. In this chapter, we characterise purified SMALP-A<sub>2a</sub>R using the radioligand binding assay and several biophysical techniques to show that the SMALP solubilisation process has not affected the receptor structure or function. Additionally, we show that a range of commonly used bioanalytical methods are not disrupted by the SMALP system.

The radioligand binding assay is used to analyse A<sub>2a</sub>R bound to its cognate ligands to prove whether the protein has maintain its activity or pharmacological properties during the solubilisation and purification steps. The biophysical tool, circular dichroism (CD), is then used to provide the information about whether SMALP solubilisation has altered the secondary structure of the protein, and its folded state. The oligomerisation state of protein is then monitored by sedimentation velocity analytical ultracentrifugation (svAUC). Additionally, we compare these experiments with detergent solubilised A<sub>2a</sub>R that provide the information whether SMALP offers improved stability over detergent.

## **4.2 Results**

### **4.2.1 Radioligand Binding Assays**

*Purified SMALP-A<sub>2a</sub>R is fully functional*

The binding capability ( $B_{\max}$ ) of the purified SMALP-A<sub>2a</sub>R (Table 4-1) was studied by radioligand binding assay using [<sup>3</sup>H] ZM241385. The value obtained in this study was close to the theoretical value of 21.3 nmol/mg for a fully active A<sub>2a</sub>R. The theoretical  $B_{\max}$  value of pure A<sub>2a</sub>R (with a predicted molecular weight of 47 kDa), was calculated by assuming a 1:1 = A<sub>2a</sub>R: [<sup>3</sup>H] ZM241385 molar binding ratio, this gave theoretical  $B_{\max}$  value of 21.3 nmol/mg. We have also shown that the affinity constant ( $K_d$ ) of ZM241385 was comparable to previous study [25].

A <sub>2a</sub> R preparation	$B_{\max}$ (pmol mg <sup>-1</sup> )	pK <sub>d</sub> (-log K <sub>d</sub> )
Yeast membrane	9.5	8.11 ± 0.18
SMALP solubilised material	9.6	-
IMAC eluate	9300	-
Gel filtration eluate	20100	8.42 ± 0.16

Table 4-1.  $B_{\max}$  and pK<sub>d</sub> of purified SMALP-A<sub>2a</sub>R from membrane preparation to gel filtration eluate. The values represented here are the mean values of 2 or 3 determinations.  $B_{\max}$  and K<sub>d</sub>/pK<sub>d</sub> values were obtained by saturation binding of [<sup>3</sup>H]-ZM 241385. The resulting binding curves were fitted to a single site model using PRISM Graphpad v4.0.

To confirm that the binding profile of SMALP solubilised A<sub>2a</sub>R was not significantly different from that observed in the native membranes (compared to previous report) [25].

SMALP solubilised A<sub>2a</sub>R was pharmacologically characterised using a range of cognate ligands including ZM241385, theophylline, XAC (Xanthine amine congener) and NECA (*N*-ethylcarboxamidoadenosine), which have various affinity and efficacy, in competition radioligand binding assays (Table 4-2 and Figure 4-1). These data showed that SMALP solubilised A<sub>2a</sub>R is still able to bind these ligands with affinities near to that of A<sub>2a</sub>R in native membranes.



Ligands	pK <sub>i</sub>	K <sub>i</sub>	K <sub>i</sub> (crude, A <sub>2a</sub> R membrane) [25]
ZM241385	9.47 ± 0.25	0.38nM	3.3 ± 0.6 nM
XAC	6.55 ± 0.16	280 nM	43.9 ± 0.4 nM
NECA	4.82 ± 0.67	15 μM	1.3 ± 0.3 μM
Theophylline	4.35 ± 28	47 μM	35.3 ± 1.9 μM

Table 4-2 Affinity values for several different ligands binding to SMALP solubilised A<sub>2a</sub>R.

This table compares the K<sub>i</sub> and the pK<sub>i</sub> values (-log(K<sub>i</sub>)), in comparison to the K<sub>i</sub> values for the same ligands on the A<sub>2a</sub> receptor expressed in *Pichia pastoris* membranes as reported by Fraser [25]. Values reported here are the mean values ± s.e.m, and n (number of repetitions) =3.

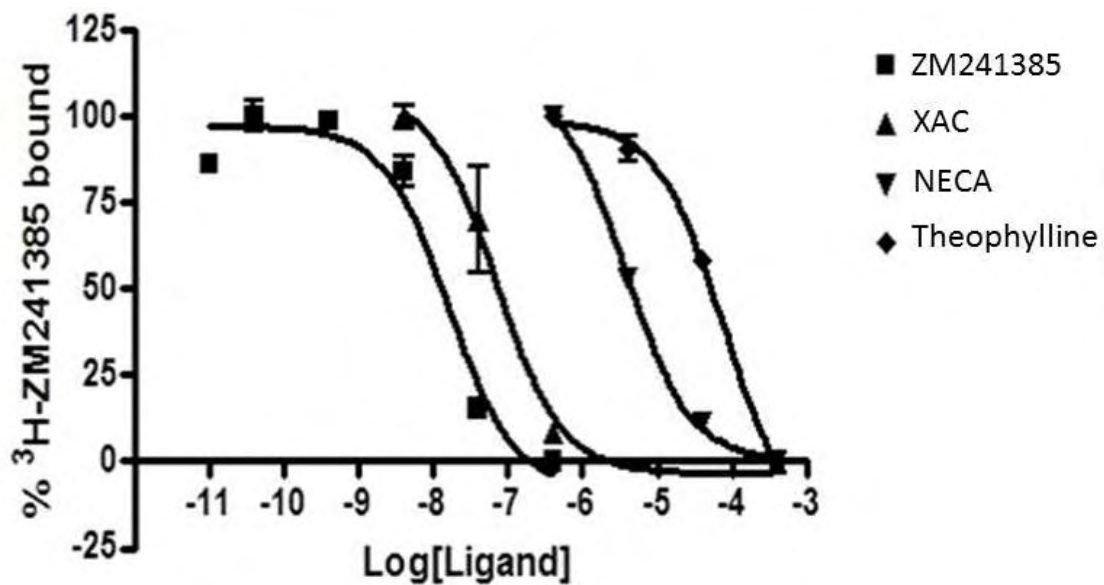


Figure 4-1. Displacement of 1nM [<sup>3</sup>H]-ZM241385 from SMALP solubilised A<sub>2a</sub>R by unlabelled ZM241385, NECA, theophylline and XAC. Representative data from an experiment repeated in triplicate. Each point is the mean value ± s.e.m.

Detergents often strip away the lipids from the receptor making membrane proteins unstable. It is therefore important to investigate whether SMALP offers a more stable environment than detergents. A preliminary report by Knowles *et al.* showed that SMALP can exert a stabilising effect on membrane proteins [49]. If, as we propose, the SMALP maintains a native-like membrane environment around A<sub>2a</sub>R, then it may be expected that the stability of the protein should be enhanced compared to A<sub>2a</sub>R solubilised in detergents. To address this, experiments that involved incubating A<sub>2a</sub>R at elevated temperatures for a set time (30 minutes) were carried out. The samples were then cooled on the ice and the retention of ligand binding activity was measured. This experiment showed that there were observable differences between the two solubilisation methods. The SMALP solubilised A<sub>2a</sub>R maintained ligand binding competency after exposure to higher temperatures than that observed for DDM solubilised A<sub>2a</sub>R (T<sub>1/2</sub> for SMALP of 49.93 ± 1.19 vs 44.40 ± 0.27 for DDM, n=3, P<0.05, Students t) (Figure 4-2). Whatever the mechanism, however, in contrast to DDM solubilised A<sub>2a</sub>R, it is clear that the SMALP protects the protein more effectively from exposure to elevated temperatures.

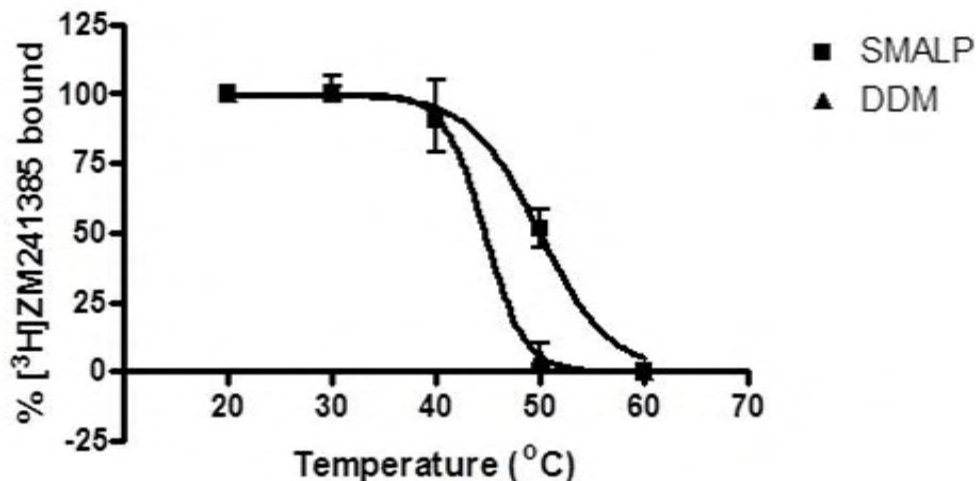


Figure 4-2. Thermostability of SMALP or DDM solubilised A<sub>2a</sub>R. Receptors solubilised with either SMALP or DDM were incubated for 30 minutes at the indicated temperature and the amount of [<sup>3</sup>H] ZM241385 bound was determined. Binding is expressed as % of [<sup>3</sup>H] ZM241385 bound at 20°C. Points are means ± s.e.m of three experiments.

#### **4.2.2 Circular Dichroism Studies**

*CD spectrum of purified SMALP-A<sub>2a</sub>R shows that the receptor is a well folded protein*

A far-UV region (195 - 260 nm) CD spectrum of purified SMALP-A<sub>2a</sub>R revealed a high  $\alpha$ -helix content (negative signal at 208 and 222 nm) indicating a well folded protein (positive signal between 190 - 200 nm) (Figure 4-3, A), it was consistent with the known structure of A<sub>2a</sub>R, the class A GPCRs with high  $\alpha$ -helical component [25, 57]. The CD data suggest that A<sub>2a</sub>R maintains a native folded structure within SMALP. Purified DDM-A<sub>2a</sub>R also showed a high  $\alpha$ -helix component, consisting with the report by Fraser (Figure 4-3, B) [25].

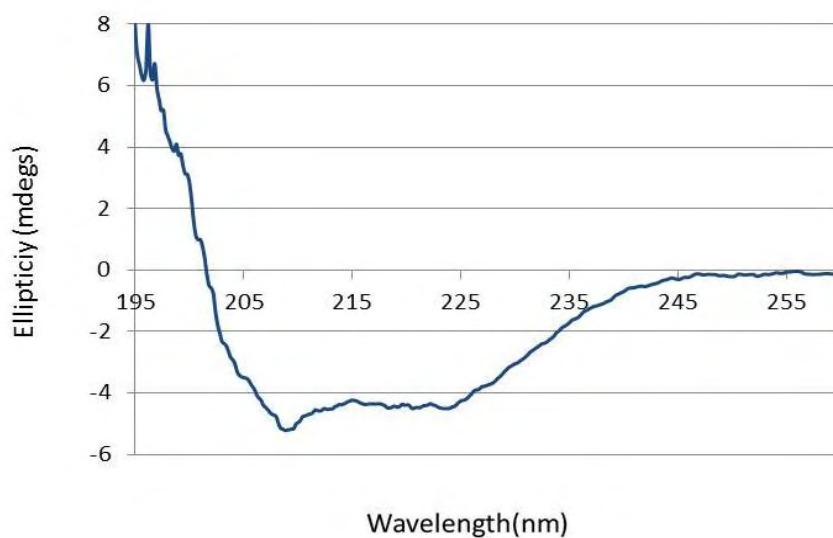


Figure 4-3 (A) CD spectrum of purified SMALP-A<sub>2a</sub>R

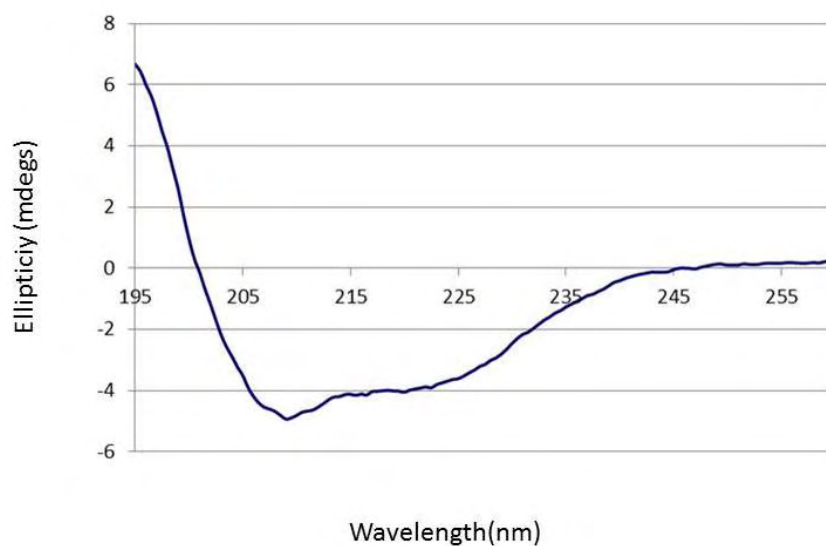


Figure 4-3 (B) CD spectrum of purified DDM-A<sub>2a</sub>R

Figure 4-3. Both of purified SMALP-A<sub>2a</sub>R and purified DDM-A<sub>2a</sub>R showed that preserved the high  $\alpha$ -helical content in their secondary structure, indicating a well-folded receptor, consists with the known structure of A<sub>2a</sub>R [25, 57]. CD data were collected using a JASCO J-715 spectropolarimeter. CD spectra were collected using a 1 mm path length cuvette and averaged over 8 scans in the far-UV domain. Spectra acquired were corrected for the buffer signal. Protein concentrations for purified SMALP/detergent A<sub>2a</sub>R were 0.05 mg/ml.

The effects of increasing temperature on the secondary structure of purified SMALP/ DDM A<sub>2a</sub>R were also studied using CD (Figure 4-4). The results showed a clear gradual decrease in amplitude of the CD signal at the wavelengths that correlate to  $\alpha$ -helix content. Surprisingly, for both samples (SMALP and detergent), the CD signal had not completely changed to that of a random coil even at 95°C (the CD spectrum of a random coil protein is characterised by an intense negative band at 200 nm and a positive band at 218 nm, sometimes, it accompanies with a very weak negative band at 235 nm [133]). This indicates that A<sub>2a</sub>R conformation was relatively resistant to thermal denaturation compared to that generally observed for globular proteins from mesotherms. Comparison of the thermal denaturation of purified SMALP/DDM A<sub>2a</sub>R showed a slight difference between the two samples when the temperature was increased to 95°C. However, the majority of the  $\alpha$ -helical secondary structure still maintained.

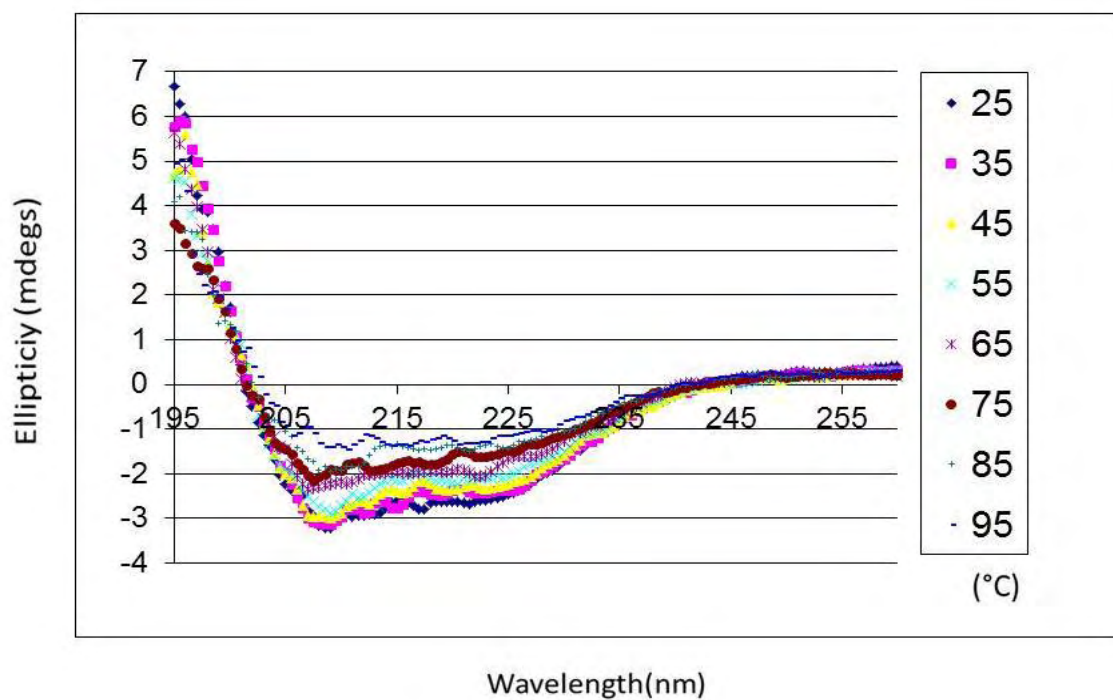


Figure 4-4 (A). CD study of the thermal stability of purified SMALP-A<sub>2a</sub>R

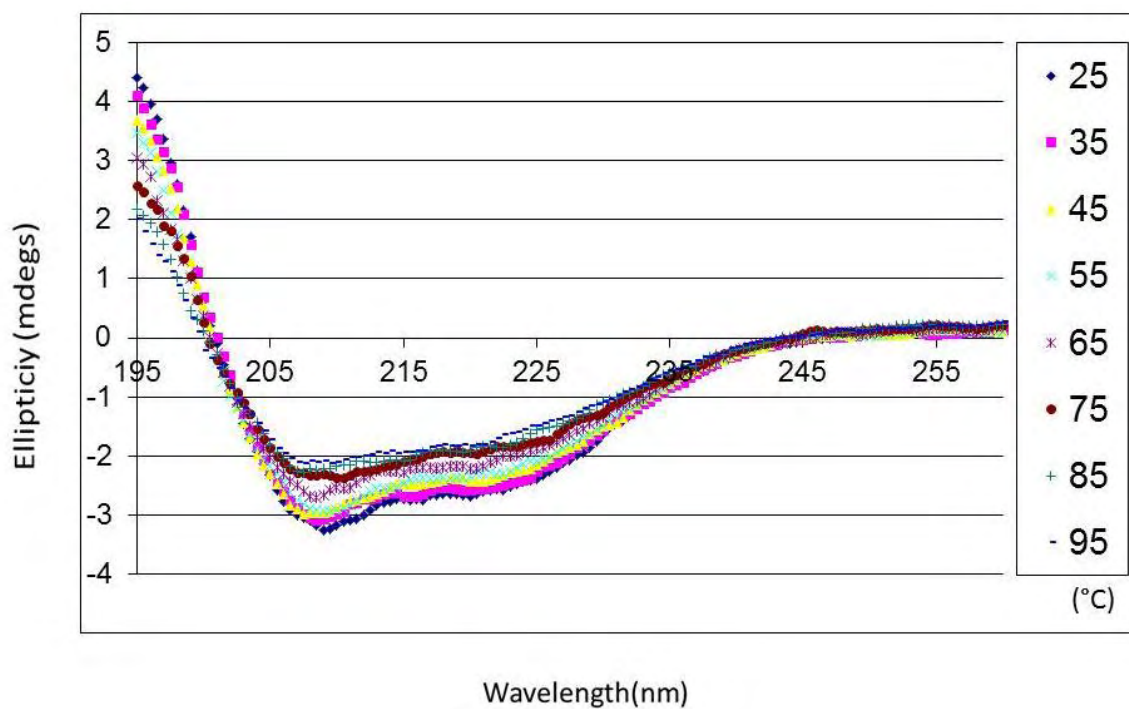


Figure 4-4 (B). CD study of the thermal stability of purified DDM-A<sub>2a</sub>R

Figure 4-4. CD spectra of the thermal stability experiment for the purified SMALP/DDM A<sub>2a</sub>R. The CD intensity (in mdegs) of the spectra increase with increasing temperature from 25°C to 95°C, (spectra

measured at intervals of 10°C). Even at the maximum temperature measured (95°C), significant secondary structure remains in both samples. CD data were collected using a JASCO J-810 spectropolarimeter. CD spectra were collected using a 1 mm path length cuvette and averaged over 8 scans in the far-UV region (from 195 to 260 nm). Spectra acquired were corrected for the buffer signal. Protein concentrations for purified SMALP/DDM A<sub>2a</sub>R were 0.03 mg/ml.

Moreover, the negative signal at 222 nm (characteristic of  $\alpha$ -helical motifs) also suggests that both purified SMALP/DDM A<sub>2a</sub>R were still folded at 95°C even CD intensity of the spectra increase with increasing temperature at 222 nm (Figure 4-5). Taken together these data indicate that at least at the level of secondary structure there is no difference in thermal stability of the two preparations.

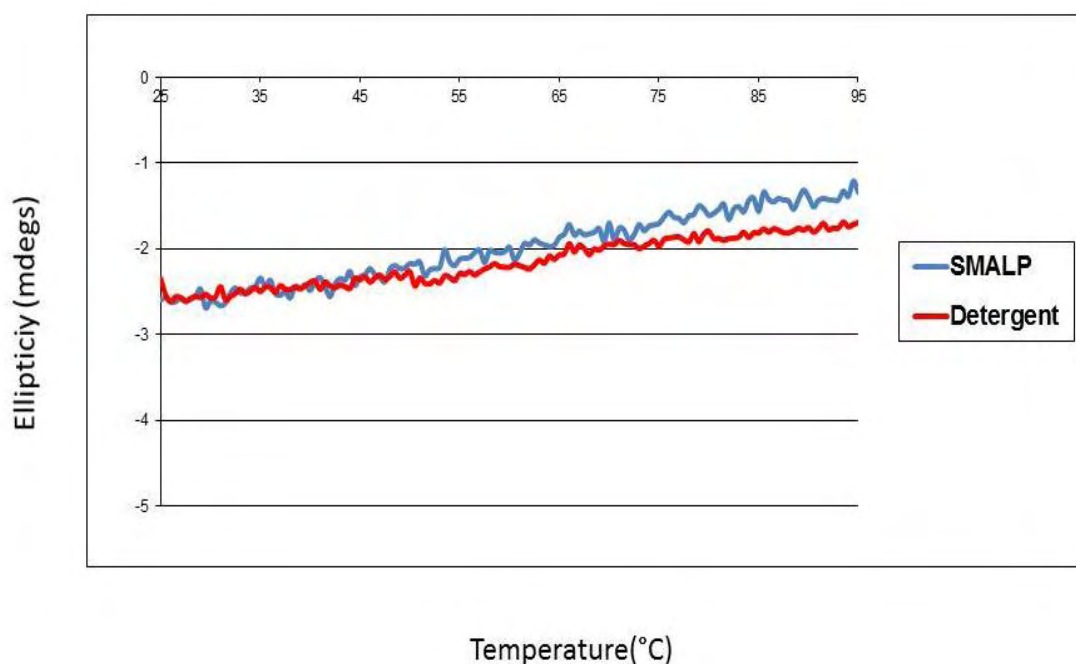


Figure 4-5. CD thermal study of purified SMALP-A<sub>2a</sub>R and DDM-A<sub>2a</sub>R monitored at 222nm showed their unfolding profiles. The data suggest both samples still maintained of their secondary structure at 95°C even though larger values at 222 nm (less negative) were observed at lower temperatures. CD data were collected using JASCO J-810. CD spectra were collected using a 1 mm path length cuvette and averaged over 8 scans at 222 nm. Spectra acquired were corrected for the buffer signal. Protein concentrations for purified SMALP/DDM A<sub>2a</sub>R were 0.03 mg/ml.

#### **4.2.3 Sedimentation Velocity Analytical Ultracentrifugation**

Given the size of the SMALP, it is possible that more than one receptor could be encapsulated into the particle. To address this issue, sedimentation velocity analytical ultracentrifugation (svAUC) was used to probe the oligomerisation of the protein in the particle (Figure 4-6). SEDFIT analysis of these data using the c(M) model produced an intense peak at 91 kDa, this is likely to be a A<sub>2a</sub>R encapsulated in SMALP accompanied by



two minor peaks at 16 and 51 kDa. The first minor peak (16 kDa) had the molecular masses close to the data from equivalent svAUC experiments carried out on free SMA (16 kDa). This peak is also commonly observed in other SMALP purifications (Dr. Tim Dafforn, personal communication). The other minor peak (51 kDa) is likely to be empty SMALP, however, this peak had a different molecular mass peak to that from equivalent svAUC experiments carried out on other SMALP purifications, such as purified SMALP-ZipA (data shown in 6.2.2). This different behaviour could be the empty SMALP since it has been suggested that SMALP may contain different lipid components within different conditions, for example, yeast and bacterial cell membranes have different lipid components. The intense higher molecular peak can therefore be attributed to the presence of purified SMALP-A<sub>2a</sub>R (91kDa).

An approximate measure of the mass of the encapsulated A<sub>2a</sub>R can then be determined by subtraction of the mass of the empty SMALP, which yields a mass of approximately 40 kDa. However, this mass does not completely match the expected theoretical size of 47 kDa. This might be due to a different volume of lipid between empty SMALP and purified SMALP-A<sub>2a</sub>R, therefore, resulting in this shifting.

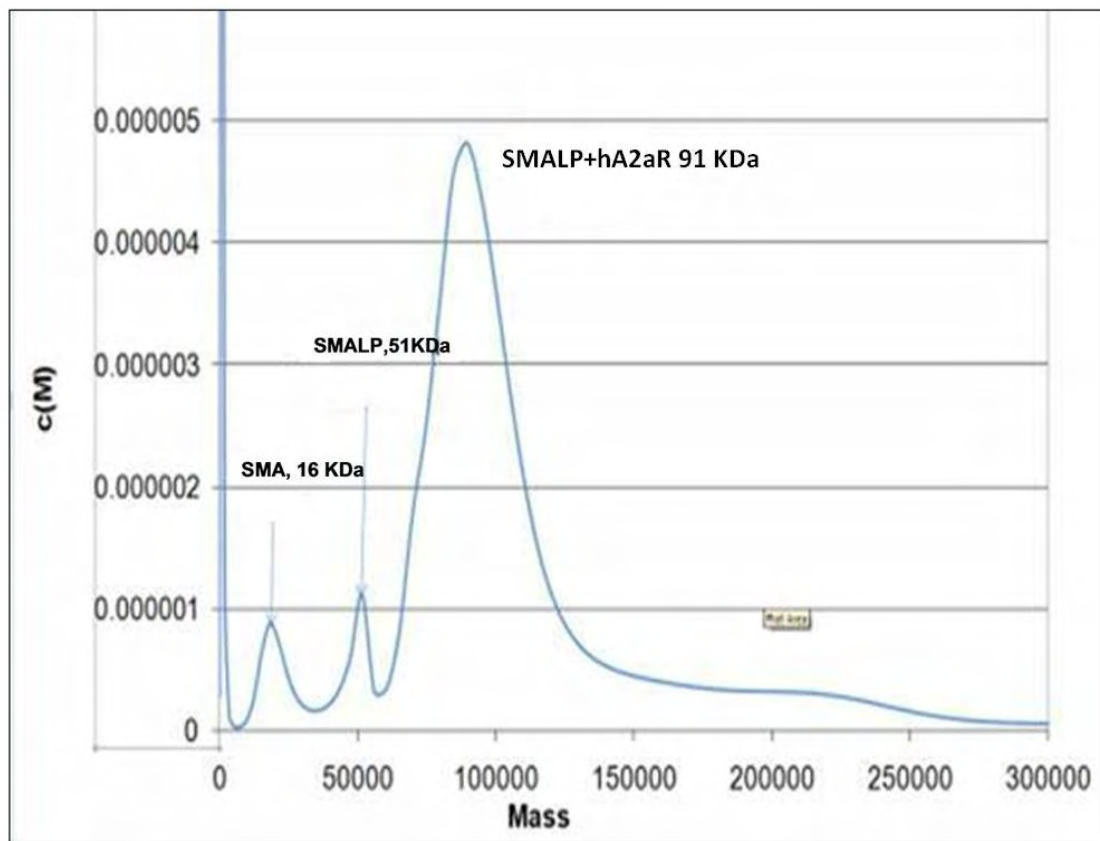


Figure 4-6. A SEDFIT  $c(M)$  deconvolution of Sedimentation Velocity Analytical ultracentrifugation data collected on purified SMALP-A<sub>2a</sub>R showing the presence of 3 peaks corresponding to SMA (16 kDa), the empty SMALP (51 kDa) and A<sub>2a</sub>R encapsulated in SMALP (91 kDa). Data were collected on a Beckman XL-I proteome lab at 40,000 rpm with the migration of the particles being monitored by scanning the cells at 280 nm.

#### **4.2.4 Electron Microscopy**

It has been shown that purified SMALP-PagP has a nanodisk structure with diameter of  $11.2 \pm 1.4$  nm [49]. A<sub>2a</sub>R is a 7 transmembranes protein which is larger than PagP, additionally, the lipid component in the yeast cell membrane is different to that of bacterial cell membranes. It is possible that the purified SMALP-A<sub>2a</sub>R should be a nanodisk structure and it may have

different dimensions compared to purified SMALP-PagP. TEM is the best way to visualise purified SMALP-A<sub>2a</sub>R. TEM micrograph of purified SMALP-A<sub>2a</sub>R (×40,000) showed purified SMALP-A<sub>2a</sub>R was a nanodisk structure (Figure 4-7). This nanodisk structure had a diameter approximately  $20 \pm 2.5$  nm, it suggests SMALP is highly flexible which can be incorporated with the different size of proteins.

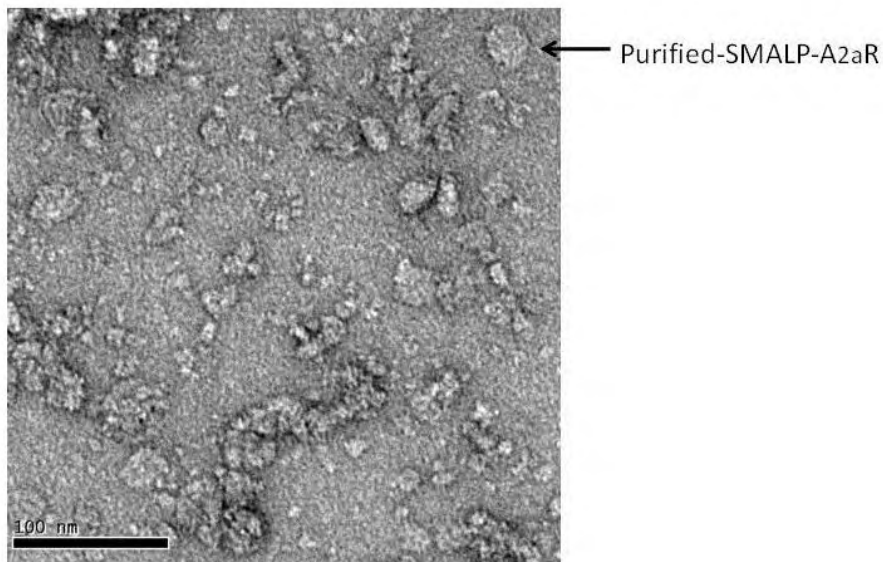


Figure 4-7. TEM micrograph of uranyl acetate stained purified SMALP-A<sub>2a</sub>R (×40, 000) showed purified SMALP-A<sub>2a</sub>R is a nanodisk structure. This nanodisk structure has a diameter approximately  $20 \pm 2.5$  nm. Selected areas were photographed at ×40,000. Scale bar represents 100 nm. The experiment was carried out using a JEOL 2011 transmission electron microscope. The sample was stained with 1% uranyl acetate solution.

### **4.3 Discussion**

Numerous systems have been developed for studying membrane proteins that claim to maintain them in a native-like membrane environment, but all have drawbacks (described in the chapter 1). In the chapter 3, we have addressed the purification results of A<sub>2a</sub>R using SMALP method. In this chapter, we have shown the subsequent studies for the purified SMALP-A<sub>2a</sub>R that confirms that the protein has both structure and activity.

Radioligand binding assays showed purified SMALP-A<sub>2a</sub>R is fully functional. In addition, SMALP solubilised A<sub>2a</sub>R was pharmacologically characterised using a range of ligands including ZM241385, theophylline, XAC and NECA, these data showed that SMALP solubilised A<sub>2a</sub>R is still able to bind to these ligands and the affinities are near A<sub>2a</sub>R in the native membrane. Subsequent CD study showed purified SMALP-A<sub>2a</sub>R is a well folded protein. Taken together these data confirm that A<sub>2a</sub>R maintain its native activity and structure during the solubilisation and purification using SMALP method. svAUC data showed purified SMALP-A<sub>2a</sub>R is mainly monomeric. In addition, TEM data indicated SMALP is flexible due to the size of purified SMALP-A<sub>2a</sub>R is obviously different from purified SMALP-PagP. Therefore, SMALP system could be incorporated with more different architectures of proteins.

The thermal stability experiments using radioligand binding assay and CD showed the different results. The radioligand binding assay showed SMALP solubilised A<sub>2a</sub>R maintains higher activity open exposure to elevated temperature than DDM solubilised A<sub>2a</sub>R, but CD data indicated that at least at the level of secondary structure there is no difference in thermal stability between SMALP and DDM samples. The reason for this difference could either be due to differences in the methods used or an indication that loss of activity is not accompanied by a change in secondary structure. The samples used for radioligand binding assay were incubated at elevated temperatures for 30 minutes, and then placed on the ice. However, the samples used for CD thermal stability were heated at elevated temperatures for a minute and measure the signal continuously. These data indicated, upon cooling, SMALP sample returns to an active conformation, and hence SMALP offers a better thermal stable environment than detergent. This may mean that the SMALP protein is protected from some kind of aggregation compared to the DDM solubilisation. This is backed up by the lack of a CD signal difference as aggregation can sometimes occur without significant unfolding of the protein [145].

Overall, SMALP provides a novel method for membrane protein study which might be suitable for most analytical study tools. Furthermore, SMALP offers more thermal stable environment than detergent. Purified SMALP-A<sub>2a</sub>R is fully functional and well-folded.

Therefore, SMALP may offer a solution to obtain “native” GPCRs crystal structure in the future.

## **CHAPTER 5: Expression and Purification of ZipA**

### **5.1 Introduction**

The previous chapter showed how SMALP could be used to purify a mammalian protein with 7 transmembrane helices from a yeast expression system. In this chapter we showed how the same system can be used to purify a protein with a completely different architecture from a different expression system. It is hoped that the results from this study will demonstrate the wide applicability of this technique.

Cell division is a critical process for all living organism by which a cell divides into two or more daughter cells. In *E.coli* cells, there are at least 15 proteins involved in cell division. One of these proteins, FtsZ, is the first protein appears at the division site, it is an essential protein for bacterial cell division and it forms FtsZ-ring. Another cell division protein, FtsZ-interacting protein A (ZipA), is an integral inner-membrane protein contains a single transmembrane domain. ZipA is located in a FtsZ-ring structure at division site, and fulfils an essential role on the assembly and function of FtsZ-ring. In fact, it has been found that cells depleted of ZipA can grow, but can not divide [100].

However, the mechanism of how ZipA interact with FtsZ is not clear. This is because, as with most membrane proteins, it is difficult to maintain protein in native-like environment to preserve its native structure and function. Therefore, in this study, we purified ZipA using SMALP system to maintain the protein in a native-like membrane environment.

In this chapter, we showed the results of the expression and purification of ZipA using expression plasmid in an *E. coli* host to obtain the purified SMALP-ZipA. The purification progress was monitored by SDS-PAGE gels, and the identification of ZipA was confirmed by FT-ICR mass spectrometry. Moreover, we also showed the data for the expression and purification of FtsZ. These two proteins will be used for subsequent FtsZ-ZipA interaction experiments (describe in the chapter 6).

## **5.2 Results**

### **5.2.1 Plasmid Construction, *Escherichia coli* Strains and Transformation**

#### **5.2.1.1 Extraction of *Escherichia coli* Genomic DNA**

Genomic DNA was extracted from TOP10 *E. coli* cells. The concentration of DNA was determined by absorbance at 260 nm. The quality of DNA can be determined by the ratio of  $Abs_{260}/Abs_{280}$  (Table 5-1). This ratio should be located between 1.8 and 2.0 (If the ratio is below 1.8, it represents the sample is protein contamination; the ratio is over 2.0, it represents



the sample is RNA contamination). Table 5-1 showed that the concentration and quality of sample 1 was better than sample 2, thus sample 1 was diluted 100 times by deionised water, and then used for further experiments.

	Concentration (ng/μl)	A <sub>260</sub> /A <sub>280</sub>
Sample 1	5008.3	1.88
Sample 2	4768.8	1.69

Table 5-1. Genomic DNA extraction. Sample 1 showed a higher concentration and better quality than sample 2. The DNA concentration and the ratio of A<sub>260</sub>/A<sub>280</sub> of were measured using a NanoDrop ND - 1000 spectrophotometer and blanked using water.

### 5.2.1.2 Polymerase Chain Reaction

Table 5-2 showed the different conditions used for PCR to amplify ZipA gene. The results were determined by 1% agarose gel (Figure 5-1). One strong band was observed at approximately 1,000 bp, it was close to full length of fusion ZipA gene (984 bp). The other band, shown on the bottom of the gel (less than 200 bp), could be a product of primer self-annealing, frequently observed from PCR reaction (Dr. Jet Lee, personal communication). The results showed the sample 4 has the weakest reaction (lower concentration of MgCl<sub>2</sub>, higher primer concentration), and other samples showed the similar results. Sample 2 and 3 were chosen for further experiments due to they showed the strongest signal for the band ~ 1,000 bp, and the weakest signal for the small size band (a band less than 200 bp). A band ~

1,000 bp was cut and purified using a QIA quick gel extraction kit. The concentration and quality of the purified DNA was measured by absorbance at 260 nm and 280 nm (Table 5-3).

Components	Sample 1	Sample 2	Sample 3	Sample 4	Sample 5	Sample 6
H <sub>2</sub> O	.45 µl	29.45 µl	26.45 µl	30.15 µl	27.85 µl	24.85 µl
10 × reaction buffer	10 µl	10 µl	10 µl	10 µl	10 µl	10 µl
MgCl <sub>2</sub> (1, 2, 4 mM)	2 µl	5 µl	8 µl	2 µl	5 µl	8 µl
dNTP (0.2 mM)	1 µl	1 µl	1 µl	1 µl	1 µl	1 µl
Forward Primer (0.5-1 mM)	1 µl	1 µl	1 µl	2 µl	2 µl	2 µl
Reverse Primer (0.5-1 mM)	1.3 µl	1.3 µl	1.3 µl	2.6 µl	2.6 µl	2.6 µl
Genomic DNA (0.1 µg)	2 µl	2 µl	2 µl	2 µl	2 µl	2 µl
Taq polymerase (1.25 U)	0.25 µl	0.25 µl	0.25 µl	0.25 µl	0.25 µl	0.25 µl

Table 5-2. The six different conditions used to PCR reaction. The reactions were applied different concentration of primer and MgCl<sub>2</sub>. Sample 2 and 3 (blue colour) showed the best results and were chosen for further experiments.

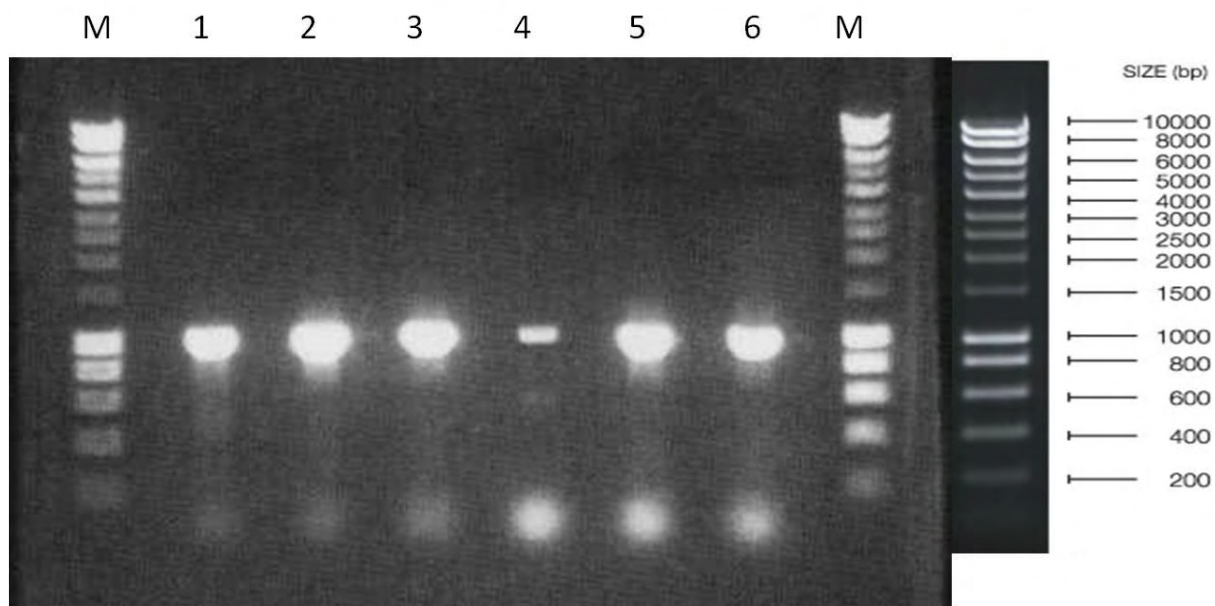


Figure 5-1. 1% agarose gel electrophoresis showed the results of PCR reaction. M represents molecular marker. Sample 2 and 3 were chosen for further experiments. The band ~1000 bp expected ZipA gene was purified using a QIA quick gel extraction kit.

	Concentration (ng/ $\mu$ l)	$A_{260}/A_{280}$
Sample 2	20	1.95
Sample 3	12	1.91

Table 5-3. The concentration and the ratio of  $A_{260}/A_{280}$  of purified DNA. PCR products were purified from 1% agarose gel using a QIA quick gel extraction kit. The DNA concentration and the ratio of  $A_{260}/A_{280}$  of were measured using a NanoDrop ND -1000 spectrophotometer and blanked using water. The results showed sample 2 has higher concentration, and was then diluted to 3 or 18 ng/ $\mu$ l used for following ligation experiment.

### 5.2.1.3 Ligation, Transformation and Extraction of Plasmid DNA

3 ng and 18 ng of purified DNA from PCR reaction were used in ligation reaction. The reactions were transformed into TOP10 *E.coli* cells, and the cells were cultured on LB agar plate containing the 100 µg/ml Ampicillin. All LB agar plates showed a large number of colonies after incubated at 37°C overnight, indicating that the ligation and transformation reactions were successful. Twelve single colonies were chosen for purification of plasmid DNA. Figure 5-2 showed a 1% agarose gel of purified plasmid DNA, sample 3, 4, 5, 6, 9, 10 and 12 showed the size of ~5,000 bp, they are smaller than expected (vector + ZipA gene ~ 6,737 bp). This could be the result of the plasmid DNA being circular, therefore, it ran faster than expected compared to linear DNA ladder (Dr. Jet Lee, personal communication). These samples were then sequenced and the data showed the plasmid DNA (sample 3, 4, 5, 6, 9, 10 and 12) contain ZipA gene. Sample 1, 2, 7 and 8 showed the size of ~ 4000 bp, and the sequencing data revealed these samples did not contain ZipA gene, therefore, these samples might only contain a vector. Sample 11 showed large size ~ 10,000 bp, it could be multi ZipA gene included in plasmid.

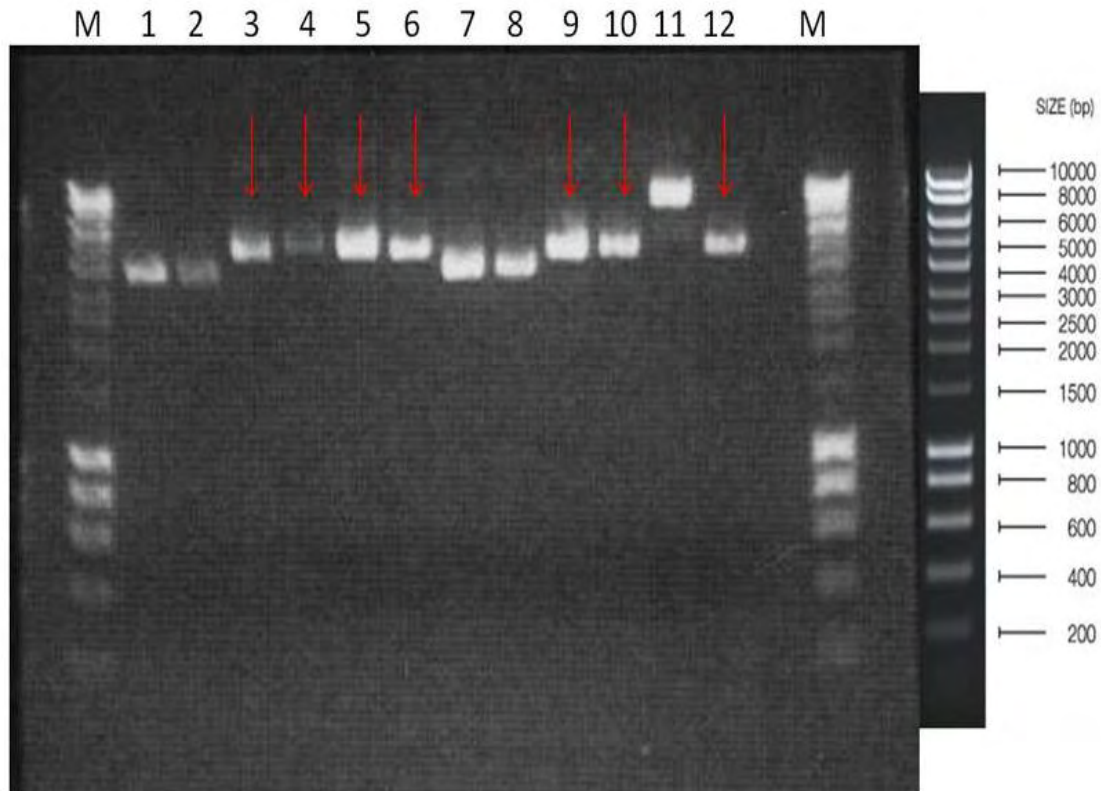


Figure 5-2. 1% agarose gel of purified plasmid DNA. Sample 3, 4, 5, 6, 9, 10 and 12 (red arrow) showed the size of ~5,000 bp, smaller than expected, more commonly observed from circular of plasmid DNA. The sequence data confirmed these samples contain ZipA gene.

### **5.2.2 Expression Screening and Small-scale of Protein Purification**

The plasmid containing ZipA gene was then transformed to BL21 star (DE3) One Shot *E. coli* cells for ZipA protein expression. A large number of colonies were observed after incubated at 37°C overnight on LB agar plate containing the 100 µg/ml Ampicillin. 3 colonies (including negative control) were chosen for expression screening. The ZipA fusion protein has a 6xHis-tag in the C-terminal, therefore, we examined ZipA expression by Western blotting using anti-His-tagged monoclonal antibody (Figure 5-3). The blotting

showed the band at ~ 52 kDa in all samples (apart from negative control, the sample only contains vector without ZipA gene). The positive band showed on SDS-PAGE gel was close to the previous report of ZipA by Hale and de Boer [100]. Therefore, we conclude a band at ~ 52 kDa was ZipA. Sample 2 showed the strongest signal at 52 kDa than the other samples. Therefore, we chose this sample for the further experiments.

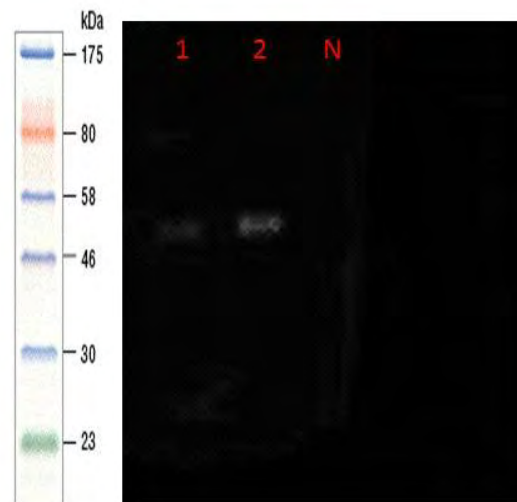


Figure 5-3. Western blotting using anti-His-tagged antibody for ZipA protein expression screening. The fusion ZipA protein has a 6xHis-tag in the C-terminal enables examined ZipA expression by Western blotting using anti-His-tagged Monoclonal antibody. A band showed at ~ 52 kDa was observed at all samples (lane 1 and 2), excluding negative control (N). Sample 2 showed the strongest signal on this band, and was chosen for the further experiments. The cell pellets were mixed with 1x SDS-PAGE sample buffer and then incubated at 95°C for 10 minutes. 20  $\mu$ l of mixture were then loaded onto the 10% SDS-PAGE gel and then transferred to a nitrocellulose membrane. The primary antibody was used anti-His-tagged Monoclonal antibody with 1: 5,000 dilutions and the secondary antibody was used anti-mouse IgG HRP-conjugated with 1: 10,000 dilutions.

The solubilisation of bacterial cell membrane used the same protocol as for yeast membrane. Adding SMA into bacterial membrane resulted in the solubilisation of most of the membranes hence less material transferred in the pellet than observed for yeast (data not shown). These data suggest that SMA has better solubilised efficiency on bacterial membranes than for yeast. The solubilised samples were then purified by using Ni<sup>2+</sup>-NTA resin. A band at ~52 kDa with strong signal was observed in the elution fractions (with 250 mM imidazole) (Figure 5-4). This suggests this protein binds strongly to Ni<sup>2+</sup>-NTA and is likely to be our fusion ZipA protein (with 6xHis tag at its C-terminus). Furthermore, the size of this protein showed on the SDS-PAGE gel was close to previous report [100]. Therefore, we conclude this protein is our ZipA. These cells which have successfully expressed ZipA were saved as glycerol stock for large-scale ZipA protein expression and purification.

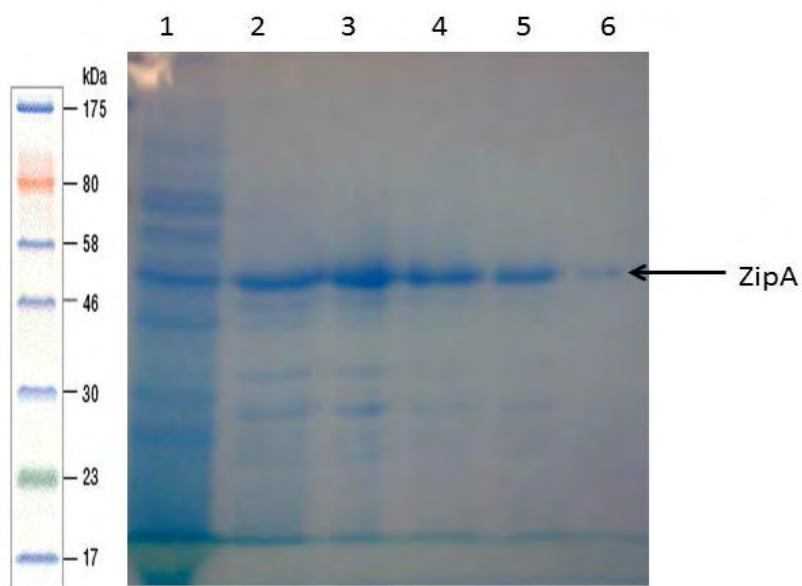


Figure 5-4. Small scale of ZipA purification. Lane 1: wash with 60 mM imidazole. Lane 2 to 6: eluted with 250 mM imidazole. The band at ~52 kDa is likely to be ZipA protein, the size is close to previous report [100].

### **5.2.3 Large-scale of Protein Expression and Purification**

*Purified SMALP-ZipA is approached by a simple two-step purification process*

On average, approximately 3.5 ~ 4 g of *E.coli* cells were obtained from a litre of flask culture. The membranes prepared from these cells were then solubilised by SMALP method. Most of membranes were solubilised and remained in the solubilised fractions (supernatant). The solubilised materials containing ZipA protein were then purified to homogeneity by a two-step purification process similar to A<sub>2a</sub>R purification process, this including the use of IMAC and gel filtration methods.



The first step was to use IMAC method, and the data showed a very good purification efficiency for SMALP solubilised ZipA using this method. Silver stained SDS-PAGE gel showed the proteins from IMAC elutions (Figure 5-5, lane 5 to 8) were already substantially pure, however, two weak bands (at ~28 kDa and ~ 80 kDa) also showed on the gel. Therefore, the elutions were further purified by gel filtration column to remove these contaminating proteins, improving purity of protein (Figure 5-6 and 5-7).

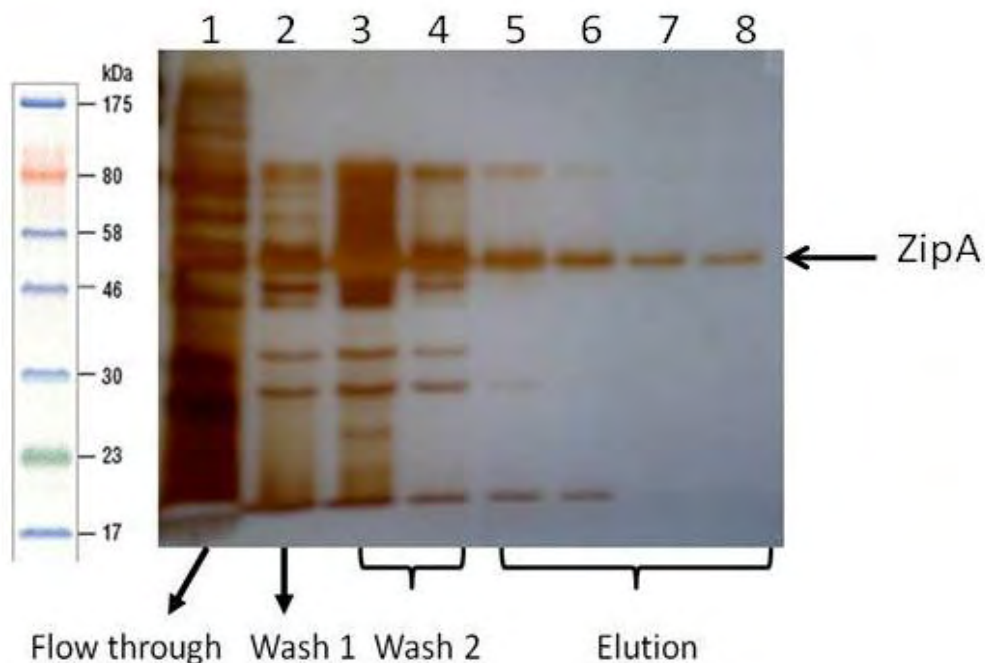


Figure 5-5. Purification of ZipA using IMAC method. The fractions were analysed by SDS-PAGE gel and silver staining. Lane 1 (from the left of the gel): Flow through: the materials that did not bind to the resin. Lane 2: first wash with 60 mM imidazole. Lane 3 and 4: second wash with 80 mM imidazole. Lane 5 to 8: elute with 250 mM imidazole.

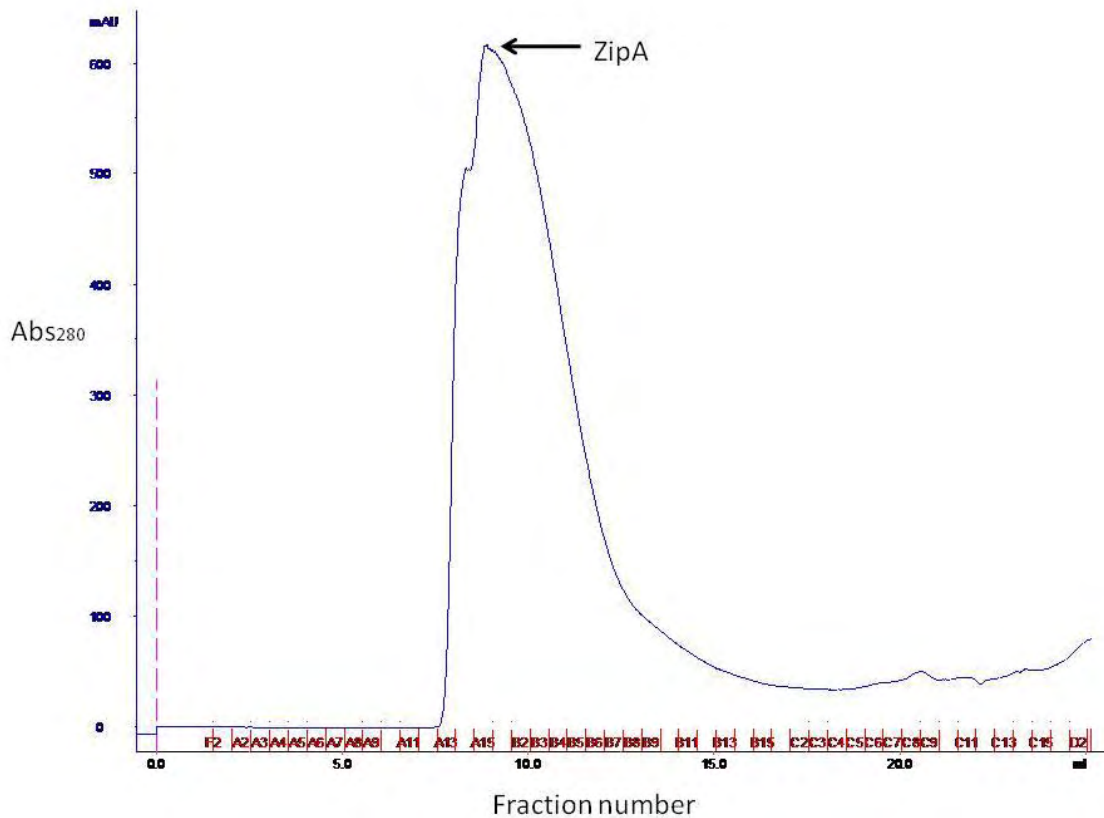


Figure 5-6. Gel filtration of ZipA. The IMAC elutions were loaded into gel filtration column. The progress was monitored by absorbance at 280 nm. The data showed a few larger proteins (observed at 80 kDa on SDS-PAGE gel) was eluted before the major protein, ZipA was eluted. The fractions containing ZipA were mixed and then examined by SDS-PAGE gel (Figure 5-7). The experiments were carried out using a Superdex 200 10/300 GL column attached to an ÄKTA™ FPLC purification system. A flow rate was set at 1 ml/min.

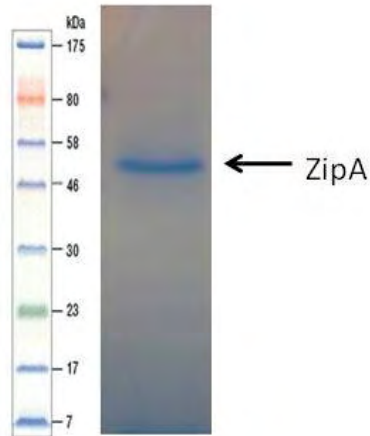


Figure 5-7. SDS-PAGE gel for the purification of ZipA using gel filtration. The IMAC elution was loaded to gel filtration Superdex 200 10/300 GL column to remove aggregation protein to reach homogeneity. The fractions containing ZipA were examined by SDS-PAGE gel. Only single band was observed at *ca.* 52 kDa. This showed that the protein has reached homogeneity after a two-step purification process.

#### **5.2.4 Protein Identification and Western Blotting Analysis**

*A band at 52 kDa is an intact ZipA*

The band observed at ~52 KDa was larger than calculated molecular weight (fusion ZipA: 38.7 kDa). This protein has been shown before to migrate aberrantly in SDS-PAGE gel [100].

To confirm a band at ~52 kDa is our purified SMALP-ZipA. FT-ICR mass spectrometry was applied to the band cut from SDS-PAGE gel (Figure 5-7), the sample was digested with trypsin to produce several short segments for FT-ICR mass spectrometry experiment. Five peptides fragments were identified which were cross referenced with the bacterial proteome and the protein was identified as FtsZ-interacting protein A (Table 5-4). These peptides are

found in the different domain of ZipA protein (highly charged region: amino acid from 29 - 85, P/Q domain: 86 - 185, and globular domain: 186 - 328).

Peptide Fragments	Peptide Sequence	Peptide Location (amino acid)
1	SKRDDDSYDEDVEDDEGVGEVR	46-67
2	VNHAPANAQEHEAARSPQHQQYQPPYASAQPR	70-92
3	RHLSPDGSGPALFSLANMVKPGTFDPEMKPGTFDPEMK	230-259
4	LMLQSAQHIADEVGGVVLDDQR	283-305
5	LREYQDIIR	312-321

Table 5-4. The identification of ZipA was using FT-ICR mass spectrometry. A band at *ca.* 52 kDa was cut from instant blue stained 10% SDS-PAGE gel for trypsin digestion before identified by FT-ICR mass spectrometry. Five peptides fragments are found in the different domain of ZipA protein including highly charged region, P/Q domain and globular domain). Peptide location (amino acid) represents the location of this peptide, for example, 46-67 represents this peptide located from 46 to 67 amino acid residue of ZipA protein.

Additionally, in order to demonstrate purified SMALP-ZipA is intact, the purified protein was analysed by Western blotting using anti-His-tagged antibody and N-terminus sequencing. Western blotting using anti-His-tagged antibody can be used for determining

whether C-terminus of ZipA is intact due to anti-His-tagged antibody bound to C-terminus of ZipA. Only one band showed on the blot, it suggests the C-terminus of ZipA is intact (Figure 5-8). The N-terminus sequencing of purified SMALP-ZipA showed a sequence was found at N-terminus of protein, namely M-M-Q-D-L corresponds to the N-terminus of ZipA. Therefore, it indicates the N-terminus of ZipA is intact, too. Taken together these data, we conclude a band showed on SDS-PAGE gel at ~52 kDa is an intact ZipA.

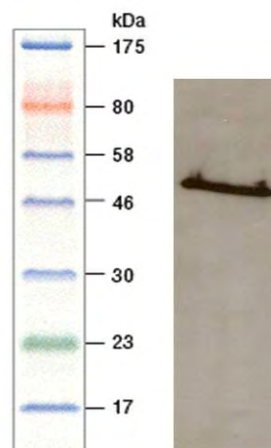


Figure 5-8. Western blotting of purified SMALP-ZipA. The purified SMALP-ZipA obtained from a simple two-step purification process was analysed by Western blotting. Only one band was observed at 52 kDa. This concludes the C-terminus of ZipA is intact due to anti-His-tagged antibody bound to C-terminus of ZipA. 20  $\mu$ l of mixtures (proteins and loading buffer) were loaded onto the 10% SDS-PAGE gel and then transferred to a nitrocellulose membrane. The primary antibody was used anti-His-tagged Monoclonal antibody with 1: 5,000 dilutions and the secondary antibody was used anti-mouse IgG HRP-conjugated with 1: 10,000 dilutions.

### **5.2.5 FtsZ Protein Expression and Purification**

An initial sample of FtsZ protein used in FtsZ-ZipA interaction experiments was kindly provided from Dr. Raul Pacheco-Gomez. However, the protein was insufficient to complete the whole project. Therefore, we also purified FtsZ protein used for FtsZ-ZipA interaction experiments.

#### **5.2.5.1 Expression Screening of FtsZ**

The FtsZ expression plasmid was obtained from Dr. Raul Pacheco-Gomez (University of Birmingham). The plasmid was transformed to BL21 star (DE3) One Shot *E.coli* cells for FtsZ protein expression. A large number of colonies were observed after incubated at 37°C overnight on LB agar plate containing the 100 µg/ml Ampicillin. Six colonies (including one sample for negative control, without adding IPTG for the induction) were chosen for expression screening. The SDS-PAGE gel showed a strong band at ~40 kDa appeared on all samples apart from negative sample (Figure 5-9), it is consistent with previous report [133]. Therefore, we conclude FtsZ protein was successfully expressed in BL21 star (DE3) One Shot *E.coli* cells.

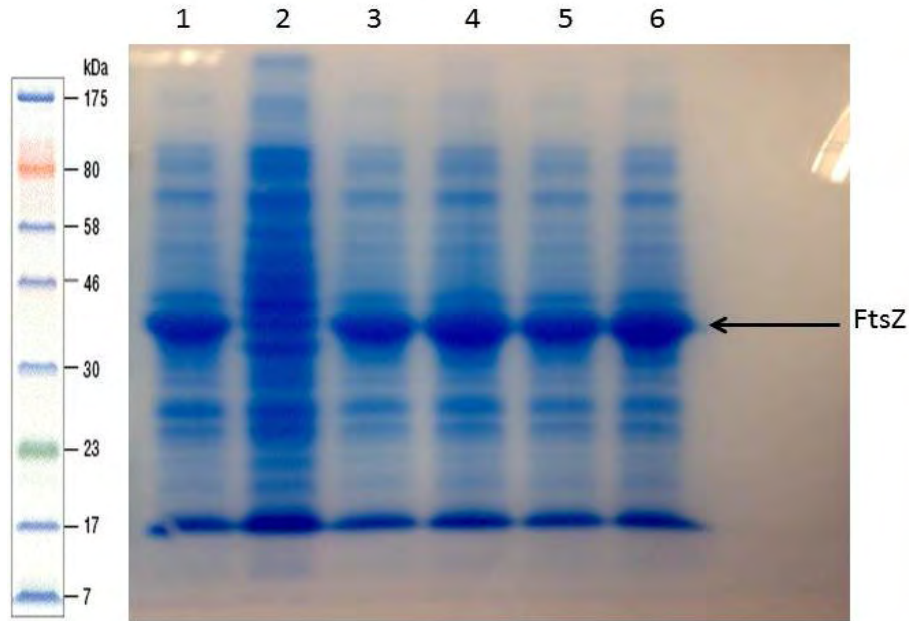


Figure 5-9 .Over-expression of FtsZ. The gel showed a strong band ~40 kDa, the size of this protein consists with previous report for FtsZ protein. We conclude a band at ~40 kDa is FtsZ. Lane 1, 3, 4, 5 and 6: the samples added IPTG. Lane 2: the sample did not add IPTG. The cells grew at 37°C and until OD<sub>600</sub> of 0.4. A stock IPTG was then added into culture to make a final IPTG concentration of 0.84 mM for the protein induction. The cell pellets were mixed with 1xSDS-PAGE sample buffer and then incubated at 95°C for 10 minutes. 20 µl of mixture were then loaded onto the 10% SDS-PAGE gel.

#### 5.2.5.2 Large-scale FtsZ Expression and Purification

The colonies which have been shown successfully expressed FtsZ protein were then used in large-scale protein expression and purification. Unlike A<sub>2a</sub>R and ZipA, FtsZ is a cytoplasmic protein and hence the membrane fraction was removed for the purification of FtsZ. Figure 5-10 showed a SDS-PAGE gel of the FtsZ fractions eluted from the ion-exchange column (Q Sepharose). FtsZ was eluted at 250 mM KCl (Figure 5-10, lane 1 to 6), and the gel showed FtsZ was already substantially pure, and approximately 25 - 30 mg of FtsZ was obtained from

one litre culture. Purified FtsZ was stored at  $-80^{\circ}\text{C}$  at least a year and showed no loss of polymerisation or GTPase activities. Moreover, freezing and thawing FtsZ up to five times did not affect activity.

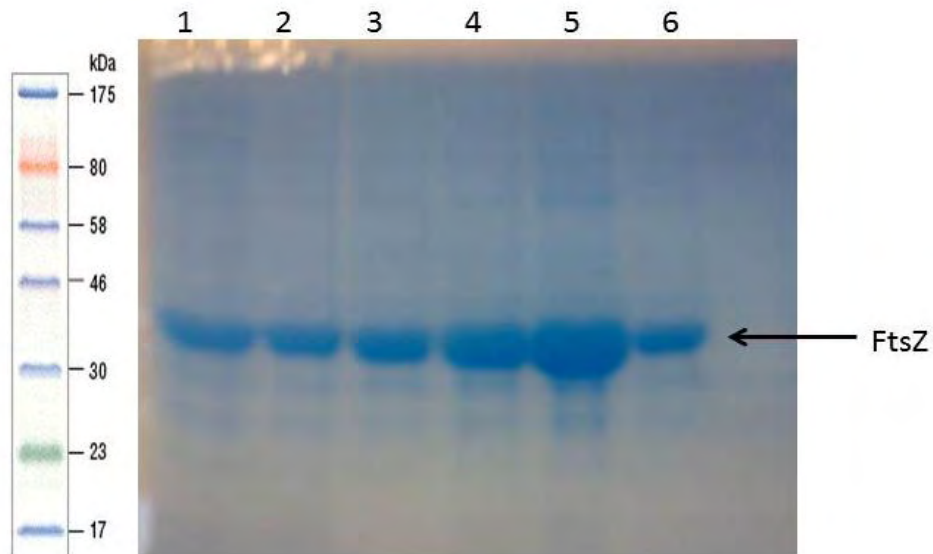


Figure 5-10. 10% SDS-PAGE of FtsZ fractions eluted from ion-exchange column (Q Sepharose). Lanes 1-6: elution, FtsZ was eluted at 250 mM KCl. The elution showed a major single band with little or no contamination.

#### 5.2.5.3 Activity Test for FtsZ

In order to study the interaction between FtsZ and ZipA we must first establish that FtsZ is active. The easiest and quickest way is to measure FtsZ polymerisation activity using a right angled light scattering (RALS) experiment (§ 2.5.2). Figure 5-11 showed a rapid increase in light scattering that was known to occur within the first minute of the reaction after adding GTP. The large light scattering signal was sustained for several minutes, and then decreased.



This is consistent with previous observations that FtsZ undergoes rapid polymerisation and reaches a steady state. The length of steady state was proportional to the GTP concentration. While we added 0.2 mM of GTP into the sample and the length of steady state maintain about 5 minutes. A rapid decrease in the light scattering suggests FtsZ depolymerisation happened as GTP depletion due to GTP hydrolysis. This is consistent with previous reports of FtsZ polymerisation [133]. The data suggest the FtsZ protein we purified is active.

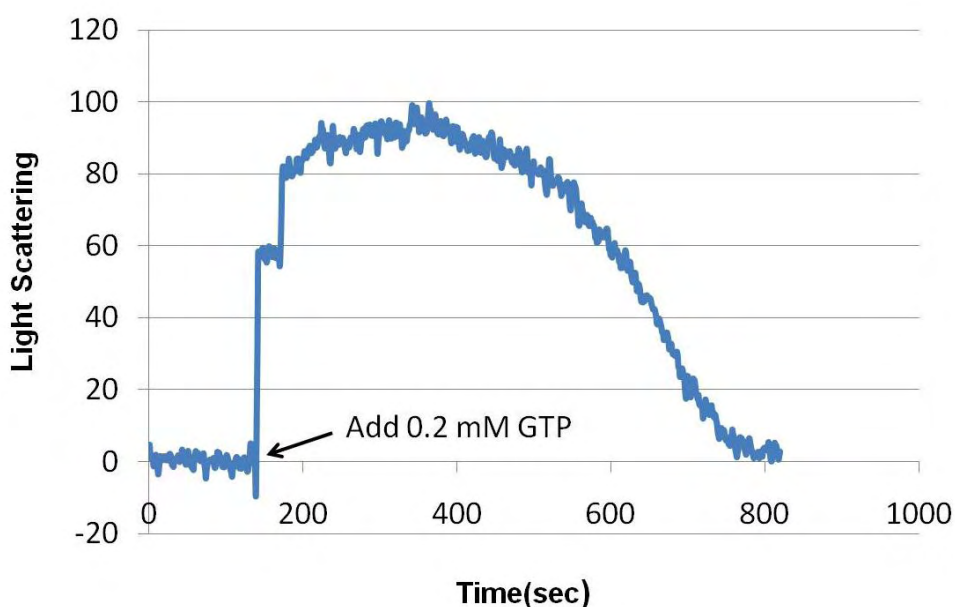


Figure 5-11. Light scattering assay for polymerisation of FtsZ. Data showed a rapid increase in light scattering occurred within the first minute of the reaction after adding GTP. The light scattering signal decreased while GTP depletion due to GTP hydrolysis. This suggests that FtsZ undergoes rapid polymerisation and reaches a steady state, and then FtsZ is depolymerised as GTP is depleted. These data suggest the purified FtsZ is active. The experiment was performed using a Perkin Elmer LS50B spectrofluorimeter. Data were collected every second at room temperature in a 0.3 cm path length fluorescence cuvette (typically with 100  $\mu$ l volume) The excitation and emission wavelengths were set at

500 nm, and the excitation and emission slit widths were set at 2.5 nm. A baseline was collected for 150 seconds before 0.2 mM was added to the sample.

### **5.3 Discussion**

The ZipA genetic construct was designed to attach a 6xHis at C-terminus of protein enabling the use of the same purification protocol as A<sub>2a</sub>R to purify ZipA. On average, it took 5 ~6 working day to obtain a purified ZipA from the expression step to the purification step, and 10 ~ 11 working day for obtaining a purified A<sub>2a</sub>R. Therefore, this single transmembrane membrane protein (ZipA) is easier to be obtained comparing to A<sub>2a</sub>R. The purified SMALP-ZipA showed a size at ~52 kDa on the SDS-PAGE gel. This is much larger than expected size 38.7 kDa. This atypical running behaviour, we also observed on A<sub>2a</sub>R and has described in section 3.2.5. To confirm the identity of the protein in the band, FT-ICR mass spectrometry experiments were carried out showing the presence of peptides throughout the ZipA sequence.

Additionally, the protein was analysed by Western blotting using anti-His-tagged antibodies proving that the C-terminus of ZipA is intact. However, this fusion ZipA protein does not have any tag in the N-terminus. Therefore, we used N-terminus sequencing to determine whether the N-terminus of ZipA is intact. The data showed a sequence that consists with the N-terminus sequence of wild type ZipA. These data demonstrate SMALP system can be

applied to an integral inner-membrane protein with a significantly different architecture to those so far purified using SMALP.

In conclusion, in this chapter, we have proved that SMALP can be used to produce ZipA using the same protocol as well as  $A_{2a}R$ . In the future, this protocol could be used for many other membrane proteins to be an universal method for membrane protein study.

## **CHAPTER 6: Characterisation of ZipA**

### **6.1 Introduction**

ZipA is a protein involved in bacterial cell division that contains a single transmembrane domain that has been shown to be involved in stabilisation of FtsZ-ring [110,111]. However, the FtsZ-ZipA interactions have not been that well studied due to the difficulty of purifying and handling ZipA (which is a membrane protein). In the previous chapter, we used the novel SMALP system to produce ZipA, now we use a range of techniques to characterise purified SMALP-ZipA and also study the FtsZ-ZipA interaction.

First of all, we use CD to determine the secondary structure of purified SMALP-ZipA, and its folded state. We also use svAUC to monitor the oligomerisation state of purified SMALP-ZipA. Moreover, we address the FtsZ-ZipA interaction via RALS assay, sedimentation assay, LD, GTPase assay and TEM. These data provide the information about the protein-protein interactions and allow us to build a model to describe how ZipA affect FtsZ polymers during the cell division. Furthermore, we attempt to reconstitute ZipA and FtsZ into a GUV to create an artificial FtsZ-ring inside a GUV. This could provide us a new route to understand the mechanism of cell division *in vitro* and in particular how the division machinery alters membrane morphology.

## **6.2 Results**

### **6.2.1 Circular Dichroism**

*CD spectrum of purified SMALP-ZipA presents a native folded protein*

To date, the full structure of ZipA has not been solved. However, the crystal structure exists of C-terminal of ZipA shows both  $\alpha$ -helices and  $\beta$ -sheets character [105]. The remaining parts of the protein are made up of a single  $\alpha$ -helices transmembrane domain and a region that is predicted to be unstructured [99]. From these data we can predict that ZipA consists of  $\alpha$ -helices,  $\beta$ -sheets and extensive unstructured region from its sequence of amino acids.

Our CD data showed purified SMALP-ZipA consists of  $\alpha$ -helices (29%),  $\beta$ -sheets (35%) and 36% unfolded of secondary structure (Figure 6-1). Additionally, the CD signal at 190 nm is lower than that expected for a folded protein, representing the protein was not fully folded (a folded protein should present a positive signal at 190 nm, Dr. Tim Dafforn, personal communication). This correlates with the presence of an unstructured region in the purified SMALP-ZipA and is consistent with the predicted structure of ZipA.

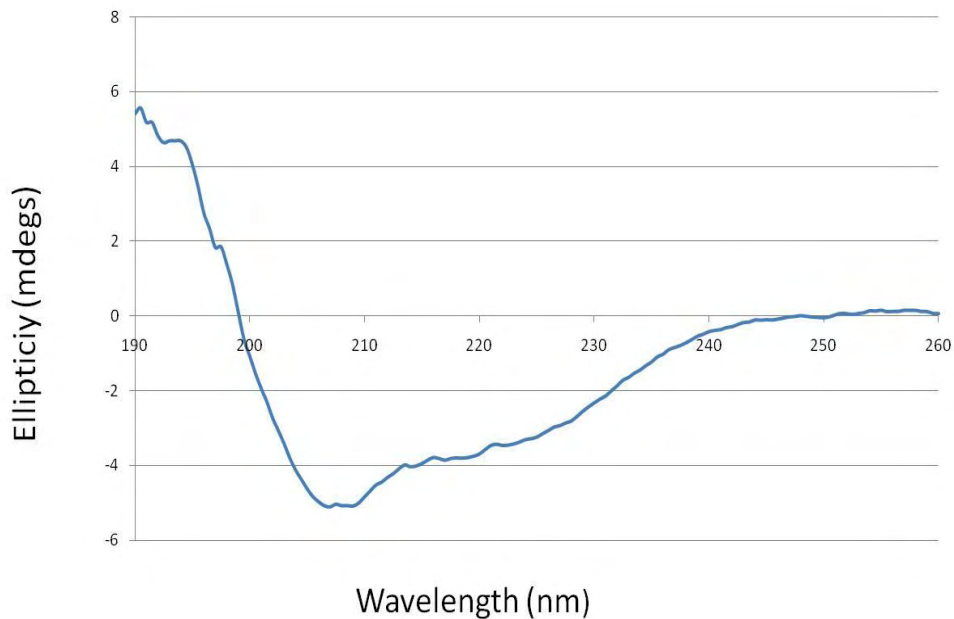


Figure 6-1. CD spectrum of purified SMALP-ZipA. The CD data showed purified SMALP-ZipA consists of  $\alpha$ -helices,  $\beta$ -sheets and unstructured region, consists with the predicted structure of ZipA. It suggests purified SMALP-ZipA maintained its native secondary structure after solubilisation and purification steps. CD data were collected using a JASCO J-715. CD spectra were collected using a 1 mm path length cuvette and averaged over 8 scans in the far-UV domain. Spectra acquired were corrected for the buffer signal. Protein concentration of purified SMALP-ZipA was 0.05 mg/ml.

### **6.2.2 Sedimentation Velocity Analytical Ultracentrifugation**

*svAUC data shows purified SMALP-ZipA is mainly monomeric*

In the chapter 4, sedimentation velocity analytical ultracentrifugation was shown to have potential utility for monitoring oligomerisation of proteins in SMALP (Figure 6-2). SEDFIT analysis of data from a sample of purified SMALP-ZipA using the c(M) model produced an intense peak at 78 kDa, that is likely to be a ZipA encapsulated in SMALP, accompanied by two minor peaks at 10 and 30 kDa. The first minor peak (10 kDa) is likely to be free SMA

(10 kDa) and the other minor peak (30 kDa) is likely to be empty SMALP. This second peak has the molecular mass different from equivalent svAUC experiments carried out on purified SMALP-A<sub>2a</sub>R (§ 4.2.3). This could be the result of these protein-free SMALP having different components of lipids as they were derived from *E.coli* membranes, rather than the yeast cell membrane used in the previous study in the chapter 4.

The intense higher molecular peak can therefore be attributed to the presence of purified SMALP-ZipA. An approximate measure of the mass of the encapsulated ZipA can then be determined by subtraction of the mass of the empty SMALP, which yields a mass of approximately 48 kDa. However, this does not completely match the expected size of ZipA (38.7 kDa) The difference is likely to result from either a variance in the amount of lipid maintained in the protein free SMALP and protein loaded SMALP, or perhaps the presence of a mixed population containing dimeric and monomeric ZipA. Although it is clear that even if there is some dimeric contaminant, it constitutes only a small proportion of the sample.

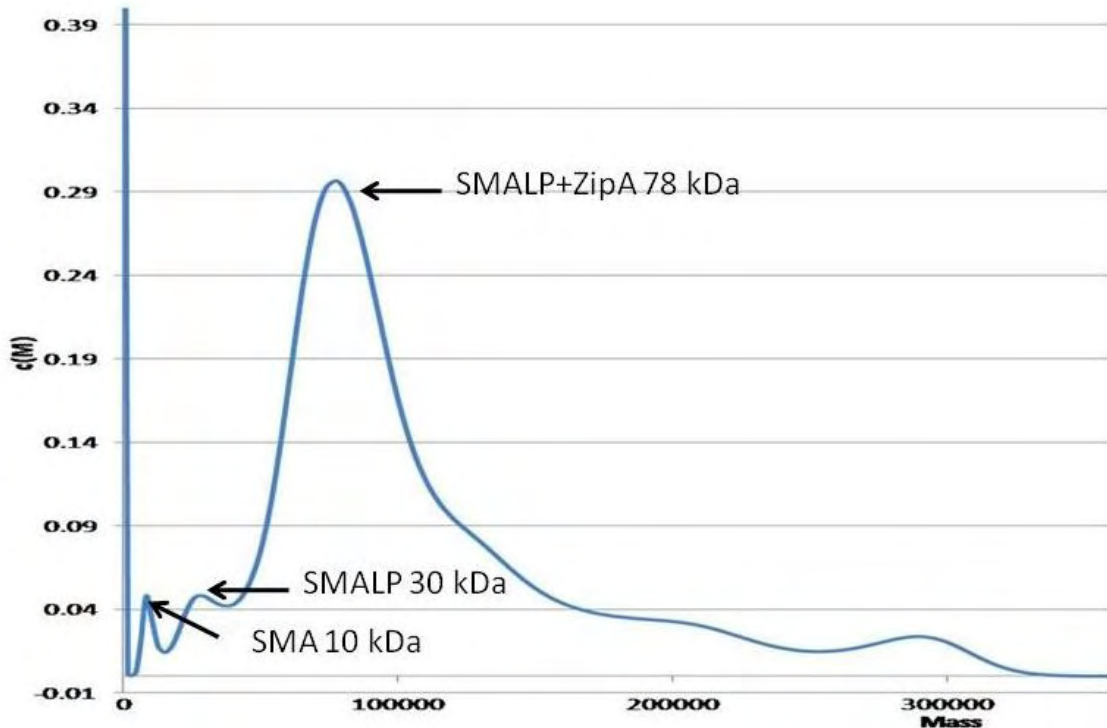


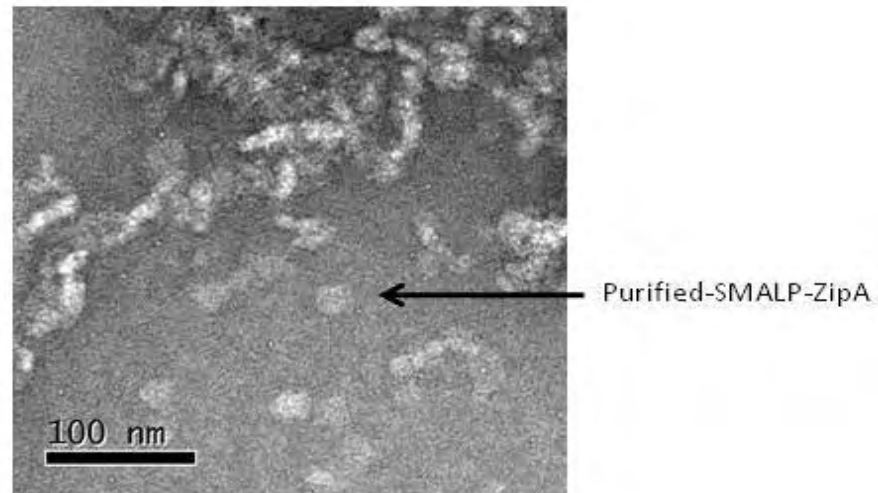
Figure 6-2. A SEDFIT  $c(M)$  deconvolution of sedimentation velocity analytical ultracentrifugation data collected on purified-SMALP-ZipA showing the presence of 3 peaks corresponding to SMA (10 KDa), the empty SMALP (30 KDa) and ZipA encapsulated in SMALP (78 KDa). Data were collected on a Beckman XL-I proteome lab at 40,000 rpm with the migration of the particles being monitored by scanning the cell at 280 nm.

### **6.2.3 Electron Microscopy**

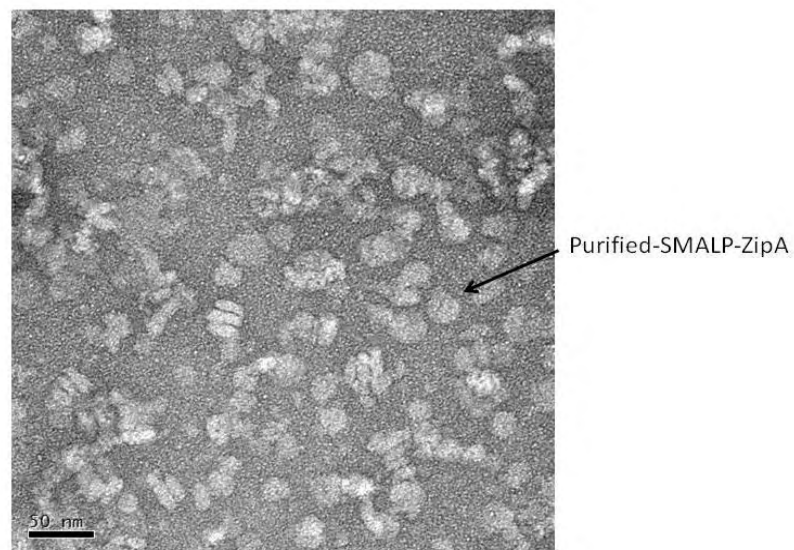
It has been shown that purified SMALP-PagP and purified SMALP-A<sub>2a</sub>R are nanodisk-like structures. TEM micrograph of purified SMALP-ZipA ( $\times 30,000$ ) ( $\times 50,000$ ) showed purified SMALP-ZipA was also in a nanodisk structure (Figure 6-3). Moreover, on average, the structure of purified SMALP-ZipA ( $17.5 \pm 2.5$  nm) was a little smaller than purified SMALP-



A<sub>2a</sub>R (20 ± 2.5 nm). It is probably that ZipA only contains a single transmembrane domain, and it is a smaller protein (38.7 kDa) than A<sub>2a</sub>R (47 kDa).



(A) TEM of purified SMALP-ZipA (×30, 000)



(B) TEM of purified SMALP-ZipA (×50, 000)

Figure 6-3. (A) TEM micrograph of purified SMALP-ZipA (×30, 000) showed purified SMALP-ZipA as a nanodisk structure. On average, the structure of purified SMALP-ZipA was a little smaller than purified SMALP-A<sub>2a</sub>R. Selected areas were photographed at ×30,000. Scale bar represents 100 nm. (B) TEM micrograph of purified SMALP-ZipA (×50, 000). Selected areas were photographed at ×50,000. Scale bar

represents 50 nm. The experiments carried out using a JEOL 2011 transmission electron microscope. The samples were stained with 1% uranyl acetate solution.

### **The Interaction Experiments Between FtsZ and ZipA**

The sections from 6.2.4 to 6.2.9 described the methods used to characterise the FtsZ-ZipA interaction.

#### **6.2.4 Right Angle Light Scattering**

*RALS signal of FtsZ polymerisation is significant increased in the presence of ZipA*

Changes in RALS signal reflect the changes in the size distribution of particles in a sample.

In this study, we used RALS to study the dynamics of FtsZ polymerisation in the presence or absence of ZipA. According to the previous published protocol, the buffer used for FtsZ polymerisation should contain a concentration of 10 mM MgCl<sub>2</sub>, at pH of 6.5. However, SMA polymer is pH-sensitive leading to precipitation at pH <6.5. In addition the polymer is precipitated by high concentrations of MgCl<sub>2</sub>. Therefore, before we study the interaction of SMALP-ZipA with FtsZ, we have to investigate if purified SMALP-ZipA is stable in the assay buffer (10 mM MgCl<sub>2</sub>, pH 6.5).

However, our initial studies showed the purified SMALP-ZipA was affected by 10 mM MgCl<sub>2</sub> (Figure 6-4). The RALS signal of purified SMALP-ZipA in 10 mM MgCl<sub>2</sub> continually

increased suggesting that the purified SMALP-ZipA particle was dissociated leading to the formation of SMA polymer precipitate. To address this, we decreased the concentration of  $\text{MgCl}_2$  to 2.5 mM and determined if this still affects the purified SMALP-ZipA. The data showed, in this low concentration of  $\text{MgCl}_2$ , the RALS signal was very steady suggesting that the purified SMALP-ZipA was stable in the lower concentration of  $\text{MgCl}_2$ .

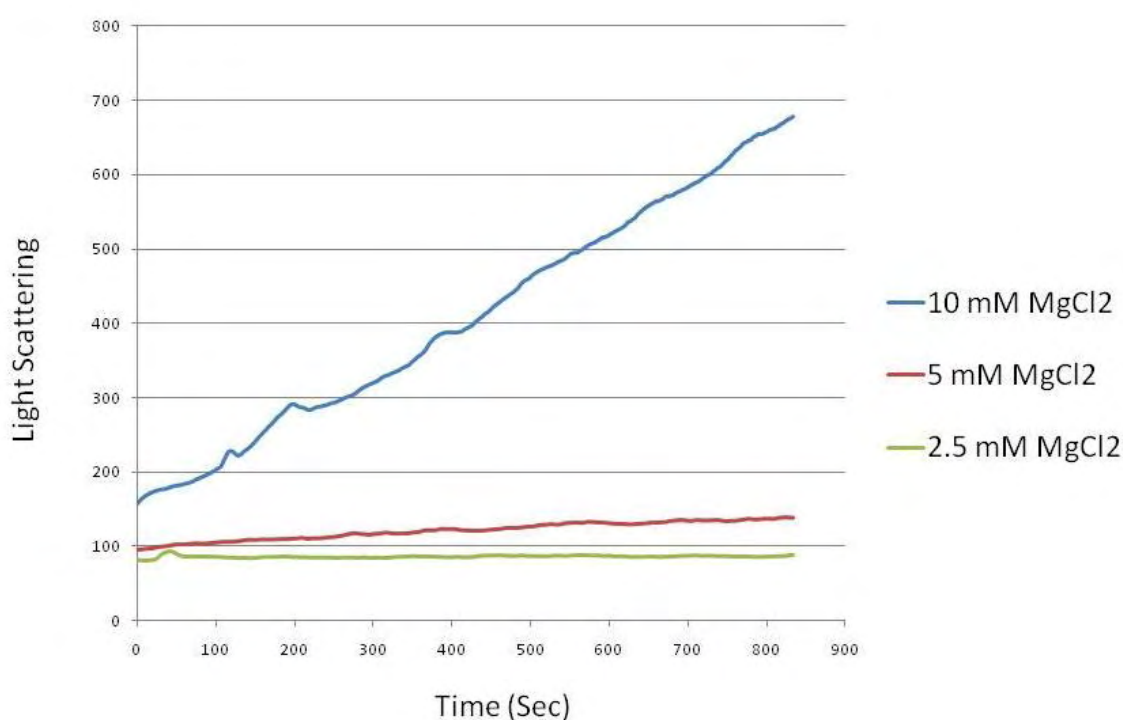


Figure 6-4. The effect of  $\text{Mg}^{2+}$  concentration on purified SMALP-ZipA.

Purified SMALP-ZipA was in 50 mM MES buffer pH 6.5, 50 mM KCl and 2.5 mM  $\text{MgCl}_2$  (green), 5 mM  $\text{MgCl}_2$  (red) or 10 mM  $\text{MgCl}_2$  (blue) to which 0.2 mM GTP was added. Data were collected every second at room temperature in a 0.3 cm path length fluorimeter cuvette (typically with 100  $\mu\text{l}$  volume). The excitation and emission wavelengths were set at 500 nm, and the excitation and emission slit widths were set at 2.5 nm. The experiment was performed using a Perkin Elmer LS50B spectrofluorimeter. A baseline was collected for 60 seconds before the GTP was added to the sample.

Moreover, we also investigated if purified SMALP-ZipA is affected by pH. The data showed the purified SMALP-ZipA was stable at pH 6.5 and 7, but started to be unstable while pH was decreased to 6 (Figure 6-5).

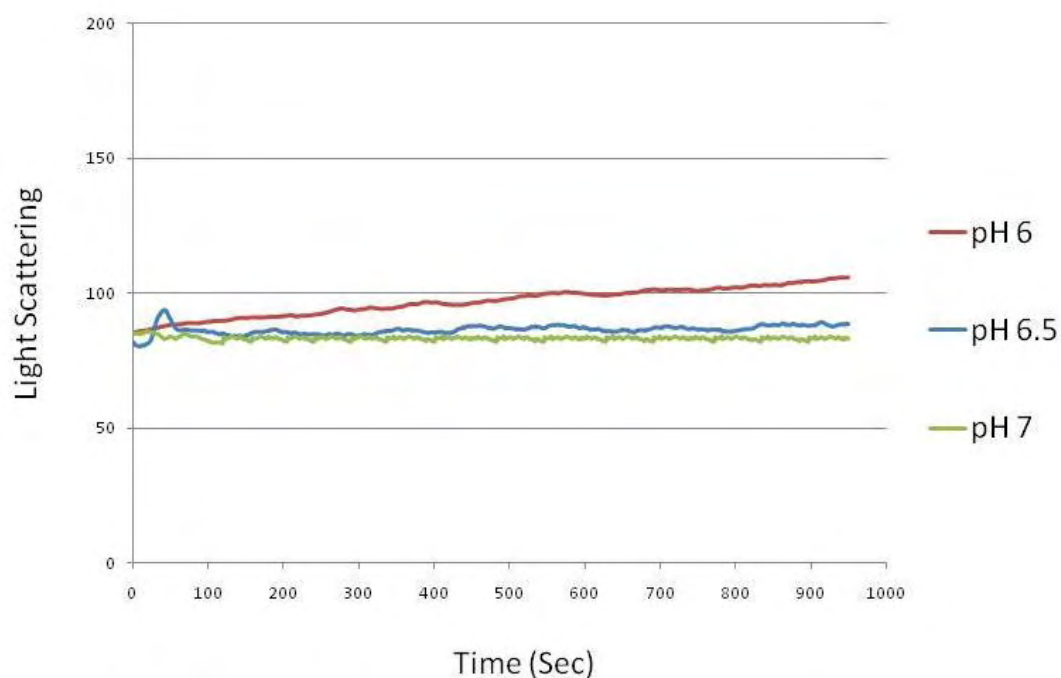


Figure 6-5. The effect of pH on purified SMALP-ZipA.

The experiment was started by adding into the sample. Purified SMALP-ZipA in 50 mM MES buffer pH 6 (red), 6.5 (blue) or 7 (green), 50 mM KCl and 2.5 mM MgCl<sub>2</sub> to which 0.2 mM GTP was added. Data were collected every second at room temperature in a 0.3 cm path length fluorimeter cuvette (typically with 100 µl volume). The excitation and emission wavelengths were set at 500 nm, and the excitation and emission slit widths were set at 2.5 nm. The experiment was performed using a Perkin Elmer LS50B spectrofluorimeter. A baseline was collected for 60 seconds before GTP was added into the sample.

Furthermore, we determined whether the FtsZ polymerisation is affected by the concentration of  $\text{MgCl}_2$  (Figure 6-6). The data showed the RALS signal of FtsZ polymerisation became smaller and a cycle of FtsZ polymerisation also became shorter while the  $\text{MgCl}_2$  was decrease to 2.5 mM, consists with previous reports [133,137]. However, given that 10 mM  $\text{MgCl}_2$  can affect the structural integrity of the purified SMALP-ZipA, the assay conditions were chosen with 2.5 mM of  $\text{MgCl}_2$  as compromise between FtsZ polymerisation and SMALP integrity.

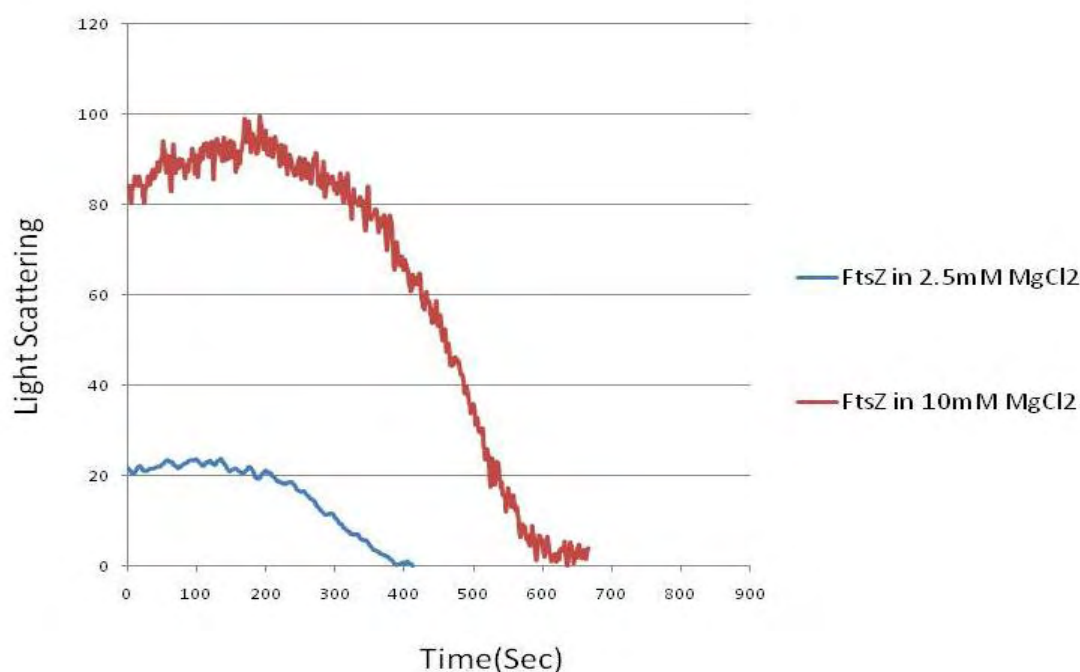


Figure 6-6. The effect of  $\text{Mg}^{2+}$  concentration on FtsZ polymerisation

FtsZ was in 50 mM MES buffer pH 6.5, 50 mM KCl and 10 mM  $\text{MgCl}_2$  (red) / 2.5 mM  $\text{MgCl}_2$  (blue). Data were collected every second at room temperature in a 0.3 cm path length fluorimeter cuvette (typically with 100  $\mu\text{l}$  volume). The excitation and emission wavelengths were set at 500 nm, and the excitation and emission slit widths were set at 2.5 nm. A baseline was collected for 2 minutes before 0.2 mM of GTP was added to the sample. The experiment was performed using a Perkin Elmer LS50B spectrofluorimeter. A baseline was collected for 120 seconds before GTP was added into the sample.

Previously study has shown FtsZ polymerisation to be sustained at lower pH condition, such as pH of 6 [133]. Our previous study (Figure 6-5), however, showed the requirement for the assay buffer have to be a pH over 6.5 to allow the SMALP structure to be stable. It meant we had to study the effect of increasing pH on FtsZ polymerisation (Figure 6-7). These data showed FtsZ polymerisation was decreased (shorter and smaller) by increasing pH. At pH 6, the RALS reached a maximum value of 34 units and then it took approximately 500 seconds to return to a value of 0 units. At pH 6.5, the RALS reached a maximum value of 23 units and then it took approximately 400 seconds to return to a value of 0 units. This (at pH 6.5) only represents a slight loss in activity and is thought to be permissible in this study, and pH 6 can affect the structural integrity of the purified SMALP-ZipA, therefore, the assay conditions were chosen at at pH 6.5 for studying FtsZ-ZipA interaction experiments.

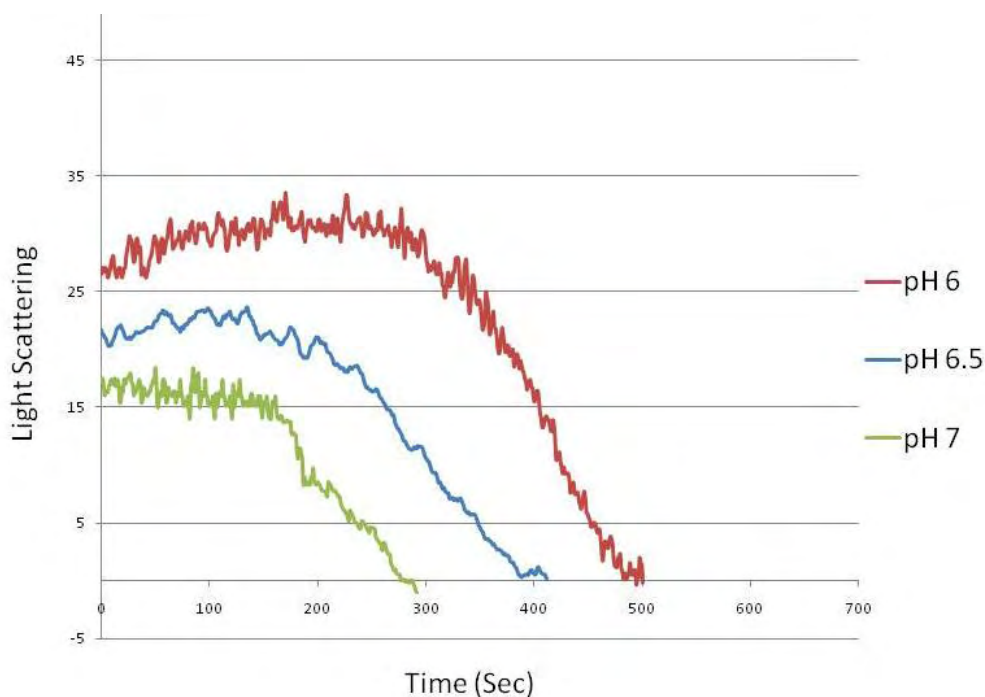


Figure 6-7. The effect of pH on FtsZ polymerisation

FtsZ was in 50 mM MES buffer pH 6 (red), 6.5 (blue) or 7 (green) 50 mM KCl and 2.5 mM MgCl<sub>2</sub>. Data were collected every second at room temperature in a 0.3 cm path length fluorimeter cuvette (typically with 100 µl volume). The excitation and emission wavelengths were set at 500 nm, and the excitation and emission slit widths were set at 2.5 nm. A baseline was collected for 2 minutes before 0.2 mM of GTP was added to the sample. The experiment was performed using a Perkin Elmer LS50B spectrofluorimeter. A baseline was collected for 120 seconds before GTP was added into the sample.

Figure 6-8 showed the RALS data of FtsZ polymerisation in the presence of different concentrations of ZipA. In the absence of ZipA, the RALS reached a maximum value of 20 units and then it took approximately 400 seconds to return to a value of 0 units. In the presence of ZipA, the RALS reached a maximum value of 50 units. More interestingly, the signal did not come back to zero even after 30 minutes. In the presence of more ZipA, the maximum of RALS increased to approximately 110 units. These data suggest that in the

presence of ZipA, the size of FtsZ polymers become larger and it takes much longer for FtsZ polymers dissociate back to FtsZ monomers.

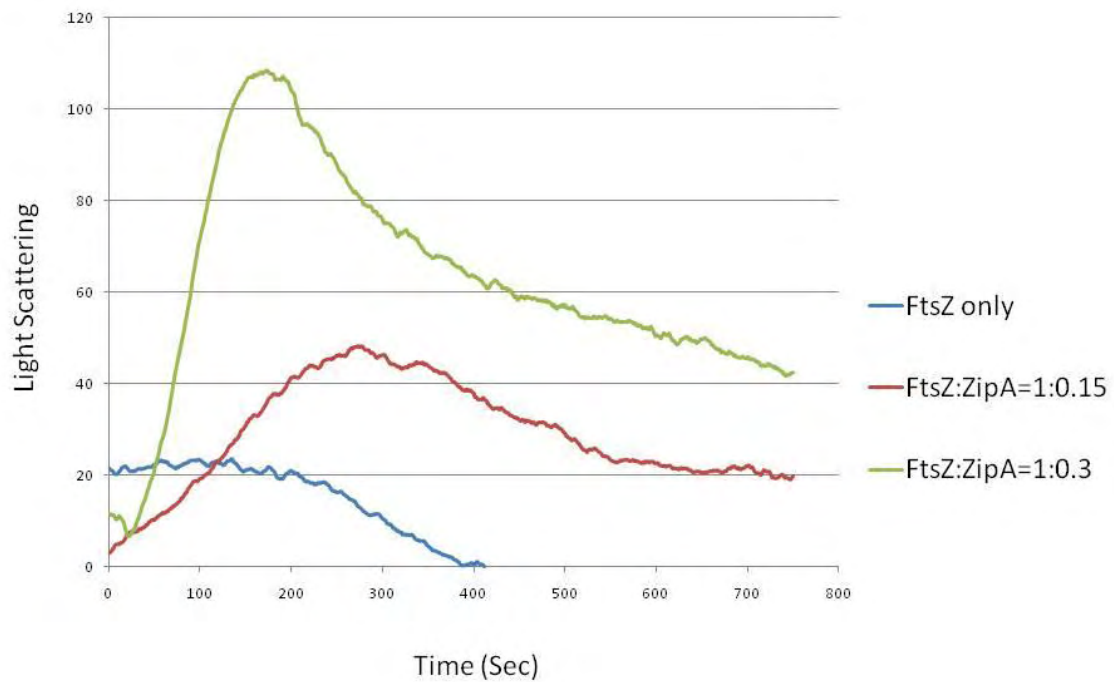


Figure 6-8. The effect of ZipA on FtsZ polymerisation

FtsZ was in 50 mM MES buffer pH 6.5, 50 mM KCl and 2.5 mM MgCl<sub>2</sub> in the presence of different concentration of ZipA. Data were collected every second at room temperature in a 0.3 cm path length fluorimeter cuvette (typically with 100  $\mu$ l volume). The excitation and emission wavelengths were set at 500 nm, and the excitation and emission slit widths were set at 2.5 nm. The experiment was performed using a Perkin Elmer LS50B spectrofluorimeter. A baseline was collected for 120 seconds before 0.2 mM was added into the sample.



### **6.2.5 Sedimentation Assay**

FtsZ polymerisation can also be measured using sedimentation assay. FtsZ polymers can be selectively pelleted over the monomer by centrifugation due to its heavier mass, the resulting pellet can then be analysed using SDS-PAGE gel. To test the effect of the purified SMALP-ZipA on FtsZ polymerisation, the sedimentation assay was carried out using the conditions described in 6.2.4. The importance of reducing  $Mg^{2+}$  ions in SMALP solutions was again underlined by data that showed a strong ZipA band in the pellet of samples containing 10 mM  $MgCl_2$  (Figure 6-9). However, the majority of purified SMALP-ZipA remained on the supernatant when the concentration of  $MgCl_2$  was decreased to 2.5 mM  $MgCl_2$  (Figure 6-9).

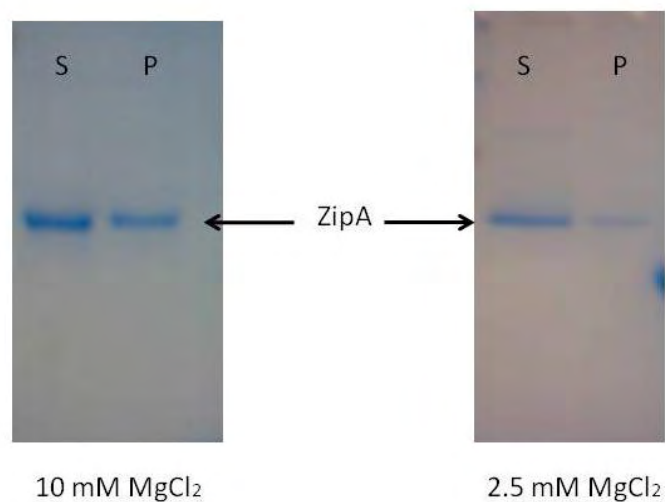


Figure 6-9. The effect of  $Mg^{2+}$  concentration on purified SMALP-ZipA using sedimentation assay

The SDS-PAGE gel showed the effect of  $MgCl_2$  on purified SMALP-ZipA was decreased to minimum by decreasing the concentration of  $MgCl_2$ . Supernatant (S) and pellet (P).  $3.3 \mu M$  ZipA was in polymerisation buffer (50 mM MES pH 6.5, 50 mM KCl, and 10 or 2.5 mM  $MgCl_2$ ) and 2 mM GTP. 2 mM GTP was immediately added to the sample to make up a final volume of 250  $\mu l$  before centrifugation at 80,000 rpm for 10 minutes. 125  $\mu l$  of supernatant was collected and the pellet was resuspended in 250  $\mu l$  of polymerisation buffer. The protein samples were mixed with 5xSDS-PAGE sample buffer. 20  $\mu l$  of mixture were then loaded onto the 10% SDS-PAGE gel.

Similar experiments to those mentioned above were also carried out to determine whether the FtsZ polymers sedimentation assay is affected by the concentration of  $MgCl_2$  (Figure 6-10). These data showed fewer FtsZ polymers were found in the pellet sample when the  $MgCl_2$  concentration was decreased to 2.5 mM. Although FtsZ polymers were decreased at the lower concentration of  $MgCl_2$  (2.5 mM), but it does not significantly affect the study on FtsZ-ZipA interaction.

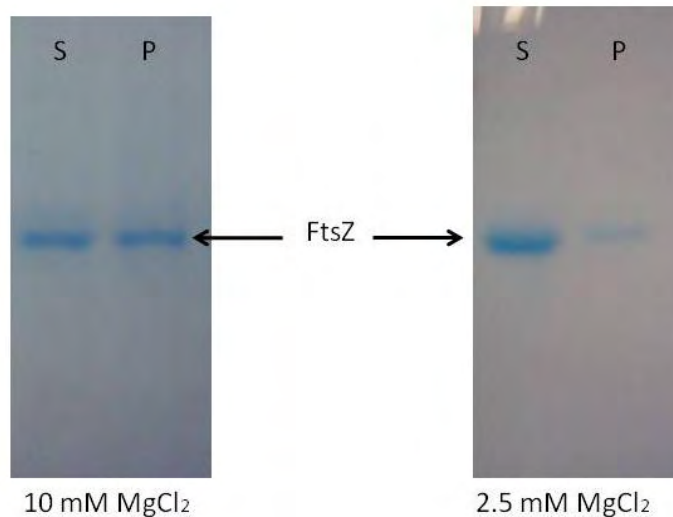


Figure 6-10. The effect of  $Mg^{2+}$  concentration on FtsZ polymerisation using sedimentation assay

The SDS-PAGE gel showed the FtsZ polymerisation was decreased by decreasing  $MgCl_2$  to 2.5 mM (less FtsZ found in the pellet). Supernatant (S) and pellet (P). Supernatant (S) and pellet (P). 3.67  $\mu$ M FtsZ was in polymerisation buffer (50 mM MES pH 6.5, 50 mM KCl, and 10 or 2.5 mM  $MgCl_2$ ) and 2 mM GTP. 2 mM GTP was immediately added to the sample to make up a final volume of 250  $\mu$ l before centrifugation at 80,000 rpm for 10 minutes. 125  $\mu$ l of supernatant was collected and the pellet was resuspended in 250  $\mu$ l of polymerisation buffer. The protein samples were mixed with 5xSDS-PAGE sample buffer. 20  $\mu$ l of mixture were then loaded onto the 10% SDS-PAGE gel.

When the polymerisation of FtsZ in the presence of ZipA was eventually carried out, these data showed more FtsZ polymers were found in the pellet in the presence of ZipA (Figure 6-11). This confirms that ZipA binds to FtsZ and suggests that ZipA promotes FtsZ polymerisation due to increase the number of FtsZ polymers found in the pellet.

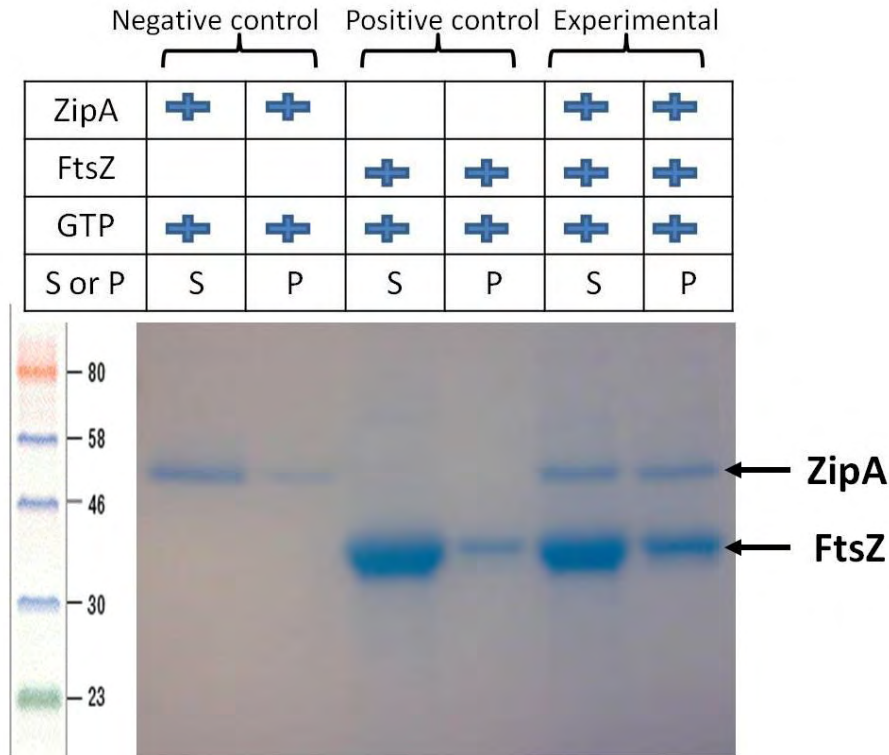


Figure 6-11. Sedimentation assay for polymerisation of FtsZ in the presence or absence of ZipA

The SDS-PAGE gel showed ZipA promotes FtsZ polymerisation and thus more FtsZ polymers were found in the pellet. Supernatant (S) and pellet (P). Lane 1 and 2 (from the left), negative control, where represent  $\mu\text{M}$  ZipA was in polymerisation buffer (50 mM MES pH 6.5, 50 mM KCl, and 2.5 mM  $\text{MgCl}_2$ ) and 2 mM GTP. Lane 3 and 4, positive control, represent  $\mu\text{M}$  FtsZ was in polymerisation buffer and 2 mM GTP. Lane 5 and 6, experimental, represent ZipA and FtsZ was at 3.3  $\mu\text{M}$  and 11 $\mu\text{M}$ , respectively, in polymerization buffer and 2 mM GTP. 2 mM GTP was immediately added to the sample to make up a final volume of 250  $\mu\text{l}$  before centrifugation at 80,000 rpm for 10 minutes. 125  $\mu\text{l}$  of supernatant was collected and the pellets were resuspended in 250  $\mu\text{l}$  of polymerisation buffer. The protein samples were mixed with 5xSDS-PAGE sample buffer. 20  $\mu\text{l}$  of mixture were then loaded onto the 10% SDS-PAGE gel.

### **6.2.6 GTPase Assay**

Previous studies have shown that FtsZ polymerisation is triggered by the presence of GTP, once GTP is depleted, the FtsZ polymers are disassociated [133]. In order to determine whether ZipA affects the GTPase activity of FtsZ, we used GTPase assay to examine the GTPase activity of FtsZ in the presence of different concentrations of ZipA. The experiment was started by adding 0.2 mM GTP into the sample. The data were transferred to the percentage of  $P_i$  released at any given time (100% represent the complete hydrolysis of GTP to GDP) (Figure 6-12). These data showed ZipA does not affect the GTPase activity of FtsZ, and this result is consistent with the observation by Haney *et al* and Liu *et al* [107, 146].

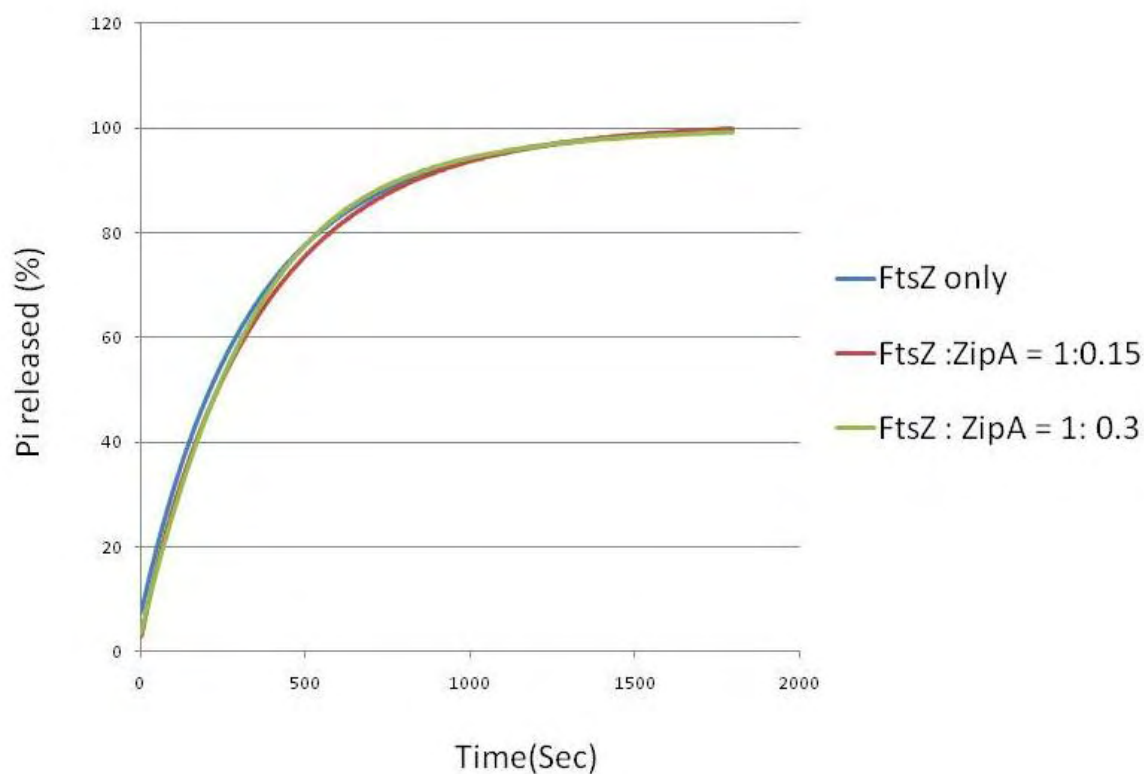


Figure 6-12. The effect of ZipA on the GTPase activity of FtsZ.

The  $P_i$  was released from the enzymatic conversion of GTP to GDP catalysed by FtsZ in the presence or absence of ZipA. The data showed ZipA does not affect the GTPase activity of FtsZ. The assay was performed by measuring  $Abs_{360}$  between the substrate (MESG) and its products (ribose 1-phosphate and 2-amino-6-mercapto-7-methylpurine). The experiment was carried out using a Jasco V-550 spectrometer at room temperature, and the wavelength was set up at 360 nm. The  $Abs_{360}$  was zeroed before adding 0.2 mM GTP into the sample. Data were collected every 1 second for 1800 seconds in a 0.5 cm path length cuvette. The data were transformed to the percentage of  $P_i$  released at any given time (100% represent the complete hydrolysis of GTP to GDP).

### **6.2.7 Linear Dichroism**

LD spectroscopy can be used to study the orientations of biomolecules in ordered arrays [114]. LD gives information about the spatial orientation of subunits of a system with respect to the orientation axis as well as the specific binding of ligands. LD experiments can be performed in systems that are intrinsically oriented or systems that can be oriented using external forces. LD has been previously used to detect FtsZ polymers as well as the orientation of chromophores within FtsZ fibres [113]. FtsZ polymerises upon GTP addition which means that the monomers (globular) are invisible to LD, however, when GTP is added to the solution, FtsZ forms the FtsZ polymers and these polymers can be oriented and have a large aspect ratio which LD spectrum can record.

In this section, we have used LD to examine the structure of the FtsZ polymers in the presence or absence of ZipA. The data presented here show that the LD signal at 211 nm in backbone region (190 to 260 nm) decreased in the presence of ZipA (Figure 6-13, A). These data suggest that either the FtsZ polymers have decreased in length or have become more curved upon addition of ZipA since in both cases a reduction in the LD signal would be obtained and therefore do not align as well as FtsZ polymers in the absence of ZipA.

We have also analysed if there was any change of the orientation of chromophores within the FtsZ polymers in order to get an insight of the possible mechanism of FtsZ protofilament formation and/or FtsZ protofilament/ZipA interaction. Examination of the LD region from 240 to 290 nm, which has been previously studied to report the orientation of GTP bound to FtsZ [133]. Figure 6-13 (B) showed the LD spectra of FtsZ in the absence or presence of increasing amounts of ZipA and it provides an insight into the possible mechanism of the GTP reorientation. The data showed a very slight difference in one of the guanine transitions (long axis) at ~250 nm from positive to negative when ZipA is present. This change is likely to be a reorientation of the guanine in the GTP due to the protofilaments lateral associations when ZipA is present.



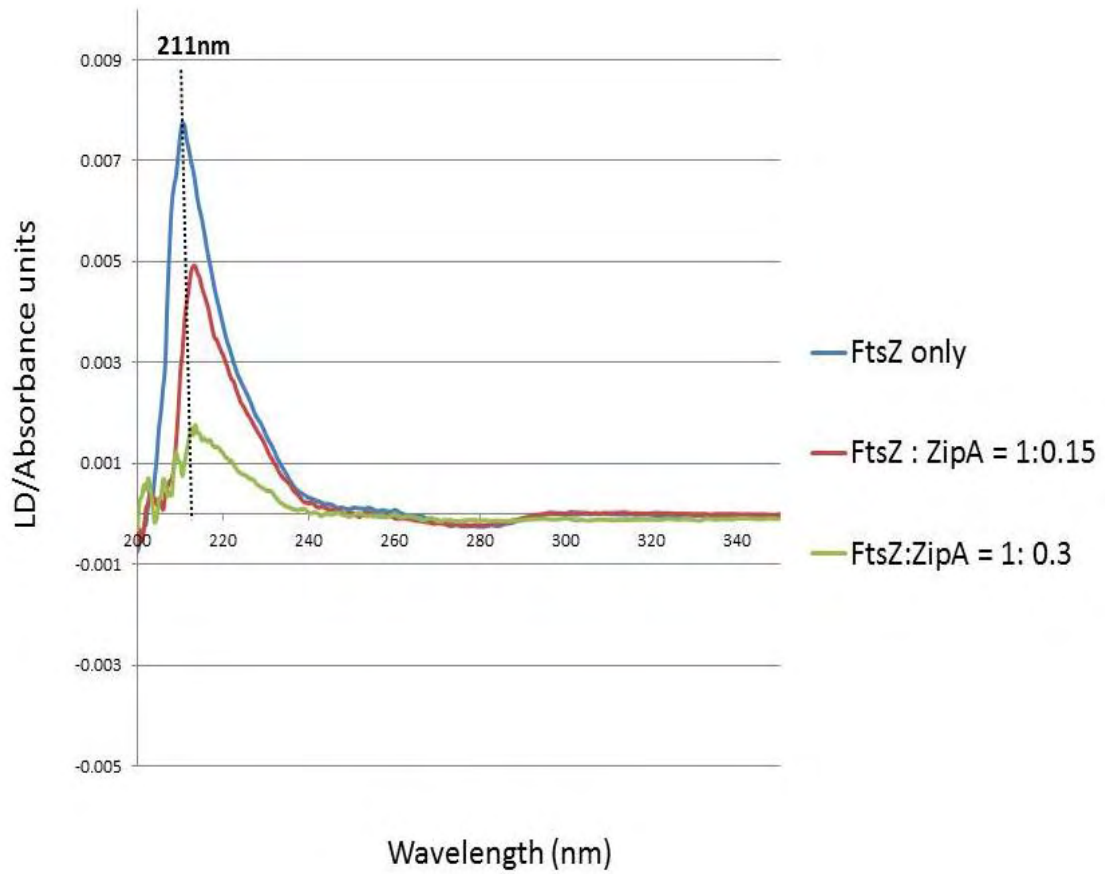


Figure 6-13(A) LD signal at 211 nm in backbone region

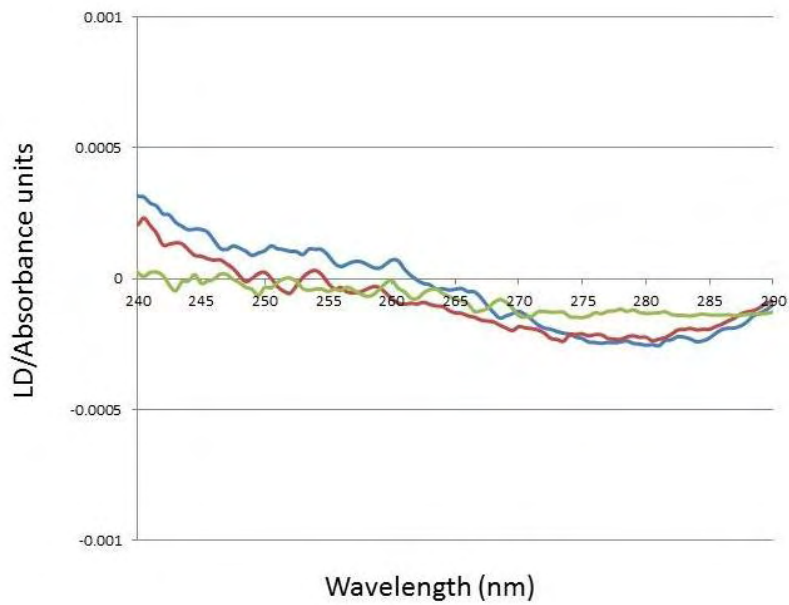


Figure 6-13 (B) Region from 240 to 290 nm

Figure 6-13 LD spectra of FtsZ protofilaments in the presence or absence of ZipA.

Increasing concentrations of ZipA (FtsZ :ZipA =1:0.15(red), FtsZ :ZipA =1:0.3(green)) were added to FtsZ protofilaments (to a final concentration of FtsZ 11  $\mu$ M). The samples were incubated at 25°C for 10 minutes in polymerization buffer (50 mM MES, pH 6.5, 50 mM KCl, and 2.5 mM MgCl<sub>2</sub>) to give a final volume of 90  $\mu$ l. (A) In the presence of increasing concentrations of ZipA, the LD backbone signal decreased. (B) The data showed a very slight difference in one of the guanine transitions (long axis) at ~250 nm from positive to negative when ZipA is present. The data were collected using a Jasco J-715 spectropolarimeter adapted for LD spectroscopy. The experiment was carried out with a rotation (7 V) and a blank (non-rotation) was subtracted from each sample measured. Data were recorded using an interval scan measurement programme. The wavelength range was set between 190 nm and 350 nm with a scanning speed of 200 nm/min and data pitch was set 0.5 seconds.

### **6.2.8 Electron Microscopy**

The effect of ZipA on FtsZ polymerisation was directly visualised by TEM. 0.2 mM GTP was added into the sample immediately before the sample was transferred to the carbon side of grid. The TEM data showed that in the absence of ZipA, FtsZ formed numerous straight or curved single protofilaments (Figure 6-14, A). In the presence of ZipA, the TEM micrograph showed these straight or curved protofilaments trended to bundle together (Figure 6-15, B), it suggests that ZipA promoted the bundling of FtsZ protofilaments.

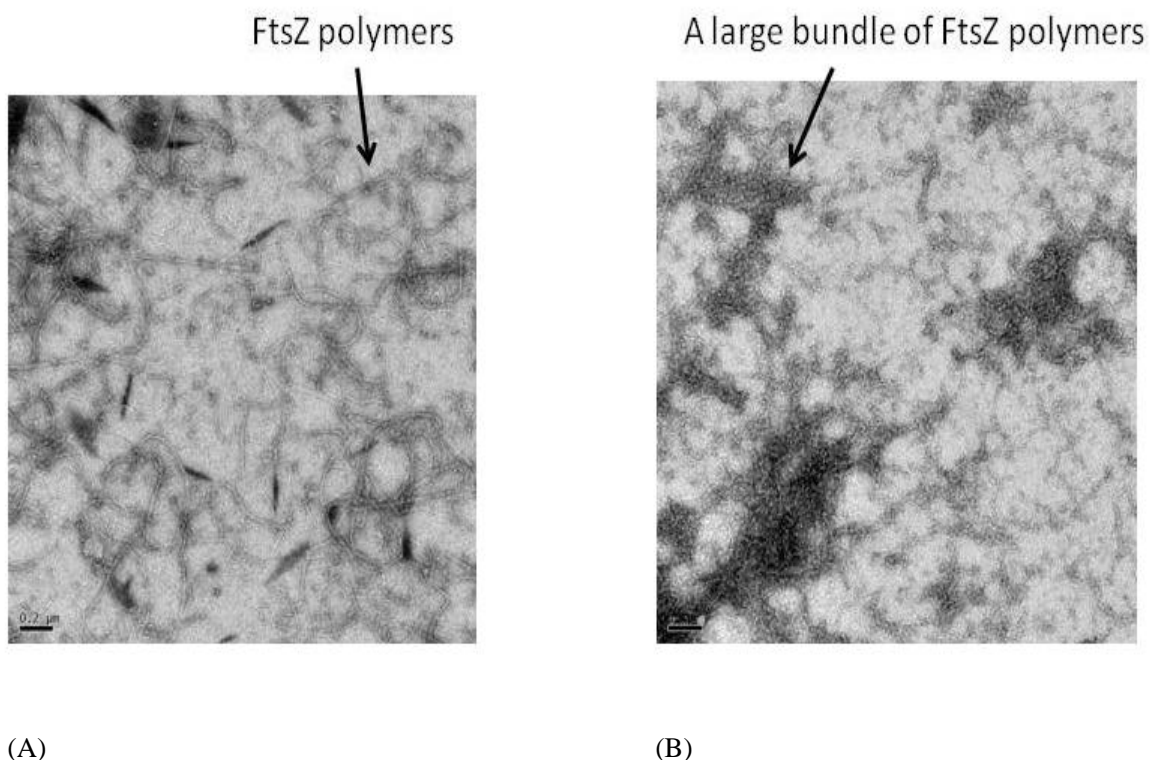


Figure 6-14. The effect of ZipA on FtsZ polymerisation. (A) In the absence of ZipA, FtsZ formed a lot of straight or curved single protofilaments. The length of these protofilaments was various. (B) In the presence of ZipA, these straight or curved protofilaments trended to bundle together. 100  $\mu$ l reactions contained 11  $\mu$ M FtsZ with or without 3.3  $\mu$ M ZipA were made up in the polymerization buffer and then incubated at 25°C for 10 minutes. 0.2 mM GTP was added to the mixture immediately before 5  $\mu$ l of the mixture was transferred to the carbon side of grid for 1 minute. The sample was stained by washing 1% uranyl acetate solution for 45 seconds. The experiment was carried out using a JEOL 2011 transmission electron microscope (TEM). Selected areas were photographed at  $\times 10,000$ . Scale bar represents 0.2  $\mu$ m.

### **6.2.9 Reconstitution of FtsZ-ring Inside A Giant Unilamellar Vesicle**

SMA polymer can be removed from pure SMALP solubilised protein by decreasing pH or adding  $MgCl_2$ , the process we termed “de-SMALP”. The protein can be inserted to the mimic

membrane system such as giant unilamellar vesicles (GUVs), one type of liposomes. This could allow us to create an artificial FtsZ-ring inside a GUV and then provide us a new route to understand the mechanism of cell division *in vitro* and in particular how the division machinery alters membrane morphology. These large vesicles with diameters of 5  $\mu\text{m}$  ~300  $\mu\text{m}$  have the advantage of being easily visualised using optical microscopy. Moreover, labelling GUVs with rhodamine 6G that allows GUVs to be seen by fluorescence confocal microscopy. It was decided that using the low pH method for the de-SMALP may destabilise protein. Therefore, we carried out the de-SMALP by adding 50 mM  $\text{MgCl}_2$ . CD data showed the de-SMALP ZipA inside a labelled GUV still maintained its native secondary structure (Figure 6-15).

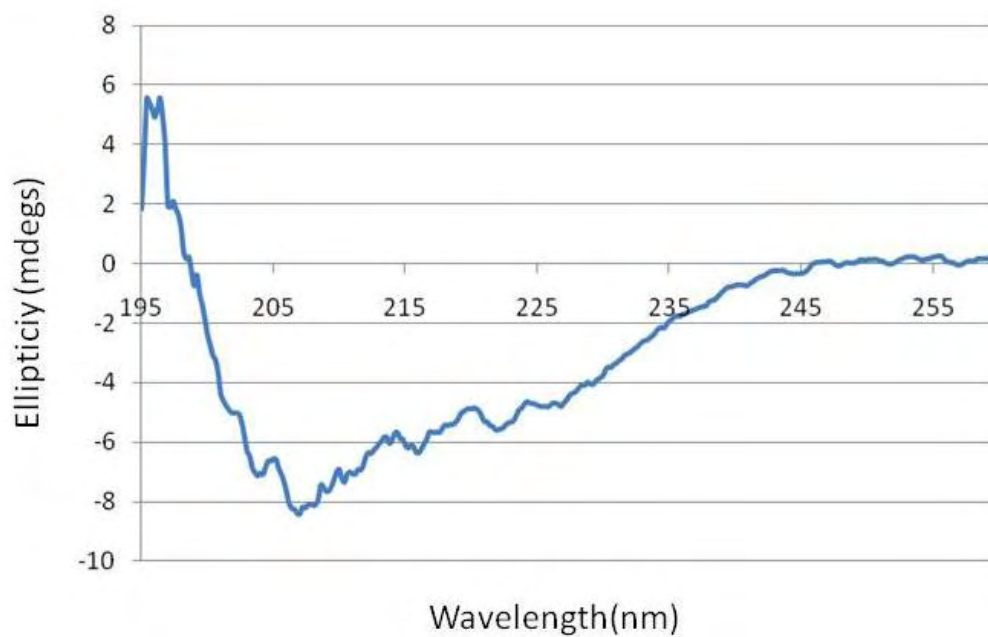
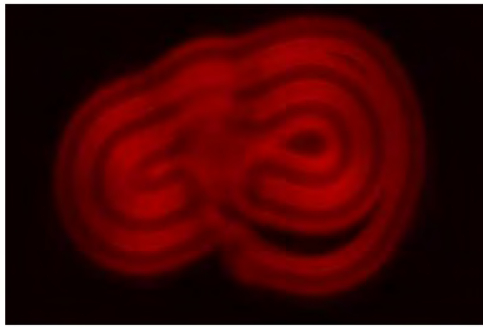


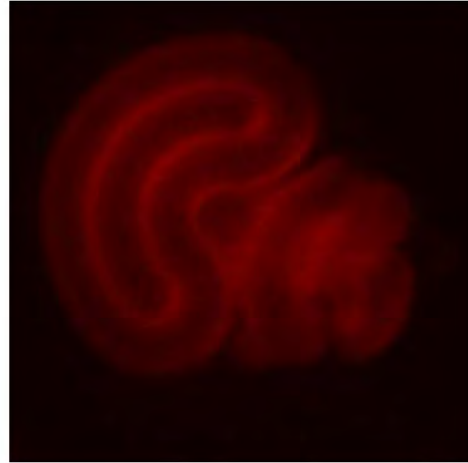
Figure 6-15. CD spectrum of de-SMALP ZipA inside a labelled GUV.

The CD data showed de-SMALP ZipA inside a GUV still maintained its native secondary structure during de-SMALP and reconstitution into a labelled GUV step. The de-SMALP ZipA was added into labelled GUV, mixed by gentle pipetting and then incubated at 37°C for 15 minutes. CD data were collected using JASCO J-715. CD spectra were collected using a 1 mm path length cuvette and averaged over 8 scans in the far-UV domain. Spectra acquired were corrected for the buffer signal.

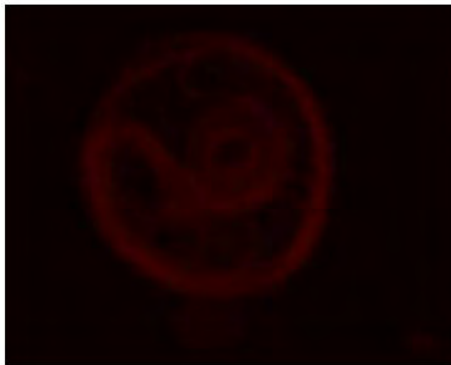
FtsZ was then added into labelled GUVs in the presence or absence of de-SMALP ZipA. The samples were then observed by confocal microscope. In the absence of ZipA, the photographs of confocal microscope showed the most of GUVs presented a shape which is like an “onion” (Figure 6-16, A and B). In the presence of ZipA, the most of GUVs were changed to many irregular shapes. Unfortunately, we did not observe any the structure is like a “ring” (Figure 6-16, C and D).



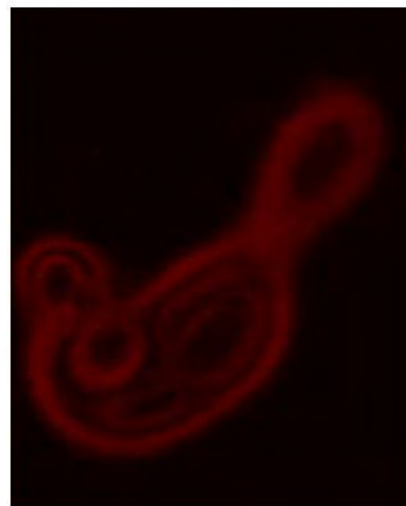
(A)



(B)



(C)



(D)

Figure 6-16. Confocal microscope of reconstitution of FtsZ-ring Inside a GUV. The ZipA (de-SMALP) and FtsZ were prepared in the polymerisation buffer to give a final protein concentration of 3.3  $\mu\text{M}$  and 11  $\mu\text{M}$ , respectively. (A) and (B), GUVs only contained 11  $\mu\text{M}$  FtsZ. (C) and (D), GUVs contained 11  $\mu\text{M}$  FtsZ and 3.3  $\mu\text{M}$  ZipA. The 67.5  $\mu\text{l}$  of proteins in the polymerisation buffer were added into GUVs to make up a final volume of 135  $\mu\text{l}$ , the sample was mixed by gentle pipetting and then incubated at 37°C for 15 minutes. GTP was added into the sample to give a final concentration of 2 mM, and then the reaction was observed immediately by Nikon A1R Inverted Confocal microscope at 60 times magnification.

### **6.3 Discussion**

In this chapter, we have shown the biophysical characterisation of purified SMALP-ZipA using a range of techniques including CD, svAUC, RALS assay, LD, GTPase and TEM. CD data showed purified SMALP-ZipA consists of  $\alpha$ -helices,  $\beta$ -sheets, it is consistent with its predicted structure. Moreover, the data also indicates that purified SMALP-ZipA contains a significant amount of unfolded structure, it is consistent with the presence of a P/Q domain which is predicted to be a largely unfolded polypeptide [99]. We also used svAUC to monitor the oligomerisation state of purified SMALP-ZipA. The data suggest that purified SMALP-ZipA is mainly monomeric (intense peak at 78 kDa). Taking the CD and svAUC data together, the purified SMALP-ZipA maintains its native structure at least at the level of secondary structure and it is mainly monomeric.

The FtsZ-ZipA interactions were then studied by various biophysical tools. These data showed ZipA affects the polymerisation of FtsZ but without affecting the GTPase activity of FtsZ. Data from LD studies showed that the presence of ZipA reduces the LD signal from the FtsZ fibres. This could be because the ZipA is disrupting the FtsZ, making it less long and hence less able to align. However, the results from sedimentation experiments showed different levels of FtsZ in the pellet with or without ZipA showing that this is not the case. Another possibility would be that the ZipA has changed the shape of the polymers making

them less linear. Examination of the TEM pictures suggest that this may be the case as more convoluted structures are observed in the FtsZ + ZipA experiments. This information is enough to begin to build a model to describe how ZipA affect FtsZ-ring during the cell division (see chapter 7).

Furthermore, we also attempt to reconstitute of FtsZ-ring inside a GUV. The experiment involved a process we termed “de-SMALP”, and then inserted ZipA into a GUV. Importantly, CD data shows no significant difference between SMALP-ZipA and de-SMALP ZipA inside a GUV. Studies of the effect of FtsZ polymerisation on the structure of GUVs containing ZipA showed the significant changes in morphology, indicating that a simple preliminary *in vitro* cell division system may have been reconstituted. However, we do not observe any the structure is like a “ring”. Therefore, the conditions of this experiment will require further development in the future.



## **CHAPTER 7: General Discussion, Conclusions and Future Work**

### **7.1 General Discussion**

Since the first membrane protein structure was solved in 1985, it has become possible to obtain atomic level structural information for membrane proteins. However, for the past 26 years, the production and study of membrane proteins has been limited by the ability to produce sufficient quantities of pure membrane protein. In particular the absence of a simple and universal protocol for extracting membrane proteins from the native membrane environment while at the same time maintaining their native structures and functions has been a real problem. This insufficiency has limited the study of the human biology and pharmaceuticals development as membrane proteins are central to a wide range of biological processes such as signal transduction, molecular transport, and respiration [129].

The main reason membrane protein is difficult to extract is their low solubility in water, which leads to instability and loss of activity. Most conventional methods require the use of detergent as an extraction agent from the cell membranes which often leads to the stripping of lipids from the protein and, as result, alteration of its activity. To address this problem, several model systems including the use of liposomes, amphipols, nanodiscs, and bicelles have allowed studying membrane proteins *in vitro* in a native-like membrane environment. All these current systems, however, have drawbacks and each of these methods require the

use of detergents to extract proteins from the cell membrane, and hence the stripping away of their native lipids. In addition, no single method has been universally satisfactory for its posterior biophysical study and characterisation. It is therefore crucial to develop a novel system which can be used to produce membrane proteins, ideally keeping them in their native environment without adding any detergents as well as being suitable for most techniques used to characterise membrane proteins.

SMALP, a novel method to study membrane proteins, has been reported in this thesis. This method has been successfully previously used to study two naturally abundant bacterial membrane proteins, PagP and bR [49]. In this project, we have demonstrated that SMALP can be used for studying more challenging membrane proteins, such as A<sub>2a</sub>R. We have showed for the first time that the SMALP system can be used to extract A<sub>2a</sub>R directly from *Pichia pastoris* cell membranes. The SMALP method performed equally well when compared to an existing detergent method (as it can be concluded from the radioligand binding assay results, data shown in the chapter 3). In pharmacological studies, the data showed that SMALP solubilised A<sub>2a</sub>R can bind to a number of small molecule ligands with native-like affinities, it demonstrates that SMALP maintains an environment similar to the native membrane. In addition, our industrial collaborator has demonstrated that SMALP can be used to solubilise membrane proteins directly from a mammalian cell membrane. It is

therefore clear that SMALP has applications across a wide range of expression systems (bacterial, yeast and mammalian cells). Another advantage of the SMALP system is that it is simple to use. The protocol that we have developed only requires adding SMA polymer (also supplied with the extra lipids) to extract the protein from the cell membrane. The downstream experiments do not require addition of extra polymer or lipids to maintain this condition. Other systems often require careful control of the experimental condition during the purification and subsequent analytical studies. For example, maintaining micelles require careful control the concentration to ensure that it is kept above CMC [8, 20], however, that is not the case if SMALP was to be used.

Continuing the comparison with detergent based preparation, one of the advantages of the SMALP system is that, in some cases, it leads to a reduction in the number of purification steps required to produce pure protein (2 versus 3 for A<sub>2a</sub>R). It is a good thing to decrease the number of purification steps when purifying a protein, especially for the low abundance protein such as GPCR as each step potentially decreases yield. We have also showed that SMALP can provide a more thermostable environment than detergent as suggested by the study of its thermal stability using radioligand binding assays. Figure 7-1 shows a model of a purified SMALP-A<sub>2a</sub>R.

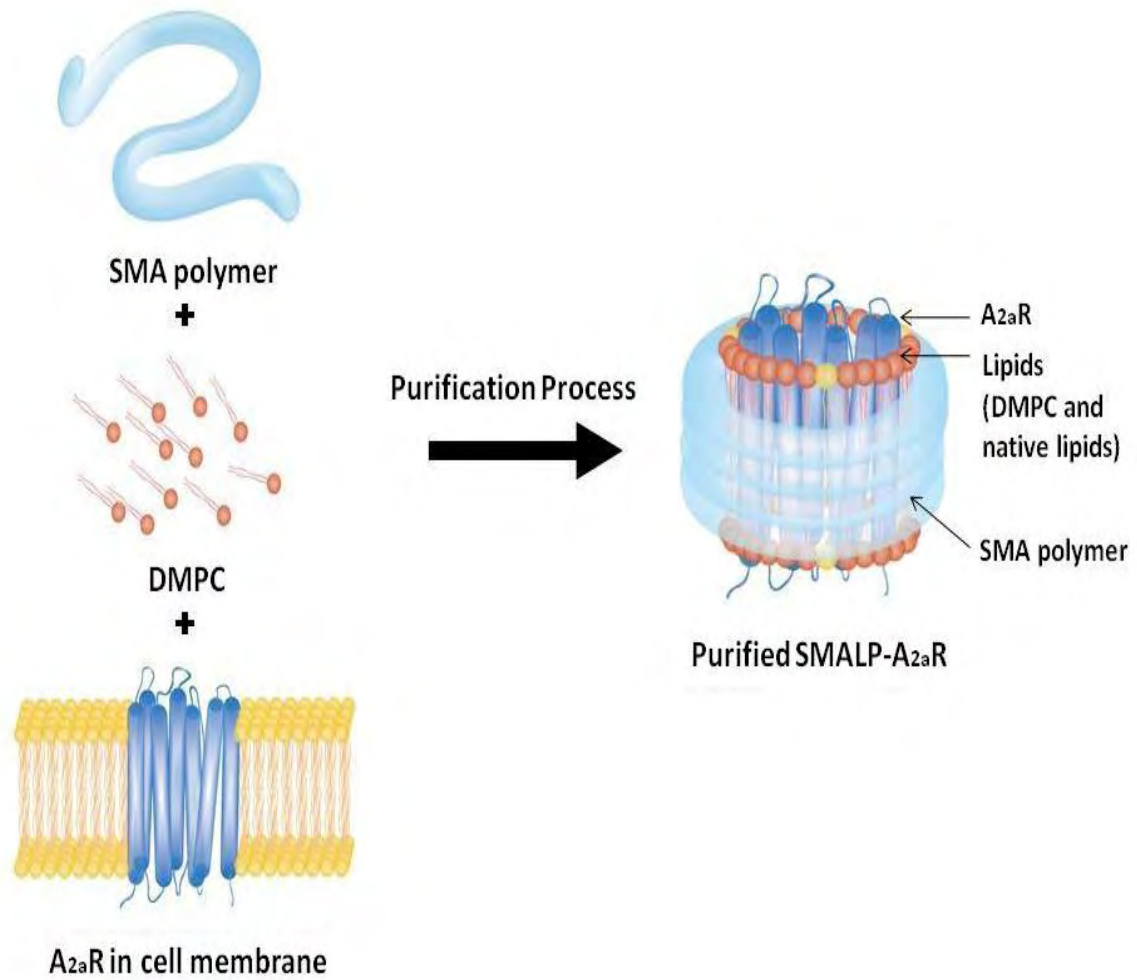


Figure 7-1. Model of a purified SMALP-A<sub>2a</sub>R

Cartoon shows the formation of purified SMALP-A<sub>2a</sub>R SMA polymer and DMPC are added into cell membranes containing A<sub>2a</sub>R. The final SMALP-A<sub>2a</sub>R is obtained after subsequent purification steps.

Moreover, we have also used this novel method to study the bacterial membrane protein ZipA, which is involved in bacterial cell division. We have characterised and studied ZipA protein and its interaction with FtsZ protein, which forms a ring in the inner membrane of bacteria that recruits approximately 15 auxiliary proteins including ZipA. ZipA was purified using the same protocol to purify A<sub>2a</sub>R demonstrating the universal nature of the SMALP method. The secondary structure of the purified SMALP-ZipA was characterised using CD, and the size was studied by svAUC. These data combined showed that the purified SMALP-ZipA maintained its native structure and it is mainly monomeric. Analysis of the FtsZ-ZipA interaction, showing that SMALP is complementary with several commonly used protein analysis methods including RALS assay, sedimentation assay, LD, GTPase assay and TEM.

In RALS assay, the signal was increased while FtsZ polymerisation (Figure 7-2, A). In the presence of ZipA, the signal has been shown a significant increase, this because ZipA induce the bundling of FtsZ polymers and thus produce the larger FtsZ polymers (Figure 7-2, B) [110,111].

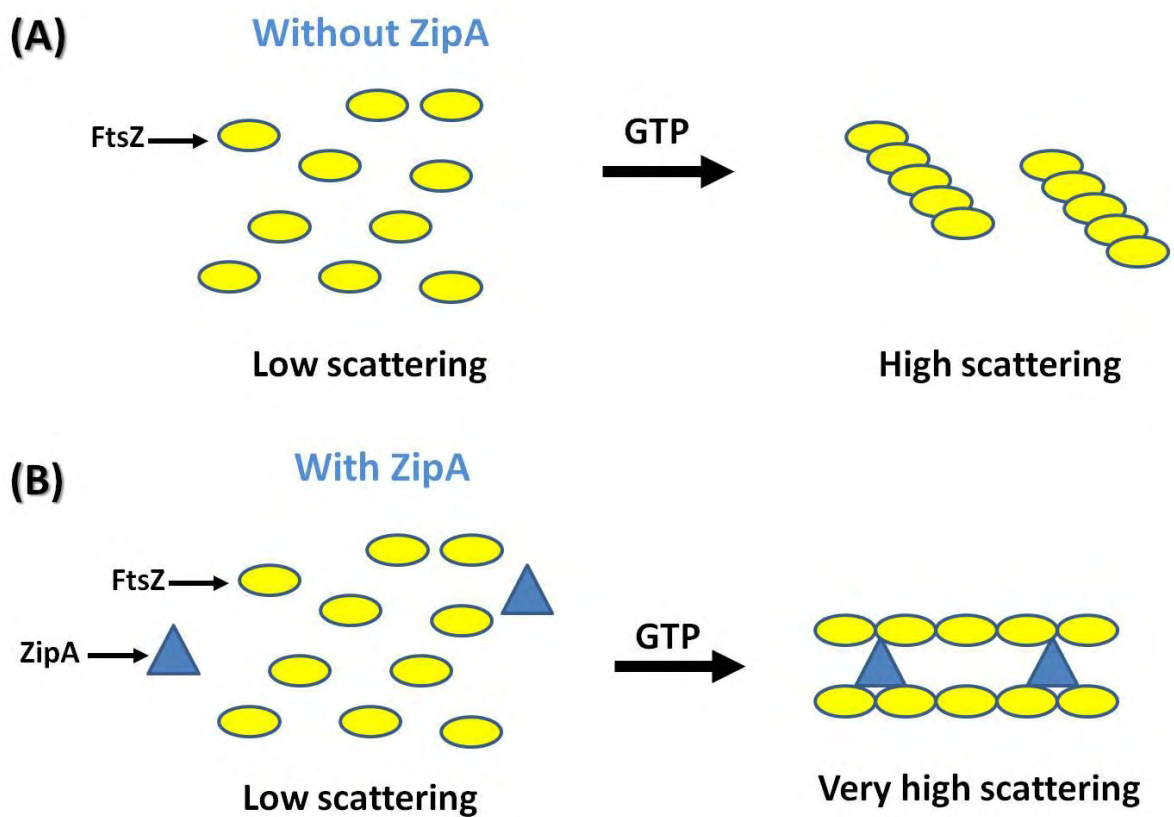


Figure 7-2 Schematic representation of the possible mechanism of FtsZ-ZipA interaction (A) Without ZipA, the signal is increased while FtsZ polymerisation. (B) In the presence of ZipA, ZipA induce bundling of FtsZ polymers and thus the signal has been shown a significant increase.

The sedimentation assay showed that FtsZ was presented in the pellet when GTP was added to FtsZ monomers indicating the formation of FtsZ polymers. In the presence of ZipA, more

intense band corresponding to the approximate molecular weight of FtsZ was observed in the SDS-PAGE gel of the pellet sample, suggesting that ZipA induces the bundling of FtsZ polymers. In addition, ZipA was also observed in the pellet, confirming that ZipA bound to FtsZ polymers. Figures 7-3 shows a schematic representation of the possible mechanism.

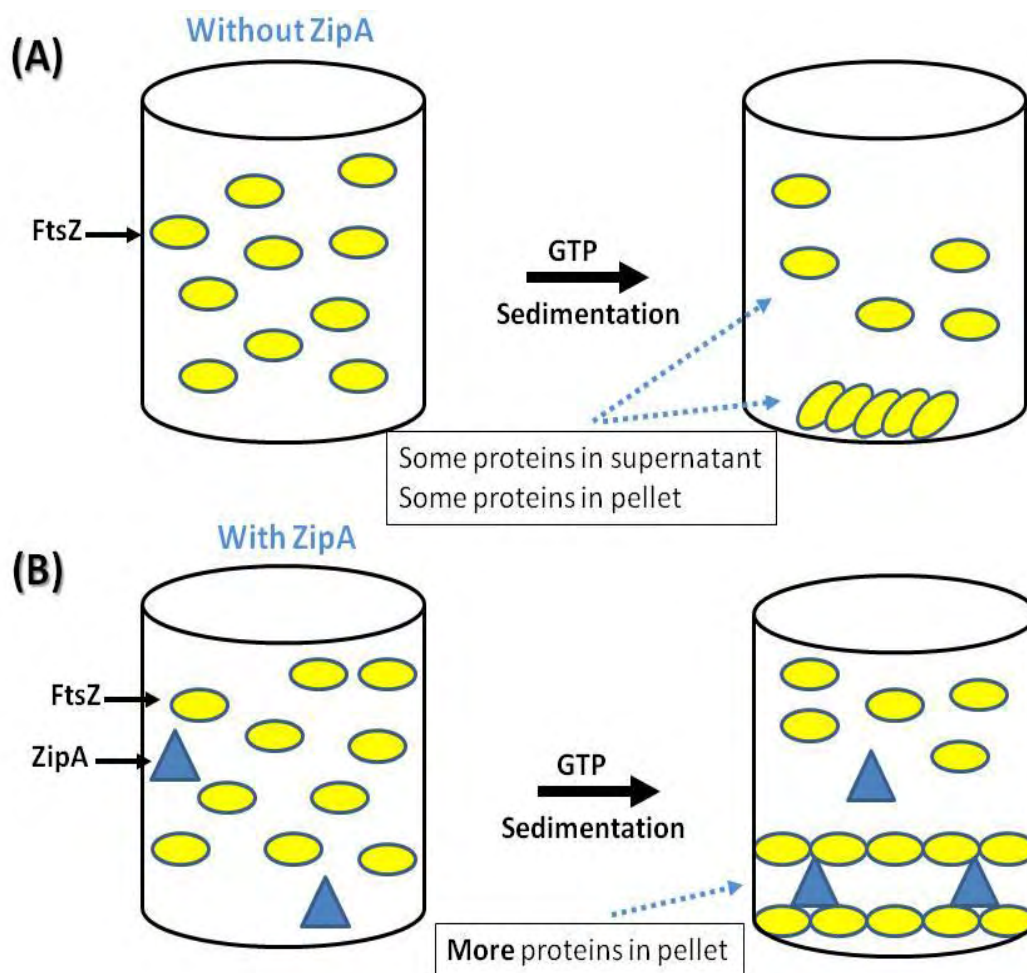


Figure 7-3. Schematic representation of the sedimentation assay performed on (A) in the absence of ZipA, FtsZ was presented in the pellet when GTP was added to FtsZ monomers indicating the formation of FtsZ polymers and (B) in the presence of ZipA, more FtsZ protein observed in the SDS-PAGE gel of the pellet sample, suggesting that ZipA induces the bundling of FtsZ polymers.

The LD data showed that the backbone far-UV signal decreased when increasing the concentration of ZipA which was added to FtsZ polymers. These data could be interpreted as three distinct possibilities: (1) ZipA makes the FtsZ polymers more flexible or curved; (2) the FtsZ polymerisation is reduced by ZipA (the polymers become shorter); (3) a combination of both. Figure 7-4 shows a schematic representation of these possible mechanisms. However, taking all the data together (RALS, sedimentation assay, LD and TEM) together, it is more likely to be the FtsZ polymers becoming more flexible or curved in the presence of ZipA.



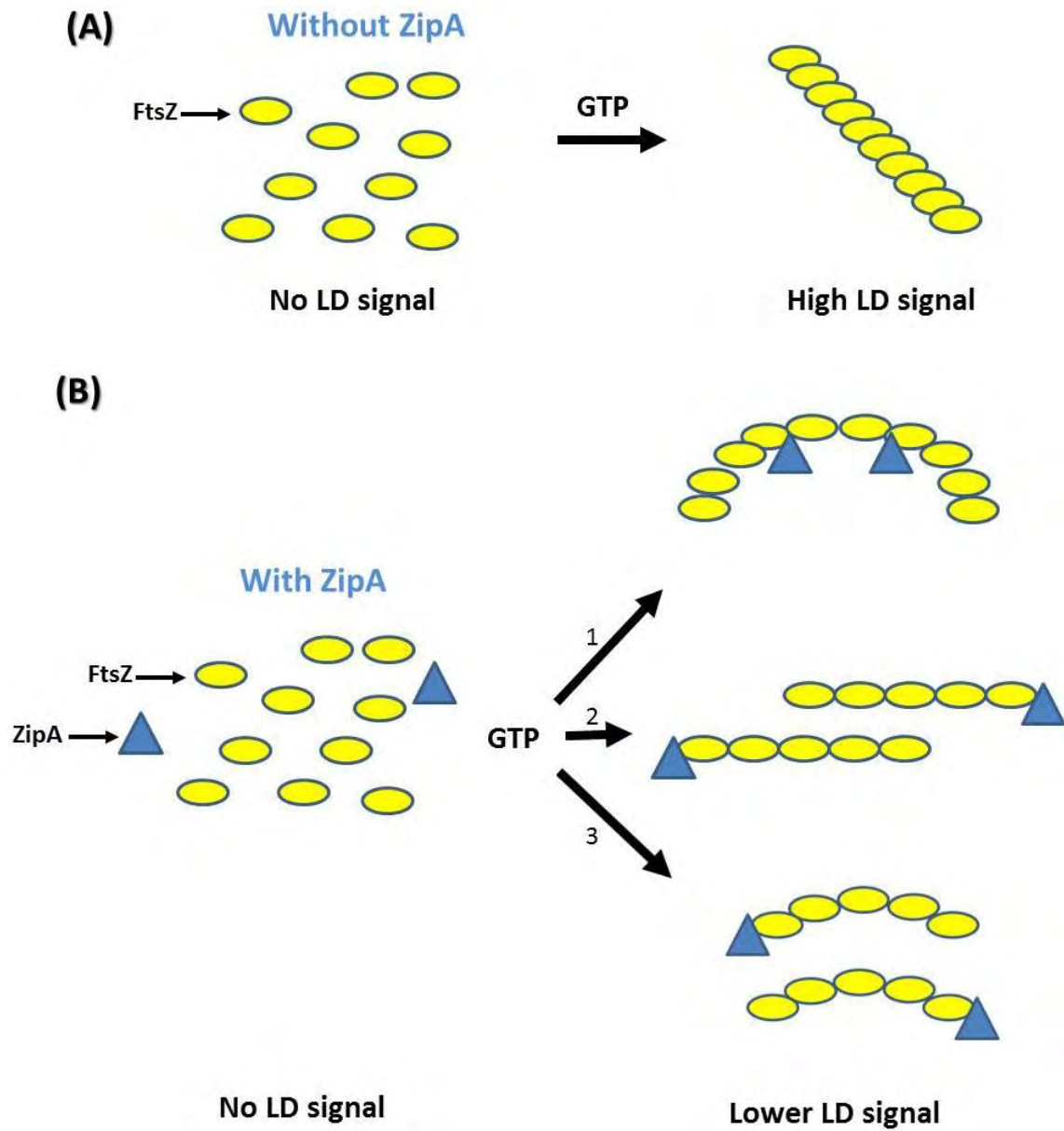


Figure 7-4. In the presence of increasing concentrations of ZipA, the backbone far-UV LD signal decreases. This indicates three possibilities (1) ZipA makes the FtsZ polymer more flexible or curved (2) the FtsZ polymerisation is reduced by ZipA or (3) a combination of both.

Overall, ZipA not only induces the bundling of FtsZ polymers, but also makes the polymers more flexible or curved (Figure 7-5). These data corroborates our previous results and agree with previous studies [107,110-112]. Our studies showed FtsZ can form FtsZ polymers, however, these polymers are more rigid in the absence of ZipA. In the presence of ZipA, these FtsZ polymers must be very flexible in order to form the FtsZ-ring. The data presented here support this mechanism and the biological role of this type of interaction.

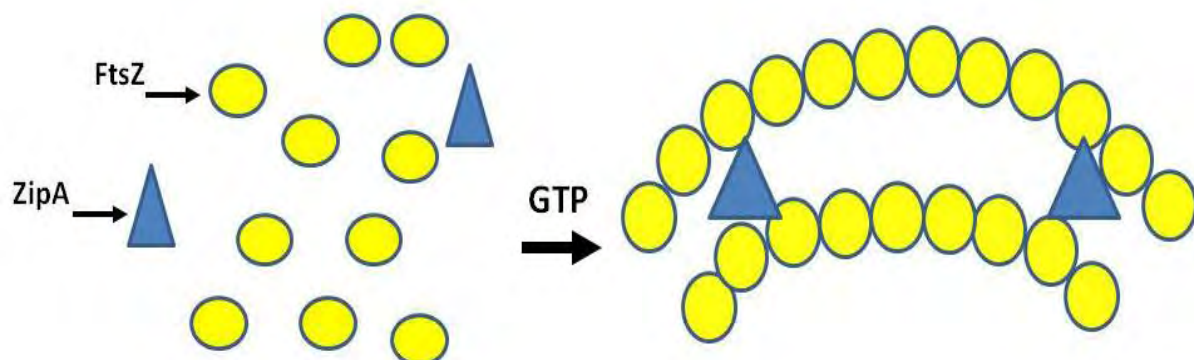


Figure 7-5. ZipA not only induces bundling of FtsZ polymers, but also makes the polymers more flexible or curved.

## **7.2 Conclusions**

The first aim of this project was to develop the SMALP method in order to use it with more challenging membrane proteins, such as G-protein coupled receptors. Our study has been successful and it has produced pure and active  $A_{2a}R$  without adding any detergent, the first

time that a GPCR has been purified in this way. Moreover, the results presented here show SMALP can impart added stability to the protein. The second aim of this project was to use SMALP to produce ZipA. This was successful and the resulting sample has been used to study the FtsZ-ZipA interaction, providing more information into the role of ZipA and FtsZ during the cell division. These results have significant implications for future membrane proteins providing a simple protocol to produce pure and active proteins in their native lipid environment for future studies. Table 7-1 shows a summary of the advantages and disadvantages of using SMALP method.

Advantages	Provide a native lipid environment
	Maintain lateral pressure
	Size homogeneity
	The protein can be extracted directly from the membrane without adding any detergent
	It is simple and easy to use
Disadvantages	It is affected by the magnesium concentration

Table 7-1: The advantages and disadvantages of SMALP

### **7.3 Future Work**

The very promising results obtained from this project have allowed us to demonstrate that SMALP can be used to produce membrane proteins. Further analytical and biophysical studies on the samples have the potential to gain a very important insight into these proteins.

Subsequent to the completion of this study, the methods pioneered in this project have been successfully applied to the purification of more than 10 membrane proteins. It would be important, however, to use SMALP solubilisation proteins in structural determination studies, such as crystallography. In addition, the attempt to reconstruct the FtsZ-ring inside a GUV presented in this project has shown some very promising results, however, it does not achieve our main aim, to see the ring inside a GUV, it still requires amending experiment protocol to approach it in the future.

## **CHAPTER 8: References**

- [1] E. Pebay-Peyroula (2007) *Biophysical Analysis of Membrane Proteins: Investigating Structure and Function* Wiley-VCH, Heppenheim.
- [2] D. Filmore (2004) "It's a GPCR world" *Mod. Drug. Discov.* 7 (11): 24-28.
- [3] Y. Okuno, A. Tamon, H. Yabuuchi, S. Nijima, Y. Minowa, K. Tonomura, R. Kunimoto and C. Feng.(2007) "GLIDA: GPCR—ligand database for chemical genomics drug discovery-atabase and tools update" *Nucl. Acids Res.* 36 (Database issue): 907-912.
- [4] J. Kendrew, R. Dickerson, B. Strandberg, R. Hart, and D. Davies (1960) "Structure of myoglobin: A three-dimensional Fourier synthesis at 2 Å resolution" *Nature* 185 (4711): 422-427.
- [5] J. Deisenhofer, K.Miki, R. Huber and H. Michel (1985) "Structure of the protein subunits in the photosynthetic reaction centre of Rhodospseudomonas viridis at 3Å resolution" *Nature* 318 (6047): 618-624.
- [6] S. White (2010) *Membrane protein of known 3D structure* [on-line] Available: [http://blanco.biomol.uci.edu/Membrane\\_Proteins\\_xtal.html](http://blanco.biomol.uci.edu/Membrane_Proteins_xtal.html) [date accessed: Dec 2010].
- [7] Protein data bank [on-line] Available: <http://www.pdb.org/pdb/home/home.do> [date accessed: Dec 2010].
- [8] M. Luckey (2008) *Membrane structural biology: with biochemical and biophysical foundations*, Cambridge University Press, New York.
- [9] T. Bayburt and S. Sligar. (2003) "Self-assembly of single integral membrane proteins into soluble nanoscale phospholipid bilayers" *Protein Sci.* 12 (11): 2476-2481.
- [10] A . Leitz, T. Bayburt, A. Barnakov, B.Springer, and S. Sligar1 (2006) "Functional reconstitution of β2-adrenergic receptors utilizing self-assembling Nanodisc technology" *BioTechniques* 40 (5): 601-612.

- [11] E. Carpenter, K. Beis, A. Cameron, and S. Iwata. (2008) "Overcoming the challenges of membrane protein crystallography" *Curr. Opin. Struct. Biol.* 18 (5): 581-586.
- [12] D. Nelson and M. Cox (2000) *Lehninger Principles of Biochemistry Third Edition* Worth, New York.
- [13] W. Dowhan (1997) "Molecular basis for membrane phospholipid diversity: Why Are There So Many Lipids?" *Annu. Rev. Biochem.* 66: 199-232.
- [14] A. Lee. (2003) "Lipid-protein interactions in biological membranes: a structural perspective" *Biochim. Biophys. Acta.* 1612 (1): 1-40.
- [15] K. Charalambous, D. Miller, P. Curnow and P. Booth. (2008) "Lipid bilayer composition influences small multidrug transporters" *BMC Biochemistry* 9: 31.
- [16] A. Seddon, M. Lorch, O. Ces, R. Templer, F. Macrae and P. Booth. (2008) "Phosphatidylglycerol Lipids Enhance Folding of an  $\alpha$  Helical Membrane Protein" *J. Mol. Biol.* 380 (3): 548-556.
- [17] A. Starling, J. Malcolm and A. Lee. (1995) "Phosphatidylinositol 4-Phosphate Increases the Rate of Dephosphorylation of the Phosphorylated  $\text{Ca}^{2+}$ -ATPase" *J. Biol. Chem.* 270: 14467-14470.
- [18] T. Fong, M. McNamee. (1986) "Correlation between acetylcholine receptor function and structural properties of membranes" *Biochemistry* 25 (4): 830-840.
- [19] S. White, W. Wimley. (1999) "Membrane protein folding and stability: physical principles" *Annu. Rev. Biophys. Biomol. Struct.* 28: 319-365.
- [20] C. Hunte, G. Jagow, H. Schagger (2003) *Membrane Protein Purification and Crystallization, Second Edition: A Practical Guide* Academic Press, London.
- [21] F. Junge, B. Schneider, S. Reckel, D. Schwarz, V. Detsch and F. Bernhard. (2008) "Large-scale production of functional membrane proteins" *Cell. Mol. Life Sci.* 65 (11): 1729-1755.
- [22] M. Lu and D. Fu (2007) "Structure of the zinc transporter YiiP" *Science* 317 (5845): 1746-1748.

- [23] Y. Yin, X. He, P. Szewczyk, T. Nguyen and G. Chang (2006) "Structure of the multidrug transporter EmrD from *Escherichia coli* " *Science* 312 (5774): 741-744.
- [24] A. Boutigny S, Kunji and N. Rolland (2010) "Membrane protein expression in *Lactococcus lactis* " *Methods Mol. Biol.* 601: 67-85.
- [25] N. Fraser. (2006) "Expression and functional purification of a glycosylation deficient version of the human adenosine 2a receptor for structural studies" *Protein Expr. Purif.* 49 (1): 129-137.
- [26] M. O'Malley, T. Lazarova, Z. Britton and A. Robinson. (2007) "High-level expression in *Saccharomyces cerevisiae* enables isolation and spectroscopic characterization of functional human adenosine A2a receptor " *J. Struct. Biol.* 159 (2): 166-78.
- [27] Z. Wang, J. Ma, L. Zhou, X. Zhang, H. Du , S. Yang, Y. Zeng (2010) "Expression and purification of EBV-LMP2 protein" *Zhonghua Shi Yan He Lin Chuang Bing Du Xue Za Zhi.* 24(3): 168-70.
- [28] P.Reeves, N. Callewaert, R. Contreras, and G. Khorana (2002) "Structure and function in rhodopsin: high-level expression of rhodopsin with restricted and homogeneous N-glycosylation by a tetracycline-inducible *N*-acetylglucosaminyl- achtungternung transferase I-negative HEK293S stable mammalian cell line" *PNAS* 99 (21): 13419-13424.
- [29] F. Katzen, T. Peterson and W. Kudlicki. (2009) "Membrane protein expression: no cells required " *Trends Biotechnol.* 27 (8): 455-460.
- [30] S. Singh, A. Gras, C. Fiez-Vandal, J. Ruprecht, R. Rana, M. Martinez, P. Strange, R. Wagner and B. Byrne. (2008) "Large-scale functional expression of WT and truncated human adenosine A2A receptor in *Pichia pastoris* bioreactor cultures" *Microb. Cell Fact.* 7: 28.
- [31] M. Opekarova and W. Tanner (2003) "Specific lipid requirements of membrane proteins – a putative bottleneck in heterologous expression." *Biochim. Biophys. Acta* 1610 (1): 11-22.
- [32] A. Lee (2004) "How lipids affect the activities of integral membrane proteins" *Biochim. Biophys. Acta.* 1666 (1-2): 62-87.

- [33] C. Hunte (2005) "Specific protein-lipid interactions in membrane proteins" *Biochem. Soc. Trans.* 33 (Pt5): 938-942.
- [34] L. Zhang. *Summary of methods to prepare lipid vesicles*. [on-line] Available <http://mit.edu/sjiang2/www/Resources/Prepare%20Lipid%20Vesicles.pdf> [date accessed: Nov 2010].
- [35] J. Popot. (2010) "Amphipols, Nanodiscs, and Fluorinated Surfactants: Three Nonconventional Approaches to Studying Membrane Proteins in Aqueous Solutions" *Annu. Rev. Biochem.* 79: 737-75.
- [36] C. Tribet, R. Audebert and J. Popot. (1996) "Amphipols: Polymers that keep membrane proteins soluble in aqueous solutions" *PNAS* 93 (26): 15047-15050.
- [37] S. Rajesh, T. Knowles and M. Overduin. (2010) "Production of membrane proteins without cells or detergents" *N. Biotechnol.* 2010 Jul 21.
- [38] C. Diab , C. Tribet, Gohon, J. Popot and F. Winnik (2007) "Complexation of integral membrane proteins by phosphorylcholine - based amphipols" *Biochim. Biophys. Acta.* 1768 (11): 2737-2747.
- [39] M. Bonnie, Gorzelle, A. Hoffman, M. Keyes, D. Gray, D. Ray and C. Sanders. (2002). "Amphipols can support the activity of a membrane enzyme." *J. Am. Chem. Soc.* 124 (39): 11594-11595.
- [40] P. Champeil, T. Menguy, C. Tribet, J. Popoti and M. Maire. (2000) "Interaction of amphipols with sarcoplasmic reticulum Ca<sup>2+</sup>-ATPase" *J. Biol. Chem.* 275 (25): 18623-18637.
- [41] T. Dahmane, M. Damian, S. Mary, J. Popot and J. Banères. (2009) "Amphipol-assisted in vitro folding of G protein – coupled receptors" *Biochemistry* 48 (27): 6516-6521.
- [42] T. Bayburt, Y. Grinkova, and S. Sligar. (2002) "Self-assembly of discoidal phospholipid bilayer nanoparticles with membrane scaffold proteins" *Nano Lett.* 2 (8): 853-856.
- [43] K. Glover, J. Whiles, G. Wu, N. Yu, R. Deems, J. Struppe, R. Stark , E. Komives and R. Vold (2001) "Structural evaluation of phospholipid bicelles for solution-state studies of membrane-associated biomolecules" *Biophys J.* 81 (4): 2163-2171.



- [44] J. Whiles, R. Deems, R. Vold and E. Dennis. (2002) "Bicelles in structure–function studies of membrane-associated proteins." *Bioorg. Chem.* 30 (6): 431-442.
- [45] R. Vold and R. Prosser (1996) "Magnetically Oriented Phospholipid Bilayered Micelles for Structural Studies of Polypeptides. Does the Ideal Bicelle Exist?" *Mag. Reson. B* 113 (3): 267-271.
- [46] P. Mohanty, J. Lee, K. Glover and K. Landskron (2011) "Discoid bicelles as efficient templates for pillared lamellar periodic mesoporous silicas at pH 7 and ultrafast reaction times" *Nanoscale Res. Lett.* 6: 61.
- [47] A. Seddon, P. Curnow, P. Booth (2004) "Membrane proteins, lipids and detergents: not just a soap opera" *Biochim Biophys Acta* 1666(1-2): 105-17.
- [48] S. Tonge and B. Tighe. (2001) "Responsive hydrophobically associating polymers: a review of structure and properties" *Adv. Drug Deliv. Rev.* 53 (1): 109-122.
- [49] T. Knowles, R. Finka, S. Corinne, Y. Lin, T. Dafforn, M. Overduin (2009) "Membrane proteins solubilized intact in lipid containing nanoparticles bounded by styrene maleic acid copolymer" *J Am Chem Soc.* 131(22): 7484-5.
- [50] A. Howard, G. McAllister, D Feighner, Y. Liu, P. Nargund, T. Van der Ploeg and A. Patchett (2001) "Orphan G-protein-coupled receptors and natural ligand discovery" *Trends Pharmacol. Sci.* 22 (3): 132-140.
- [51] C. Venter (2001) "The sequence of the human genome " *Science* 291 (5507): 1304-1351.
- [52] G. Vauquelin and B. Mentzer (2007) *Protein-coupled Receptors, Molecular Pharmacology, From Academic Concept to Pharmaceutical Research*  
John Wiley & Sons, Chichester.
- [53] S. Ahn, C. Nelson, T. Garrison, W. Miller and R. Lefkowitz. (2003) "Desensitization, internalization, and signaling functions of  $\beta$ -arrestins demonstrated by RNA interference " *PNAS.* 100 (4): 1740-1744.
- [54] B. Cen; Q. Yu, J. Guo, Y. Wu, K. Ling, Z. Cheng, L. Ma and G. Pei. (2001) "Direct binding of beta-arrestins to two distinct intracellular domains of the delta opioid receptor" *J. Neurochem.* 76 (6): 1887-1894.

- [55] A. Claing; W. Chen, W. Miller, N. Vitale, J. Moss, R. Premont and R. Lefkowitz (2001) "Beta-Arrestin-mediated ADP-ribosylation factor 6 activation and beta 2-adrenergic receptor endocytosis " *J. Biol. Chem.* 276 (45): 42509-42513.
- [56] A. Conlan, M. Lindus and T. Gillespie (2002) "The COOH-terminus of parathyroid hormone-related protein (PTHrP) interacts with beta-arrestin 1B" *FEBS Lett.* 527 (1-3): 71-75.
- [57] V. Jaakola, M. Griffith, M. Hanson, V. Cherezov, Y. Chien, J. Lane, A. Ijzerman and R. Stevens. (2008) "The 2.6 angstrom crystal structure of a human A2A adenosine receptor bound to an antagonist" *Science* 322 (5905): 1211-1217.
- [58] K. Palczewski, T. Kumasaka, T. Hori, C. Behnke, H. Motoshima, B. Fox, I. Trong, D. Teller, T. Okada, R. Stenkamp, M. Yamamoto and M. Miyano. (2000) "Crystal structure of rhodopsin: a G protein-coupled receptor " *Science* 289 (5480): 739-745.
- [59] S. Rasmussen, H. Choi, D. Rosenbaum, T. Kobilka, F. Thian, P. Edwards, M. Burghammer, V. Ratnala, R. Sanishvili, R. Fischetti, G. Schertler, W. Weis and B. Kobilka. (2007) "Crystal structure of the human  $\beta_2$ adrenergic G-protein-coupled receptor" *Nature* 450 (7168): 383-384.
- [60] V. Cherezov, D. Rosenbaum, M. Hanson, S. Rasmussen, F. Thian, T. Kobilka, H. Choi, P. Kuhn, W. Weis, B. Kobilka and R. Stevens. (2007) "High-resolution crystal structure of an engineered human  $\beta_2$ -adrenergic G Protein-coupled receptor" *Science* 318 (5854): 1258-1265.
- [61] T. Warne, M. Serrano-Vega, J. Baker, R. Moukhametzianov, P. Edwards, R. Henderson, A. Leslie, C. Tate and G. Schertler. (2008) "Structure of a  $\beta_1$ -adrenergic G-protein-coupled receptor" *Nature* 454 (7203): 486-492.
- [62] B. Wu, Y. Chien, C. Mol, G. Fenalti, W. Liu, V. Katritch, R. Abagyan, A. Brooun, P. Wells, F. Bi, D. Hamel, P. Kuhn, T. Handel, V. Cherezov and R. Stevens (2010) "Structures of the CXCR4 Chemokine GPCR with Small-Molecule and Cyclic Peptide Antagonists." *Science* 330 (6007): 1066-1071.

- [63] T. Chien, W. Liu, W. Han, V. Katritch, Q. Zhao, V. Cherezov and C. Stevens  
*Accelerated Technologies Center for Gene to 3D Structure (ATCG3D)*  
[on-line] Available: <http://www.pdb.org/pdb/home/home.do> [date accessed: Dec 2010].
- [64] T. Dunwiddie and S. Masino. (2001) "The role and regulation of adenosine in the central nervous system " *Annu. Rev. Neurosci.* 24:31-55.
- [65] Y. Shi, X. Liu, D. Gebremedhin, J. Falck, D. Harder and R. Koehler. (2008) "Interaction of mechanisms involving epoxyeicosatrienoic acids, adenosine receptors and metabotropic glutamate receptors in neurovascular coupling in rat whisker barrel cortex" *J. Cereb. Blood. Flow. Metab.* 28 (1): 111-125.
- [66] S. Lahiri, C. Mitchell, D. Reigada, A. Roy and N. Cherniack. (2007) "Purines, the carotid body and respiration" *Respir. Physiol. Neurobiol.* 157 (1): 123-129.
- [67] E. Ongini, M. Adami, C. Ferri and R. Bertorelli (1997) "Adenosine A2A receptors and neuroprotection " *Ann. N Y Acad. Sci.* 825 (1): 30-48.
- [68] M. Hernan, B. Takkouche, F. Caamano-Isorna and J. Gestal-Otero. (2002)  
"A meta-analysis of coffee drinking, cigarette smoking, and the risk of Parkinson's disease."  
*Ann. Neurol.* 52 (3): 276-284.
- [69] M. Guzman, S. Weiss and J. Beckwith (1997) "Domain-Swapping analysis of FtsI, FtsL and FtsQ, Bitopic membrane proteins essential for cell division in *Escherichia coli*" *J. Bacteriology* 179(16): 5094-5103.
- [70] J. Lutkenhaus (1993) "FtsZ-ring in bacterial cytokinesis" *Molecular Microbiology* 9(3): 403-409.
- [71] J. Lutkenhaus and S. Addinall,. (1997) "Bacterial cell division and the Z ring" *Annu. Rev. Biochem.* 66: 93-116.
- [72] N. Goehring and J. Beckwith. (2005) "Diverse Paths to Midcell: Assembly of the Bacterial Cell Division Machinery" *Curr. Bio.* 15: 514-526.
- [73] J. Errington A. Daniel and J. Scheffers (2003) "Cytokinesis in bacteria Microbiol " *Mol. Biol. Rev.* 67 (1): 52-65.

- [74] N. Buddelmeijer and J. Beckwith (2002) "Assembly of cell division proteins at the *E. coli* cell center " *Curr. Opin. Microbiol.* 5 (6): 553-557.
- [75] B. Lewin (2007) *Genes IX* Jones & Bartlett Learning, Sudbury.
- [76] S. Pichoff and J. Lutkenhaus (2005) " Tethering the Z-ring to the membrane through a conserved membrane targeting sequence in FtsA" *Mol. Microbiol.* 55 (6): 1722-1734.
- [77] J. Gueiros-Filho and R. Losick (2002) "A widely conserved bacterial cell division protein that promotes assembly of the tubulin-like protein FtsZ" *Genes Dev.* 16 (19): 2544-2556.
- [78] E. Bi, and J. Lutkenhaus, (1993) "Cell division inhibitors Sula and MinCD prevent formation of the FtsZ-ring " *J. Bacteriol.* 175 (4): 1118-1125.
- [79] D. Raskin and P. Boer, (1999) " Rapid pole-to-pole oscillation of a protein required for directing division to the middle of *Escherichia coli* " *PNAS* 96 (9): 4971-4976.
- [80] D. Raskin, and P. Boer, (1999) " MinDE-dependent pole-topole oscillation of division inhibitor MinC in *Escherichia coli* " *J. Bacteriol.* 181 (20): 6419-6424.
- [81] K. Suefuji, R. Valluzzi, and D. RayChaudhuri, (2002) "Dynamic assembly of MinD into filament bundles modulated by ATP, phospholipids, and MinE " *PNAS* 99 (26): 16776-16781.
- [82] L. Ma, G. King, and L. Rothfield, (2004) "Positioning of the MinE binding site on the MinD surface suggests a plausible mechanism for activation of the *Escherichia coli* MinD ATPase during division site selection" *Mol. Microbiol.* 54 (1): 99-108.
- [83] Z. Hu, C. Saez, and J. Lutkenhaus, (2003) "Recruitment of MinC, an inhibitor of Z-ring formation, to the membrane in *Escherichia coli*: role of MinD and MinE" *J. Bacteriol.* 185 (1): 196-203.
- [84] P. de Boer, R. Crossley and L. Rothfield (1992) " The essential bacterial cell-division protein FtsZ is a GTPase " *Nature* 359 (6392): 254-256.
- [85] D. RayChaudhuri and J. Park (1992) "*Escherichia coli* cell-division gene *ftsZ* encodes a novel GTP-binding protein" *Nature* 359 (6392): 251-254.

- [86] B. Beall and J. Lutkenhaus (1991) "FtsZ in *Bacillus subtilis* is required for vegetative septation and for asymmetric septation during sporulation" *Genes Dev.* 5 (3): 447-455.
- [87] K. Dai and J. Lutkenhaus (1991) "FtsZ is an essential cell division gene in *Escherichia coli*" *J. Bacteriol.* 173 (11): 3500-3506.
- [88] A. Katharine and J. Löwe. (2006) "Dynamic filaments of the bacterial cytoskeleton" *Annu. Rev. Biochem.* 75: 467-492.
- [89] J. Glass, E. Lefkowitz, J. Glass, C. Heiner, E. Chen and G. Cassell. (2000) "The complete sequence of the mucosal pathogen *Ureaplasma urealyticum*" *Nature* 407 (6805): 757-762.
- [90] R. Stephens, S. Kalman, C. Lammel, J. Fan, R. Marathe, L. Aravind, W. Mitchell, L. Olinger, R. Tatusov, Q. Zhao, E. Koonin and R. Davis (1998) "Genome sequence of an obligate intracellular pathogen of humans: *Chlamydia trachomatis*" *Science* 282 (5389): 754-759.
- [91] Y. Kawarabayashi, Y. Hino, H. Horikawa, S. Yamazaki, Y. Haikawa, K. Jin-no, M. Takahashi, M. Sekine, S. Baba, A. Ankai, H. Kosugi, A. Hosoyama, S. Fukui, Y. Nagai, K. Nishijima, H. Nakazawa, M. Takamiya, S. Masuda, T. Funahashi, T. Tanaka, Y. Kudoh, J. Yamazaki, N. Kushida, A. Oguchi and H. Kikuchi (1999) "Complete genome sequence of an aerobic hyper-thermophilic crenarchaeon, *Aeropyrum pernix* K1" *DNA Res.* 6 (2): 83-101, 145-152.
- [92] P. Beech, T. Nheu, T. Schultz, S. Herbert, T. Lithgow, P. Gilson and G. McFadden (2000) "Mitochondrial FtsZ in a chromophyte alga." *Science* 287 (5456): 1276-1279.
- [93] K. Osteryoung and E. Vierling. (1995) "Conserved cell and organelle division" *Nature* 376 (6540): 473-474.
- [94] J. Löwe and L. Amos (1998) "Crystal structure of the bacterial cell-division protein FtsZ" *Nature* 391: 203-206.
- [95] M. Oliva, S. Cordell and J. Löwe (2004) "Structural insights into FtsZ protofilament formation" *Nature Struct. Mol. Biol.* 11 (12): 1243-1250.

- [96] X. Ma, and W. Margolin. (1999) "Genetic and functional analyses of the conserved c-terminal core domain of *Escherichia coli* ftsZ " *J. Bacteriol.* 181 (24): 7531-7544.
- [97] S. Pichoff, and J. Lutkenhaus, (2002) "Unique and overlapping roles for ZipA and FtsA in septal ring assembly in *Escherichia coli* " *EMBO J.* 21 (4): 685-693.
- [98] S. Shuman, (1994) "Novel Approach to Molecular Cloning and Polynucleotide Synthesis Using Vaccinia DNA Topoisomerase" *J. Biol. Chem.* 269, 32678-32684.
- [99] T. Ohashi, C. Hale, P. de Boer and H. Erickson (2002). "Structural evidence that the P/Q domain of ZipA is an unstructured, flexible tether between the membrane and the c-terminal FtsZ-binding domain " *J. Bacteriol.* 184 (15): 4313-4315.
- [100] C. Hale and P. de Boer. (1997) " Direct binding of FtsZ to ZipA, an essential component of the septal ring structure that mediates cell division in *E. coli* " *Cell* 88 (2): 175-185.
- [101] A. Pugsley, (1993) " The complete general secretory pathway in Gram-negative bacteria " *Microbiol. Rev.* 57 (1): 50-108.
- [102] H. Erickson, (2001) " The FtsZ protofilament and attachment of ZipA structural constraints on the FtsZ power stroke" *Curr. Opin. Cell Biol.* 13 (1): 55-60.
- [103] C. Hale, A. Rhee and P. de Boer. (2000) "ZipA-induced bundling of FtsZ polymers mediated by an interaction between C-terminal domains " *J. Bacteriol.* 182 (18): 5153-5166.
- [104] F. Moy, E. Glasfeld, L. Mosyak and R. Powers. (2000) "Solution structure of ZipA, a crucial component of *Escherichia coli* cell division " *Biochemistry* 39 (31): 9146-9156.
- [105] L. Mosyak, Y. Zhang, E. Glasfeld, S. Haney, M. Stahl, J. Seehra and W. Somers. (2000) " The bacterial cell-division protein ZipA and its interaction with an FtsZ fragment revealed by X-ray crystallography" *EMBO J.* 19 (13): 3179-3191.
- [106] S. Haney, E. Glasfeld, C. Hale, D. Keeney, Z. He and P. de Boer (2001) "Genetic analysis of the *E. coli* FtsZ-ZipA interaction in the yeast two-hybrid system: characterization of FtsZ residues essential for the interactions with ZipA and with FtsA" *J. Biol. Chem.* 276 (15): 11980-11987.

- [107] Z. Liu, A. Mukherjee and J. Lutkenhaus. (1999). "Recruitment of ZipA to the division site by interaction with FtsZ." *Mol. Microbiol.* 31 (6): 1853-1861.
- [108] H. Erickson. (2001) " The FtsZ protofilament and attachment of ZipA-structural constraints on the FtsZ power stroke " *Curr. Opin. Cell Biol.* 13(1): 55-60.
- [109] NCBI (2010) [on-line] Available :<http://blast.ncbi.nlm.nih.gov/Blast.cgi> [date accessed: Oct 2010].
- [110] C. Hale, A. Rhee, and P. De Boer. (2000) " ZipA-induced bundling of FtsZ polymers mediated by an interaction between C-terminal domains" *J. Bacteriol.* 182 (18): 5153-5166.
- [111] D. Chaudhuri. (1999)."ZipA is a MAP-Tau homolog and is essential for structural integrity of the cytokinetic FtsZ-ring during bacterial cell division." *EMBO J.* 18 (9): 2372-2383.
- [112] A. Mukherjee and J. Lutkenhaus. (1999) "Analysis of FtsZ assembly by light scattering and determination of the role of divalent metal cations" *J. Bacteriol.* 181 (3): 823-832.
- [113] E. Small, R. Marrington, A. Rodger, D. Sloan, D. Roper, T. Dafforn and S. Addinall. (2007)"FtsZ polymer-bundling by the *Escherichia coli* ZapA Orthologue, YgfE, involves a conformational change in bound GTP " *J. Mol. Biol.* 369 (1): 210-221.
- [114] T. Dafforn and A. Rodger. (2004) "Linear dichroism of biomolecules: which way is up?" *Curr. Opin. Struct. Biol.* 14 (5): 541-546.
- [115] A. Rodger and B. Nordén. (1997). *Circular dichroism and linear dichroism* Oxford University Press, Oxford.
- [116] J. Lin-Cereghino, W. Wong, S. Xiong, W. Giang, L. Luong, J. Vu, S. Johnson and G. Lin-Cereghino (2005) "Condensed protocol for competent cell preparation and transformation of the methylotrophic yeast *Pichia pastoris*." *BioTechniques* 38 (1): 44-48.
- [117] W. Zhang, L. Smith, B. Plantz, V. Schlegel and M. Meagher (2002) "Design of methanol feed control in *Pichia pastoris* fermentations based upon a growth model" *Biotechnol. Prog.* 18 (6): 1392-1399.

- [118] D. Mattanovich, B. Gasser, H. Hohenblum and M. Sauer. (2004) "Stress in recombinant protein producing yeasts" *J Biotechnol.* 113 (1-3): 121-135.
- [119] J. Porath, J. Carlsson, I. Olsson and G. Belfrage, (1975) "Metal chelate affinity chromatography, a new approach to protein fractionation" *Nature* 258 (5536): 598-599.
- [120] E. Sulkowski, (1985) "Purification of proteins by IMAC " *Trends Biotechnol.* 3 (1): 1-7.
- [121] H. Nakata. (1989) "Purification of AI Adenosine Receptor from RaBt rain Membranes" *J. Biol. Chem.* 264 (28): 16545-16551.
- [122] H. Markus, B. Wei and R. Grisshammer. (2002) "Purification and characterization of the human adenosine A2a receptor functionally expressed in *Escherichia coli* " *Euro. J. Biochem.* 269 (1): 82-92.
- [123] W. Heidcamp (1995) *Cell Biology Laboratory Manual* [on-line] Available <http://homepages.gac.edu/~cellab/index-1.htm> [date accessed: Sept 2010].
- [124] P. Smith, R. Krohn, G. Hermanson, A. Mallia, F. Gartner ,M. Provenzano, E. Fujimoto,N. Goeke, B. Olson and D. Klenk (1985) "Measurement of protein using bicinchoninic acid " *Anal. Biochem.* 150 (1): 76-85.
- [125] T. Kendall-Harden (2010) [on-line] Available <http://www.signaling-gateway.org/molecule/query?afcsid=A000209> [date accessed: Sept 2010].
- [126] T. Bylund, K. Toews and J. Lung. (1993) "Radioligand binding methods: practical guide and tips" *Cell Mol. Physiol.* 265 (5 Pt 1): L421-L429.
- [127] L. Limbird. (1996). *Cell surface receptors: A short course on theory and methods.* Springer, Berlin.
- [128] H. Yamamura, S. Enna and M. Kuhar (1990) *Methods in Neurotransmitter receptor analysis.* Raven Press, New York.
- [129] P. Atkins, and J. De Paula, (2005) *Elements of Physical Chemistry 4<sup>th</sup> edition,* Oxford University Press, Oxford.



- [130] I. Serdyuk, N. Zaccai and J. Zaccai (2007) *Methods in Molecular Biophysics Structure, Dynamics, Function* Cambridge University Press, New York.
- [131] S. Harding and B. Chowdhry (2001) *Protein-ligand interactions, structure and spectroscopy: a practical approach*. Oxford University Press, Oxford.
- [132] P. Schuck. (2000) "Size distribution analysis of macromolecules by sedimentation velocity ultracentrifugation and Lamm equation modelling " *Biophys J.* 78 (3): 1606-1619.
- [133] R. Pacheco-Gómez (2008) *Structural studies and assembly dynamics of the bacterial cell division protein FtsZ* The University of Warwick, Coventry.
- [134] E. Small, and S. Addinall, (2003) "Dynamic FtsZ polymerization is sensitive to the GTP to GDP ratio and can be maintained at steady state using a GTP-regeneration system " *Microbiology* 149 (Pt 8): 2235-2242.
- [135] A. Mukherjee and J. Lutkenhaus, (1999) "Analysis of FtsZ assembly by light scattering and determination of the role of divalent metal cations" *J. Bacteriology* 181 (3): 823-832.
- [136] S. Ennaceur, M. Hicks, C. Pridmore, T. Dafforn, A. Rodger and J. Sanderson, (2009) "Peptide adsorption to lipid bilayers: Slow processes revealed by linear dichroism spectroscopy" *Biophysical J.* 96 (4): 1399-1407.
- [137] E. White, L. Ross, R. Reynolds, L. Seitz, G. Morre and D. Borhani. (2000) "Slow polymerization of *Mycobacterium tuberculosis* FtsZ " *J. Bacteriology* 182 (14): 4028-4034.
- [138] M. Webb, (1992) "A continuous spectrophotometric assay for inorganic phosphate and for measuring phosphate release kinetics in biological systems" *PNAS* 89 (11): 4884-4887.
- [139] A. Mukherjee and J. Lutkenhaus (1998) "Purification, assembly, and localization of FtsZ " *Methods Enzymol.* 298: 296-305.
- [140] M. Osawa, D. Anderson and H. Erickson (2009) "Reconstitution of contractile FtsZ-rings in liposomes " *Science* 320 (5877): 792-794.
- [141] A. Moscho, O. Orwar, D. Chiu, B. Modi and R. Zare, (1996) "Rapid preparation of giant unilamellar vesicles" *PNAS* 93 (21): 11443-11447.

- [142] A. Ratha, M. Glibowickaa, V. Nadeaua, G. Chena and C. Debera. (2009) "Detergent binding explains anomalous SDS-PAGE migration of membrane proteins" *PNAS*. 106 (6): 1760-1765.
- [143] M. Wallsten and K. Perlundahl.(1990) "Binding of sodium dodecyl sulphate to an integral membrane protein and to a water-soluble enzyme. Determination by molecular-sieve chromatography with flow scintillation detection" *J. Chromutography* 5 (12): 3-12.
- [144] J. Lacapère (2010) *Membrane Protein Structure Determination: Methods and Protocols* Human Press, New York.
- [145] T. Dafforn, R. Mahadeva, P. Elliott, P. Sivasothy, D. Lomas. (1999) "A kinetic mechanism for the polymerization of alpha1-antitrypsin " *J. Biol. Chem.* 274 (14): 9548-9555.
- [146] S. Haney, E Glasfeld, C. Hale, D. Keeney, Z. He and P. de Boer. (2001) "Genetic analysis of the *Escherichia coli* FtsZ-ZipA interaction in the yeast two-hybrid system" *J. Biol. Chem.* 276 (15): 11980-11987.
- [147] H. Schägger (2006) "Tricine-SDS-PAGE" *Nature Protocols* 1, 16-22.
- [148] R. Garavito , S. Ferguson-Miller (2001) "Detergents as tools in membrane biochemistry" *J Biol Chem.* 276(35): 32403-6.
- [149] A. Helenius and K. Simons (1975) "Solubilization of membranes by detergents" *Biochim Biophys Acta.*415(1): 29-79.
- [150] F. Menger, R. Zana, and B. Lindman. (1998) "Portraying the Structure of Micelles" *J Chem Educ*, 75 (1): 115.
- [151] M. le Maire, P. Champeil and JV. Moller (2000) "Interaction of membrane proteins and lipids with solubilizing detergents". *Biochim Biophys Acta.* 1508(1-2): 86-111.
- [152] J. Rigaud and B. Pitard. (1995) "Reconstitution of membrane proteins into liposomes: application to energy-transducing membrane proteins". *Biochim Biophys Acta*1231(3): 223-46.
- [153] M. Jones and D. Chapman (1995) *Micelles, monolayers and biomembranes.* Wiley–Liss, New York.

- [154] P. Walde, K. Cosentino, H. Engel, P. Stano (2010) "Giant vesicles: preparations and applications" *Chem biochem* 11(7): 848-65
- [155] M. Luckey, H. Nikaido (1980) "Specificity of diffusion channels produced by lambda phage receptor protein of *Escherichia coli*" *PNAS* 77(1): 167-71.
- [156] G. Beschiaschvili, J. Seelig . (1992) "Peptide binding to lipid bilayers. Nonclassical hydrophobic effect and membrane-induced pK shifts" *Biochemistry* 31(41): 10044-53.
- [157] M. Costello, P. Viitanen, N. Carrasco, D. Foster, H. Kaback (1984) "Morphology of proteoliposomes reconstituted with purified lac carrier protein from *Escherichia coli*" *J Biol Chem.* 259(24): 15579-86.
- [158] T. Knowles (2007) *Lipodisqs: A novel method for the : study of membrane proteinsstudy proteins* University of Birmingham, Birmingham.
- [159] S. Jähnichen (2006) *Activation cycle of G-proteins by G-protein-coupled receptors* [on-line] Available:<http://commons.wikimedia.org/wiki/File:GPCR-Zyklus.png> [date accessed: Nov 2010].
- [160] E. Kelly, C. Bailey and G. Henderson (2008) "Agonist-selective mechanisms of GPCR desensitization". *Br J Pharmacol* 153 Suppl 1: S379-88
- [161] I. Database (2010) [on-line] Available :<http://www.iuphar-db.org/DATABASE/ObjectDisplayForward?objectId=19> [date accessed: Nov 2010].
- [162] M. Thanbichler and L. Shapiro (2008) "Getting organized — how bacterial cells move proteins and DNA" *Nature Rev Micro* (6) 28-40
- [163] E. Hochuli, (1989) "Genetically designed affinity chromatography using a novel metal chelate absorbent" *Biologically Active Molecules* 217-239.
- [164] J. Löwe, F. Ent, and L. (2004) "Molecules of the bacterial cytoskeleton" *Annu Rev Biophy Biomol Struct* 33: 177-198

## **CHAPTER 9: Appendices**

### **A2aR Protein Wild Type Sequence (412 Amino Acid Residues)**

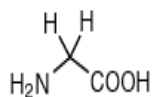
MPIMGSSVYITVELAIAVLAILGNVLCWAVWLNSNLQNVTNYFVVSLAAADIAVGVLAIPF  
AITISTGFCAACHGCLFIACFVLVLTQSSIFSLAIAIDRYIAIRIPLRYNGLVTGTRAKGIIAICW  
VLSFAIGLTPMLGWNNCGQPKEGKNHSQGC GEGQVACLFEDVVP MNYMVYFNFFACVLVP  
LLMLGVYLRIFLAARRQLKQMESQPLGERARSTLQKEVHAAKSLAIIVGLFALCWLPLHII  
NCFTFFCPDCSHAPLWLMYLAIVLSHTNSV VNPFIAYRIREFRQTFRKIIRSHVLRQQEPFKA  
AGTSARVLA AHGSDGEQVSLRLNGHPPGVWANGSAPHPERRPNGYALGLVSGGSAQESQG  
NTGLPDVELLSHELKGVCPPEPGLDDPLAQDGAGVS

### **ZipA Protein Wild Type Sequence (328 Amino Acid Residues)**

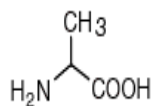
MMQDLRLILIIVGAIAIIALLVHGFWTSRKERSMFRDRPLKRMKSKRDDDSYDEDVEDDEG  
VGEVRVHRVNHAPANAEHEAARSPQH QYQPPYASAQPRQP VQPPEAQVPPQHAPHPAQ  
PVQQPAYQPQPEQLQQPVSPQVAPAPQPVHSAPQPAQQA FQPAEPVAAPQPEPVAEPAPVM  
DKPKRKEAVIIMNVAAHHGSELNGEALLNSIQQAGFIFGDMNIYHRHLSPDGSGPALFSLAN  
MVKPGTFDPEMKDFTTPGV TIFMQVPSYGDELQNFKLMLQSAQHIADEVGGVV LDDQRRM  
MTPQKLREYQDIIREVKDANA

**Standard 3 and 1 Letter Amino Acid Abbreviations and Structures**

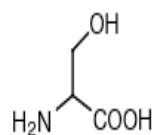
**Small**



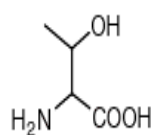
Glycine (Gly, G)  
MW: 57.05



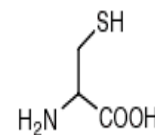
Alanine (Ala, A)  
MW: 71.09



Serine (Ser, S)  
MW: 87.08, pK<sub>a</sub> ~ 16

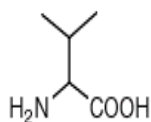


Threonine (Thr, T)  
MW: 101.11, pK<sub>a</sub> ~ 16

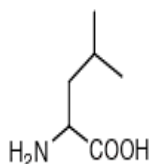


Cysteine (Cys, C)  
MW: 103.15, pK<sub>a</sub> = 8.35

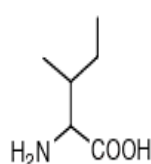
**Hydrophobic**



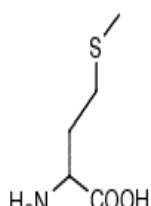
Valine (Val, V)  
MW: 99.14



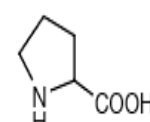
Leucine (Leu, L)  
MW: 113.16



Isoleucine (Ile, I)  
MW: 113.16

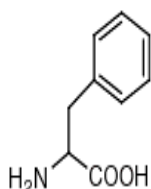


Methionine (Met, M)  
MW: 131.19

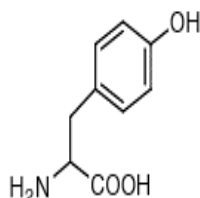


Proline (Pro, P)  
MW: 97.12

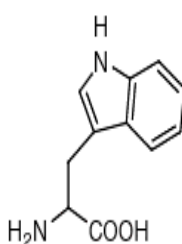
**Aromatic**



Phenylalanine (Phe, F)  
MW: 147.18

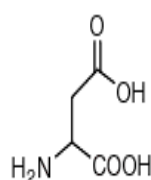


Tyrosine (Tyr, Y)  
MW: 163.18

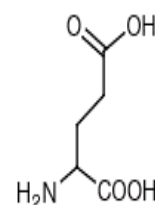


Tryptophan (Trp, W)  
MW: 186.21

**Acidic**

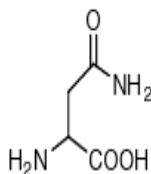


Aspartic Acid (Asp, D)  
MW: 115.09, pK<sub>a</sub> = 3.9

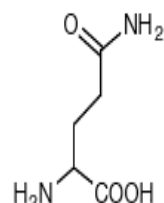


Glutamic Acid (Glu, E)  
MW: 129.12, pK<sub>a</sub> = 4.07

**Amide**

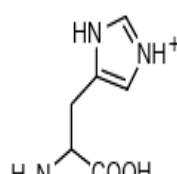


Asparagine (Asn, N)  
MW: 114.11

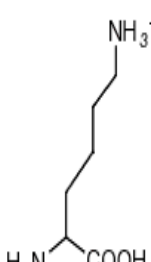


Glutamine (Gln, Q)  
MW: 128.14

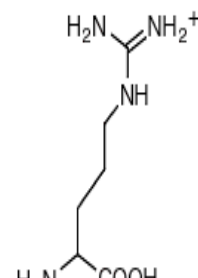
**Basic**



Histidine (His, H)  
MW: 137.14, pK<sub>a</sub> = 6.04



Lysine (Lys, K)  
MW: 128.17, pK<sub>a</sub> = 10.79



Arginine (Arg, R)  
MW: 156.19, pK<sub>a</sub> = 12.48

<http://www.neb.com>